Dissertation

submitted to the

Combined Faculties of the Natural Sciences and Mathematics

of the Ruperto-Carola-University of Heidelberg, Germany

for the degree of

Doctor of Natural Sciences

Put forward by

Sebastian Meuren

born in Wittlich

Oral examination: 24.6.2015

Nonlinear quantum electrodynamic and electroweak processes in strong laser fields

Referees:

Honorarprof. Dr. Christoph H. Keitel

Prof. Dr. Jan M. Pawlowski

Zusammenfassung

Die vorliegende Arbeit betrachtet verschiedene nichtlineare elektrodynamische und elektroschwache Prozesse, die in starken Laserfeldern auftreten können; ein Schwerpunkt liegt auf Kurzpulseffekten. Insbesondere erfolgt eine numerische Berechnung der Impulsverteilung für photonenproduzierte Elektron-Positron-Paare und eine semiklassische Interpretation ihrer charakteristischen Eigenschaften. Durch den Beweis des optischen Theorems ergibt sich eine kompakte Doppelintegraldarstellung für die totale Paarerzeugungswahrscheinlichkeit, die numerisch ausgewertet wird. Die Einbeziehung des exponentiellen Zerfalls der Photonenwellenfunktion in einer ebenen Welle erfolgt durch Lösen der Schwinger-Dyson-Gleichungen in führender Ordnung unter Anwendung der quasistatischen Näherung. In diesem Zusammenhang wird der Polarisationsoperator für eine ebene Welle untersucht und seine Ward-Takahashi-Identität überprüft. Eine klassische Analyse zeigt, dass photonenproduzierte Elektron-Positron-Paare unter bestimmten Bedingungen rekollidieren können. Die auf solche Rekollisionen zurückführbaren Beiträge zum Polarisationsoperator werden identifiziert und sowohl analytisch als auch numerisch berechnet. Darüber hinaus wird die Existenz einer nicht-trivialen Dynamik des Elektronenspins in ultrakurzen Laserpulsen nachgewiesen, die auf Quantenfluktuationen zurückzuführen ist. Abschließend erfolgt eine Betrachtung des Austauschs von schwachen Eichbosonen, der für Neutrino-Photon Wechselwirkungen essenziell ist. Insbesondere wird der Tensor, welcher die Kopplung zwischen dem Axialvektor- und dem Vektorstrom beschreibt, berechnet und die sogenannte Adler-Bell-Jackiw (ABJ) Anomalie untersucht.

Abstract

Various nonlinear electrodynamic and electroweak processes in strong plane-wave laser fields are considered with an emphasis on short-pulse effects. In particular, the momentum distribution of photoproduced electron-positron pairs is calculated numerically and a semiclassical interpretation of its characteristic features is established. By proving the optical theorem, compact double-integral expressions for the total pair-creation probability are obtained and numerically evaluated. The exponential decay of the photon wave function in a plane wave is included by solving the Schwinger-Dyson equations to leading-order in the quasistatic approximation. In this respect, the polarization operator in a plane wave is investigated and its Ward-Takahashi identity verified. A classical analysis indicates that a photoproduced electron-positron pair recollides for certain initial conditions. The contributions of such recollision processes to the polarization operator are identified and calculated both analytically and numerically. Furthermore, the existence of nontrivial electron-spin dynamics induced by quantum fluctuations is verified for ultra-short laser pulses. Finally, the exchange of weak gauge bosons is considered, which is essential for neutrino-photon interactions. In particular, the axial-vector–vector coupling tensor is calculated and the so-called Adler-Bell-Jackiw (ABJ) anomaly investigated.

List of Publications

Publications covered by this thesis

[1] **Quantum Electron Self-Interaction in a Strong Laser Field**,
S. Meuren and A. Di Piazza,
Phys. Rev. Lett. **107**, 260401 (2011)
5 pages, 2 figures, doi:10.1103/PhysRevLett.107.260401, arXiv:1107.4531

[2] **Tests of Classical and Quantum Electrodynamics with Intense Laser Fields**,
S. Meuren, O. Har-Shemesh, and A. Di Piazza,
Progress in Ultrafast Intense Laser Science **X**, (Springer, 2014),
25 pages, 7 figures, doi:10.1007/978-3-319-00521-8_8

[3] **Polarization operator for plane-wave background fields**,
S. Meuren, C. H. Keitel, and A. Di Piazza,
Phys. Rev. D **88**, 013007 (2013)
19 pages, 2 figures, doi:10.1103/PhysRevD.88.013007, arXiv:1304.7672

[4] **Polarization-operator approach to pair creation in short laser pulses**,
S. Meuren, K. Z. Hatsagortsyan, C. H. Keitel, and A. Di Piazza,
Phys. Rev. D **91**, 013009 (2015)
20 pages, 14 figures, doi:10.1103/PhysRevD.91.013009, arXiv:1406.7235

[5] **High-Energy Recollision Processes of Laser-Generated Electron-Positron Pairs**,
S. Meuren, K. Z. Hatsagortsyan, C. H. Keitel, and A. Di Piazza,
Phys. Rev. Lett. **114**, 143201 (2015)
7 pages, 4 figures, doi:10.1103/PhysRevLett.114.143201, arXiv:1407.0188

[6] **Semiclassical description of nonlinear electron-positron photoproduction in strong laser fields**,
S. Meuren, C. H. Keitel, and A. Di Piazza,
submitted (2015)
16 pages, 4 figures, arXiv:1503.03271

[7] **Nonlinear neutrino-photon interactions inside strong laser pulses**,
S. Meuren, C. H. Keitel, and A. Di Piazza,
submitted (2015)
18 pages, 4 figures, arXiv:1504.02722

Publications not related to this thesis

[8] **Measurement of the autoionization lifetime of the energetically lowest doubly excited $Q_1\,^1\Sigma_u^+$ state in H2 using electron ejection asymmetry**,
A. Fischer, A. Sperl, P. Cörlin, M. Schönwald, S. Meuren, J. Ullrich, T. Pfeifer, R. Moshammer and A. Senftleben,
J. Phys. B: At. Mol. Opt. Phys. **47** 021001 (2014)
5 pages, 4 figures, doi:10.1088/0953-4075/47/2/021001

Contents

Contents

Appendix 163

Summary of the Notation

Physical constants		
c	$2.998 \times 10^{10}\,\text{cm/s}$	speed of light in vacuum
$\hbar = h/(2\pi)$	$6.582 \times 10^{-16}\,\text{eV s}$	reduced Planck constant[a]
μ_0	$4\pi \times 10^{-7}\,\text{N/A}^2$	magnetic permeability of vacuum
$\epsilon_0 = 1/(\mu_0 c^2)$	$8.854 \times 10^{-12}\,\text{F/m}$	electric permittivity of vacuum
m_e	$511.0\,\text{keV/c}^2$	electron mass[b]
m_μ	$105.7\,\text{MeV/c}^2$	muon mass
m_τ	$1.777\,\text{GeV/c}^2$	tau mass
$|e|$	$1.602 \times 10^{-19}\,\text{C}$	elementary charge[c]
$\lambdabar_c = \hbar/(mc)$	$3.862 \times 10^{-11}\,\text{cm}$	reduced Compton wavelength (electron)
$\alpha = e^2/(4\pi\epsilon_0 \hbar c)$	$1/137.0$	fine-structure constant
$G_F/(\hbar c)^3$	$1.166 \times 10^{-5}\,\text{GeV}^{-2}$	Fermi coupling constant

[a] $\hbar c = 197.3\,\text{MeV fm}$
[b] Normally, we denote the electron mass simply by m.
[c] Note that $e = -|e| < 0$ denotes the electron charge as in Ref. [LL82].

Tab. 1: Summary of the most important physical constants used in this thesis. For more precise numerical values see Ref. [MTN12].

The notation employed in this thesis agrees with Landau and Lifshitz [LL82], except that for charge Heaviside-Lorentz units are used[1], i.e. $\alpha = e^2/(4\pi) \approx 1/137$. Furthermore, we set $\hbar = c = 1$ in most equations (c and $\hbar$ are sometimes reinstated for clarity).

Four-dimensional space-time indices are denoted by lowercase Greek letters ($\mu, \nu \ldots$), taking the values $0, 1, 2, 3$ and three-dimensional space indices by lowercase Latin letters ($i, j, \ldots$), taking the values $1, 2, 3$ or equivalently x, y, z. The Einstein summation convention is always implicitly assumed for all types of repeated indices which appear only on one side of an equation. The metric $g^{\mu\nu} = g_{\mu\nu} = \text{diag}\,(+, -, -, -)$ is used to raise and lower Lorentz indices $a_\mu = g_{\mu\nu}a^\nu$, the unit and the totally anti-symmetric tensor are denoted by $\delta_\nu^\mu = g^{\mu\rho}g_{\rho\nu} = \text{diag}(1,1,1,1)$ ($\delta_\mu^\mu = 4$) and $\epsilon^{\mu\nu\rho\sigma}$ ($\epsilon^{0123} = -\epsilon_{0123} = 1$), respectively. Scalar products of two four-vectors are denoted by $ab = a^\mu b_\mu = a^\mu g_{\mu\nu}b^\nu$, they are sometimes enclosed with brackets for clarity $(ab) = a^\mu b_\mu$. For contractions of second-rank tensors and vectors the following matrix notation is often used: $aTb = a_\mu T^{\mu\nu}b_\nu$, $(T_1 T_2)^{\mu\nu} = T_1{}^\mu_\rho T_2^{\rho\nu}$, $T^{2\mu\nu} = T^{\mu\rho}T_\rho{}^\nu$, $(Ta)^\mu = T^{\mu\nu}a_\nu$, $(aT)^\mu = a_\nu T^{\nu\mu}$. The Lorentz index of the Dirac gamma matrices (see App. D) is treated as a four-vector index, e.g. $\gamma T\gamma = \gamma^\mu T_{\mu\nu}\gamma^\nu$.

Dirac spinor indices are denoted by lowercase Latin letters ($a, b, \ldots$), taking the values $1, 2, 3, 4$ and are normally suppressed [$\bar{u}_{p'}\gamma^\mu u_p = (u_{p'})_a^* \gamma_{ab}^0 \gamma_{bc}^\mu (u_p)_c$].

---

[1]Note that the replacement $\epsilon_0 \to 1$ is not sufficient, in addition one also has to "rescale" the magnetic field $\boldsymbol{B}_{\text{SI}} = \frac{1}{c}\boldsymbol{B}_{\text{HL}}$. This ensures that the electric and the magnetic field have the same units.

Common symbols	
$g^{\mu\nu} = \mathrm{diag}\,(+,-,-,-)$	space-time metric
δ^{μ}_{ν}, δ_{ij}	unit tensors (Kronecker symbols)
$\epsilon^{\mu\nu\rho\sigma}$, $\epsilon^{0123} = -\epsilon_{0123} = 1$ ϵ^{ijk}, $\epsilon^{123} = 1$	totally antisymmetric tensors
$\boldsymbol{a}^i = (\boldsymbol{a}^1, \boldsymbol{a}^2, \boldsymbol{a}^3)$	three-vector (bold Latin letters)
$a^{\mu} = (a^0, \boldsymbol{a})$	four-vector (italic Latin letters)
$(\boldsymbol{a} \times \boldsymbol{b})^i = \epsilon^{ijk}\boldsymbol{a}^j\boldsymbol{b}^k$	cross product
$\boldsymbol{ab} = \boldsymbol{a}^i\boldsymbol{b}^i$	scalar product of two three-vectors
$ab = a_{\mu}b^{\mu} = a_0 b_0 - \boldsymbol{ab}$	scalar product of two four-vectors
$x^{\mu} = (t, \boldsymbol{x}) = (t, x, y, z)$	four-position vector
$d^4x = dx^0 dx^1 dx^2 dx^3$	four-dimensional volume element
$\partial_{\mu} = \partial/\partial x^{\mu} = (\partial/\partial t, \nabla)$	four-dimensional differentiation operator
$\partial_{\mu}x_{\nu} = g_{\mu\nu}$	defining relation for the four-derivative
$\nabla = (\partial_1, \partial_2, \partial_3)$	three-dimensional differentiation operator
$\square = \partial^2 = \partial^{\mu}\partial_{\mu}$	D'Alembert operator
$\Delta = \nabla^2$	Laplace operator
$f'(x)$	derivative with respect to the argument[a]
$[A, B] = AB - BA$	commutator
$\{A, B\} = AB + BA$	anticommutator
$T^{[\mu\nu]} = \frac{1}{2}(T^{\mu\nu} - T^{\nu\mu})$	anti-symmetric part of a tensor
$T^{(\mu\nu)} = \frac{1}{2}(T^{\mu\nu} + T^{\nu\mu})$	symmetric part of a tensor
$T^{*\mu\nu} = \frac{1}{2}\epsilon^{\mu\nu\rho\sigma}T_{\rho\sigma}$	dual tensor[b]
$A^{\dagger}, A^{\mathrm{T}}, A^{-1}$	Hermitian conjugate, transpose, inverse
$A^{\dagger} = A$	Hermitian matrix or operator
$A^{\dagger} = -A$	anti-Hermitian matrix or operator
$A^{\dagger} = A^{-1}$	unitary matrix or operator
$\gamma = 1/\sqrt{1 - (\boldsymbol{v}/c)^2}$	relativistic Lorentz factor
γ^{μ}	Dirac gamma matrices (see App. D)
$\gamma^5 = -i\gamma^0\gamma^1\gamma^2\gamma^3$	fifth gamma matrix
$\sigma^{\mu\nu} = (\gamma^{\mu}\gamma^{\nu} - \gamma^{\nu}\gamma^{\mu})/2$	commutator of two gamma matrices
$\mathbf{1}$	unit matrix in spinor space
$\slashed{a} = \gamma^{\mu}a_{\mu}$	Feynman's slash notation
$\bar{\psi} = \psi^{\dagger}\gamma^0$	Dirac conjugated spinor
$\bar{M} = \gamma^0 M^{\dagger}\gamma^0$	Dirac conjugated matrix
$\hat{\psi}, \hat{a}, \hat{a}^{\dagger}$	Fock-space operators are written with hat
$\delta(x)$	Dirac delta function
$\delta^{(3)}(\boldsymbol{x}) = \delta(\boldsymbol{x}^1)\delta(\boldsymbol{x}^2)\delta(\boldsymbol{x}^3)$	three-dimensional Dirac delta function
$\delta^{(4)}(x) = \delta(x_0)\delta^{(3)}(\boldsymbol{x})$	four-dimensional Dirac delta function
$i0 = i\epsilon$, $\epsilon \to 0_+$	Limiting procedure for propagators
$\mathbf{tr}$, $\det$	trace/determinant of a matrix or operator
$\Re$; $\Im$	real/imaginary part of a complex number

[a] If no explicit argument is present (e.g., for f'), the prime is a part of the symbol name and does not indicate a derivative.

[b] If the tensor contains complex entries, $(T^{\mu\nu})^*$ denotes the complex conjugate.

Tab. 2: Summary of commonly used (mathematical) symbols and how they are defined here. The symbols and definitions used for special mathematical functions agree with those in [Olv+10]. More details can be found in the appendices.

Special symbols		
$\epsilon_{\boldsymbol{p}} = \sqrt{M^2 + \boldsymbol{p}^2}$	energy[a]	
ϵ^μ	polarization four-vector of a photon	
$p^\mu = (p^0, \boldsymbol{p})$	four-momentum vector[b]	
$k^\mu = \omega(1, \boldsymbol{n})$	laser-photon four-momentum	
$\phi = kx$	laser phase at the space-time point x^μ	
$F^{\mu\nu}$	background field tensor	Eq. (1.17)
$\psi_i(\phi)$	laser shape functions	
a_i^μ	laser field-strength four-vectors	Eq. (1.18)
$f_i^{\mu\nu}$	constant background field tensors	
A^μ	background four-potential	Eq. (1.19)
ξ_i, ξ	classical intensity parameters	Eq. (1.20)
χ_i, χ	quantum-nonlinearity parameters[c]	Eq. (1.21)
$\mathfrak{F}^{\mu\nu}(\phi, \phi_0)$	integrated field tensor	Eq. (1.29)
$\mathfrak{F}^{\mu\nu}(\phi)$		
$\bar{k}^\mu$	conjugate laser four-momentum	Eq. (1.31)
$v^-, v^+, v^{\mathrm{I}}, v^{\mathrm{II}}$	light-cone components of v^μ ($\perp = \mathrm{I}, \mathrm{II}$)	Eq. (1.37)
$\delta^{(-,\perp)}(a)$	delta function in light-cone coordinates	Eq. (1.42)
$\Lambda_1^\mu, \Lambda_2^\mu$	Lambda four-vectors associated with q^μ	Eq. (1.48)
$E_{p,x} = E_p(x),$	Ritus matrices	Eq. (1.55)
$\bar{E}_{p,x} = \bar{E}_p(x)$		
$\Gamma^\rho(p', q, p)$	dressed vertex	Eq. (1.67)
S_Γ	quantities related to	Eq. (1.69)
$G^{\mu\rho}, G_5^{\mu\rho}$	the dressed vertex	Eq. (1.70)
G_1, G_2, G_3		Eq. (1.71)
$\mathcal{G}^\rho(p', q, p)$	nonsingular part of the dressed vertex	Eq. (1.79)
t_i	invariant transverse momenta	Eq. (1.83)
w	third invariant momentum parameter	Eq. (1.84)
$\bar{w}$	conjugated momentum parameter	Eq. (1.86)
$\mathfrak{G}_0, \mathfrak{G}_{j,l}$	master integrals	Eq. (1.89)
$\mathcal{Q}_1^\mu, \mathcal{Q}_2^\mu$	four-vectors associated with q_i^μ	Eq. (3.35)
$\Lambda_1^{*\mu}, \Lambda_2^{*\mu}$	Dual lambda four-vectors[d]	Eq. (C.4)
Λ_5^μ	pseudo four-vector associated with k^μ	Eq. (C.7)
$f(x), f'(x), f_1(x)$	Ritus functions	Eq. (F.1)

[a] For a particle with mass M and momentum $\boldsymbol{p}$.
[b] The four-momentum is on shell if $p^2 = M^2$, implying $p^0 = \epsilon_{\boldsymbol{p}}$.
[c] In Chap. 5 a different notation is used, see Eq. (5.14).
[d] The star is part of the symbol.

Tab. 3: Summary of important symbols which are frequently used in the text.

Introduction

At present the Standard Model of particle physics describes all observed quantum phenomena with an outstanding precision. Its long lasting success story culminated in the recent discovery of the Higgs boson at the LHC [ATLAS12; CMS12], which confirmed the generation of particle masses via spontaneous symmetry breaking in the electroweak sector. Nevertheless, many fundamental questions remain unanswered and most physicists believe that the Standard Model represents only the low-energy limit of a more complete "grand unified theory" (GUT). Similar to the unification of the electric and the weak force for energies higher than the weak scale ($\sim 10^2\,$GeV), it is expected that above a hypothetical GUT scale ($\sim 10^{16}\,$GeV) also the strong and the electroweak force are described on a common footing. Finally, a "theory of everything" should also comprise a quantum description of gravity at the Planck scale ($\sim 10^{19}\,$GeV).

In the past, many extensions of the Standard Model have been considered. However, it is rather unpredictable which approach is heading in the right direction, as nearly all measurements carried out so far are consistent with the predictions of the Standard Model[1]. Therefore, our effort to attain a deeper understanding of nature would certainly benefit from an unexpected experimental finding. In order to provide the Standard Model a possibility to fail, it is desirable to test it in yet unexplored parameter regions.

An approach complementary to ordinary collider-based experiments are investigations of highly nonlinear or even nonperturbative phenomena. The probably most prominent example is the confinement phase of QCD, which is not very well understood so far. In the present thesis, we consider nonlinear electrodynamic and electroweak processes inside strong laser fields. The calculated probabilities often experience a nonperturbative coupling between electrons (or positrons) and the background field or require the simultaneous absorption of many laser photons within the formation region of the process. Notably, most of our predictions could be tested either with existing technology or at planned near-future laser facilities by colliding high-energy electrons, positrons, photons or neutrinos with ultra-strong laser pulses.

The peak electric field strength E_0 and the angular frequency ω are the two most important parameters of a laser pulse. According to the Lorentz force law, a constant electric field with field strength E_0 can transfer the energy $\epsilon \sim |eE_0ct|$ to an electron during the time t in the relativistic regime (e denotes the electron charge) [LL87]. For on-shell electrons the characteristic time scale t is set by the angular frequency ω of the laser ($t \sim 1/\omega$). Correspondingly, an electron at rest becomes relativistic within one laser cycle ($\epsilon \sim mc^2$) if the classical intensity parameter $\xi = |e|\,E_0/(mc\omega)$ is of order unity (ξ is both gauge and Lorentz invariant, see Chap. 1). Here and in the following we focused on electrons, as they represent the lightest electrically charged particles (all considerations apply equally

---

[1]We assume here that neutrino masses are taken into account. Notable exceptions are the anomalous magnetic moment of the muon [Hag+07] and the size of the proton [Poh+13].
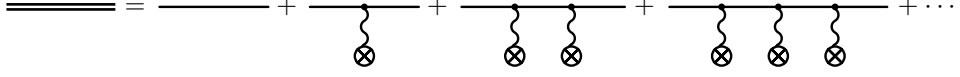
Fig. 1: Perturbative expansion of the dressed electron/positron propagator with respect to the external field $A^\mu \sim E_0/\omega$ (denoted by $\otimes$). For each additional coupling we obtain one more vertex/free propagator, which multiplies the probability amplitude with a factor $\sim \xi$ in the perturbative regime.

to positrons). Correspondingly, they set the scale at which nonlinear QED effects become important.

In the so-called relativistic regime $\xi \gtrsim 1$, which corresponds to the intensity $I \gtrsim 10^{18}\,\mathrm{W/cm^2}$ for optical lasers ($\omega \sim 1\,\mathrm{eV}$), a perturbative expansion of the S-matrix with respect to the background laser field breaks down (note that, e.g., the laser system described in [Yan+08] achieves the intensity $2 \times 10^{22}\,\mathrm{W/cm^2}$ for $\omega = 1.55\,\mathrm{eV}$, which corresponds to $\xi \approx 70$). The threshold $\xi \gtrsim 1$ can be understood qualitatively from a comparison of two Feynman diagrams which differ by only one external field interaction (see Fig. 1): Each coupling to the background field adds a factor eA^μ and each additional propagator a factor $\sim 1/m$ to the transition amplitude ($A^\mu \sim E_0/\omega$ denotes the four-potential of the field and the propagator is evaluated heuristically for zero momentum). Therefore, we expect that in the regime $\xi \ll 1$ the probability to absorb n photons from the laser field scales as $\sim \xi^{2n}$, which is indeed observed in actual calculations [Di+12; Rit85]. Accordingly, the exchange of multiple laser photons starts to play an important role for relativistically strong background fields ($\xi \gtrsim 1$).

The present thesis devises special attention to the strong-field regime $\xi \gg 1$, which is particularly interesting from a theoretical point of view. Besides, it is accessible experimentally with existing optical petawatt laser systems. Since the first experimental realization of an optical laser in 1960 [Mai60], the available laser peak intensities steadily increased due to a continuous flow of innovations like the chirped pulse amplification technique [MTB06; SM85]. Nowadays various optical petawatt laser systems are operating all over the world, capable of producing intensities in the range of $10^{20} - 10^{22}\,\mathrm{W/cm^2}$ [Chu+13; Gau+10; Kir+12; Sun+10; Wan+11; Yu+12].

Furthermore, multi-petawatt laser systems are under construction, with envisaged intensities up to $\sim 10^{23-25}\,\mathrm{W/cm^2}$ [Kor+11]. Among them are the APOLLON-10P laser [Ché+12], the Extreme Light Infrastructure [ELI], the Vulcan 10 PW laser [Lya+11] at the Central Laser Facility [CLF], and the Exawatt Center for Extreme Light Studies [XCELS]. In the near future, these facilities will provide unique opportunities for studying quantum processes inside ultra-strong electromagnetic background fields. In order to describe experiments carried out in the nonlinear regime $\xi \gtrsim 1$, the coherent part of the photon field must be taken into account exactly in the calculations. This is possible in the Furry picture [Fur51], i.e. by expanding the electron/positron field operator using dressed (Volkov) states (see Chap. 1) [LL82; Vol35].

So far we considered only the classical intensity parameter ξ, which admits

a straightforward interpretation for real electrons and positrons. However, an electromagnetic background field also acts on virtual particles, which are always present in the form of quantum fluctuations. Owing to the equivalence of mass and energy and the Heisenberg uncertainty relation, an electron-positron pair with energy $\epsilon \gtrsim mc^2$ can spontaneously appear in the vacuum for a short time $\tau \lesssim \hbar/\epsilon$. Pictorially speaking, the vacuum contains many virtual electron-positron pairs with a life time on the Compton scale $\tau_c = \hbar/(mc^2) \approx 1.3 \times 10^{-21}$ s. According to the above classical considerations, an electric background field can bring a virtual electron-positron pair on shell if it reaches the QED critical field strength $E_{\mathrm{cr}} = m^2 c^3/|e|\,\hbar \approx 1.3 \times 10^{16}$ V/cm. This process is called spontaneous or Schwinger pair creation from the vacuum [Sch51]; it was first suggested by Sauter [Sau31] as an explanation for the Klein paradox [Kle29]. Even if the Dirac sea picture is obsolete, it is often employed to illustrate Schwinger pair creation as a tunneling process from the occupied negative-energy states to the positive-energy continuum. As the definition of the critical field involves the reduced Planck constant $\hbar$, it represents a genuine quantum scale which does not admit a completely classical explanation.

Unfortunately, the laser intensity $I_{\mathrm{cr}} = 4.6 \times 10^{29}$ W/cm^2, which corresponds to the QED critical field strength E_{cr}, is not attainable in the near future. Therefore, several catalyzing mechanisms for vacuum pair production below the Schwinger limit have been considered. One suggested possibility is the so-called assisted Schwinger mechanism [DGS09; SGD08], where a strong, low-frequency and a weak, high-frequency field are combined. Pictorially speaking, the effective tunneling barrier is reduced by absorbing several photons from the high-frequency field [Di+09]. Alternatively, the critical field is attainable in a boosted Lorentz frame even if the laser pulse has a subcritical intensity in the laboratory. This approach is considered here, namely pair creation induced by high-energy gamma photons (nonlinear Breit-Wheeler process [BW34]). However, the energy $\hbar\omega_\gamma$ of the incoming gamma photon must substantially exceed the threshold mc^2 in order to produce an ultra-relativistic electron-positron pair. More precisely, the threshold condition for nonlinear Breit-Wheeler pair production is given by $\chi \gtrsim 1$, where χ denotes the quantum-nonlinearity parameter [$\chi = (2\hbar\omega_\gamma/mc^2)(E_0/E_{cr})$ for a head-on laser–high-energy photon collision, see Chap. 1].

Due to the unitarity of the S-matrix, the total electron-positron photoproduction probability is related to the imaginary part of the polarization operator, which describes photon forward scattering (see Chap. 3 and Ref. [3]). By proving this so-called optical theorem for arbitrary plane-wave background fields, we obtain compact double-integral expressions for the total nonlinear Breit-Wheeler pair-creation probability (see Chap. 2 and Ref. [4]). Our numerical calculations indicate that pair-production probabilities of the order of ten percent could be reached for the collision between a single GeV photon and a strong optical laser pulse (GeV photons are available from Compton backscattering [Mur+14; SPring8]; they could also be produced in an all-optical setup by employing electron wakefield acceleration [ESL09; Lee+06; Phu+12; Pow+14; Wan+13]). So far only the E-144 experiment at SLAC was dedicated to nonlinear QED processes in strong laser

fields. In this experiment, nonlinear Compton scattering [Bul+96] and electron-positron pair creation via the trident process [Bur+97] were observed by colliding a 46.6 GeV electron beam with relativistically intense optical laser light. According to our findings, the nonlinear Breit-Wheeler process is a promising candidate for the first direct conversion of light into matter using a light-by-light scattering experiment.

As the probability for pair creation is substantial for next-generation laser parameters, a straightforward application of perturbation theory becomes inadequate and also the exponential decay of the photon wave function must be taken into account. In vacuum, the modifications induced by loop diagrams are usually small, which is the reason why they are called radiative corrections. Inside a strong background field, however, the exact wave functions defined via the Schwinger-Dyson equation are unstable. Correspondingly, the polarization operator (which describes quantum fluctuations for photons, see Chap. 3 and Ref. [3]) and the mass operator (which describes quantum fluctuations for electrons and positrons, see Chap. 5 and Refs. [1] and [2]) are of central importance for a unitary time evolution. Especially in the regime where cascade reactions are expected [BK08; Bul+10a; Bul+13; Elk+11; Fed+10; Ner+11], the wave-function decay becomes important. Due to its significance, we present here a new derivation of the leading-order contribution to the polarization operator, which is very similar to the corresponding calculations in vacuum QED (see Chap. 3 and Ref. [3]; the adaptation of the calculation method to the mass operator is straightforward). Notably, the physical interpretation of the appearing integration variables becomes particularly transparent in our approach and facilitated the identification of the recollision contribution to the polarization operator (see Chap. 4 and Ref. [5]).

In Chap. 2 (see also Ref. [6]) we verify that photoproduced electron-positron pairs behave like classical particles after they have left the formation region (in the ultra-relativistic regime $\xi \gg 1$). Correspondingly, many features of the asymptotic momentum distribution become intuitively understandable from the classical equations of motion. Remarkably, they predict for linearly polarized laser fields high-energy recollision processes, which could subsequently prime new reactions as in an ordinary collider experiment [HMK06; Kuc07]. Recollision processes are well known from atomic physics, where they are routinely employed in laboratories, e.g., for high-harmonic generation (HHG). Semiclassically, they can be described using a three-step model: Firstly, the atom is ionized by the laser field, subsequently the laser accelerates the electron and finally the electron recollides with the parent ion [Cor93; Koh+12; Kuc87]. From a pictorial point of view one could expect that in the realm of quantum field theory recollisions of photoproduced electron-positron pairs are described by loop diagram like the polarization operator. However, high-energy recollision contributions to the polarization operator, which permit the efficient absorption of many laser photons, remained unnoticed until we identified them in Ref. [5] (see Chap. 4). So far, only the quasistatic approximation (i.e. the limit $\xi \to \infty$) was considered in the regime $\xi \gg 1$. In this limit, the creation and the annihilation vertex of the electron-positron loop are located very close to each other and the whole process happens effectively inside a constant-crossed

field. Correspondingly, only a few laser photons can be absorbed by the electron-positron loop (see also [Di+13] for a more general argument). The detailed analysis presented in Chap. 4 reveals that the absence of recollision contributions in the limit $\xi \to \infty$ can be attributed to the wave-packet spreading of the electron-positron pair inside the laser field, which suppresses recollision processes with respect to the immediate annihilation of the electron-positron pair within the formation region of pair creation. Nonetheless, they are responsible for a large plateau-region in the polarization operator spectrum, which renders the absorption of $\sim \xi^3$ laser photons feasible. Our calculation represents the first full ab initio quantum calculation for recollision processes of electron-positron pairs created from vacuum. Furthermore, we firmly established the validity of the above mentioned semiclassical three-step model (pair creation – acceleration – recollision) by showing that it predicts the same scaling laws for the width and the height of the plateau-region in the spectrum as the full quantum calculation. Even if the center-of-mass energy of the resulting electron-positron "vacuum collider" are smaller than those routinely obtained at existing large accelerator facilities, the electron and the positron are entangled during their propagation and the process is intrinsically coherent. In comparison with vacuum fluctuations [which happen on the Compton scale $\sim \hbar/(mc)$] the laser enlarges the extend of the electron-positron loop by several orders of magnitude (laser-induced recollision processes occur on the scale set by the laser wavelength $\sim c/\omega$). Therefore, recollision processes constitute a novel test for the Standard Model and the predictions of loop Feynman diagrams on a scale which is unexplored so far.

Recollision processes represent a very incisive example for properties of the quantum vacuum which change profoundly in the presence of external background fields. Another, well known effect is birefringence, normally derived using an effective action approach [Aff88; BB67; BB70; DG00; Din+14b]. Noteworthy, it is self-consistently contained in our derivation of the exact photon wave function (see Chap. 3 and Ref. [3]). While birefringence is well explored for photons, the analogous phenomenon for electrons has not attracted much attention yet. In Refs. [1] and [2] (see Chap. 5) we showed for the first time that the spin-dependence of the electron dispersion relation could be measured using strong laser fields. As the orientation of the magnetic field oscillates, also the sign of the spin-dependent contribution to the quasi-energy continuously changes its sign. Therefore, the importance of the electron spin orientation averages out for long laser pulses, which probably explains why the effect has not been investigated previously. However, due to the nonlinear dependence of the electron anomalous magnetic moment on the effective laser intensity, a finite spin rotation is obtained for ultra-short laser pulses with an asymmetric pulse profile. Correspondingly, the spin degree of freedom exhibits nontrivial dynamics due to quantum fluctuations which are not predicted by the Dirac equation. The effect is closely related to the Lamb shift in atoms [LR47] and provides an alternative probe of the quantum vacuum.

Finally, we consider also neutrino interactions inside strong laser fields in Chap. 6 (see also Ref. [7]). Even though neutrinos are neutral particles and interact only

via the exchange of weak gauge bosons, charged leptons and quarks mediate a coupling to the photon field beyond tree level. Therefore, loop diagrams represent the leading-order contribution to processes like photon emission or trident pair creation by neutrinos. In addition to the polarization operator (see Chap. 3 and Ref. [3]) also the axial-vector–vector current-coupling pseudo tensor appears in this context. Here, we present the first calculation of the leading-order contribution to the current-coupling tensor inside an arbitrary plane-wave laser field. As it represents the simplest Feynman diagram in an external field which exhibits the Adler-Bell-Jackiw (ABJ) anomaly [Adl69; BJ69], it is also interesting from a fundamental point of view. By employing a suitable regularization procedure, we explicitly calculate the anomalous contribution to the Ward-Takahashi identity and show that no nonperturbative contributions arise inside a plane-wave field at one loop. Despite the fact that the probabilities for nonlinear neutrino-photon interactions are small, the electromagnetic background field enhances them by several orders of magnitude in comparison with the vacuum case [GMV93; GMV94a; GMV96]. In the future, laser-neutrino experiments could provide useful insights concerning electromagnetic catalyzing mechanisms, which presumably play an important role in astrophysical environments with strong magnetic fields [GMV92; IR97].

1

QED with strong plane-wave background fields

The basic concepts of quantum field theory have been discussed in many textbooks (see, e.g., the Refs. [GR96; IZ05; LL82; Mag05; PS95; Sre07; Wei95; Wei96]). Therefore, the main intention of this chapter is to summarize the most important results and to introduce our notation. We start with the quantization of the photon field, following Gupta [Gup50] and Bleuler [Ble50] (see Sec. 1.1). Subsequently, coherent states are introduced [Gla63], as they are a good theoretical description of strong laser pulses (see Sec. 1.2). From a mathematical point of view, the presence of the laser field leads to a vacuum expectation value (VEV) for the photon field operator. If the laser field is strong, the coherent part of the photon field must be included exactly in all calculations and only the quantum fluctuations around the classical expectation value can be treated perturbatively[1].

In this thesis, the coherent part of the photon field is always described by a plane wave (see Sec. 1.3). As a plane-wave field depends nontrivially only on the phase $\phi = kx$ (k^μ denotes the laser four-momentum), the calculations become particularly transparent in light-cone coordinates (see Sec. 1.4). The presence of a plane-wave background does not affect the stability of the vacuum. Therefore, the quantization of the Dirac field is not substantially altered in comparison with the vacuum case (see, e.g., the Refs. [DG00; FGS91; Mit75; Rit85] and the reviews [BR13; Di+12; EKK09; MS06; MTB06]). Furthermore, the Dirac equation can be solved analytically in closed form for a plane-wave background field and a dressed-state expansion of the fermionic field operator becomes feasible (see Sec. 1.5). Therefore, the Feynman rules for QED inside strong plane-wave background fields differ only by the employed wave functions from those in vacuum. In momentum space, this leads to a modification of the vertex. The so-called dressed vertex is thoroughly discussed in Sec. 1.6.

1.1. Quantization of the photon field

QED is described by the following Lagrangian density [LL82; Wei95]

$$\mathcal{L}_{\mathrm{QED}} = \bar{\psi} \left(i\slashed{\partial} - m \right) \psi - \frac{1}{4} \mathcal{F}_{\mu\nu} \mathcal{F}^{\mu\nu} - e\bar{\psi}\gamma_\mu \psi \mathcal{A}^\mu, \tag{1.1}$$

where ψ and $\mathcal{A}^\mu$ are the Dirac spinor field and the photon vector field, respectively. Furthermore, $\mathcal{F}^{\mu\nu} = \partial^\mu \mathcal{A}^\nu - \partial^\nu \mathcal{A}^\mu$ denotes the electromagnetic field tensor.

---

[1]This is true for experimental parameters achievable now and in the near future. For very strong background fields, however, QED becomes strongly coupled and also the quantum fluctuations cannot be treated perturbatively anymore [Di+12; Rit85].

The free photon field is described by the Lagrangian density

$$\mathcal{L}_{\text{em}} = -\frac{1}{4}\mathcal{F}_{\mu\nu}\mathcal{F}^{\mu\nu}. \tag{1.2}$$

As $\mathcal{A}^0$ is not a dynamical field, we cannot straightforwardly employ the canonical quantization procedure (for more details see Ref. [Wei95], Chap. 8). The problem is solved by giving up gauge invariance. Working in the Lorentz gauge $\partial_\mu \mathcal{A}^\mu = 0$, we add a so-called gauge-fixing term to the Lagrangian density [GR96; IZ05; Pok00; Ryd96]

$$\mathcal{L}'_{\text{em}} = -\frac{1}{4}\mathcal{F}_{\mu\nu}\mathcal{F}^{\mu\nu} - \frac{1}{2}\zeta\left(\partial_\rho \mathcal{A}^\rho\right)^2, \tag{1.3}$$

where ζ is called gauge-fixing parameter[2]. After fixing the gauge, the photon field can be quantized like four ordinary scalar fields. Finally, the field operator is given by

$$\hat{\mathcal{A}}^\mu(x) = \hat{\mathcal{A}}^\mu_+(x) + \hat{\mathcal{A}}^{\dagger\mu}_+(x), \quad \hat{\mathcal{A}}^\mu_+(x) = \sum_{\sigma=1,2}\int\frac{d^3q}{(2\pi)^3}\frac{1}{\sqrt{2\omega_{\boldsymbol{q}}}}\,\hat{c}_{\boldsymbol{q},\sigma}e^{-iqx}\epsilon^\mu_{\boldsymbol{q},\sigma}, \tag{1.4}$$

where $\omega_{\boldsymbol{q}} = \sqrt{\boldsymbol{q}^2}$ and $\epsilon^\mu_{\boldsymbol{q},\sigma}$ are orthogonal polarization four-vectors

$$(\epsilon^*_{\boldsymbol{q},\sigma})^\mu(\epsilon_{\boldsymbol{q},\tau})_\mu = -\delta_{\sigma\tau} \tag{1.5}$$

[for simplicity we consider here only the two physical degrees of freedom $(\sigma,\tau = 1,2)$, see, e.g., Refs. [Ble50; Gup50; Wei95] for further details].

In Eq. (1.4) the same normalization is used as, e.g., in Refs. [Mag05; PS95] (note that it differs from Ref. [LL82]). Correspondingly, the photon creation $\hat{c}^\dagger_{\boldsymbol{q},\sigma}$ and annihilation operators $\hat{c}_{\boldsymbol{q},\sigma}$ obey the canonical commutation relations

$$[\hat{c}_{\boldsymbol{p},\sigma}, \hat{c}^\dagger_{\boldsymbol{q},\tau}] = (2\pi)^3\delta^3(\boldsymbol{p} - \boldsymbol{q})\delta_{\sigma\tau}. \tag{1.6}$$

1.2. Coherent states of the photon field

In the presence of a strong laser field the photon field operator $\hat{\mathcal{A}}^\mu(x)$ obtains a vacuum expectation value (VEV), i.e. it is shifted $\hat{\mathcal{A}}^\mu(x) \to \hat{\mathcal{A}}^\mu_{\text{rad}}(x) + \mathcal{A}^\mu_{\text{ext}}(x)$ by the classical background field $\mathcal{A}^\mu_{\text{ext}}(x) = A^\mu(x)$. While $A^\mu(x)$ describes the coherent part of the laser field (by assumption, it is not affected by the quantum processes happening inside the field), $\hat{\mathcal{A}}^\mu_{\text{rad}}(x)$ represents the quantum fluctuations around the VEV. In the following, we will justify this approach following Refs. [FGS91; Gla63; HHI09].

A strong laser field represents a very good experimental realization of a coherent state $|A\rangle$ of the photon field. Using the same notation as in the previous section,

---

[2]Sometimes the inverse of ζ is used. We have to ensure that all physical observable results (e.g., the *S*-Matrix) are independent of ζ. If this is established on general grounds, particular calculations often simplify for certain values of ζ. By "abuse of language" we call $\zeta = 1$ the t'Hooft-Feynman gauge and $\zeta \to \infty$ the Landau gauge. The gauge-fixing parameter can be interpreted as a Lagrange-multiplier for the Lorentz-gauge constraint $\partial_\mu \mathcal{A}^\mu = 0$, see [GR96].

it can be written as [Gla63]

$$|A\rangle = \hat{D} |0\rangle, \tag{1.7}$$

where $|0\rangle$ is the vacuum state of the photon Fock space ($\hat{c}_{\boldsymbol{q},\sigma} |0\rangle = 0$ for all $\boldsymbol{q}$ and σ, and $\langle 0|0\rangle = 1$) and $\hat{D}$ is a unitary displacement operator. If the classical four-potential $A^\mu(x)$ associated with the coherent state is given by [compare with Eq. (1.4)]

$$A^\mu(x) = A_+^\mu(x) + A_+^{*\mu}(x), \tag{1.8a}$$

with

$$A_+^\mu(x) = \sum_{\sigma=1,2} \int \frac{d^3q}{(2\pi)^3} \frac{1}{\sqrt{2\omega_{\boldsymbol{q}}}} C_{\boldsymbol{q},\sigma} e^{-iqx} \epsilon_{\boldsymbol{q},\sigma}^\mu, \tag{1.8b}$$

the displacement operator $\hat{D}$ has the form

$$\hat{D} = \exp\Big[\sum_{\sigma=1,2} \int \frac{d^3q}{(2\pi)^3} \Big(C_{\boldsymbol{q},\sigma} \hat{c}_{\boldsymbol{q},\sigma}^\dagger - C_{\boldsymbol{q},\sigma}^* \hat{c}_{\boldsymbol{q},\sigma} \Big) \Big] \tag{1.9}$$

and the properties

$$\hat{D}^{-1} \hat{c}_{\boldsymbol{q},\sigma} \hat{D} = \hat{c}_{\boldsymbol{q},\sigma} + C_{\boldsymbol{q},\sigma}, \quad \hat{D}^{-1} \hat{c}_{\boldsymbol{q},\sigma}^\dagger \hat{D} = \hat{c}_{\boldsymbol{q},\sigma}^\dagger + C_{\boldsymbol{q},\sigma}^*. \tag{1.10}$$

From Eq. (1.10) we obtain

$$\hat{\mathcal{A}}_+^\mu(x) |A\rangle = A_+^\mu(x) |A\rangle. \tag{1.11}$$

Due to the relation

$$\langle A|\hat{\mathcal{A}}^\mu(x)|A\rangle = A^\mu(x), \tag{1.12}$$

a coherent state can be considered as the most "classical" state of the photon field.

If the coherent part of the photon field is not substantially changed during the interaction, the same coherent state appears on both sides of the S-matrix element(s) of an arbitrary QED process,

$$\langle A| \cdots |A\rangle = \langle 0|\hat{D}^{-1} \cdots \hat{D}|0\rangle. \tag{1.13}$$

Physically, this amounts to the assumption that the laser field is not significantly depleted or enhanced during the interaction. To justify this approximation, we note that typical available optical petawatt lasers, which are suitable for the investigation of QED processes in a strong laser field, have an energy of the order of 100 J [Di+12], i.e., a total number of $\sim 10^{20}$ photons. At an intensity of $\sim 10^{22}\,\mathrm{W/cm^2}$ (which is, in principle, attainable with a petawatt laser), $\sim \xi^3 \sim 10^6$ photons are absorbed from the laser by each electron (positron) [Di+12]. By assuming that $\sim 10^9$ electrons (positrons) interact with the laser, we obtain that $\sim 10^{15}$ photons are expected to be absorbed from the laser field, which remains then practically

unaffected. Therefore, the coherent part of the photon field can be treated as a given, classical background field which does not change during the interaction (see also Refs. [Ber69; BV81; ER66; FE64; Fil85]).

By applying this approximation, we can include the coherent part of the photon field nonperturbatively if we adopt the transformation in Eq. (1.10). In particular, we obtain [see Eqs. (1.4) and (1.8)]

$$\hat{D}^{-1}\hat{\mathcal{A}}^\mu(x)\hat{D} = \hat{\mathcal{A}}^\mu(x) + A^\mu(x). \tag{1.14}$$

Thus, instead of calculating S-matrix elements between coherent states, we can apply the shift $\hat{\mathcal{A}}^\mu(x) \rightarrow \hat{\mathcal{A}}^\mu_{\text{rad}}(x) + A^\mu(x)$ and consider S-matrix elements between vacuum states as usual [FGS91; HHI09].

To estimate the laser intensity at which we can start to treat the laser as a classical field, we follow Ref. [LL82], Sec. 5. In natural units, the energy density of a laser field with intensity I and central angular frequency ω is of the order of I, and the density of modes is of the order of ω^3. Correspondingly, each mode contains N_γ photons, where N_γ is of the order of I/ω^4. If $N_\gamma \gg 1$, due to the correspondence principle, it is possible to describe the laser modes by a classical field. Thus, we obtain the following condition for the laser intensity

$$I \gg \omega^4 \approx 6 \times 10^5 \, \text{W/cm}^2 \times \left(\frac{\omega}{1 \, \text{eV}}\right)^4, \tag{1.15}$$

which is well fulfilled at the relativistic intensities ($I \gtrsim 10^{18} \, \text{W/cm}^2$) in the optical regime ($\omega \sim 1 \, \text{eV}$) we are interested in here.

1.3. Classical plane-wave fields

In this thesis only plane-wave external fields are considered, i.e., we require that the field tensor $F^{\mu\nu}(x)$ of the classical background field depends only on the plane-wave phase $\phi = kx$, where k^μ ($k^2 = 0$) is the characteristic four-momentum of the laser photons (see Sec. 1.3.4). In this case the Dirac equation can be solved analytically (see Sec. 1.5.1) and thus it is feasible to construct a Fock space with dressed states and perform nonperturbative calculations with respect to the background field in the Furry picture [Fur51].

1.3.1. Field tensor

In the absence of charges and currents, the field tensor $F^{\mu\nu}(x)$ of the background field must obey the homogeneous Maxwell equations [LL87]:

$$\partial_\mu F^{\mu\nu}(x) = k_\mu F'^{\mu\nu}(x) = 0, \quad \partial^\mu F^*_{\mu\nu}(x) = k^\mu F'^*_{\mu\nu}(x) = 0. \tag{1.16}$$

The most general (antisymmetric) field tensor obeying Eq. (1.16) is given by the following expression [Sch51]

$$F^{\mu\nu}(kx) = f_1^{\mu\nu}\psi_1'(kx) + f_2^{\mu\nu}\psi_2'(kx) = \sum_{i=1,2} f_i^{\mu\nu}\psi_i'(kx), \tag{1.17}$$

where

$$f_i^{\mu\nu} = k^\mu a_i^\nu - k^\nu a_i^\mu, \quad f_{i\,\rho}^\mu f_j^{\rho\nu} = -\delta_{ij} a_i^2 \, k^\mu k^\nu, \quad k_\mu f_i^{\mu\nu} = 0 \qquad (1.18)$$

and $ka_i = 0$, $a_1 a_2 = 0$ (see also Sec. 1.4). The scalar functions $\psi_i(kx)$ are arbitrary, restricted only by the physical requirement that the external field is of finite extent and has no dc component[3] [i.e., $\psi_i(\pm\infty) = \psi'_i(\pm\infty) = 0$, with $\psi_i(kx)$, $\psi'_i(kx)$ vanishing fast enough at infinity]. Furthermore, we adopt (without restriction) the normalization condition $|\psi_i(kx)|, |\psi'_i(kx)| \lesssim 1$. This implies that the strength of the field along the two polarization directions is characterized by the two four-vectors a_i^μ (for more details see Sec. 1.3.2).

In the Lorentz gauge ($\partial_\mu A^\mu = 0$) the four-potential corresponding to the field tensor in Eq. (1.17) can be chosen as

$$A^\mu(kx) = a_1^\mu \psi_1(kx) + a_2^\mu \psi_2(kx), \quad F^{\mu\nu}(kx) = \partial^\mu A^\nu(kx) - \partial^\nu A^\mu(kx). \qquad (1.19)$$

1.3.2. Classical intensity parameters

Due to the normalization conditions employed for the shape functions $\psi_i(\phi)$ [see Eq. (1.17)], the laser field strength is characterized by the so-called classical intensity parameters ξ_i, which are gauge and Lorentz invariant [see Eq. (1.21)] [HI09]

$$\xi_i = \frac{|e|}{m} \sqrt{-a_i^2}, \quad \xi = \sqrt{\xi_1^2 + \xi_2^2}, \quad \hat{\xi}_i = \xi_i/\xi. \qquad (1.20)$$

As pointed out in the introduction, the plane-wave background field must be taken into account exactly in the calculations if $\xi \gtrsim 1$ [Di+12]. Modern laser facilities can reach this ultra-relativistic regime, e.g., in Ref. [Yan+08] $\xi \sim 100$ was obtained.

1.3.3. Quantum-nonlinearity parameters

Using the tensors $f_i^{\mu\nu}$ and an arbitrary four-momentum vector q^μ (most commonly the four-momentum of an incoming particle), we define the following quantum-nonlinearity parameters [Di+12]:

$$\chi_i = \frac{|e|\sqrt{q f_i^2 q}}{m^3} = \eta\, \xi_i, \quad \eta = \frac{\sqrt{(kq)^2}}{m^2}. \qquad (1.21)$$

Since both η and χ_i are manifestly gauge and Lorentz invariant, this also holds for the parameters ξ_i. Furthermore, we define

$$\chi = \sqrt{\chi_1^2 + \chi_2^2}, \quad \hat{\chi}_i = \chi_i/\chi. \qquad (1.22)$$

---

[3]Note that the dc component vanishes if $\psi_i(\pm\infty) = 0$, as

$$\int\limits_{-\infty}^{+\infty} d\phi\, \psi'_i(\phi) = \psi_i(\infty) - \psi_i(-\infty) = 0.$$
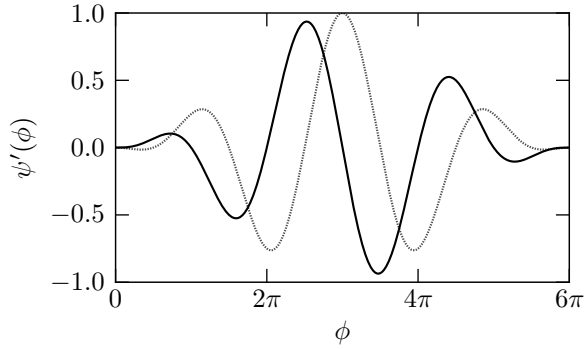
Fig. 2: Laser pulse with $\sin^2$-envelope [see Eq. (1.23)] for different carrier-envelope phases [$\phi_0 = 0$ (solid line) and $\phi_0 = -\pi/2$ (dotted line), $N = 3$ cycles]. Depending on the CEP we obtain either one strong peak or two peaks with slightly less strength.
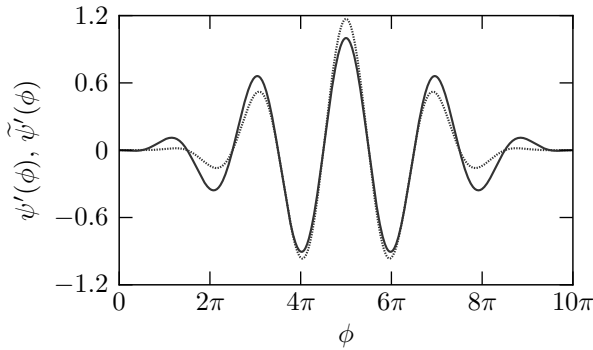
Fig. 3: In the numerical calculations we considered either a laser pulse with $\sin^2$ (solid line) or with $\sin^4$ envelope (dotted line), plotted here for $N = 5$ cycles and a CEP of $\phi_0 = -\pi/2$ [see Eq. (1.23) and Eq. (1.24)]. As the $\sin^4$ pulse falls off faster at the edges, it must have a higher peak strength in comparison with a $\sin^2$ envelope in order to describe a pulse with the same total energy.

1.3.4. Laser pulse shape and photon four-momentum

In the numerical calculations we normally employ a linearly polarized laser pulse $[\psi_1(\phi) = \psi(\phi), \psi_2(\phi) = 0]$ with a $\sin^2$-envelope given by [see Eq. (1.17)]

$$\psi'(\phi) = \sin^2[\phi/(2N)] \sin(\phi + \phi_0) \tag{1.23}$$

for $\phi = kx \in [0, 2\pi N]$ and zero otherwise. Here N characterizes the number of cycles in the pulse and ϕ_0 its carrier-envelope phase (CEP, see Fig. 2). To estimate the effect of the pulse shape we have sometimes repeated the calculations also for a $\sin^4$-envelope

$$\psi'(\phi) \longrightarrow \widetilde{\psi}'(\phi) = \mathcal{R} \sin^4[\phi/(2N)] \sin(\phi + \phi_0). \tag{1.24}$$

Here, the scaling parameter $\mathcal{R}$ is chosen such that

$$\int\limits_0^{2\pi N} d\phi \, [\psi'(\phi)]^2 = \int\limits_0^{2\pi N} d\phi \, [\widetilde{\psi}'(\phi)]^2, \tag{1.25}$$

as in most experiments the total energy of the laser pulse is fixed and only its shape may change (see Fig. 3). As long as N is an integer and $N \geq 2$ for ψ' and $N \geq 3$ for $\widetilde{\psi}'$, the above shape functions describe a laser pulse without dc

Fig. 4: If the laser pulse has a finite extend, its spectrum must have a finite width and the four-momentum of the laser photons is not well defined. Here we plotted the normalized spectrum [see Eq. (1.28)] for the $\sin^2$-pulse given in Eq. (1.23) with a CEP of $\phi_0 = 0$ for $N = 5$ (solid line), $N = 10$ (dashed line) and $N = 20$ (dotted line) cycles. The larger the pulse, the more monochromatic it becomes.
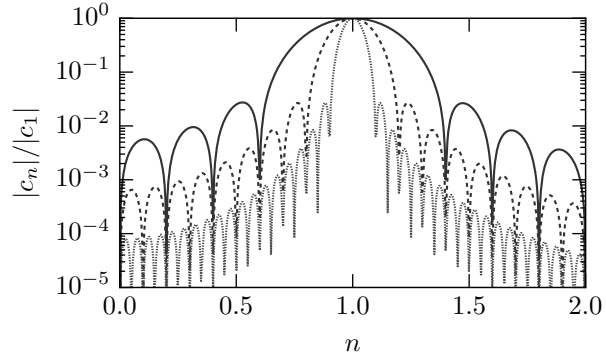
component, i.e.

$$\int\limits_0^{2\pi N} d\phi\, \psi'(\phi) = \int\limits_0^{2\pi N} d\phi\, \widetilde{\psi}'(\phi) = 0 \tag{1.26}$$

and the energy in the pulse is independent of the CEP.

A plane-wave laser pulse with a finite duration must contain photons with different four-momenta nk^μ (n is not restricted to integers). This becomes obvious from the following Fourier transformation

$$\psi'(\phi) = \int\limits_{-\infty}^{+\infty} dn\, e^{in\phi} c_n = \int\limits_0^{\infty} dn \left(e^{in\phi} c_n + e^{-in\phi} c_n^* \right), \tag{1.27}$$

where the complex coefficients $c_{-n} = c_n^*$ are given by

$$c_n = \int\limits_{-\infty}^{+\infty} \frac{d\phi}{2\pi}\, e^{-in\phi} \psi'(\phi) = \int\limits_0^{2\pi N} \frac{d\phi}{2\pi}\, e^{-in\phi} \psi'(\phi). \tag{1.28}$$

In Fig. 4 the absolute value of the coefficients c_n normalized to $c_{n=1}$ has been plotted for different pulse lengthes. Despite this ambiguity and the fact that we treat the laser field as a classical field, we will call $k^\mu = \omega(1, \boldsymbol{n})$ the (characteristic) four-momentum of the laser photons and ω their (characteristic) angular frequency.

1.3.5. Integrated field tensor

We will use the following symbol for the integrated field tensor

$$\mathfrak{F}^{\mu\nu}(\phi, \phi_0) = \int\limits_{\phi_0}^{\phi} d\phi'\, F^{\mu\nu}(\phi'), \quad \frac{\partial \mathfrak{F}^{\mu\nu}(\phi, \phi_0)}{\partial \phi} = F^{\mu\nu}(\phi). \tag{1.29a}$$

Furthermore, we define

$$\mathfrak{F}^{\mu\nu}(\phi) = \mathfrak{F}^{\mu\nu}(\phi, -\infty) = \int\limits_{-\infty}^{\phi} d\phi' \, F^{\mu\nu}(\phi') \qquad (1.29b)$$

and introduce the compact notation $\mathfrak{F}_x^{\mu\nu} = \mathfrak{F}^{\mu\nu}(kx)$. Using Eq. (1.17), we conclude that in the Lorentz gauge

$$\mathfrak{F}^{\mu\nu}(\phi, \phi_0) = k^\mu[A^\nu(\phi) - A^\nu(\phi_0)] - k^\nu[A^\mu(\phi) - A^\mu(\phi_0)]$$
$$= \sum_{i=1,2} f_i^{\mu\nu}[\psi_i(\phi) - \psi_i(\phi_0)], \quad (1.30a)$$

$$\mathfrak{F}^{\mu\nu}(\phi) = k^\mu A^\nu(\phi) - k^\nu A^\mu(\phi) = \sum_{i=1,2} f_i^{\mu\nu}\psi_i(\phi). \qquad (1.30b)$$

1.4. Light-cone coordinates

As a plane-wave laser field depends nontrivially only on the phase $\phi = kx$ (see Sec. 1.3), it naturally introduces the four-vector k^μ which characterizes the four-momentum of the laser photons (see Sec. 1.3.4). As $k^2 = 0$, any basis including k^μ will be a light-cone basis which defines so-called light-cone coordinates [Dir49; Mit75; NR71]. Calculations involving plane-wave background fields become particular transparent if light-cone coordinates are used.

1.4.1. Light-cone basis

We call the set of four four-vectors k^μ, $\bar{k}^\mu$, e_i^μ ($i \in 1, 2$) a light-cone basis if they obey

$$k^2 = \bar{k}^2 = 0, \quad ke_i = \bar{k}e_i = 0, \quad k\bar{k} = 1, \quad e_ie_j = -\delta_{ij}. \qquad (1.31)$$

Using the above properties and the determinant identity for $\epsilon^{\mu\nu\rho\sigma}\epsilon^{\alpha\beta\gamma\delta}$, it is possible to show that any such light-cone basis obeys $\Omega^2 = 1$, where

$$\Omega = \epsilon_{\mu\nu\rho\sigma}k^\mu \bar{k}^\nu e_1^\rho e_2^\sigma \qquad (1.32)$$

is called the orientation of the basis. To be more specific, we can, in a reference system where the plane wave propagates along the direction $\boldsymbol{n}$, take the following four-vectors

$$k^\mu = \omega(1, \boldsymbol{n}), \quad \bar{k}^\mu = \frac{1}{2\omega}(1, -\boldsymbol{n}), \quad e_i^\mu = (0, \boldsymbol{e}_i) \sim a_i^\mu,$$
$$\boldsymbol{n}^2 = 1, \quad \boldsymbol{e}_i\boldsymbol{e}_j = \delta_{ij}, \quad \boldsymbol{n} = \boldsymbol{e}_1 \times \boldsymbol{e}_2 \qquad (1.33)$$

($\boldsymbol{e}_i$ represent the two polarization directions of the plane-wave field, and ω has the dimension of a frequency).

In light-cone coordinates the metric is given by

$$g^{\mu\nu} = k^\mu \bar{k}^\nu + \bar{k}^\mu k^\nu - e_1^\mu e_1^\nu - e_2^\mu e_2^\nu. \qquad (1.34)$$

This allows us to define the transformation to light-cone coordinates (primed indices) by

$$a^{\mu'} = \Lambda^{\mu'}{}_{\nu} a^{\nu}, \quad b_{\mu'} = b_{\nu} \Lambda^{-1\nu}{}_{\mu'}, \quad \Lambda^{-1\rho}{}_{\mu'} \Lambda^{\mu'}{}_{\sigma} = \delta^{\rho}_{\sigma}, \tag{1.35}$$

where the components denote contractions with the following four-vectors

$$\begin{aligned} \Lambda^{-}{}_{\mu} &= k_{\mu}, & \Lambda^{+}{}_{\mu} &= \bar{k}_{\mu}, & \Lambda^{\mathrm{I}}{}_{\mu} &= e_{1\mu}, & \Lambda^{\mathrm{II}}{}_{\mu} &= e_{2\mu}, \\ \Lambda^{-1\mu}{}_{-} &= \bar{k}^{\mu}, & \Lambda^{-1\mu}{}_{+} &= k^{\mu}, & \Lambda^{-1\mu}{}_{\mathrm{I}} &= -e_1^{\mu}, & \Lambda^{-1\mu}{}_{\mathrm{II}} &= -e_2^{\mu}. \end{aligned} \tag{1.36}$$

(we label light-cone components by $+,-,\mathrm{I},\mathrm{II}$). This implies that we obtain for an arbitrary four-vector v^{μ} the light-cone components

$$v^{-} = vk, \quad v^{+} = v\bar{k}, \quad v^{\mathrm{I}} = ve_1, \quad v^{\mathrm{II}} = ve_2. \tag{1.37}$$

We point out that k^{μ} has dimension of momentum and therefore $\bar{k}^{\mu}$ must have dimension of inverse momentum (e_i^{μ} are dimensionless). Hence, the dimensions of v^{+} and v^{-} differ from those of v^{μ}. The different dimensions of the light-cone components can be circumvented by defining $k^{\mu} = \omega n^{\mu}$ and using the dimensionless quantity n^{μ} in place of k^{μ}. Then, however, nv is not a Lorentz scalar (contrary to $kv = v^{-}$), and ω has to appear explicitly in many places.

In light-cone coordinates, the metric is given by

$$g_{\mu'\nu'} = g_{\rho\sigma} \Lambda^{-1\rho}{}_{\mu'} \Lambda^{-1\sigma}{}_{\nu'} = \delta^{+}_{\mu'} \delta^{-}_{\nu'} + \delta^{-}_{\mu'} \delta^{+}_{\nu'} - \delta^{\mathrm{I}}_{\mu'} \delta^{\mathrm{I}}_{\nu'} - \delta^{\mathrm{II}}_{\mu'} \delta^{\mathrm{II}}_{\nu'}, \tag{1.38}$$

which allows us to write the scalar product of two four-vectors as

$$a_{\mu} b^{\mu} = a^{+} b^{-} + a^{-} b^{+} - a^{\mathrm{I}} b^{\mathrm{I}} - a^{\mathrm{II}} b^{\mathrm{II}} \tag{1.39}$$

(we also use the short notation $a^{\perp} b^{\perp} = a^{\mathrm{I}} b^{\mathrm{I}} + a^{\mathrm{II}} b^{\mathrm{II}}$). Due to Eq. (1.32), we obtain

$$\left| \det \Lambda^{\mu'}{}_{\nu} \right| = \left| \Lambda^{+}{}_{\mu} \Lambda^{-}{}_{\nu} \Lambda^{\mathrm{I}}{}_{\rho} \Lambda^{\mathrm{II}}{}_{\sigma} \epsilon^{\mu\nu\rho\sigma} \right| = 1. \tag{1.40}$$

Thus, the four-dimensional integration measure becomes

$$\int d^4 a = \int da^{+} da^{-} da^{\perp}, \quad da^{\perp} = da^{\mathrm{I}} da^{\mathrm{II}}. \tag{1.41}$$

Furthermore, the following notation for light-cone momentum conserving delta functions is used

$$\delta^{(-,\perp)}(a) = \delta(a^{-}) \delta(a^{\mathrm{I}}) \delta(a^{\mathrm{II}}) \tag{1.42}$$

($\perp$ summarizes I and II).

1.4.2. Equivalence of different light-cone bases

As any set of four four-vectors e_i^{μ} ($i \in 1, 2$), $\bar{k}^{\mu}$ and k^{μ} obeying the relations given in Eq. (1.31) represents a light-cone basis, it is natural to ask which expressions

are invariant under a change of the underlying light-cone basis. To this end we consider two different bases $\bar{k}^\mu$, e_i^μ and $\bar{k}'^\mu$, $e_i'^\mu$ and denote the corresponding components of a four-vector v^μ by

$$
\begin{aligned}
v^+ &= \bar{k}^\mu v_\mu, \quad v^{\mathrm{I}} = e_1^\mu v_\mu, \quad v^{\mathrm{II}} = e_2^\mu v_\mu, \\
v'^+ &= \bar{k}'^\mu v_\mu, \quad v'^{\mathrm{I}} = e_1'^\mu v_\mu, \quad v'^{\mathrm{II}} = e_2'^\mu v_\mu,
\end{aligned}
\tag{1.43}
$$

$(v^- = v'^- = kv)$. The three coordinates $(-, \mathrm{I}, \mathrm{II})$ define a closed subspace and we obtain the relation

$$
\begin{pmatrix} v'^- \\ v'^{\mathrm{I}} \\ v'^{\mathrm{II}} \end{pmatrix} = \begin{pmatrix} 1 & 0 & 0 \\ e_1'\bar{k} & -e_1'e_1 & -e_1'e_2 \\ e_2'\bar{k} & -e_2'e_1 & -e_2'e_2 \end{pmatrix} \cdot \begin{pmatrix} v^- \\ v^{\mathrm{I}} \\ v^{\mathrm{II}} \end{pmatrix}.
\tag{1.44}
$$

In order to show that its determinant has magnitude one, we use the expansions

$$
\begin{aligned}
e_1'^\mu &= ae_1^\mu + be_2^\mu + \lambda k^\mu, \\
e_2'^\mu &= ce_1^\mu + de_2^\mu + \mu k^\mu.
\end{aligned}
\tag{1.45}
$$

As $e_1'^2 = e_2'^2 = -1$ and $e_1'e_2' = 0$, we obtain $a^2 + b^2 = c^2 + d^2 = 1$ and $ac + bd = 0$. Without restricting generality, we set $a = \cos\varphi$, $b = \sin\varphi$ and $d = \cos\theta$, $c = \sin\theta$. Finally, we obtain the two solutions $\theta = -\varphi$ and $\theta = -\varphi + \pi$, which correspond to $ad - bc = \pm 1$. Therefore, the measure $dv^- dv^\perp = dv'^- dv'^\perp$ and the delta function

$$
\delta^{(-,\perp)}(v) = \delta(v^-)\delta(v^{\mathrm{I}})\delta(v^{\mathrm{II}}) = \delta(v'^-)\delta(v'^{\mathrm{I}})\delta(v'^{\mathrm{II}}) = \delta^{(-,\perp)}(v')
\tag{1.46}
$$

are invariant under a change of the light-cone basis. If $v^- = v^\perp = 0$, also the component $v^+ = \bar{k}^\mu v_\mu$ is invariant.

1.4.3. Canonical light-cone basis

For any four-vector q^μ with $kq \neq 0$ we define an associated canonical light-cone basis k^μ, $\bar{k}^\mu$, Λ_1^μ and Λ_2^μ, where[4]

$$
\bar{k}^\mu = \frac{1}{kq}q^\mu - \frac{q^2}{2(kq)^2}k^\mu
\tag{1.47}
$$

and

$$
\Lambda_1^\mu = \frac{f_1^{\mu\nu}q_\nu}{kq\sqrt{-a_1^2}}, \quad \Lambda_2^\mu = \frac{f_2^{\mu\nu}q_\nu}{kq\sqrt{-a_2^2}}.
\tag{1.48}
$$

If q^μ is also light-like ($q^2 = 0$), the basis is particularly simple (this is not in general required, though).

---

[4]The notation $\bar{k}_q^\mu$ and $\Lambda_{q,i}^\mu$ would be more explicit. For simplicity, the index q is dropped.

Now, we can expand an arbitrary four-momentum vector p^μ as follows:

$$p^\mu = rq^\mu + sk^\mu + Mt_1\Lambda_1^\mu + Mt_2\Lambda_2^\mu \tag{1.49a}$$

where M represents a mass scale and

$$p^- = rkq, \quad p^+ = \frac{q^2}{2kq}r + s, \quad p^{\mathrm{I}} = -Mt_1, \quad p^{\mathrm{II}} = -Mt_2. \tag{1.49b}$$

If the four-momentum is on shell (i.e. $p^2 = M^2$), we can eliminate one of the four expansion parameters, e.g.,

$$s = \frac{M^2}{kq}\left[\frac{1}{2r}(1 + t_1^2 + t_2^2) - \frac{r}{2}\frac{q^2}{M^2}\right]. \tag{1.50}$$

1.4.4. On-shell momentum integrals in light-cone coordinates

During the calculation of matrix elements one often encounters three-dimensional on-shell momentum integrals. Since plane-wave background fields conserve three of four light-cone momenta [see Eq. (1.80)], it is often convenient to rewrite such integrals in light-cone coordinates as follows

$$\int \frac{d^3p}{(2\pi)^3}\frac{1}{2\epsilon_{\boldsymbol{p}}}f(p) = \int \frac{d^4p}{(2\pi)^3}\delta(p^2 - m^2)\theta(p^0)f(p) = \int \frac{dp^-dp^\perp}{(2\pi)^3}\frac{\theta(p^-)}{2p^-}f(p) \tag{1.51}$$

($\epsilon_{\boldsymbol{p}} = \sqrt{M^2 + \boldsymbol{p}^2}$). Here, M is the particle mass, θ is the step function and we require that $p^2 = M^2$ with $p^0 \geq 0$. This implies that $p^0 = \epsilon_{\boldsymbol{p}}$ if we integrate over $\boldsymbol{p}$ (in the first expression) and $p^+ = (p^\perp p^\perp + M^2)/(2p^-)$ if we integrate over $p^-, p^\perp$ (in the last expression). We note that $p^0 = \epsilon_{\boldsymbol{p}}$ corresponds to $p^- > 0$ and $p^0 = -\epsilon_{\boldsymbol{p}}$ to $p^- < 0$ ($p^- = 0$ is only reached in the limit $\epsilon_{\boldsymbol{p}} \to \infty$). In particular, using the expansion given in Eq. (1.49), we obtain the relation

$$\int \frac{d^3p}{(2\pi)^3}\frac{1}{2\epsilon_{\boldsymbol{p}}}f(p) = M^2\int \frac{dr\,dt_1dt_2}{(2\pi)^3\,2r}\,\theta(rkq)\,f(p). \tag{1.52}$$

1.5. Quantization with plane-wave background fields

As pointed out in the introduction, for very strong background fields the coherent part $A^\mu(x)$ of the photon field [see Eq. (1.14)] must be taken into account exactly in the calculations. For plane-wave fields this is possible by solving the interaction Dirac equation analytically (see Sec. 1.5.1) and an subsequent expansion of the fermionic field operator using the obtained Volkov states (see Sec. 1.5.2).

1.5.1. Volkov solution of the Dirac equation

For a classical plane-wave field $A^\mu = A^\mu(\phi)$ (see Sec. 1.3) the interacting Dirac equation

$$(i\slashed{\partial} - e\slashed{A} - m)\psi = 0 \tag{1.53}$$

can be solved analytically and one obtains the so-called Volkov states $\Psi_p(\phi)$ [LL82; Vol35], which we will also call dressed states. If we require that they turn into plane-waves for $\phi \to -\infty$ $[\Psi_p(x) \to \psi_p(x)]$, we obtain the representation [Mit75; Rit72a]

$$\Psi_p(x) = E_{p,x} u_p, \quad \psi_p(x) = e^{-ipx} u_p, \tag{1.54}$$

where the so-called Ritus matrices $E_{p,x} = E_p(x)$ are defined by

$$E_{p,x} = \left[1 + \frac{e\slashed{k}\slashed{A}(kx)}{2\,kp} \right] e^{iS_p(x)}, \quad \bar{E}_{p,x} = \left[1 + \frac{e\slashed{A}(kx)\slashed{k}}{2\,kp} \right] e^{-iS_p(x)} \tag{1.55}$$

(in the literature different normalization conditions are used). Note that

$$\bar{E}_{p,x} E_{p,x} = E_{p,x} \bar{E}_{p,x} = 1. \tag{1.56}$$

The constant Dirac spinors u_p and v_p for the electron and the positron, respectively, are defined by [LL82; PS95]

$$(\slashed{p} - m)u_p = 0, \quad (\slashed{p} + m)v_p = 0 \tag{1.57a}$$

and obey the normalization conditions

$$\bar{u}_p u_p = 2m, \quad \bar{v}_p v_p = -2m \tag{1.57b}$$

(the spin degree of freedom is discussed in Chap. 5).

Although the Volkov states are exact solutions of the interacting Dirac equation, their phase corresponds to the classical action [LL87]

$$S_p(x) = -px - \int\limits_{-\infty}^{kx} d\phi' \left[\frac{e\, pA(\phi')}{kp} - \frac{e^2 A^2(\phi')}{2\,kp} \right]. \tag{1.58}$$

Therefore, many aspects of the theory can be understood from the classical equations of motion (see App. A.3).

Analogously to Eq. (1.54), the dressed electron propagator is given by

$$iG(x, y) = i \int \frac{d^4 p}{(2\pi)^4} E_{p,x} \frac{\slashed{p} + m}{p^2 - m^2 + i0} \bar{E}_{p,y} \tag{1.59}$$

(see Sec. 2.2.2 for a thorough analysis).

The given representations for the Volkov states [see Eq. (1.54)] and the dressed propagator [see Eq. (1.59)] can be verified by proving that the Ritus matrices convert momentum operators into momentum variables [Rit72a]

$$[i\slashed{\partial}_x - e\slashed{A}(kx)]E_{p,x} = E_{p,x}\slashed{p}, \quad -i\partial_x^\mu \bar{E}_{p,x}\gamma_\mu - e\bar{E}_{p,x}\slashed{A}(kx) = \slashed{p}\bar{E}_{p,x} \tag{1.60}$$

(these identities hold only if the derivative acts solely on $E_{p,x}$ and $\bar{E}_{p,x}$, respectively).

Finally, we point out that the Ritus matrices form a complete set [Rit72a]

$$\int \frac{d^4 p}{(2\pi)^4} \, E_{p,x} \bar{E}_{p,x'} = \delta^4(x - x'), \quad \int d^4 x \, \bar{E}_{p',x} E_{p,x} = (2\pi)^4 \, \delta^4(p' - p) \qquad (1.61)$$

(the verification of these relations is particularly simple in light-cone coordinates, see Sec. 1.4).

1.5.2. Dressed-state expansion of the field operator

As both field invariants

$$\mathcal{F}_{\text{inv}} = -\frac{1}{4} F_{\alpha\beta} F^{\alpha\beta}, \quad \mathcal{G}_{\text{inv}} = -\frac{1}{4} F^*_{\alpha\beta} F^{\alpha\beta} \qquad (1.62)$$

vanish for a plane-wave background field, the vacuum remains stable (no spontaneous pair creation) [Di+12; Sch51]. Therefore, the quantization procedure for the fermionic fields is not altered substantially in comparison with vacuum QED.

Instead of expanding the fermionic field operator in terms of the free wave functions, we use now the Volkov states given in Eq. (1.54). This implies that the coherent part of the photon field (which is left unchanged by the interaction) is already taken into account exactly

$$\hat{\psi}(x) = \sum_{\sigma=1,2} \int \frac{d^3 p}{(2\pi)^3 \sqrt{2\epsilon_{\boldsymbol{p}}}} \left[\hat{a}_{\boldsymbol{p},\sigma} \, E_p(x) \, u_{p,\sigma} \, + \, \hat{b}^\dagger_{\boldsymbol{p},\sigma} \, E_{-p}(x) \, v_{p,\sigma} \right]. \qquad (1.63)$$

Here, $\hat{a}_{\boldsymbol{p},\sigma}$ and $\hat{b}_{\boldsymbol{p},\sigma}$ denote the annihilation operators for fermions and anit-fermions, respectively (note that we use here the same normalization for the field operators as, e.g., in [Mag05; PS95], which differs from [LL82]).

By comparing Eq. (1.63) with the vacuum expression we see that, effectively, only the free wave functions must be replaced by the Ritus matrices [see Eq. (1.54)]

$$\exp(-ipx) \longrightarrow E_p(x), \quad \exp(+ipx) \longrightarrow \bar{E}_p(x), \qquad (1.64)$$

which depend nontrivially on the plane-wave phase $\phi = kx$. As the abelian photon field has no tree-level self interactions, the Feynman rules for the photon sector remain unaffected by the background field.

1.5.3. Summary of the Feynman rules in position space

Finally, we obtain the Feynman rules summarized in Tab. 4 [DG00; FGS91; Mit75; Rit85]. In Feynman gauge the photon propagator $-iD_{\mu\nu}(x - y)$ is given by

$$-iD_{\mu\nu}(x - y) = -i \int \frac{d^4 k}{(2\pi)^4} \, e^{-ik(x-y)} \frac{4\pi}{k^2 + i0} \, g_{\mu\nu} \qquad (1.65)$$

Feynman rules in position space

Vertex	$-ie\gamma^\mu$	
Photon propagator	$-iD_{\mu\nu}(x-y)$	x,μ ~~~~~ y,ν
Dirac propagator	$iG(x,y)$	x ═══ y
Incoming fermion	$E_p(x)\,u_{p,\sigma}$	x ═══ p
Outgoing fermion	$\bar{u}_{p,\sigma}\,\bar{E}_p(x)$	p ═══ x
Incoming anti-fermion	$\bar{v}_{p,\sigma}\,\bar{E}_{-p}(x)$	x ═══ $\leftarrow p$
Outgoing anti-fermion	$E_{-p}(x)\,v_{p,\sigma}$	$\leftarrow p$ ═══ x
Incoming photon	$\epsilon^\mu\,e^{-ikx}$	x ~~~ $\leftarrow k$
Outgoing photon	$\epsilon^{*\mu}\,e^{ikx}$	~~~ x $\leftarrow k$

Tab. 4: Feynman rules for the calculation of QED *S*-matrix elements in the presence of a plane-wave background field. We use a double line for (anti-) fermions to stress the fact that the dressed states and propagators include the exact interaction with the classical background field. In the limit $A^\mu(x) \to 0$ the Feynman rules for vacuum QED are obtained.

and the Volkov propagator $iG(x,y)$ reads [see Eq. (1.59)]

$$iG(x,y) = i \int \frac{d^4p}{(2\pi)^4}\, E_p(x)\, \frac{\slashed{p} + m}{p^2 - m^2 + i0}\, \bar{E}_p(y). \tag{1.66}$$

Note that we have to integrate over all possible space-time positions of the vertices. Furthermore, a closed fermionic loop requires a trace in spinor space and an additional minus sign.

1.6. Dressed vertex

To obtain Feynman rules in momentum space, the Ritus E_p matrices [see Eq. (1.55)] are combined with the vertex, analogously as in vacuum QED [Mit75; Rit72a]. Correspondingly, we define the dressed vertex by (see Fig. 5)

$$\Gamma^\rho(p',q,p) = -ie \int d^4x\, e^{-iqx}\, \bar{E}_{p',x}\gamma^\rho E_{p,x}. \tag{1.67}$$

Working in momentum space, the only difference between vacuum QED and strong-field QED is a more complicated interaction vertex [i.e., the free vertex $-ie\gamma^\rho$ is re-
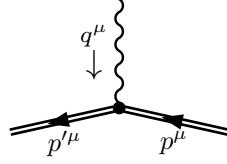
Fig. 5: In the presence of an external background field the dressed vertex must be used in momentum space [see Eq. (1.67)]. We adopt the following sign convention: the electron with four-momentum p^μ and the photon with four-momentum q^μ are incoming and the electron with four-momentum p'^μ is outgoing.

placed by the dressed vertex defined in Eq. (1.67)].

1.6.1. Gauge-invariant representation

After some Gamma-matrix algebra (see App. D), we obtain the following simplified expression for the dressed vertex

$$\Gamma^\rho(p', q, p) = -ie \int d^4x \left[\gamma_\mu G^{\mu\rho}(kp', kp; kx) \right.$$
$$\left. + i\gamma_\mu \gamma^5 G_5^{\mu\rho}(kp', kp; kx) \right] e^{iS_\Gamma(p',q,p;x)}, \quad (1.68)$$

where the phase and the coupling tensors are given by

$$S_\Gamma(p', q, p; x) = -S_{p'}(x) - qx + S_p(x) = (p' - q - p)x$$
$$+ \int\limits_{-\infty}^{kx} d\phi' \left[\frac{ep_\mu p'_\nu \mathfrak{F}^{\mu\nu}(\phi')}{(kp)(kp')} + \frac{e^2(kp - kp')}{2(kp)^2(kp')^2} p_\mu p'_\nu \mathfrak{F}^{2\mu\nu}(\phi') \right], \quad (1.69)$$

$$G^{\mu\rho}(kp', kp; kx) = g^{\mu\rho} + G_1(kp', kp)\, \mathfrak{F}_x^{\mu\rho} + G_2(kp', kp)\, \mathfrak{F}_x^{2\mu\rho},$$
$$G_5^{\mu\rho}(kp', kp; kx) = G_3(kp', kp)\, \mathfrak{F}_x^{*\mu\rho}, \quad (1.70)$$

$$G_1(kp', kp) = -e\,\frac{kp + kp'}{2kp\, kp'}, \quad G_2(kp', kp) = \frac{e^2}{2kp\, kp'},$$
$$G_3(kp', kp) = -e\,\frac{kp - kp'}{2kp\, kp'} \quad (1.71)$$

(note that G_1 and G_2 are even in the permutation $kp \leftrightarrow kp'$ while G_3 is odd). As it depends on the external field only through the tensor $\mathfrak{F}^{\mu\nu}$, the expression given in Eq. (1.68) is manifestly gauge invariant (with respect to the external field) [Mit75].

37

1.6.2. Algebraic properties

As $q^\mu = p'^\mu - p^\mu$, we obtain for the free vertex the following contraction relation

$$\slashed{q} = (\slashed{p}' - m)\,\mathbf{1} - \mathbf{1}\,(\slashed{p} - m). \tag{1.72}$$

The dressed vertex obeys a similar algebraic identity [Mit75]

$$q_\rho \Gamma^\rho(p',q,p) = (\slashed{p}' - m)I(p',q,p) - I(p',q,p)(\slashed{p} - m), \tag{1.73}$$

where

$$I(p',q,p) = -ie \int d^4x\, e^{-iqx}\, \bar{E}_{p',x} E_{p,x}. \tag{1.74}$$

Furthermore, we note the following representation

$$I(p',q,p) = -ie \int d^4x \left[\mathbf{1} + \frac{G_3}{2}\sigma^{\alpha\beta}\mathfrak{F}_{\alpha\beta}(kx) \right] e^{iS_\Gamma}. \tag{1.75}$$

The identity given in Eq. (1.73) plays a central role in the proof of the Ward-Takahashi identity. To verify Eq. (1.73), we use Eq. (1.60) and [Mit75]

$$\int d^4x\, i\partial_\mu [\bar{E}_{p',x}\gamma^\mu e^{-iqx} E_{p,x}] = 0. \tag{1.76}$$

Typically, $(\slashed{p}' - m)$ and $(\slashed{p} - m)$ in Eq. (1.73) cancel an adjacent propagator, and the associated momentum-integral can be taken using the relations

$$\begin{aligned}
\int \frac{d^4p''}{(2\pi)^4} I(p,q',p'')\Gamma^\mu(p'',q,p') &= -ie\Gamma^\mu(p,q+q',p'), \\
\int \frac{d^4p''}{(2\pi)^4} \Gamma^\mu(p,q,p'')I(p'',q',p') &= -ie\Gamma^\mu(p,q+q',p'),
\end{aligned} \tag{1.77}$$

which follow from Eq. (1.61). Using Eqs. (1.73) and (1.77), we can simplify diagrams which contain dressed vertices contracted with the corresponding photon four-momenta.

Finally, we note the relation [see Eq. (D.2)]

$$\overline{\Gamma}^\rho(p',q,p) = -\Gamma^\rho(p,-q,p'). \tag{1.78}$$

1.6.3. Momentum conservation

In light-cone coordinates (see Sec. 1.4) the dressed vertex defined in Eq. (1.68) depends nontrivially only on $\phi = kx = x^-$. Therefore, we can take the integrals in dx^+ and $dx^\perp$ and obtain momentum-conserving delta functions in three of four light-cone components,

$$\Gamma^\rho(p',q,p) = (2\pi)^3 \delta^{(-,\perp)}(p'-q-p)\,\mathcal{G}^\rho(p',q,p). \tag{1.79}$$

Here, $\mathcal{G}^\mu(p',q,p)$ denotes the nonsingular part of the dressed vertex [the notation used for the delta function is introduced in Eq. (1.42)]. Note that its definition is in-

dependent of the light-cone basis chosen (see Sec. 1.4.2).

In contrary to vacuum QED, four-momentum is only conserved up to a multiple of the plane-wave four-momentum k^μ at the dressed vertex. We point out that we always implicitly assume the presence of this momentum-conserving delta function if we discuss the quantity $\mathcal{G}^\rho(p', q, p)$ (or functions related to it), i.e. we assume that it is only evaluated for four-momenta which obey $p'^\mu - q^\mu - p^\mu = 0$ for the light-cone components $(-, \perp)$.

After the integrals in dx^+ and $dx^\perp$ are taken, the first part of the phase reduces to [see Eq. (1.69)]

$$(p' - q - p)^+ x^- = n\, kx, \tag{1.80a}$$

where we introduced the parameter n by

$$p'^\mu = p^\mu + q^\mu + nk^\mu. \tag{1.80b}$$

Thus, the integral in $kx = x^-$ determines the amount of laser four-momentum nk^μ which is absorbed from the background field. For simplicity, we will call n the number of absorbed laser photons (note that n is not restricted to integers, see Sec. 1.3.4).

1.6.4. Canonical parametrization

To simplify the phase $S_\Gamma(p', q, p; x)$ given in Eq. (1.69) further, we use the incoming photon momentum q^μ to define the canonical light-cone basis associated with this vertex (see Sec. 1.4.3) and introduce the two four-vectors [see Eq. (1.48)]

$$\Lambda_i^\mu = \frac{f_i^{\mu\nu} q_\nu}{kq \sqrt{-a_i^2}} \tag{1.81}$$

($i = 1, 2$). After parametrizing the integrated field tensor as in Eq. (1.30), we obtain the following expression for the phase [see Eq. (1.69); the classical intensity parameters ξ_i are defined in Eq. (1.20)]

$$S_\Gamma(p', q, p; x) = (p' - q - p)x + \frac{1}{2}\frac{m^2}{kq} w \sum_{j=1,2} \int_{-\infty}^{kx} d\phi' \left[\xi_j^2 \psi_j^2(\phi') - 2t_j \xi_j \psi_j(\phi') \right], \tag{1.82}$$

where we introduced the parameters [see Eq. (1.80)]

$$t_i = -\frac{p_\mu \Lambda_i^\mu}{m} = -\frac{p'_\mu \Lambda_i^\mu}{m} = -\frac{(p + p')_\mu \Lambda_i^\mu}{2m} = \frac{e\, p^\mu p'^\nu f_{i\mu\nu}}{kq\, m^2\, \xi_i} \tag{1.83}$$

to characterize the transverse momenta and

$$w = -\frac{(kq)^2}{(kp)(kp')} \tag{1.84}$$

to characterize the longitudinal momentum of the fermions which interact at the vertex. More precisely, we expand their momenta as follows [see Eq. (1.49)]

$$p^\mu = rq^\mu + sk^\mu + t_1\, m\Lambda_1^\mu + t_2\, m\Lambda_2^\mu,$$
$$p'^\mu = r'q^\mu + s'k^\mu + t_1'\, m\Lambda_1^\mu + t_2'\, m\Lambda_2^\mu. \tag{1.85}$$

The momentum-conserving delta functions included in the vertex [see Eq. (1.80)] imply $r' = r + 1$ and $t_i' = t_i$. We call this the "canonical" parametrization of the momenta, because the resulting phase of the dressed vertex [see Eq. (1.82)] has a particularly simple structure.

The quantities kq and w specify kp and kp' up to the sign of

$$\bar{w} = \frac{(kp + kp')}{kq}\, w, \quad \frac{(kp + kp')}{kq} = \pm\sqrt{1 - \frac{4}{w}}, \tag{1.86}$$

which can be seen from the solutions

$$kp = \left(-\frac{1}{2} \pm \sqrt{\frac{1}{4} - \frac{1}{w}}\right) kq, \quad kp' = \left(+\frac{1}{2} \pm \sqrt{\frac{1}{4} - \frac{1}{w}}\right) kq. \tag{1.87}$$

Finally, we obtain [see Eq. (1.71)]

$$G_1(\bar{w}, kq) = \frac{e}{2}\frac{\bar{w}}{kq}, \quad G_2(w, kq) = -\frac{e^2}{2}\frac{w}{(kq)^2}, \quad G_3(w, kq) = -\frac{e}{2}\frac{w}{kq}. \tag{1.88}$$

Thus, up to the sign of the coefficient G_1, the whole nontrivial momentum-dependence of the dressed vertex is contained in the parameters t_i and w.

1.6.5. Master integrals

To simplify the dressed vertex given in Eq. (1.68) further, we take the integrals in dx^+ and $dx^\perp$ to obtain momentum-conserving delta functions [see Eq. (1.79)] and introduce the following master integrals

$$\mathfrak{G}_0(p', q, p) = \int\limits_{-\infty}^{+\infty} d\phi\, e^{i\widetilde{S}_\Gamma(p', q, p; \phi)}, \quad \mathfrak{G}_{j,l}(p', q, p) = \int\limits_{-\infty}^{+\infty} d\phi\, [\psi_j(\phi)]^l e^{i\widetilde{S}_\Gamma(p', q, p; \phi)}, \tag{1.89}$$

where the remaining part of the action is given by [see Eq. (1.82)]

$$\widetilde{S}_\Gamma(p', q, p; \phi) = n\phi + \frac{1}{2}\frac{m^2}{kq}w \sum_{i=1,2} \int\limits_{-\infty}^{\phi} d\phi' \left[\xi_i^2\psi_i^2(\phi') - 2t_i\xi_i\psi_i(\phi')\right] \tag{1.90}$$

$[n = (p' - q - p)^+$, see Eq. (1.80)]. For $\mathfrak{G}_{j,l}(p', q, p)$ with $l > 0$ the integration range is automatically limited to the pulse duration. Assuming that $n \neq 0$ (which is required if the in- and outgoing particles are on-shell), we integrate by parts and

obtain

$$\mathfrak{G}_0(p', q, p) = -\frac{1}{2n}\frac{m^2}{kq}w \sum_{i=1,2}\left[\xi_i^2\mathfrak{G}_{i,2}(p', q, p) - 2t_i\xi_i\mathfrak{G}_{i,1}(p', q, p)\right] \qquad (1.91)$$

(the boundary terms at infinity are dropped).

Finally, we can express the nonsingular part $\mathcal{G}^\rho(p', q, p)$ [see Eq. (1.79)] of the dressed vertex $\Gamma^\rho(p', q, p)$ defined in Eq. (1.67) as

$$\mathcal{G}^\rho(p', q, p) = (-ie)\Bigg\{\gamma_\mu\Big[\mathfrak{G}_0 g^{\mu\rho} + \sum_{j=1,2}(G_1\mathfrak{G}_{j,1}f_j^{\mu\rho} + G_2\mathfrak{G}_{j,2}f_j^{2\mu\rho})\Big]$$
$$+ i\gamma_\mu\gamma^5\sum_{j=1,2}G_3\mathfrak{G}_{j,1}f_j^{*\mu\rho}\Bigg\}, \quad (1.92)$$

where $G_i = G_i(kp', kp)$ [see Eq. (1.88)], $\mathfrak{G}_0 = \mathfrak{G}_0(p', q, p)$, $\mathfrak{G}_{i,j} = \mathfrak{G}_{i,j}(p', q, p)$ [see Eq. (1.89)] and we implicitly assume that $p'^\mu = p^\mu + q^\mu$ for the components $(-, \perp)$, which is ensured by momentum conservation [see Eq. (1.80)].

1.6.6. Dressed vertex with on-shell momenta

The case where all momenta of the dressed vertex are on shell (i.e. $p^2 = p'^2 = m^2$, $q^2 = 0$) is of central importance for tree-level processes (note that the dressed vertex represents the leading-order contribution to nonlinear Breit-Wheeler pair creation and nonlinear Compton scattering, see Chap. 2, where all external momenta are necessarily on shell). In this case the representation given in Sec. 1.6.4 can be simplified even further. In particular, the fact that $q^2 = 0$ implies that the canonical light-cone basis associated with the vertex has a very simple structure [see Eq. (1.85) and Sec. 1.4.3].

For each momentum which is on shell, we can eliminate one degree of freedom. Using the parametrization [see Eq. (1.85)] [Rit85]

$$\begin{aligned} p^\mu &= rq^\mu + sk^\mu + t_1\, m\Lambda_1^\mu + t_2\, m\Lambda_2^\mu, \\ p'^\mu &= r'q^\mu + s'k^\mu + t_1'\, m\Lambda_1^\mu + t_2'\, m\Lambda_2^\mu \end{aligned} \qquad (1.93)$$

$(r' = r + 1,\ t_i' = t_i)$ we obtain[5] [see Eq. (1.50)]

$$s = \frac{1}{2}\frac{m^2}{kp}(1 + t_1^2 + t_2^2), \quad s' = \frac{1}{2}\frac{m^2}{kp'}(1 + t_1^2 + t_2^2), \qquad (1.94)$$

where $kp = rkq$ and $kp = r'kq$. Therefore, the amount $n = (p' - q - p)^+$ of absorbed laser photons [see Eq. (1.80)] is now determined by the external momenta and given by

$$n = s' - s = \frac{1}{2}w\frac{m^2}{kq}(1 + t_1^2 + t_2^2), \quad \frac{m^2}{kp'} - \frac{m^2}{kp} = w\frac{m^2}{kq}, \qquad (1.95)$$

---

[5]Since the parameters r and t_i (or r' and t_i') are conserved at the vertex, we chose them as independent variables and express s and s' using the on-shell condition.

where [see Eq. (1.83) and Eq. (1.84)]

$$t_i = -\frac{p_\mu \Lambda_i^\mu}{m}, \quad w = -\frac{(kq)^2}{(kp)(kp')} = -\frac{1}{rr'}. \tag{1.96}$$

Due to the relation given in Eq. (1.95) the phase of the master integrals [see Eq. (1.89) and Eq. (1.91)]

$$\mathfrak{G}_{j,l}(p',q,p) = \mathfrak{G}_{j,l}(w,t_1,t_2) = \int\limits_{-\infty}^{+\infty} d\phi \, [\psi_j(\phi)]^l e^{i\widetilde{S}_\Gamma(w,t_1,t_2;\phi)} \tag{1.97}$$

simplifies and is given by [see Eq. (1.90)]

$$\widetilde{S}_\Gamma(w,t_1,t_2;\phi) = \frac{1}{2} w \frac{m^2}{kq} \mathfrak{S}_\Gamma(t_1,t_2;\phi),$$

$$\mathfrak{S}_\Gamma(t_1,t_2;\phi) = (1 + t_1^2 + t_2^2)\phi + \sum_{i=1,2} \int\limits_{-\infty}^{\phi} d\phi' \left[\xi_i^2 \psi_i^2(\phi') - 2t_i \xi_i \psi_i(\phi') \right]. \tag{1.98}$$

We note that for on-shell momenta the phase of the master integrals is monotonic, which can be seen from

$$\widetilde{S}_\Gamma'(p',q,p;\phi) = \widetilde{S}_\Gamma'(w,t_1,t_2;\phi) = \frac{1}{2} w \frac{m^2}{kq} \mathfrak{S}_\Gamma'(t_1,t_2;\phi),$$

$$\mathfrak{S}_\Gamma'(t_1,t_2;\phi) = 1 + \sum_{i=1,2} \left[t_i - \xi_i \psi_i(\phi) \right]^2 \tag{1.99}$$

(for $\widetilde{S}$ and $\mathfrak{S}$ the prime denotes the partial derivative with respect to the laser phase ϕ). Thus, $\widetilde{S}_\Gamma'(p',q,p;\phi)$ is always different from zero for on-shell momenta (note that $w \geq 4$).

1.6.7. Fourier representation for the master integrals

Due to the simple dependence of $\widetilde{S}_\Gamma(w,t_1,t_2;\phi)$ on w [see Eq. (1.98)], we can efficiently calculate the master integrals for many different values of w using only a single fast Fourier transform (see App. I.1 and Chap. 2). To this end we define for on-shell momenta [see Eq. (1.97)]

$$\mathfrak{G}_{j,l}(\tilde{x},t_1,t_2) = \int\limits_{-\infty}^{+\infty} dw \, e^{-i\frac{1}{2}w\frac{m^2}{kq}\tilde{x}} \mathfrak{G}_{j,l}(w,t_1,t_2) = 4\pi \frac{kq}{m^2} \frac{[\psi_j(\phi_{\tilde{x}})]^l}{|\mathfrak{S}_\Gamma'(t_1,t_2;\phi_{\tilde{x}})|}, \tag{1.100}$$

where we interchanged the integration order (resulting in a delta function) and $\phi_{\tilde{x}}$ is the unique solution of $\mathfrak{S}_\Gamma(w,t_1,t_2;\phi_{\tilde{x}}) = \tilde{x}$. Correspondingly, we obtain the following representation

$$\mathfrak{G}_{j,l}(w,t_1,t_2) = \int\limits_{-\infty}^{+\infty} d\tilde{x} \, e^{i\frac{1}{2}w\frac{m^2}{kq}\tilde{x}} \frac{[\psi_j(\phi_{\tilde{x}})]^l}{|\mathfrak{S}_\Gamma'(t_1,t_2;\phi_{\tilde{x}})|}. \tag{1.101}$$

2 Nonlinear Breit-Wheeler pair production

The possibility to create matter from pure light is one of the most appealing predictions of quantum electrodynamics. So far, however, it has never been observed experimentally. In this chapter we consider a special type of light-by-light scattering scheme, namely the collision between a highly-energetic gamma photon and a strong optical laser pulse. It is shown that for available experimental parameters electron-positron photoproduction probabilities of the order of ten percent are achievable. Correspondingly, this setup is a promising candidate for the first conversion of light into matter in a laboratory.

In vacuum the decay of a photon into an electron-positron pair is forbidden due to energy-momentum conservation (also for photon energies $\hbar\omega_\gamma$ above the threshold $2mc^2$). To catalyze the decay, for example, a second photon (Breit-Wheeler process [BW34]) or the Coulomb field of a nucleus (Bethe-Heitler pair creation [BH34; OP33]) is needed. Inside relativistically strong laser fields ($\xi \gg 1$) even the simultaneous absorption of many laser photons becomes feasible and the Breit-Wheeler process is called nonlinear (see Fig. 6). Therefore, electron-positron photoproduction is also possible using optical laser pulses, i.e. if the laser photon energy $\hbar\omega \sim \text{eV}$ is much smaller than the electron (positron) mass.

Shortly after the first experimental realization of an optical laser by Maiman [Mai60], several authors started to consider nonlinear quantum processes inside strong electromagnetic background fields (see e.g. Refs. [NNR65; NR64a; NR64b; NR67; Rei62] for the Breit-Wheeler process). However, the required laser intensities
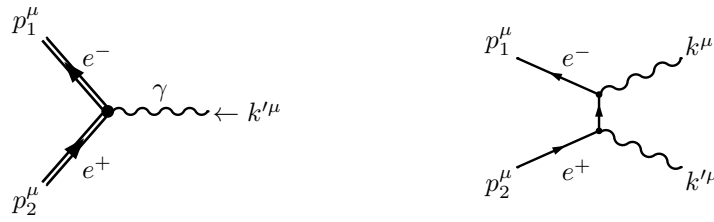
a) Nonlinear Breit-Wheeler process   **b)** Breit-Wheeler pair creation

Fig. 6: a) Leading-order Feynman diagram for the decay of a photon into an electron-positron pair inside a background field. **b)** In vacuum this process is always kinematically forbidden and must be catalyzed, e.g., by a second photon (Breit-Wheeler pair creation; the two interaction vertices may also be interchanged) [BW34]. Inside a strong laser field even the simultaneous absorption of many laser photons (nonlinear Breit-Wheeler process) becomes feasible. Here, the dressed (Volkov) states for the fermions are denoted by double lines (solutions of the Dirac equation, which take the interaction with the background field exactly into account) [LL82; Vol35]. The four-vectors indicate the four-momenta of the particles; they are described in the text (time axis from right to left).

a) Nonlinear Compton scattering   **b)** Ordinary Compton process
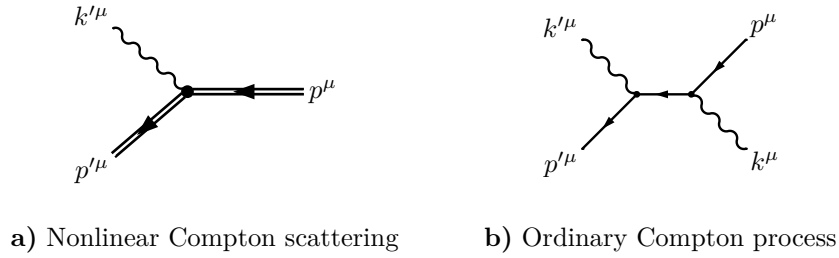
Fig. 7: a) Leading-order Feynman diagram for the emission of a photon by an electron or a positron inside a background field (nonlinear Compton scattering). **b)** As the electron (positron) is stable in vacuum, at least one additional interaction is needed to emit a photon (ordinary Compton process; the two interaction vertices may also be interchanged). Nonlinear Compton scattering and nonlinear Breit-Wheeler pair creation (see Fig. 6) are related via a crossing symmetry (solid lines denote fermions in vacuum, double lines dressed fermion states and wiggly lines photons; time axis from right to left).

for laboratory observations have become available only recently due to impressive technological advances. The experimental progress triggered new theoretical investigations over the past years, with an emphasis on both nonlinear Breit-Wheeler pair production (see Fig. 6) [Bul+10b; Bul+13; FM13; HIM10; HIM11; Ipp+11; JM13; KER13; KK12a; KK14; Nou+12; OHA11; Tit+12; Tit+13; Tuc10] and non-linear Compton scattering (see Fig. 7) [BDF12a; BDF12b; BF11; GH14; HSK10; Kin15; KK12b; KK13; MD11; MD13; MDK10; SK11; SK12; SK13; SK14]. A detailed summary of the existing literature can be found, e.g., in the review articles [BR13; Di+12; EKK09; MS06; MTB06; RVX10].

In this chapter, which is mainly based on the publications [4] and [6], we will consider both the differential and the total probabilities for electron-positron photoproduction inside an arbitrary plane-wave laser field. As near future experiments will probably use short laser pulses to obtain high intensities, we focus on few-cycle pulses in the numerical calculations. Below, we summarize the main achievements of our work.

Proof of the optical theorem for the polarization operator

The optical theorem relates the total probability for particle production processes to the imaginary part of corresponding loop diagrams; it is a direct consequence of a unitary time evolution [PS95; Sre07; Wei95]. More specifically, the total pair-creation probability must be related to the imaginary part of the photon forward-scattering amplitude (described by the polarization operator, see Chap. 3) due to probability conservation (see Fig. 8) [FGS91; Rit85]. However, it is instructive to verify this by an explicit calculation, which leads to the so-called "cutting" or "cutkosky rules" for Feynman diagrams (for QED in vacuum this derivation was first given in Refs. [Cut60; Lan59]).

Here, the optical theorem for the polarization operator in the presence of an arbitrary plane-wave background field is proven (to leading order) by generalizing the calculation presented in Ref. [Sre07] for vacuum Feynman diagrams (see Sec. 2.2). The application of the optical theorem to the nonlinear Breit-Wheeler process results in a compact double-integral representation for the total electron-positron photoproduction probability (see Sec. 2.4). By evaluating the remaining two in-

a) pair production   **b)** polarization operator
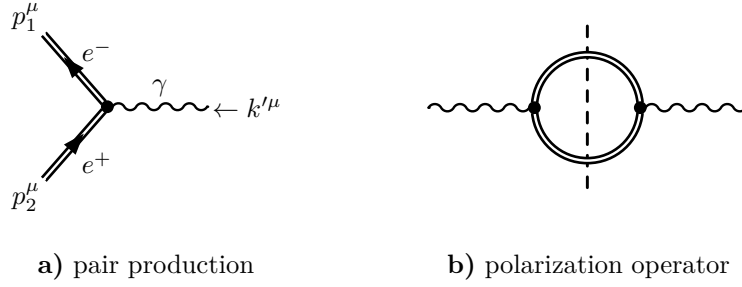
Fig. 8: The total probability for electron-positron photoproduction is related via the optical theorem to the imaginary part of the polarization operator, which describes photon forward scattering (see Chap. 3).

tegrals numerically (see Sec. 4.5), the dependence of the total pair-production probability on the energy of the incoming photon, the intensity of the laser pulse, the number of cycles, the global pulse shape and the carrier-envelope phase (CEP) has been studied in detail (see Sec. 2.5).

Note that the optical theorem is also used in Refs. [Di+09; Mil+06] to investigate the nonlinear Bethe-Heitler process. Alternatively, total probabilities could be calculated efficiently using the approach introduced in Ref. [Din13] for nonlinear Compton scattering.

Verification of the local constant-crossed field approximation

It is well known that for relativistically strong laser fields ($\xi \gg 1$) the formation region of the basic QED processes nonlinear Compton scattering and nonlinear Breit-Wheeler pair production is much smaller than the laser wavelength [Di+12; Rit85]. Therefore, it is possible to calculate the total nonlinear Breit-Wheeler pair-creation probability by averaging the corresponding quantity inside a constant-crossed field over the laser pulse shape in the regime $\xi \gg 1$ (see Sec. 2.4). By comparing this so-called local constant-crossed field approximation with a full numerical calculation, we show that already for $\xi \gtrsim 10$ both results are in very good agreement.

However, the local constant-crossed field approximation breaks down in the regime $\xi \lesssim 1$. There, the global properties of the laser pulse become important, which is demonstrated by analyzing the CEP-dependence of the total probability (see Sec. 2.5).

Furthermore, we prove that the local constant-crossed field approximation is also applicable for the calculation of the asymptotic momentum distribution of the pair if interference effects between different formation regions are properly taken into account (see Sec. 2.7).

Inclusion of the exponential photon wave-function decay

In the regime where the total pair-production probability is of order unity, the standard evaluation of the leading-order Feynman diagram given in Fig. 6 results in unphysical predictions. To resolve the contradiction, the back-reaction of the pair-creation process on the photon wave function must be taken into account. Here, a self-consistent description is obtained by solving the Schwinger-Dyson equation [LL82; Sch51], which leads to an exponential decay of exact photon wave function

45

(see Sec. 2.3). It is shown that already for available laser parameters and gamma photon energies this effect plays an important role and that it cannot be ignored at next-generation laser facilities (see Sec. 2.5).

Moreover, the birefringence of the quantum vacuum is obtained from the exact photon wave function. Normally, this effect is derived from the effective action, see, e.g., Refs. [Aff88; BB67; BB70; BMS76; DG00; Din+14b].

Semiclassical explanation for the asymptotic momentum distribution

By applying a stationary-phase analysis to the leading-order S-matrix element of the Breit-Wheeler process (see Fig. 6), we establish a semiclassical description for electron-positron photoproduction valid in the regime $\xi \gg 1$ (see Sec. 2.7). Accordingly, the asymptotic electron-positron momentum distribution is mainly determined by the classical equations of motion inside the laser field. To obtain the correct initial conditions for the classical propagation, the differential pair-creation probability inside the constant-crossed field at the creation point has to be considered. In addition, the interference between pairs produced within different formation regions must be taken into account if the asymptotic momenta after the classical propagation coincide [Rit85]. As a laser field is oscillatory, each laser cycle typically contributes two interference paths to the final probability amplitude. Therefore, nonlinear Breit-Wheeler pair production can also be interpreted as an optical multi-slit experiment (for the importance of interference effects in Schwinger pair production see, e.g., Ref. [DD11]).

We point out that the developed intuitive picture reveals many similarities between Breit-Wheeler pair creation and atomic tunnel ionization [Cor93; Koh+12; Kuc87]. Furthermore, it provides a clear explanation for the extend of the spectrum, the region of highest probability and the strong dependence on the carrier-envelope phase (CEP) for ultra-short laser pulses reported in Ref. [KK12a] (see Sec. 2.8).

Note that semiclassical methods are also used in Refs. [MD11; MD13; MDK10] to interpret the emission spectra obtained for nonlinear Compton scattering.

High-resolution calculation of the spectrum to resolve interferences

In order to establish the validity of the semiclassical description outlined above, the asymptotic momentum distribution of photoproduced electron-positron pairs is calculated fully numerically without any approximation. In particular, it is shown that already for $\xi \gtrsim 10$ the interference structure obtained from the local constant-crossed field approximation applied on the probability amplitude level is in very good agreement with full numerical predictions (see Sec. 2.8).

As the appearing integrals are highly oscillating in the regime $\xi \gg 1$, the exact numerical calculation is a challenging task [KK12a; Tit+12]. To accomplish it, we presented a scheme which is substantially more efficient than other employed methods (see Sec. 1.6). Consequently, it became feasible to evaluate the three-dimensional differential probability on a grid which is fine enough to completely resolve the interference structure of the spectrum.

2.1. Derivation of the pair-creation probability

To calculate the pair-creation probability, we describe the incoming photon by a wave packet

$$|\Phi, \eta\rangle = \int \frac{d^3 q'}{(2\pi)^3 \, 2\epsilon_{q'}} \, \eta(q') \, |\Phi_{q'}\rangle \, , \tag{2.1}$$

where $\epsilon_{q'} = \sqrt{q'^2}$. As shown in [IT13; PS95; Ryd96], this has the advantage of avoiding the appearance of squared delta functions and ambiguities in interpreting volume factors. In Eq. (2.1) we assume that all components of the wave packet have the same polarization (the polarization indices are suppressed) and are on shell, i.e. $q'^2 = 0$. Furthermore, $|\Phi_{q'}\rangle$ denotes a momentum eigenstate of the photon field with relativistic normalization

$$\langle \Phi_q | \Phi_{q'} \rangle = 2\epsilon_q (2\pi)^3 \delta^3(q - q'). \tag{2.2}$$

The wave-packet state describes a single particle [$\langle \Phi, \eta | \Phi, \eta \rangle = 1$] if the envelope function obeys the covariant normalization condition

$$\int \frac{d^3 q'}{(2\pi)^3 \, 2\epsilon_{q'}} \, |\eta(q')|^2 = 1 \tag{2.3}$$

(this is assumed in the following discussion).

The probability that a single photon decays into an electron-positron pair inside a plane-wave background field is now given by

$$W = \sum_{\sigma, \sigma'} \int \frac{d^3 p \, d^3 p'}{(2\pi)^6 \, 2\epsilon_p 2\epsilon_{p'}} \, |\langle \Phi_{p,\sigma,p',\sigma'} | S | \Phi, \eta \rangle|^2 \, , \tag{2.4}$$

where $|\Phi_{p,\sigma,p',\sigma'}\rangle$ describes an electron and a positron with momenta[1] $p^\mu = (\epsilon_p, p)$ and $p'^\mu = (\epsilon_{p'}, p')$, respectively ($\sigma, \sigma' \in [1, 2]$ label the different spin states, $\epsilon_p = \sqrt{m^2 + p^2}$, $\epsilon_{p'} = \sqrt{m^2 + p'^2}$). Equation (2.4) holds if the one-particle momentum eigenstates for the electron and the positron are relativistically normalized [see Eq. (2.2)] [Mag05],

$$\langle \Phi_{p,\sigma} | \Phi_{p',\sigma'} \rangle = 2\epsilon_p (2\pi)^3 \delta^3(p - p')\delta_{\sigma\sigma'}. \tag{2.5}$$

Then, the identity operator (in the one-particle subspace) is given by

$$\mathbf{1} = \sum_{\sigma=1,2} \int \frac{d^3 p}{(2\pi)^3 \, 2\epsilon_p} \, |\Phi_{p,\sigma}\rangle \langle \Phi_{p,\sigma}| \, , \tag{2.6}$$

which explains the density of states employed in Eq. (2.4).

In the following we drop the spin labels and write $|\Phi_{p,p'}\rangle = |\Phi_{p,\sigma,p',\sigma'}\rangle$ for simplicity. Note that W is a probability (not a rate), as the duration of the process is naturally limited if the background field has only a finite extend.

---

[1]Note that in the first part of this chapter (i.e. from Sec. 2.1 to Sec. 2.5) the notation for the momenta agrees with the one used in Ref. [4] but differs from the one used in the second part of this chapter (i.e. starting from Sec. 2.6). There, the notation agrees with Ref. [6].

Using Eq. (2.1) we rewrite the squared matrix element in Eq. (2.4) as

$$|\langle \Phi_{\boldsymbol{p},\boldsymbol{p'}} | S | \Phi, \eta \rangle|^2 = \int \frac{d^3 q_1 \, d^3 q_2}{(2\pi)^6 \, 2\epsilon_{\boldsymbol{q}_1} 2\epsilon_{\boldsymbol{q}_2}} \eta(q_1) \eta^*(q_2) \mathfrak{M}(p, p'; q_1) [\mathfrak{M}(p, p'; q_2)]^*, \quad (2.7)$$

where

$$i\mathfrak{M}(p, p'; q) = \langle \Phi_{\boldsymbol{p},\boldsymbol{p'}} | S | \Phi_{\boldsymbol{q}} \rangle \quad (2.8)$$

[for simplicity we often suppress some of the labels, i.e. $\mathfrak{M}(p, \sigma, p', \sigma'; q) = \mathfrak{M}(p, p'; q) = \mathfrak{M}(q)$].

From now on we consider only plane-wave external fields (see Sec. 1.3). Then, the S-matrix contains three overall momentum-conserving delta functions [see Eq. (1.79)] and it is useful to define the reduced matrix element $\mathcal{M}$ by

$$i\mathfrak{M}(p, p'; q) = (2\pi)^3 \delta^{(-,\perp)}(p + p' - q) \, i\mathcal{M}(p, p'; q). \quad (2.9)$$

After transforming the on-shell momentum integrals to light-cone coordinates using Eq. (1.51), we can rewrite Eq. (2.7) as follows

$$|\langle \Phi_{\boldsymbol{p},\boldsymbol{p'}} | S | \Phi, \eta \rangle|^2 = \int \frac{dq_1^- \, dq_1^\perp}{(2\pi)^3} \frac{\theta(q_1^-)}{2q_1^-} \, |\eta(q_1)|^2$$
$$\times \frac{1}{2q_1^-} |\mathcal{M}(p, p'; q_1)|^2 \, (2\pi)^3 \delta^{(-,\perp)}(p + p' - q_1). \quad (2.10)$$

Finally, the total pair-creation probability is given by [see Eq. (2.4)]

$$W = \int \frac{d^3 q'}{(2\pi)^3 \, 2\epsilon_{\boldsymbol{q'}}} |\eta(q')|^2 \, W(q'), \quad (2.11\text{a})$$

where

$$W(q) = \sum_{\text{spin}} \int \frac{d^3 p \, d^3 p'}{(2\pi)^6 \, 2\epsilon_{\boldsymbol{p}} 2\epsilon_{\boldsymbol{p'}}} \frac{1}{2q^-} |\mathcal{M}(p, p'; q)|^2 \, (2\pi)^3 \delta^{(-,\perp)}(p + p' - q). \quad (2.11\text{b})$$

Using the Feynman rules for QED with plane-wave background fields (see Sec. 1.5.3 for details), we obtain the following expression for the electron-positron photoproduction matrix element[2] (see Fig. 6)

$$i\mathfrak{M}(p, \sigma, p', \sigma'; q) = \epsilon_\mu \, \bar{u}_{p,\sigma} \Gamma^\mu(p, q, -p') v_{p',\sigma'}, \quad (2.12)$$

where ϵ_μ is the polarization four-vector of the incoming photon ($\epsilon q = 0$, $\epsilon^\mu \epsilon_\mu^* = -1$). Furthermore, $u_{p,\sigma}$ and $v_{p',\sigma'}$ denote the Dirac four-spinors of the electron and the positron, respectively [see Eq. (1.57)]. Correspondingly, the reduced matrix element reads [see Eqs. (2.9) and (2.12)]

$$i\mathcal{M}(p, p'; q) = \epsilon_\mu \, \bar{u}_p \mathcal{G}^\mu(p, q, -p') v_{p'}, \quad (2.13)$$

---

[2]Note that in Eq. (3) and Eq. (A19) in Ref. [4] the i is erroneously missing.

where $\mathcal{G}$ denotes the nonsingular part of the dressed vertex [see Eq. (1.79)].

We point out that the expression for the matrix element given here represents only the leading-order contribution to the pair-creation process. Furthermore, it is only possible to interpret W as the probability for pair production as long as it is small. In general, it represents the decay exponent of the exact photon wave function (see Sec. 2.3 for more details).

2.2. Optical theorem

In the last section we have clarified the relation between the pair-creation probability and the corresponding S-matrix element [see Eq. (2.11)]. By proving the so-called optical theorem [see Eq. (2.29)], we will show now that the total pair-creation probability is closely related to photon forward scattering described by the polarization operator (see Fig. 8).

The optical theorem immediately leads to the exponential decay of the exact photon wave function, which is subsequently discussed in Sec. 2.3. Furthermore, it is employed in Sec. 2.4 to obtain compact expressions for the total nonlinear Breit-Wheeler pair-creation probability.

2.2.1. Leading-order cutting rule for the polarization operator

In this section we will explicitly derive the optical theorem for nonlinear Breit-Wheeler pair production (to leading order, see Fig. 8) in the presence of an arbitrary plane-wave background field (see also [BMS76; Di+09; Din+14b; FGS91; Mil+06; Rit72b] and e.g. [Cut60; Lan59; PS95; Sre07] for the corresponding proof in vacuum QED). To this end we consider the squared matrix element [see Eq. (2.12)], which appears in Eq. (2.7)

$$\mathfrak{M}(p,\sigma,p',\sigma';q_1)[\mathfrak{M}(p,\sigma,p',\sigma';q_2)]^*$$
$$= \epsilon_\mu \epsilon_\nu^* \, \mathbf{tr} \, \rho_{p,\sigma}^u \Gamma^\mu(p,q_1,-p')\rho_{p',\sigma'}^v \overline{\Gamma}^\nu(p,q_2,-p') \quad (2.14)$$

[see Eq. (D.2) for the bar notation used]. Here, we have introduced the following density matrices

$$\rho_{p,\sigma}^u = u_{p,\sigma}\bar{u}_{p,\sigma}, \quad \rho_{p',\sigma'}^v = v_{p',\sigma'}\bar{v}_{p',\sigma'}. \quad (2.15)$$

To obtain the total pair-creation probability we have to sum/integrate over final spins and momenta [see Eq. (2.4)]

$$\sum_{\text{spin}} \int \frac{d^3p \, d^3p'}{(2\pi)^6 \, 2\epsilon_{\boldsymbol{p}} 2\epsilon_{\boldsymbol{p}'}} \, \mathfrak{M}(q_1)[\mathfrak{M}(q_2)]^*. \quad (2.16)$$

The sum over different spin states yields [LL82; PS95]

$$\sum_{\sigma=1,2} \rho_{p,\sigma}^u = \slashed{p} + m, \quad \sum_{\sigma'=1,2} \rho_{p',\sigma'}^v = \slashed{p}' - m. \quad (2.17)$$

Thus, we see that Eq. (2.16) resembles the leading-order contribution to the polarization operator (see Chap. 3)

$$i\mathcal{P}^{\mu\nu}(q_1, q_2) = \int \frac{d^4p_1\, d^4p_2}{(2\pi)^8} \frac{\mathbf{tr}[\cdots]^{\mu\nu}}{(p_1^2 - m^2 + i0)(p_2^2 - m^2 + i0)}, \qquad (2.18)$$

where

$$\mathbf{tr}[\cdots]^{\mu\nu} = \mathbf{tr}\, \Gamma^\mu(p_2, q_1, p_1)(\not{p}_1 + m)\Gamma^\nu(p_1, -q_2, p_2)(\not{p}_2 + m). \qquad (2.19)$$

To match the two expressions even further, we introduce two more integrations in p^0 and p'^0 in Eq. (2.16) together with appropriate delta and step functions to bring the momenta on shell [see Eq. (1.51)]. After applying the identity given in Eq. (1.78), using the cyclic property of the trace and the change of variables $p^\mu \to p_2^\mu$, $p'^\mu \to -p_1^\mu$ we obtain

$$\sum_{\text{spin}} \int \frac{d^3p\, d^3p'}{(2\pi)^6\, 2\epsilon_{\boldsymbol{p}} 2\epsilon_{\boldsymbol{p'}}} \mathfrak{M}(q_1)[\mathfrak{M}(q_2)]^* = \int \frac{d^4p_1\, d^4p_2}{(2\pi)^6}$$
$$\times\, \delta(p_1^2 - m^2)\delta(p_2^2 - m^2)\theta(-p_1^0)\theta(p_2^0)\epsilon_\mu \epsilon_\nu^* \, \mathbf{tr}[\cdots]^{\mu\nu}. \quad (2.20)$$

To prove the optical theorem we have to relate the imaginary part of the photon forward-scattering amplitude described by the polarization operator to the total pair-creation probability. To this end we extract the nonsingular part of the polarization operator by defining

$$\mathcal{P}^{\mu\nu}(q_1, q_2) = (2\pi)^3 \delta^{(-,\perp)}(q_1 - q_2)\, \Pi^{\mu\nu}(q_1, q_2), \qquad (2.21)$$

and consider $\Im\left[\epsilon_\mu \epsilon_\nu^* \Pi^{\mu\nu}(q, q)\right]$. We point out that the contracted trace $\epsilon_\mu \epsilon_\nu^* \, \mathbf{tr}[\cdots]^{\mu\nu}$ [see Eq. (2.19)] is purely real if evaluated at $q_1^\mu = q_2^\mu = q^\mu$ (strictly speaking, after the singular part is factorized out). This can be deduced from

$$(\mathbf{tr}[\cdots]^{\mu\nu})^* = \mathbf{tr}[\cdots]^{\nu\mu}(q_1 \leftrightarrow q_2) \qquad (2.22)$$

[note that $(\mathbf{tr}\, M)^* = \mathbf{tr}\, M^\dagger = \mathbf{tr}\, \bar{M}$]. Using the Sokhotski-Plemelj identity [Mer98; Sre07]

$$\frac{1}{p^2 - m^2 + i0} = \mathrm{P}\,\frac{1}{p^2 - m^2} - i\pi\delta(p^2 - m^2), \qquad (2.23)$$

we obtain the symbolic relation [see Eq. (2.18)]

$$\Im\left[\epsilon_\mu \epsilon_\nu^* \Pi^{\mu\nu}(q, q)\right] = -\Re\left[\epsilon_\mu \epsilon_\nu^* i\Pi^{\mu\nu}(q, q)\right] \sim \pi^2\delta\delta - \mathrm{P}\,\mathrm{P}. \qquad (2.24)$$

It is shown in Sec. 2.2.2 that the two principle value integrals are related to the on-shell contribution. Symbolically, the result can be written as

$$\mathrm{P}\,\mathrm{P} = \mathrm{sign}(p_1^-)\,\mathrm{sign}(p_2^-)\pi^2\delta\delta, \qquad (2.25)$$

implying

$$\Im\left[\epsilon_\mu\epsilon_\nu^*\Pi^{\mu\nu}(q,q)\right] \sim \left[1 - \text{sign}(p_1^-)\,\text{sign}(p_2^-)\right]\pi^2\delta\delta. \tag{2.26}$$

On the other hand, the momentum-conserving delta function $\delta^{(-)}(p_2 - q_1 - p_1)$ contained in the vertices in Eq. (2.20) ensures that only the region $p_2^- - p_1^- > 0$ contributes to the integral (assuming $q_i^- > 0$, i.e. we exclude the trivial case of a photon which is copropagating with the laser). Thus, in Eq. (2.20) we can apply the replacement

$$2\theta(-p_1^0)\theta(p_2^0) \longleftrightarrow \left[1 - \text{sign}(p_1^-)\,\text{sign}(p_2^-)\right]. \tag{2.27}$$

Finally,

$$\begin{aligned}
2\Im\left[\epsilon_\mu\epsilon_\nu^*\Pi^{\mu\nu}(q,q)\right] = \epsilon_\mu\epsilon_\nu^* \int \frac{d^3p\,d^3p'}{(2\pi)^6\,2\epsilon_{\boldsymbol{p}}2\epsilon_{\boldsymbol{p}'}} &\,(2\pi)^3\delta^{(-,\perp)}(p + p' - q) \\
&\times\ \mathbf{tr}(\not{p} + m)\mathcal{G}^\mu(p,q,-p')(\not{p}' - m)\overline{\mathcal{G}}^\nu(p,q,-p')
\end{aligned} \tag{2.28}$$

for $q^- > 0$, where $\mathcal{G}^\mu$ denotes the nonsingular part of the dressed vertex [see Eq. (1.79)].

After combining everything, we obtain the following relation between the total electron-positron photoproduction probability W and the imaginary part of the photon forward scattering amplitude, which is called the optical theorem (see also [BMS76; Di+09; Mil+06])

$$W = \int \frac{d^3q'}{(2\pi)^3\,2\epsilon_{\boldsymbol{q}'}}\,|\eta(q')|^2\,W(q'), \quad W(q) = \frac{1}{kq}\,\Im\left[\epsilon_\mu\epsilon_\nu^*\Pi^{\mu\nu}(q,q)\right] \tag{2.29}$$

$[q^2 = 0;\ W \approx W(q)$ if the wave packet of the incoming photon is sharply peaked around $q'^\mu = q^\mu$, see Eq. (2.3)].

2.2.2. Pole structure of the Volkov propagator

To prove Eq. (2.25) we have to investigate the pole structure of the the Volkov propagator [see Eq. (1.59)]

$$iG(x,y) = i\int \frac{d^4p}{(2\pi)^4}\,E_{p,x}\,\frac{\not{p} + m}{p^2 - m^2 + i0}\,\bar{E}_{p,y}. \tag{2.30}$$

This is most conveniently carried out in light-cone coordinates, where the integral in dp^+ has a simple structure [Rit72a], as the phase of the propagator depends on p^+ only via [see Eq. (1.58)]

$$\exp[-ip^+(x^- - y^-)] \tag{2.31}$$

$(A^- = k^- = 0)$. For $p^- \neq 0$ we can evaluate the integral in p^+ using the residue theorem [AF03].

In general, the point $p^- = 0$ (which corresponds to the so-called light-cone zero mode) must be treated carefully (for more details about light-cone quantization and the light-cone zero mode see e.g. Refs. [BPP98; Dir49; Hei01]). As long

51

as no singularities [e.g. a delta function $\delta(p^-)$] are encountered, a single point can always be excluded from the integration range. In the absence of external fields such a delta function appears in QED only in diagrams without external legs and for all other diagrams the light-cone zero mode can be ignored (see Sec. II.C in Ref. [CM69]). Like in vacuum QED, the light-cone zero mode does not contribute to the leading-order diagram for the polarization operator in a plane-wave background field if the incoming photon is on shell and does not propagate collinearly with the laser field. This can be seen explicitly from the final expression of the field-dependent part of the polarization operator given in Chap. 3 [see Eq. (3.56)]. In fact, the integrand of the polarization operator vanishes at the points $\tau = 0$ and $v = \pm 1$, corresponding to vanishing values of at least one of the proper-time variables s and t [see Eq. (3.24)]. Thus, the delta function used to take the p^--integral [see Eq. (3.20)] implies that $p^- \neq 0$ as long as $kq = q^- \neq 0$. In conclusion, for the discussion of the optical theorem we can ignore subtleties arising from the light-cone zero mode and assume that $p^- \neq 0$ in the following.

To take the integral in p^+ we have to close the contour in the lower complex plane if $x^- - y^- > 0$ and in the upper complex plane if $x^- - y^- < 0$. The pole of

$$\frac{1}{p^2 - m^2 + i0} = \frac{1}{2p^+ p^- - p^\perp p^\perp - m^2 + i0} \tag{2.32}$$

is located at

$$p^+ = \frac{p^\perp p^\perp + m^2 - i0}{2p^-}, \tag{2.33}$$

i.e. in the lower complex plane for $p^- > 0$ and in the upper complex plane for $p^- < 0$, in agreement with the Feynman boundary condition.

Following Ref. [Sre07], we have to consider also the retarded and advanced propagators, defined by the pole prescriptions

$$\frac{1}{p^2 - m^2 + \operatorname{sign}(p^-)i0}, \quad \frac{1}{p^2 - m^2 - \operatorname{sign}(p^-)i0}, \tag{2.34}$$

respectively. The pole of the former is always located in the lower, the pole of the latter always in the upper complex plane. Correspondingly, the propagators vanish for $x^- < y^-$ and $x^- > y^-$, respectively.

The polarization operator diagram [see Eq. (3.6)] contains both $G(x, y)$ and $G(y, x)$ or in other words the phase factor contains

$$\exp\left[-ip_1^+(x^- - y^-)\right] \exp\left[ip_2^+(x^- - y^-)\right]. \tag{2.35}$$

Correspondingly, the contour integrals in p_1^+ and p_2^+ must be closed differently. If both propagators of the polarization operator are either replaced by advanced or by retarded propagators, such that for $x^- - y^- \gtrless 0$ one propagator is always zero, the contribution of the total diagram vanishes. Using the relation [see
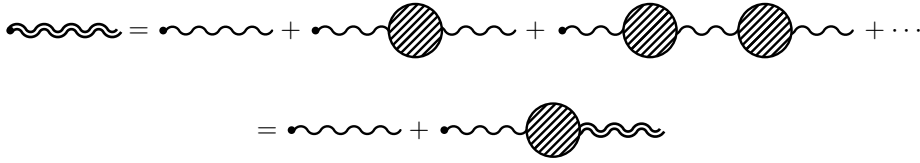
a) Exact photon wave function
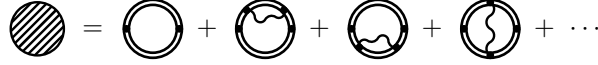
b) One-particle irreducible diagrams

Fig. 9: a) The exact photon wave function (double wiggly line) can be defined either implicitly or by an geometric expansion. **b)** One-particle irreducible (1PI) contributions to the polarization operator (see Chap. 3).

Eq. (2.23)]

$$\frac{1}{p^2 - m^2 \pm \text{sign}(p^-)i0} = \text{P}\frac{1}{p^2 - m^2} \mp i\,\text{sign}(p^-)\pi\delta(p^2 - m^2),\qquad(2.36)$$

we can now prove the identity [see Eq. (2.25)]

$$\text{P}\,\text{P} = \text{sign}(p_1^-)\,\text{sign}(p_2^-)\pi^2\delta\delta\qquad(2.37)$$

for $\Im\left[\epsilon_\mu\epsilon_\nu^*\Pi^{\mu\nu}(q,q)\right]$.

2.3. Exact photon wave function

It is shown in Sec. 2.5 that the quantity $W(q)$ [see Eq. (2.11)] may become larger than unity for next-generation laser parameters. Therefore, the common interpretation of $W(q)$ as pair-production probability must eventually be modified. The reason for this unphysical result is the fact that we neglected the exponential decay of the photon and the electron wave functions during the evaluation of the Feynman diagram shown in Fig. 6. As the photon is unstable in the external field, the phase of its exact wave function must contain an imaginary part to ensure a unitary time evolution. Due to the optical theorem [see Eq. (2.29)] the decay of the photon wave function is naturally obtained from radiative corrections (see Fig. 9). To obtain a self-consistent description, they have to be included by solving the Schwinger-Dyson equation [LL82; Sch51].

2.3.1. Schwinger-Dyson equations

In vacuum the wave function of an incoming (outgoing) photon with four-momentum q^μ is given by [LL82; PS95]

$$\Phi_{q,j}^{\text{in}\mu}(x) = \epsilon_j^\mu e^{-iqx}, \quad \Phi_{q,j}^{*\text{out}\mu}(x) = \epsilon_j^{*\mu}e^{iqx}\qquad(2.38)$$

($j = 1, 2$ labels the polarization state). However, inside a background field radiative corrections affect also the external lines (even after renormalization [Wei95]) and the exact wave function obeys the Schwinger-Dyson equation [LL82; Sch51]

$$-\partial^2 \Phi_q^{\mathrm{in}\mu}(x) = \int d^4y \, P^{\mu\nu}(x,y) \Phi_{q\nu}^{\mathrm{in}}(y),$$

$$-\partial^2 \Phi_q^{*\mathrm{out}\mu}(x) = \int d^4y \, \Phi_{q\nu}^{*\mathrm{out}}(y) P^{\nu\mu}(y,x), \tag{2.39}$$

where $P^{\mu\nu}(x,y)$ denotes the polarization operator in position space. It is related to the polarization operator in momentum space (see Chap. 3) via

$$P^{\mu\nu}(x,y) = \int \frac{d^4q_1 d^4q_2}{(2\pi)^8} \, e^{-iq_2x} \, \mathcal{P}^{\mu\nu}(-q_2, -q_1) \, e^{iq_1y},$$

$$\mathcal{P}^{\mu\nu}(q_1, q_2) = \int d^4x d^4y \, e^{-iq_1y} \, P^{\mu\nu}(y,x) \, e^{iq_2x} \tag{2.40}$$

[note that we use for $P^{\mu\nu}(x,y) = P^{\nu\mu}(y,x)$ the Schwinger notation (particle propagation from y to x) [Sch51], while in $\mathcal{P}^{\mu\nu}(q_1, q_2) = \mathcal{P}^{\nu\mu}(-q_2, -q_1)$ the incoming momentum is denoted by q_1]. As the vacuum part does not change the photon wave function (after renormalization is carried out), we will consider here only the field-dependent part of the polarization operator.

We point out that now even for a plane-wave field the states for incoming and outgoing particles are not equivalent anymore, as the quantum loop enters differently into the equations (the corresponding Schwinger-Dirac equation for an electron is discussed in Chap. 5).

To solve the Schwinger-Dyson equations [see Eq. (2.39)] we use the ansatz

$$\Phi_{q,j}^{\mathrm{in}\mu}(x) = \exp(-iqx)\mathcal{E}_{q,j}^{\mathrm{in}\mu}(kx), \quad \Phi_{q,j}^{*\mathrm{out}\mu}(x) = \mathcal{E}_{q,j}^{*\mathrm{out}\mu}(kx) \exp(iqx) \tag{2.41}$$

and require the boundary conditions

$$\mathcal{E}_{q,j}^{\mathrm{in}\mu}(-\infty) \to \epsilon_j^\mu, \quad \mathcal{E}_{q,j}^{*\mathrm{out}\mu}(+\infty) \to \epsilon_j^{*\mu} \tag{2.42}$$

(with a suitable choice for the constant polarization four-vectors ϵ_j^μ). As they denote the asymptotic momenta, the quantum numbers are left unchanged (i.e. $q^2 = 0$). However, we obtain $\mathfrak{Q}_j^2 \neq 0$, where the effective four-momentum $\mathfrak{Q}_j^\mu$ is defined as the derivative of the total wave-function phase [Din+14b], i.e. for in states

$$\mathfrak{Q}_j^\mu = -\partial^\mu S_{q,j}(x), \quad \Phi_{q,j}^{\mathrm{in}\mu}(x) \sim \exp[iS_{q,j}(x)] \tag{2.43}$$

($\mathfrak{Q}_j^\mu = q^\mu$ to leading order).

From Eq. (2.39) we obtain now the following integro-differential equations

$$i2kq \, \mathcal{E}_{q,j}^{\prime\mathrm{in}\mu}(\phi) = \int d\phi' \, P_q^{\mu\nu}(\phi, \phi') \mathcal{E}_{q,j\nu}^{\mathrm{in}}(\phi'),$$

$$-i2kq \, \mathcal{E}_{q,j}^{\prime*\mathrm{out}\mu}(\phi) = \int d\phi' \, \mathcal{E}_{q,j\nu}^{*\mathrm{out}}(\phi') \tilde{P}_q^{\nu\mu}(\phi', \phi), \tag{2.44}$$

where we defined the quantities

$$P_q^{\mu\nu}(kx, ky) = \int dy^+ dy^\perp \, e^{iq(x-y)} \, P^{\mu\nu}(x, y),$$
$$\tilde{P}_q^{\nu\mu}(ky, kx) = \int dy^+ dy^\perp \, e^{iq(y-x)} \, P^{\nu\mu}(y, x).$$
(2.45)

2.3.2. Exact photon wave function for strong background fields

From now on we focus on the in states and assume that the background field is strong ($\xi \gg 1$), i.e. we use the leading-order quasistatic approximation for the polarization operator (see Sec. 3.3.2). To determine the leading-order corrections in $\alpha\chi^{2/3} \ll 1$ [Rit85], we can apply a perturbative approach [Sch51]. As to leading order $\mathfrak{Q}_j^\mu = q^\mu$, we obtain the following differential equation[3]

$$i2kq \, \mathcal{E}_{q,j}^{\prime\text{in}\mu}(\phi) = -\left[\mathfrak{p}_1(\phi) \, \Lambda_1^\mu \Lambda_1^\nu + \mathfrak{p}_2(\phi) \, \Lambda_2^\mu \Lambda_2^\nu + \mathfrak{p}_3(\phi)\frac{q^\mu q^\nu}{m^2}\right]\mathcal{E}_{q,j\nu}^{\text{in}}(\phi),$$
(2.46)

where [see Eq. (3.96)]

$$\mathfrak{p}_1(\phi) = \alpha \, \frac{m^2}{3\pi} \int\limits_{-1}^{+1} dv \, (w-1)\frac{f'(\tilde{x})}{\tilde{x}}, \quad \mathfrak{p}_2(\phi) = \alpha \, \frac{m^2}{3\pi} \int\limits_{-1}^{+1} dv \, (w+2)\frac{f'(\tilde{x})}{\tilde{x}},$$

$$\mathfrak{p}_3(\phi) = -\alpha \, \frac{m^2}{\pi} \int\limits_{-1}^{+1} dv \, \frac{f_1(\tilde{x})}{w}$$
(2.47)

[$\frac{1}{w} = \frac{1}{4}(1 - v^2)$, $\tilde{x} = [w/|\chi(\phi)|]^{2/3}$, $\chi(\phi) = \chi\psi'(\phi)$ and the Ritus functions are defined in Eq. (F.1)]. As the incoming photon is initially transversely polarized (i.e. in the plane spanned by Λ_j^μ, $j = 1, 2$), the term proportional to $\mathfrak{p}_3(\phi)$ can be ignored.

Finally, we obtain for the exact incoming photon wave function the following expression

$$\Phi_{q,j}^{\text{in}\mu}(x) = \Lambda_j^\mu \exp\left[-iqx - i\frac{1}{2kq}\int\limits_{-\infty}^{kx} d\phi' \, \mathfrak{p}_j(\phi')\right]$$
(2.48)

($j = 1, 2$, valid for $\xi \gg 1$ and as long as $\alpha\chi^{2/3} \ll 1$ [Rit85]; similarily, the outgoing photon wave function can be derived).

According to Eq. (2.48) the effective photon four-momentum [see Eq. (2.43)] is given by

$$\mathfrak{Q}_j^\mu(\phi) = q^\mu + k^\mu \frac{1}{2kq}\mathfrak{p}_j(\phi)$$
(2.49)

and locally the well-known expression for the square of the photon mass $\mathfrak{Q}_j^2$ inside a constant-crossed field is recovered [BS71; Nar69; Rit70b; Rit72a] (for other dis-

---

[3]Note that for $\xi \gg 1$ the polarization operator is contracted to a single point (we do not consider the recollision contribution discussed in Chap. 4). Therefore, the integro-differential equation [see Eq. (2.44)] turns into an ordinary differential equation.

cussions of refractive indices and birefringence see e.g. [Aff88; BB67; BB70; BMS76; DG00; Din+14b] and the reviews [BR13; Di+12; MS06]).

2.3.3. Exponential wave-function decay

Due to the imaginary part of the polarization operator, the photon wave function decays exponentially (as expected for an unstable particle). During the calculation of the pair-creation probability the exponential decay of the wave function must be considered as soon as the approximation $W(q) \ll 1$ breaks down [see Eq. (2.11)].

The total probability that a photon with polarization four-vector $\epsilon_j^\mu = \Lambda_j^\mu$ does not decay inside the laser pulse is obtained by evaluating the square of the exact wave function at $kx \to \infty$, it is given by [BI70]

$$W_{q,j}^{\mathrm{s}} = \exp\left\{ \frac{1}{kq} \int\limits_{-\infty}^{+\infty} d\phi' \, \Im[\mathfrak{p}_j(\phi')] \right\}. \tag{2.50}$$

As the imaginary part of the polarization operator is related to the pair-creation diagram (without radiative corrections) via the optical theorem [see Eq. (2.29)]

$$W_j(q) = \frac{1}{kq} \, \Im \left[\Lambda_{j\mu} \Lambda_{j\nu} \, \Pi^{\mu\nu}(q,q) \right], \tag{2.51}$$

the survival probability can be expressed as

$$W_{q,j}^{\mathrm{s}} = \exp[-W_j(q)] \approx 1 - W_j(q) \tag{2.52}$$

[the last relation holds only if $W_j(q)$ is much smaller than unity]. Thus, $W_j(q)$ must be interpreted as the decay exponent for the photon wave function if it becomes large [nevertheless, we call $W_j(q)$ simply the probability for pair creation, keeping Eq. (2.52) in mind].

2.4. Total pair-creation probability

The total nonlinear Breit-Wheeler pair-creation probability is obtained by inserting the reduced matrix element given in Eq. (2.13) into Eq. (2.11). However, the phase-space integrals are highly oscillating in the regime $\xi \gg 1$ and a direct numerical calculation is tedious (see Sec. 2.6) [KK12a; Tit+12].

In order to circumvent this difficulty, we utilize the optical theorem [see Eq. (2.29)]. By applying it to the double-integral representation for the field-dependent part of the polarization operator given in Eq. (3.132), we obtain compact expressions for the total nonlinear Breit-Wheeler pair-creation probability $W(q)$ [see Eq. (2.11)]. For a single on-shell photon with four-momentum q^μ and polarization four-vector ϵ^μ, colliding with a plane-wave laser pulse described by the field tensor $F^{\mu\nu}(\phi) = f_1^{\mu\nu}\psi_1'(\phi) + f_2^{\mu\nu}\psi_2'(\phi)$ [see Eq. (1.17)] the total pair-creation

probability is given by

$$W(q) = -\frac{1}{kq}\frac{\alpha}{2\pi}\int\limits_0^\infty \frac{d\varrho}{\varrho}\int\limits_{-\infty}^{+\infty}dy^-\Im\,\epsilon_\mu\epsilon_\nu^*\big[P_{12}\Lambda_1^\mu\Lambda_2^\nu$$
$$+ P_{21}\Lambda_2^\mu\Lambda_1^\nu + P_{11}\Lambda_1^\mu\Lambda_1^\nu + P_{22}\Lambda_2^\mu\Lambda_2^\nu\big], \quad (2.53)$$

where [see Eq. (1.48)]

$$\Lambda_1^\mu = \frac{f_1^{\mu\nu}q_\nu}{kq\sqrt{-a_1^2}}, \quad \Lambda_2^\mu = \frac{f_2^{\mu\nu}q_\nu}{kq\sqrt{-a_2^2}} \tag{2.54}$$

and the coefficients P_{ij} [see Eq. (3.133)] are evaluated at $q_1 = q_2 = q$, $q^2 = 0$ [P_Q does not contribute for $q\epsilon = q^2 = 0$, which can be seen from the definition of the four-vectors $\mathcal{Q}_i^\mu$].

2.4.1. Linearly polarized laser fields

We consider now the important case of a linearly polarized background field [$\xi = \xi_1$, $\xi_2 = 0$; $\psi_1(\phi) = \psi(\phi)$, $\psi_2(\phi) = 0$; $F^{\mu\nu} = \psi'(\phi)f^{\mu\nu}$, $f^{\mu\nu} = k^\mu a^\nu - k^\nu a^\mu$, $P_{12} = P_{21} = 0$]. It is then useful to introduce the following two polarization four-vectors (see App. E for a detailed discussion of possible photon polarizations)

$$\epsilon_\parallel^\mu = \Lambda_1^\mu, \quad \epsilon_\perp^\mu = \Lambda_2^\mu. \tag{2.55}$$

They are real and obey $\epsilon_\parallel^2 = \epsilon_\perp^2 = -1$, $\epsilon_\parallel\epsilon_\perp = 0$. The index denotes the polarization direction of the photon with respect to the electric field of the laser (in the frame where the incoming photon and the laser pulse collide head-on).

Accordingly, we obtain for the total pair-creation probability in a linearly polarized laser pulse by an on-shell photon with polarization four-vector $\epsilon_\parallel^\mu$ and $\epsilon_\perp^\mu$ [see Eq. (2.53)]

$$
\begin{aligned}
W_\parallel(q) &= -\alpha\frac{m^2}{kq}\frac{1}{2\pi}\int\limits_{-\infty}^{+\infty}dy^-\int\limits_0^\infty\frac{d\varrho}{\varrho}\,\Im\,\widetilde{P}_{11}, \\
W_\perp(q) &= -\alpha\frac{m^2}{kq}\frac{1}{2\pi}\int\limits_{-\infty}^{+\infty}dy^-\int\limits_0^\infty\frac{d\varrho}{\varrho}\,\Im\,\widetilde{P}_{22},
\end{aligned}
\tag{2.56}
$$

where [see Eq. (3.133)]

$$\widetilde{P}_{11} = -\frac{i}{\varrho}\frac{kq}{m^2}\Big[\mathcal{W}_2(x_1)e^{-i4x_1} - \mathcal{W}_2(x_0)e^{-i4x_0}\Big]$$
$$+ \xi^2\Big[\frac{1}{2}V\mathcal{W}_0(x_1) + 2X\mathcal{W}_1(x_1)\Big]e^{-i4x_1},$$
$$\widetilde{P}_{22} = -\frac{i}{\varrho}\frac{kq}{m^2}\Big[\mathcal{W}_2(x_1)e^{-i4x_1} - \mathcal{W}_2(x_0)e^{-i4x_0}\Big] + \xi^2\frac{1}{2}V\mathcal{W}_0(x_1)e^{-i4x_1}$$

$[V = V_1, X = X_{11}$, see Eq. (3.137); x_0 and x_1 are defined in Eq. (3.135) and $\mathcal{W}_l(x)$ in Eq. (G.2)].

2.4.2. Quasistatic approximation for strong background fields

As the integrals in Eq. (2.56) are oscillatory, it is useful to derive non-oscillatory representations for important limits. In this section we consider a strong $(\xi \gg 1)$, linearly polarized background field. In this case the field-dependent contribution to the polarization operator can be written as [see Eq. (3.102)]

$$
i\mathcal{P}^{\mu\nu}(q_1, q_2) - i\mathcal{P}^{\mu\nu}_{\mathfrak{F}=0}(q_1, q_2) = i(2\pi)^3 \delta^{(-,\perp)}(q_1 - q_2) \int\limits_{-\infty}^{+\infty} dz^- \, e^{i(q_2^+ - q_1^+)z^-}
$$
$$
\times \left[\pi_1' \frac{(fq)^\mu (fq)^\nu}{(fq)^2} + \pi_2' \frac{(f^*q)^\mu (f^*q)^\nu}{(f^*q)^2} - \frac{\pi_3'}{q_1 q_2} G^{\mu\nu} \right], \quad (2.57)
$$

where $f^{*\mu\nu} = \frac{1}{2}\epsilon^{\mu\nu\rho\sigma} f_{\rho\sigma}$ and

$$
\pi_1' = \alpha \frac{m^2}{3\pi} \int\limits_{-1}^{+1} dv \, (w-1) \left[\frac{|\chi(kz)|}{w} \right]^{2/3} f'(\rho),
$$

$$
\pi_2' = \alpha \frac{m^2}{3\pi} \int\limits_{-1}^{+1} dv \, (w+2) \left[\frac{|\chi(kz)|}{w} \right]^{2/3} f'(\rho), \quad (2.58)
$$

$$
\pi_3' = -\alpha \frac{q_1 q_2}{\pi} \int\limits_{-1}^{+1} dv \, \frac{f_1(\rho)}{w},
$$

with $\frac{1}{w} = \frac{1}{4}(1 - v^2)$, $\rho = \left[\frac{w}{|\chi(kz)|} \right]^{2/3} (1 - \frac{q_1 q_2}{m^2} \frac{1}{w})$, $\chi(kz) = \chi \psi'(kz)$ and $G^{\mu\nu} = q_2^\mu q_1^\nu - q_1 q_2 \, g^{\mu\nu}$. Furthermore, the Ritus functions are defined by [see App. F]

$$
f(x) = i \int\limits_0^\infty dt \, \exp\left[-i(tx + t^3/3) \right] = \pi \, \mathrm{Gi}(x) + i\pi \, \mathrm{Ai}(x),
$$
$$
f_1(x) = \int\limits_0^\infty \frac{dt}{t} \exp\left(-itx \right) \left[\exp\left(-it^3/3 \right) - 1 \right]
$$

(2.59)

and the integration variable can be changed using

$$
\int\limits_{-1}^{+1} dv = 2 \int\limits_0^1 dv = \int\limits_4^\infty dw \, \frac{4}{w\sqrt{w(w-4)}} \quad (2.60)
$$

(valid for integrands which are even functions of v).

To determine the pair-creation probabilities we apply now the optical theorem

given in Eq. (2.29) to Eq. (2.57) and note the identities [see Eq. (1.48)]

$$\Lambda_1^\mu \Lambda_1^\nu = -\frac{(fq)^\mu (fq)^\nu}{(fq)^2}, \quad \Lambda_2^\mu \Lambda_2^\nu = -\frac{(f^*q)^\mu (f^*q)^\nu}{(f^*q)^2}. \tag{2.61}$$

Finally, the total probability for the decay of a single on-shell photon with four-momentum q^μ and polarization four-vector $\epsilon_\parallel^\mu$ ($\epsilon_\perp^\mu$) into an electron-positron pair inside a strong ($\xi \gg 1$, $\chi < \xi$), linearly polarized laser pulse with field tensor $F^{\mu\nu}(kx) = f^{\mu\nu}\psi'(\phi)$ is given by

$$W_\parallel(q) = -\alpha \frac{m^2}{kq} \int\limits_{-\infty}^{+\infty} d\phi \int\limits_{-1}^{+1} dv \, \frac{(w-1)}{3} \frac{\mathrm{Ai}'(\tilde{x})}{\tilde{x}},$$

$$W_\perp(q) = -\alpha \frac{m^2}{kq} \int\limits_{-\infty}^{+\infty} d\phi \int\limits_{-1}^{+1} dv \, \frac{(w+2)}{3} \frac{\mathrm{Ai}'(\tilde{x})}{\tilde{x}}, \tag{2.62}$$

where $\frac{1}{w} = \frac{1}{4}(1 - v^2)$, $\tilde{x} = [w/|\chi(\phi)|]^{2/3}$ and $\chi(\phi) = \chi\psi'(\phi)$ (due to $q\epsilon = q^2 = 0$ the coefficient π_3' does not contribute). We point out that Eq. (2.62) holds for an arbitrary shape of the plane-wave background field (χ should be such that $\alpha\chi^{2/3} \ll 1$, otherwise perturbation theory with respect to the radiation field is expected to break down [Di+12; Rit85]). As the formation region is small for $\xi \gg 1$, the total pair-creation probability given in Eq. (2.62) consists essentially of the probability to create a pair inside a constant-crossed field (see [Rit72a], Eq. (64) and [Rit85], Chap. 5, Eq. (60); see also [BKS98]), integrated over the pulse shape [$\chi(\phi)$ represents the instantaneous value of the quantum-nonlinearity parameter].

For comparison with the literature we consider now the monochromatic limit of Eq. (2.62), i.e. $\psi'(\phi) = \sin(\phi)$ and a counterpropagating photon. As the wave is periodic, we can split the integral in ϕ and consider only a single half-cycle (i.e. $\phi \in [0, \pi]$). As the photon is counterpropagating, it passes this half-cycle in the time $T/4$, where the laser period is given by $T = 2\pi/\omega$. Correspondingly, the rate for pair creation by a single photon inside a strong ($\xi \gg 1$), linearly polarized, monochromatic plane wave field is given by

$$W_\parallel(q) = -\alpha \frac{m^2}{q^0} \frac{1}{\pi} \int\limits_0^\pi d\phi \int\limits_{-1}^{+1} dv \, \frac{(w-1)}{3} \frac{\mathrm{Ai}'(x_m)}{x_m},$$

$$W_\perp(q) = -\alpha \frac{m^2}{q^0} \frac{1}{\pi} \int\limits_0^\pi d\phi \int\limits_{-1}^{+1} dv \, \frac{(w+2)}{3} \frac{\mathrm{Ai}'(x_m)}{x_m}, \tag{2.63}$$

where now $x_m = [w/|\chi_m(\phi)|]^{2/3}$, $\chi_m(\phi) = \chi\sin(\phi)$ [$\frac{1}{w} = \frac{1}{4}(1 - v^2)$]. Equation (2.63) coincides with the result obtained in [Rit85] [Chap. 3, Eq. (35) and Chap. 5, Eq. (60)]. It is also in agreement with the results obtained in [BMS76].

2.4.3. Small quantum parameter (exponential suppression)

For $\chi \ll 1$ the pair-creation probability is exponentially suppressed. This becomes obvious from the asymptotic expansion of the Airy function [Olv+10]

$$\mathrm{Ai}'(x) \sim -\frac{x^{1/4}\,e^{-\frac{2}{3}x^{3/2}}}{2\sqrt{\pi}}. \tag{2.64}$$

In this regime we can approximately evaluate the integrals in Eq. (2.62), resulting in a compact expression for the pair-creation probability. As the pair-creation probability is exponential suppressed, only the region around the peak of the field strength contributes to the integral in ϕ. Furthermore, we see from Eq. (2.60) that the integral in w is formed around $w = 4$. Correspondingly, we can use the relation

$$\int\limits_{4}^{\infty} dw\,\frac{1}{\sqrt{w-4}}e^{-xw} = e^{-4x}\sqrt{\frac{\pi}{x}} \tag{2.65}$$

(for $x > 0$) to evaluate the integral in w approximately. Assuming that $|\psi'(\phi)| \approx |\sin(\phi)|$ close to a field peak, the contribution from each peak can be approximately taken into account using

$$\int\limits_{0}^{\pi} d\phi\,e^{-x/\sin(\phi)} \approx \int\limits_{-\infty}^{+\infty} d\phi\,e^{-x(1+\phi^2/2)} = e^{-x}\sqrt{\frac{2\pi}{x}} \tag{2.66}$$

(if $x > 0$; for different peak shapes this relation must be modified accordingly). Combining everything, the pair-creation probability within a single peak of a linearly polarized, plane-wave laser field is in the regime $\xi \gg 1$, $\chi \ll 1$ given by

$$W_\parallel(q) = \alpha\,\frac{m^2}{kq}\frac{3\sqrt{\pi}}{8}\left(\frac{\chi}{2}\right)^{3/2}e^{-8/(3\chi)}, \tag{2.67}$$

$W_\perp(q) = 2W_\parallel(q)$. From Eq. (2.67) the pair-creation rate inside monochromatic fields can be obtained similar as above [see Eq. (2.63)]. To this end we consider again a photon counterpropagating with a monochromatic wave. A counterpropagating photon passes four field maxima during the time of one laser period $T = 2\pi/\omega$. Correspondingly, the pair-creation rate for a single photon is given by (linear polarization, $\xi \gg 1$, $\chi \ll 1$)

$$W_\parallel(q) = \alpha\,\frac{m^2}{q^0}\frac{3}{8\sqrt{\pi}}\left(\frac{\chi}{2}\right)^{3/2}e^{-8/(3\chi)}, \tag{2.68}$$

$W_\perp(q) = 2W_\parallel(q)$. The result agrees with [Rit85], Chap. 3, Eq. (33) (see also [Rei62]).

Fig. 10: Total pair-creation probability for a single photon inside a linearly polarized laser pulse ($\phi_0 = 0$, $N = 5$, $\chi = 1$). The full numerical calculation [black dots, see Eq. (2.56)] is compared with the local constant-crossed field approximation [valid for $\xi \gg 1$, dotted line, see Eq. (2.62)]. Allready for $\xi \gtrsim 10$ both results are in very good agreement.
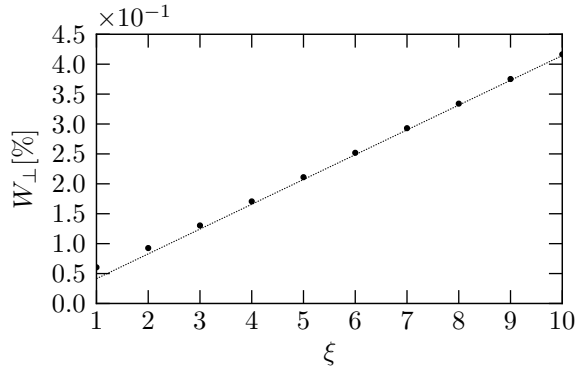
Fig. 11: Comparison between the full numerical calculation of the pair-creation probability [solid lines, see Eq. (2.56)] and the constant-crossed field approximation [valid for $\xi \gg 1$, dotted lines, see Eq. (2.62)] for $\xi = 1.0$, 1.25, 1.5, 1.75 and 2.0 (lower to upper curve), $N = 5$, $\chi = 1$. Besides underestimating the probability, the strong-field approximation fails to reproduce the correct CEP dependence in the regime $\xi \lesssim 1$.
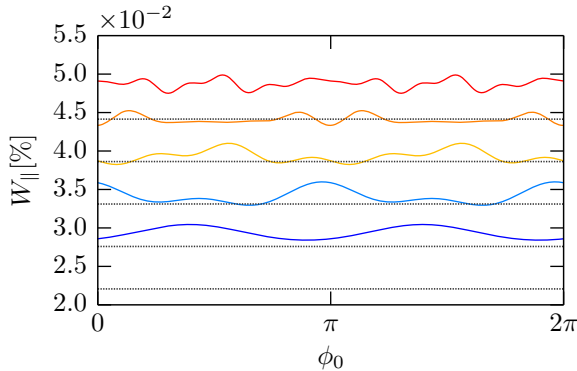
2.5. Numerical results for the total pair-creation probability

To determine for which experimental parameters the observation of the nonlinear Breit-Wheeler process is feasible, the total pair-creation probability is now evaluated numerically for a linearly polarized laser pulse. We consider its dependence on the classical intensity parameter ξ [see Eq. (1.20)], the quantum-nonlinearity parameter χ [see Eq. (1.21)], the number of cycles N and the carrier-envelope phase (CEP) ϕ_0 of the pulse. Furthermore, we compare a $\sin^2$ [see Eq. (1.23)] with a $\sin^4$-pulse [see Eq. (1.24)].

As the pair-creation probability is exponentially suppressed for $\chi \ll 1$ [see Eq. (2.67)], we are mainly interested in the nonlinear quantum regime where $\chi \gtrsim 1$. Existing optical petawatt laser systems reach already $\xi \sim 100$ [Yan+08] and photon energies $\sim 1\,\text{GeV}$ are obtainable via Compton backscattering either at conventional facilities like SPring8 [Mur+14; SPring8] or by using laser wakefield accelerators [ESL09; Lee+06; Phu+12; Pow+14; Wan+13]. Hence, it is possible to reach the regime $\chi \gtrsim 1$ with presently available technology.

2.5.1. Breakdown of the constant-crossed field approximation

In the following we will not consider the influence of the incoming photon wave packet and set $W = W(q)$, see Eq. (2.11). For $\xi \gg 1$ the total pair-creation probability can be calculated using Eq. (2.62) without further numerical difficulties, as the integrals are non-oscillatory. To verify the validity of the local constant-crossed field approximation [see Eq. (2.62)], we have compared it with the general expression given in Eq. (2.56) (the oscillatory integrals have been
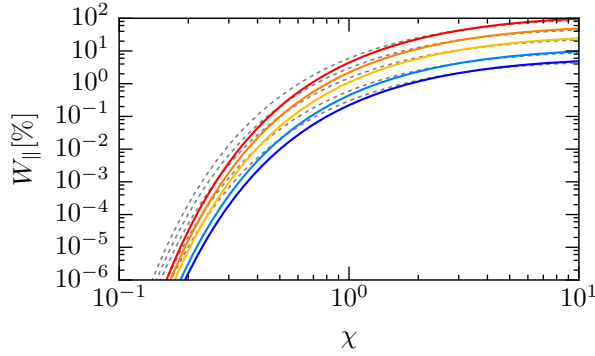
Fig. 12: Dependence of the pair-creation probability on ξ and χ ($\phi_0 = 0$, $N = 5$). For $\xi \gtrsim 1$ the pair-creation probability increases linearly with ξ (we plotted the values $\xi = 10, 20, 50, 100$ and 200, lower to upper curve). In the regime $\chi \ll 1$ pair creation is exponentially suppressed [pulse shape $\psi'(\phi)$ (solid lines), see Eq. (1.23) and $\widetilde{\psi}'(\phi)$ (dashed lines), see Eq. (1.24)].

evaluated numerically as explained in Sec. 4.5). The result is shown in Fig. 10. Already for $\xi \lesssim 10$ both equations are in good agreement. However, for $\xi \sim 1$ the constant-crossed field approximation fails to predict the CEP dependence of the total probability (see Fig. 11). As the formation region scales as $1/\xi$, the global structure of the pulse within the formation region itself [which is not included in the constant-crossed field approximation, see Eq. (2.62)] becomes important at $\xi \sim 1$.

From now on we consider the experimentally interesting regime $\xi \gg 1$ and use Eq. (2.62) to determine the total pair-creation probability. Furthermore, we compare two different pulse shapes. Solid lines are calculated using the $\sin^2$-envelope [see Eq. (1.23)], dashed lines using the $\sin^4$-envelope [see Eq. (1.24)]. In general, the results do not depend strongly on the pulse shape. However, in the regime where pair creation is exponentially suppressed ($\chi \ll 1$), the $\sin^4$-envelope is favorable, as it implies a higher peak field strength (see Fig. 3).

2.5.2. Dependence on the nonlinear quantum parameter

In Fig. 12 we plot the total pair-creation probability as a function of the parameters ξ and χ. For $\xi \gtrsim 1$ it scales linear in ξ due to the phase-space prefactor m^2/kq [see Eq. (2.62)] and only the dependence on χ is nontrivial [Rit85]. Around $\chi \sim 1$ the pair-creation probability becomes sizable and is no longer exponentially suppressed [see Eq. (2.67)] [Rit85].

2.5.3. Importance of the exponential wave-function decay

As explained in Sec. 2.3, the quantities $W_{\parallel,\perp}$ only represent the total pair-creation probability as long as they are much smaller than unity. In general, one has to consider the total probability for the decay of a photon with a given polarization [see Eq. (2.52)]

$$W_{\parallel,\perp}^d = 1 - W_{\parallel,\perp}^s = 1 - \exp[-W_{\parallel,\perp}] \approx W_{\parallel,\perp}. \tag{2.69}$$

In Fig. 13 we have compared both quantities to show when this difference becomes relevant. We point out that the decay of the photon is necessarily accompanied by the creation of at least one electron-positron pair.

In Fig. 14 we have plotted the parameter regime accessible by combining a petawatt laser system ($\xi = 100$) with a GeV photon source. Accordingly, it is

Fig. 13: Comparison between the photon-decay probability $W_\parallel^d$ (solid lines) and the pair-creation probability $W_\parallel$ obtained from the leading-order Feynman diagram shown in Fig. 6, i.e. without including radiative corrections (dashed lines). As long as the probability is small, both quantities agree. However, for $W_\parallel \sim 1$ it is important to note that $W_\parallel$ represents the decay exponent of $W_\parallel^d$ [see Eq. (2.52), the parameters are as in Fig. 12, the pulse shape is given by $\psi'(\phi)$].
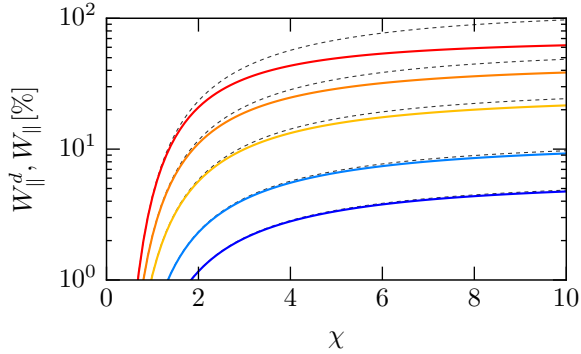
Fig. 14: Total photon-decay probability during the head-on collision between a gamma photon with energy ω_γ and a linearly polarized laser pulse with the following parameters: $\phi_0 = 0$, $N = 5$, $\omega = 1.55\,\text{eV}$, $\xi = 100$ [pulse shape $\psi'(\phi)$ (solid lines), see Eq. (1.23) and $\widetilde{\psi}'(\phi)$ (dotted lines), see Eq. (1.24)]. For parallel polarization ($W_\parallel^d$) the probabilities are smaller than for orthogonal polarization ($W_\perp^d$).
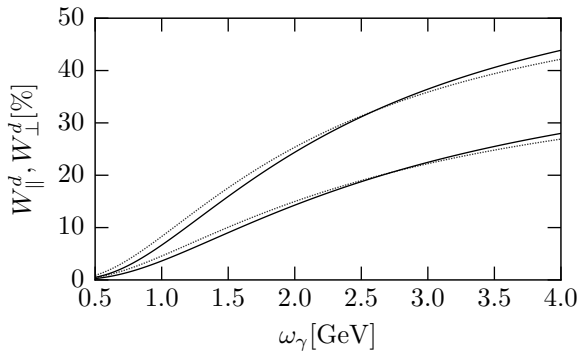
possible to obtain a large pair-creation yield even with a limited number of highly energetic photons. As expected from Eq. (2.67), the pair-creation probability for perpendicular polarization ($W_\perp$) is roughly twice as large as for parallel polarization ($W_\parallel$). Correspondingly, $W_\parallel$ can be considered as a lower bound (which is the reason why we mainly focused on this polarization).

2.5.4. Dependence on the pulse length and the CEP

The dependence of the total pair-creation probability on the pulse length N is shown in Fig. 15. As expected, the scaling in the pulse length is roughly linear in the regime $\chi \sim 1$.

Fig. 15: The scaling of the pair-creation probability is roughly linear in the pulse length (we plotted $N = 3, 5, 7, 9$ and 11, lower to upper curve; $\phi_0 = 0$, $\xi = 10$) [pulse shape $\psi'(\phi)$ (solid lines), see Eq. (1.23) and $\widetilde{\psi}'(\phi)$ (dashed lines), see Eq. (1.24)].
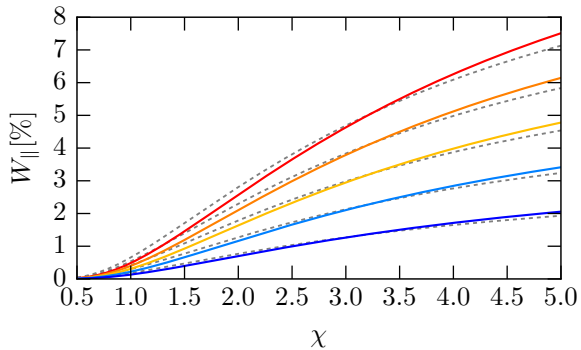
Due to the fact that the pair-creation probability is exponentially suppressed for $\chi \ll 1$, it depends very sensitively on the maximum field strength in this regime and large CEP effects can be expected. To investigate them, we introduce the CEP-averaged pair-creation probability

$$\langle W_{\parallel,\perp} \rangle = \frac{1}{2\pi} \int\limits_0^{2\pi} d\phi_0 \, W_{\parallel,\perp}(\phi_0) \tag{2.70a}$$

and the relative deviation

$$\Delta W_{\parallel,\perp}(\phi_0) = \frac{W_{\parallel,\perp}(\phi_0) - \langle W_{\parallel,\perp} \rangle}{\langle W_{\parallel,\perp} \rangle}. \tag{2.70b}$$

They are plotted in Fig. 16 and Fig. 17, respectively, for a short pulse ($N = 3$) of moderate intensity ($\xi = 10$). For $\chi \approx 0.2$ the relative CEP effect is of the order of 10%, but many photons are needed to produce a sufficient amount of electron-positron pairs. In the regime where pair creation is likely ($\chi \sim 1$), the CEP effect for the total pair-creation probability is very small (we point out that this prediction could be changed by higher-order corrections).
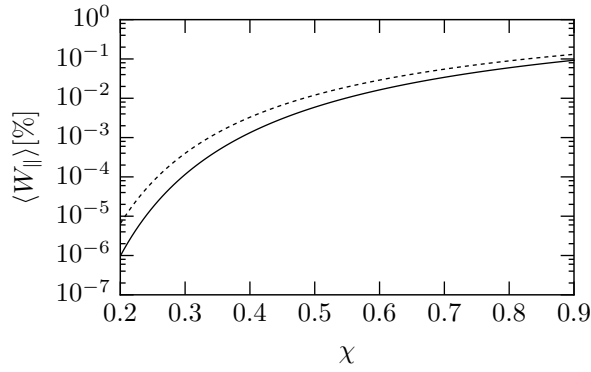
Fig. 16: The total pair-creation probability as a function of the quantum-nonlinearity parameter χ averaged over the CEP phase [see Eq. (2.70), $\xi = 10$ and $N = 3$]. The solid line correspond to the pulse shape $\psi'(\phi)$ [see Eq. (1.23)] and the dashed line to the pulse shape $\widetilde{\psi}'(\phi)$ [see Eq. (1.24)].

(a) $\sin^2$ envelope

(b) $\sin^4$ envelope
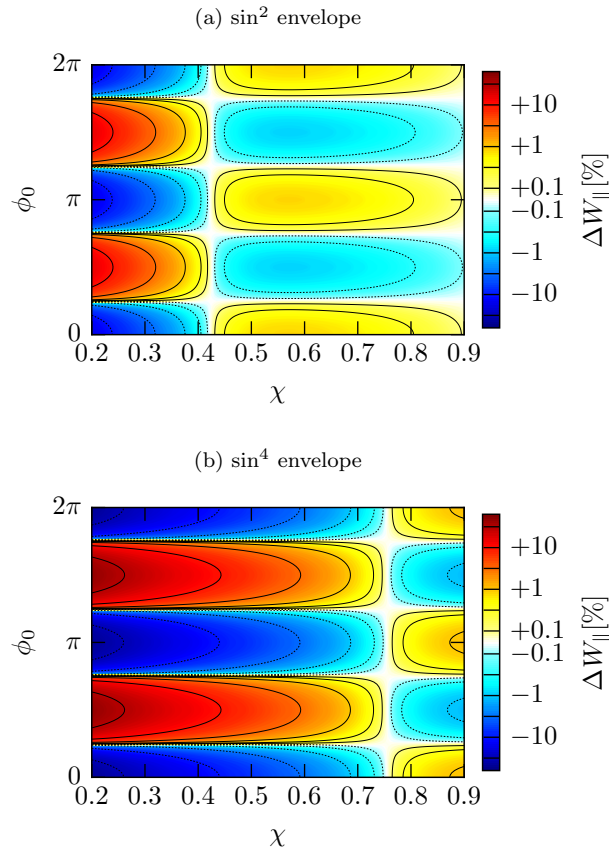
Fig. 17: The relative pair-creation probability [see Eq. (2.70)] as a function of the quantum-nonlinearity parameter χ and the CEP ϕ_0 ($\xi = 10$ and $N = 3$, for the CEP-averaged probability see Fig. 16). We used the pulse shape $\psi'(\phi)$ [see Eq. (1.23)] for the upper and $\widetilde{\psi}'(\phi)$ [see Eq. (1.24)] for the lower plot. The dependence on the CEP is quite pronounced for $\chi \ll 1$, where, however, the total probability is strongly suppressed (the intermediate color levels are located at $10^{-1/2} \approx 0.32$, $10^{1/2} \approx 3.2$ and $10^{3/2} \approx 32$).

65

2.6. Differential pair-creation probability

In the first part of this chapter we primarily considered the total pair-creation probability. In particular, we showed in Sec. 2.5 that the experimental observation of the nonlinear Breit-Wheeler process is feasible with existing technology. Therefore, also the differential probability (i.e. the asymptotic momentum distribution of the produced pairs) is of interest for upcoming experiments. The second part of this chapter focuses on its calculation and establishes an intuitive semiclassical picture for the pair-creation process valid in the regime $\xi \gg 1$.

2.6.1. Spectrum in light-cone coordinates

The calculation of the differential pair-creation probability simplifies considerably if the canonical light-cone basis (see Sec. 1.4.3)

$$k^\mu, \quad \bar{k}^\mu = \frac{1}{kq}q^\mu, \quad e_i^\mu = \Lambda_i^\mu = \frac{f_i^{\mu\nu}q_\nu}{kq\,\sqrt{-a_i^2}} \tag{2.71}$$

is used [q^μ denotes the four-momentum of the incoming photon ($q^2 = 0$), the trivial case $kq = 0$ is excluded]. Therefore, we expand the four-momentum p_1^μ (p_2^μ) of the created electron (positron) in the following way [see Eq. (1.93)]

$$p_1^\mu = r'q^\mu + s'k^\mu + t_1'm\Lambda_1^\mu + t_2'm\Lambda_2^\mu, \tag{2.72a}$$

$$p_2^\mu = -rq^\mu - sk^\mu - t_1m\Lambda_1^\mu - t_2m\Lambda_2^\mu \tag{2.72b}$$

($t_i' = t_i$ and $r' = r + 1$ due to momentum conservation). The notation for the momenta (see Fig. 18) agrees with the one used in Chap. 1 for the dressed vertex (see Sec. 1.6) if $p'^\mu = p_1^\mu$ and $p^\mu = -p_2^\mu$ (this is always assumed in the following).

In Eq. (2.72) the quantities

$$s = \frac{1}{2r}\frac{m^2}{kq}(1 + t_1^2 + t_2^2), \quad s' = \frac{1}{2r'}\frac{m^2}{kq}(1 + t_1^2 + t_2^2) \tag{2.73}$$

are determined by the on-shell conditions $p_1^2 = p_2^2 = m^2$ [see Eq. (1.94)]. Corre-
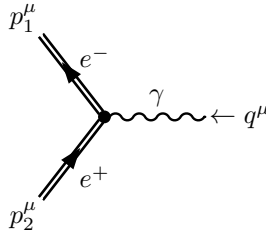
Fig. 18: Notation used throughout the calculation of the asymptotic electron (positron) momentum distribution (see also Fig. 6). The four-momenta of the electron and the positron are denoted by p_1^μ and p_2^μ, respectively, and the incoming photon four-momentum by q^μ. The particles are all on shell, i.e. $p_1^2 = p_2^2 = m^2$ and $q^2 = 0$.

spondingly, the amount n of absorbed laser photons is related to the introduced Lorentz invariant momentum parameters as follows [see Eq. (1.95)]

$$p_1^\mu + p_2^\mu = q^\mu + nk^\mu, \quad n = \frac{1}{2}w\frac{m^2}{kq}(1 + t_1^2 + t_2^2). \tag{2.74}$$

According to Eq. (2.11) the total pair-creation probability is given by

$$W(q) = \sum_{\text{spin}} \int \frac{d^3p_1\,d^3p_2}{(2\pi)^6\,2\epsilon_{\boldsymbol{p}_1}2\epsilon_{\boldsymbol{p}_2}}\,\frac{1}{2kq}\,|\mathcal{M}(p_1,p_2;q)|^2\,(2\pi)^3\delta^{(-,\perp)}(p_1 + p_2 - q)$$

$$= \sum_{\text{spin}} \int_{-1}^{0} dr \int_{-\infty}^{+\infty} dt_1 dt_2\,\frac{m^2}{(kq)^2}\frac{1}{8(-rr')}\frac{1}{(2\pi)^3}\,|\mathcal{M}(p_1,p_2;q)|^2, \tag{2.75}$$

where $i\mathcal{M}(p_1,p_2;q) = \epsilon_\mu\,\bar{u}_{p_1}\mathcal{G}^\mu(p_1,q,-p_2)v_{p_2}$ is the reduced matrix element for the process [see Eq. (2.9)], $\mathcal{G}^\mu$ the nonsingular part of the dressed vertex [see Eq. (1.79)], ϵ^μ the polarization four-vector of the incoming photon and u_{p_1} and v_{p_2} the Dirac spinors for the electron and the positron, respectively. Furthermore, we used Eq. (1.51) to rewrite the on-shell integrals in light-cone coordinates and [see Eqs. (2.71) and (2.72)]

$$\begin{aligned} p^- &= kp = rkq, \quad p^{\mathrm{I}} = p\Lambda_1 = -mt_1, \\ p^+ &= \bar{k}p = s, \qquad p^{\mathrm{II}} = p\Lambda_2 = -mt_2. \end{aligned} \tag{2.76}$$

After introducing the parameters [see Eq. (1.84)]

$$R = r + \frac{1}{2} = \frac{kp_1 - kp_2}{2kq} = \frac{1}{2}\frac{kp_1 - kp_2}{kp_1 + kp_2}, \quad w = -\frac{1}{r(r+1)} = \frac{4}{1 - 4R^2} \tag{2.77}$$

we obtain the final result

$$W(q) = \int_{-1/2}^{+1/2} dR \int_{-\infty}^{+\infty} dt_1 dt_2\,\frac{d^3W}{dRdt_1dt_2},$$

$$\frac{d^3W}{dRdt_1dt_2} = \frac{m^2}{(kq)^2}\frac{w}{8}\frac{1}{(2\pi)^3}\sum_{\text{spin}}|\mathcal{M}(p_1,p_2;q)|^2. \tag{2.78}$$

For a head-on collision the parameters t_i are related to the transverse momentum of the created pair, whereas for electrons and positrons created ultra-relativistic the parameter R is half the asymmetry of the asymptotic energies of the electron and the positron.

2.6.2. Evaluation of the trace

To determine the spectrum using Eq. (2.78) we have to analyze the square of the reduced matrix element

$$\sum_{\text{spin}} \mathcal{M}\mathcal{M}^* = \epsilon_\mu\epsilon_\nu^*\mathcal{M}^{\mu\nu}(p_1,p_2), \quad \mathcal{M}(p_1,p_2;q) = \epsilon_\mu\,\bar{u}_{p_1}\mathcal{G}^\mu(p_1,q,-p_2)v_{p_2}, \tag{2.79}$$

which contains the following trace

$$\mathcal{M}^{\mu\nu}(p_1, p_2) = -e^2 \, \mathbf{tr}[...]^{\mu\nu}(p' \to p_1, p \to -p_2),$$
$$e^2 \, \mathbf{tr}[...]^{\mu\nu} = \mathbf{tr}\, \mathcal{G}^{\mu}(p', q, p)(\slashed{p} + m)\bar{\mathcal{G}}^{\nu}(p', q, p)(\slashed{p}' + m). \tag{2.80}$$

As shown in Sec. 1.6.5 the nonsingular part of the dressed vertex can be expressed in terms of only a few master integrals [see Eq. (1.92)]

$$\mathcal{G}^{\rho}(p', q, p) = (-ie)\Bigg\{\gamma_{\mu}\Big[\mathfrak{G}_0 g^{\mu\rho} + \sum_{j=1,2} (G_1 \mathfrak{G}_{j,1} f_j^{\mu\rho} + G_2 \mathfrak{G}_{j,2} f_j^{2\mu\rho})\Big]$$
$$+ i\gamma_{\mu}\gamma^5 \sum_{j=1,2} G_3 \mathfrak{G}_{j,1} f_j^{*\mu\rho}\Bigg\}. \tag{2.81}$$

Therefore, we obtain the following result

$$\Lambda_{i,\mu}\Lambda_{j,\nu} \, \mathbf{tr}[...]^{\mu\nu} = \mathbf{tr}(\slashed{a} + i\slashed{b}\gamma^5)(\slashed{p} + m)(\slashed{c} - i\slashed{d}\gamma^5)(\slashed{p}' + m)$$
$$= 4(ac)(m^2 - pp') + 4[(ap)(cp') + (ap')(cp)]$$
$$- 4(bd)(m^2 + pp') + 4[(bp)(dp') + (bp')(dp)]$$
$$+ 4\epsilon^{\mu\nu\rho\sigma}(b_{\mu}c_{\rho} - a_{\mu}d_{\rho})p_{\nu}p'_{\sigma}, \tag{2.82}$$

where the polarization four-vector ϵ^{μ} is expressed in terms of the four-vectors Λ_i^{μ} (see App. E) and

$$a^{\mu} = \mathfrak{G}_0\Lambda_i^{\mu} - \frac{m\xi_i}{e}G_1\mathfrak{G}_{i,1}k^{\mu}, \quad b^{\mu} = -(-1)^{i'}\frac{m\xi_{i'}}{e}G_3\mathfrak{G}_{i',1}\Lambda_5^{\mu},$$
$$c^{\mu} = \mathfrak{G}_0^*\Lambda_j^{\mu} - \frac{m\xi_j}{e}G_1\mathfrak{G}_{j,1}^*k^{\mu}, \quad d^{\mu} = -(-1)^{j'}\frac{m\xi_{j'}}{e}G_3\mathfrak{G}_{j',1}^*\Lambda_5^{\mu} \tag{2.83}$$

(we use the notation $1' = 2$ and $2' = 1$ for the indices). Correspondingly, the scalar products are given by

$$ac = -\delta_{ij}\,|\mathfrak{G}_0|^2, \quad bd = 0, \tag{2.84a}$$

$$\epsilon^{\mu\nu\rho\sigma}(b_{\mu}c_{\rho} - a_{\mu}d_{\rho})p_{\nu}p'_{\sigma}$$
$$= -\frac{m^2 kq}{e}G_3(-1)^{i'}(-1)^{j'}(\xi_{i'}t_{j'}\mathfrak{G}_0^*\mathfrak{G}_{i',1} + \xi_{j'}t_{i'}\mathfrak{G}_0\mathfrak{G}_{j',1}^*) \tag{2.84b}$$

and

$$ap = -t_i m\mathfrak{G}_0 - \frac{m\xi_i}{e}G_1\mathfrak{G}_{i,1}kq\,r, \quad bp = -(-1)^{i'}\frac{m\xi_{i'}}{e}G_3\mathfrak{G}_{i',1}\Lambda_5 q\,r, \tag{2.84c}$$

$$cp = -t_j m\mathfrak{G}_0^* - \frac{m\xi_j}{e}G_1\mathfrak{G}_{j,1}^*kq\,r, \quad dp = -(-1)^{j'}\frac{m\xi_{j'}}{e}G_3\mathfrak{G}_{j',1}^*\Lambda_5 q\,r \tag{2.84d}$$

[if p^μ is replaced by p'^μ we have to replace r by r' $(t_i = t'_i)$]. Furthermore, we conclude from Eq. (1.88) that

$$(kq)^2(G_1^2/e^2) = w(w/4 - 1), \quad (kq)^2(G_3^2/e^2) = \frac{1}{4}w^2,$$
$$kq(G_1/e)(r + r') = 2(w/4 - 1), \qquad kq(G_3/e) = -\frac{1}{2}w. \tag{2.85}$$

Finally, we obtain

$$\begin{aligned}
\Lambda_{i,\mu}\Lambda_{j,\nu}\,\mathbf{tr}[...]^{\mu\nu} = &- 4\delta_{ij}\,|\mathfrak{G}_0|^2\,(m^2 - pp') \\
&+ 4m^2\Big[2t_it_j\,|\mathfrak{G}_0|^2 - 2(w/4 - 1)\xi_i\xi_j\mathfrak{G}_{i,1}\mathfrak{G}_{j,1}^* \\
&+ 2(w/4 - 1)(\xi_it_j\mathfrak{G}_0^*\mathfrak{G}_{i,1} + \xi_jt_i\mathfrak{G}_0\mathfrak{G}_{j,1}^*)\Big] \\
&- 2m^2w\,(-1)^{i'}(-1)^{j'}\xi_{i'}\xi_{j'}\mathfrak{G}_{i',1}\mathfrak{G}_{j',1}^* \\
&+ 2m^2w\,(-1)^{i'}(-1)^{j'}(\xi_{i'}t_{j'}\mathfrak{G}_0^*\mathfrak{G}_{i',1} + \xi_{j'}t_{i'}\mathfrak{G}_0\mathfrak{G}_{j',1}^*),
\end{aligned} \tag{2.86}$$

where

$$m^2 - pp' = \frac{w}{2}m^2(1 + t_1^2 + t_2^2). \tag{2.87}$$

For a linearly polarized laser field ($\psi = \psi_1$, $\psi_2 = 0$, $\xi = \xi_1$) and an incoming photon with parallel polarization ($\epsilon^\mu = \Lambda_1^\mu$, see App. E), Eq. (2.86) simplifies and the trace is given by

$$\begin{aligned}
\Lambda_{1\mu}\Lambda_{1\nu}\,\mathbf{tr}[...]^{\mu\nu} = &\,2m^2(w - 4)\big[-\xi^2\,|\mathfrak{G}_{1,1}|^2 + 2\xi t_1\Re(\mathfrak{G}_0^*\mathfrak{G}_{1,1})\big] \\
&+ 4m^2\,|\mathfrak{G}_0|^2\,\big[-(w/2)(1 + t_1^2 + t_2^2) + 2t_1^2\big].
\end{aligned} \tag{2.88}$$

2.7. Semiclassical description

The decay of a photon into an electron-positron pair is an intrinsic quantum process, which has no classical analogue and must be described in the realm of quantum field theory using the S-matrix approach [Di+12; Rit85]. This implies that we can typically determine only the probability distribution for the asymptotic momenta and all details of the actual production process are hidden. However, it is well known that inside a relativistically strong ($\xi \gg 1$) plane-wave laser field the formation region of the basic QED processes nonlinear Compton scattering and nonlinear Breit-Wheeler pair production is much smaller than the laser wavelength. Hence, the total probability for nonlinear Compton scattering and nonlinear Breit-Wheeler pair production can be calculated by applying the local constant-crossed field approximation, i.e. by averaging the corresponding probability in a constant-crossed field over the laser pulse [Di+12; NNR65; NR64a; NR64b; NR67; Rei62; Rit85]. As pointed out by Ritus [Rit85], this procedure is justified for the calculation of the total probabilities but it may not work for differential probabilities, i.e. for determining the momentum distribution of the final particles (this has also been recently observed numerically in [HIK15] for nonlinear Compton scattering). In general, interference effects arising from processes occurring at different space-time points, which are neglected from the beginning when the averaging procedure is

applied to the probabilities, can play an important role [Rit85]. Nevertheless, this is the state-of-the-art approach for the implementation of strong-field QED processes in plasma codes [BK08; Bul+10a; Bul+13; Elk+11; Fed+10; Ner+11]. Therefore, it is desirable to estimate the error of this procedure and to show how the standard approach could be extended if necessary.

By applying a stationary-phase analysis to the leading-order S-matrix element for electron-positron photoproduction, we show here that for $\xi \gg 1$ all significant features of the momentum distribution for the created electron-positron pair are obtainable from the following three-step procedure:

❶ At each laser phase the pair-production probability amplitude is calculated using the local constant-crossed field approximation

❷ The asymptotic momenta for the electron and the positron are obtained by applying the classical equations of motion

❸ Interferences between pairs which have the same asymptotic momenta but originate from different formation regions are taken into account

In Chap. 4 this simpleman's model is extend to include also a possible recollision of the created pair (see Sec. 4.4).

Note that electron-positron photoproduction has a lot of commonalities with laser-induced ionization processes. In fact, the procedure outlined above is closely related to similar approaches used in atomic physics to describe the time evolution of an electron after tunnel ionization [Cor93; Koh+12; Kuc87] (a tunneling picture for pair creation was developed in Ref. [Wöl+15], see also Ref. [Di+09]).

2.7.1. Stationary-phase analysis

If the background field becomes very strong ($\xi \gg 1$), the master integrals [see Eq. (1.97)]

$$\mathfrak{G}_0(w, t_1, t_2) = \int\limits_{-\infty}^{+\infty} d\phi \, e^{i\tilde{S}_\Gamma(t_1, t_2; \phi)}, \quad \mathfrak{G}_{j,l}(w, t_1, t_2) = \int\limits_{-\infty}^{+\infty} d\phi \, [\psi_j(\phi)]^l e^{i\tilde{S}_\Gamma(t_1, t_2; \phi)}$$

(2.89)

are highly oscillatory due to the nonlinear term in the phase [see Eq. (1.99)]

$$\mathfrak{S}'_\Gamma(t_1, t_2; \phi) = 1 + \sum_{i=1,2} \left[t_i - \xi_i \psi_i(\phi) \right]^2$$

(2.90)

$[\tilde{S}_\Gamma(t_1, t_2; \phi) = (w/2)(m^2/kq)\mathfrak{S}_\Gamma(t_1, t_2; \phi);$ the prime denotes the derivative with respect to the laser phase ϕ] and a stationary-phase analysis is applicable.

Focusing on a linearly-polarized background field ($\psi_2 = 0$, $\xi = \xi_1$, $\psi = \psi_1$), only the term containing t_1 leads to strong oscillations in the regime $\xi \gg 1$. Therefore, the master integrals are dominated by small regions around the quasi-stationary points ϕ_k defined by $t_1 = \xi\psi(\phi_k)$. Close to each quasi-stationary point ϕ_k two

true stationary points $\phi_k^{\pm}$

$$\xi\psi(\phi_k^{\pm}) = t_1 \pm i\sqrt{1 + t_2^2} \tag{2.91}$$

are located inside the complex plane but close to the real line. In the regime $\xi \gg 1$ the imaginary part in Eq. (2.91) scales as $1/\xi$ and the integral along the real line is dominated by the regions where $t_1 \approx \xi\psi(\phi_k)$ (see App. H) [Rit85]. In the following we call the quasi-stationary points ϕ_k simply stationary points and keep this subtlety in mind (an analogous situation is encountered for nonlinear Compton scattering [MD11]).

Furthermore, we assume that all stationary points are located sufficiently far away from each other, i.e. we ignore subtleties arising around the extremal points of $\psi(\phi)$ [note that pair production is ineffective in these regions, as $\psi'(\phi)$ is small]. After expanding the phase around a stationary point ϕ_k up to the cubic term we obtain

$$\begin{aligned}
\widetilde{S}_\Gamma(\phi) &\approx \widetilde{S}_\Gamma(\phi_k) + a(\phi - \phi_k) + \frac{1}{3}b(\phi - \phi_k)^3 \\
a &= \frac{w}{2}\frac{m^2}{kq}(1 + t_2^2), \quad b = \frac{w}{2}\frac{m^2}{kq}[\xi\psi'(\phi_k)]^2.
\end{aligned} \tag{2.92}$$

Since $a \sim \xi$ and $b \sim \xi^3$, the formation region $\delta\phi$ scales as ξ^{-1} and both the linear and the cubic term have to be taken into account. Higher-order terms of the expanded phase do not contribute (within the formation region) and can be neglected to leading order (a similar discussion can be found in Chap. 4 for recollision processes, see Sec. 4.2.2).

After the change of variables from ϕ to $t = \sqrt[3]{b}(\phi - \phi_k)$ the phase is approximately given by

$$\widetilde{S}_\Gamma(\phi) \approx \widetilde{S}_\Gamma(\phi_k) + xt + \frac{1}{3}t^3, \tag{2.93}$$

where

$$x = \frac{a}{\sqrt[3]{b}} = \left[\frac{w/2}{\chi(\phi_k)}\right]^{2/3}(1 + t_2^2), \quad \frac{1}{\sqrt[3]{b}} = \frac{2}{w}\frac{kq}{m^2}\left[\frac{w/2}{|\chi(\phi_k)|}\right]^{2/3}, \tag{2.94}$$

and $\chi(\phi) = \chi\psi'(\phi)$ denotes the local value of the quantum-nonlinearity parameter $\chi = (kq/m^2)\xi$ [see Eq. (1.21)].

After applying the expansions given in Eq. (2.92) to the master integrals defined in Eq. (1.89) we obtain [see Eq. (F.9)]

$$\mathfrak{G}_0(p', q, p) \approx \frac{kq}{m^2}\frac{2}{w}\left[\frac{w/2}{|\chi(\phi_k)|}\right]^{2/3} 2\pi\,\mathrm{Ai}(x)\,e^{i\widetilde{S}_\Gamma(p', q, p; \phi_k)}, \tag{2.95a}$$

$$\begin{aligned}
\mathfrak{G}_{1,1}(p', q, p) &\approx \frac{t_1}{\xi}\mathfrak{G}_0(p', q, p) \\
&- i\left(\frac{kq}{m^2}\frac{2}{w}\right)^2\psi'(\phi_k)\left[\frac{w/2}{|\chi(\phi_k)|}\right]^{4/3} 2\pi\,\mathrm{Ai}'(x)\,e^{i\widetilde{S}_\Gamma(p', q, p; \phi_k)}. \tag{2.95b}
\end{aligned}$$

Here we truncated the expansion of the preexponent after the linear term, i.e. we

used

$$\psi(\phi) \approx \psi(\phi_k) + \psi'(\phi_k)(\phi - \phi_k) = \frac{t_1}{\xi} + \psi'(\phi_k)(\phi - \phi_k) \tag{2.96}$$

as higher-order contributions vanish in the limit $\xi \to \infty$.

For a single stationary point, the well-known result for pair production within a constant-crossed field is obtained [after combining Eq. (2.88) and Eq. (2.95), see e.g. Ref. [NR67]]. In general, however, the phase factor in Eq. (2.95) leads to an interference between contributions of different stationary points (see Fig. 19).

2.7.2. Classical interpretation of the stationary points

In order to show that the stationary points have a classical interpretation, we consider now the classical evolution of the four-momenta p_1^μ and p_2^μ. According to Eq. (A.17) we obtain

$$\begin{aligned} p_1^\mu(\phi) &= r'(\phi)q^\mu + s'(\phi)k^\mu + t_1'(\phi)\, m\Lambda_1^\mu + t_2'(\phi)\, m\Lambda_2^\mu, \\ p_2^\mu(\phi) &= -r(\phi)q^\mu - s(\phi)k^\mu - t_1(\phi)\, m\Lambda_1^\mu - t_2(\phi)\, m\Lambda_2^\mu, \end{aligned} \tag{2.97}$$

where [see Eq. (A.19)]

$$t_i(\phi) = t_i - \xi_i \psi_i(\phi), \quad r(\phi) = r, \quad s(\phi) = \frac{1}{2}\frac{m^2}{kp}[1 + t_1^2(\phi) + t_2^2(\phi)],$$

$$t_i'(\phi) = t_i' - \xi_i \psi_i(\phi), \quad r'(\phi) = r', \quad s'(\phi) = \frac{1}{2}\frac{m^2}{kp'}[1 + t_1'^2(\phi) + t_2'^2(\phi)]. \tag{2.98}$$

As usual for S-matrix elements, $p_i^\mu = p_i^\mu(\pm\infty)$ denote the asymptotic four-momenta $[p_i^\mu(-\infty) = p_i^\mu(+\infty)$ follows from $\psi_k(\pm\infty) = 0$; by assumption the laser has no dc component]. Furthermore, $t_i = t_i(\pm\infty)$, $r = r(\pm\infty)$, $s = s(\pm\infty)$ and $t_i' = t_i$ implies $t_i'(\phi) = t_i(\phi)$.

Correspondingly, we obtain [see Eq. (1.95)]

$$p_1^\mu(\phi) + p_2^\mu(\phi) = q^\mu + n(\phi)k^\mu, \quad n(\phi) = \frac{1}{2}w\frac{m^2}{kq}[1 + t_1^2(\phi) + t_2^2(\phi)], \tag{2.99}$$

where $k^\mu n(\phi)$ is the four-momentum classically absorbed from the laser field. Remarkably, it determines the oscillation frequency of the phase [see Eqs. (1.95) and (1.99)]

$$\widetilde{S}_\Gamma'(p', q, p; \phi) = n(\phi) \tag{2.100}$$

(the prime denotes the derivative with respect to the laser phase ϕ). Therefore, the four-momentum conservation relation

$$p_1^\mu(\phi_s) + p_2^\mu(\phi_s) = q^\mu \tag{2.101}$$

is obeyed at a true stationary point ϕ_s of the phase $[\widetilde{S}_\Gamma'(p', q, p; \phi_s) = 0]$. As this is not possible for on-shell momenta, they must be located within the complex plane.

At the (quasi-) stationary points ϕ_k defined by $t_i = \xi_i \psi_i(\phi_k)$ [i.e. $t_i(\phi_k) = 0$] we obtain

$$p_1^\mu(\phi_k) + p_2^\mu(\phi_k) = q^\mu + \frac{1}{2} w \frac{m^2}{kq} k^\mu. \qquad (2.102)$$

Accordingly, these are the points where the least amount of laser four-momentum k^μ is needed to bring the four-momenta on shell.

For monochromatic fields the threshold condition $\chi \gtrsim 1$ for the onset of pair production is normally derived using the dressed mass ($m^* \sim \xi m$) and the fact that asymptotically the pair can absorb $n \sim \xi^3/\chi$ photons from the background field [see Eq. (2.74)] [Di+12; Rit85]. As already pointed out in Ref. [KR13], the same threshold condition is also obtained by considering the physical mass m ($4m^2 \leq 2nkq$) and noting that the pair must become real on the scale set by the formation region $\delta\phi \sim 1/\xi$ (classically, the electron and the positron may absorb together the four-momentum nk^μ with $n \sim \xi$ during the formation region).

From a quantum mechanical perspective the initial condition $t_i(\phi_k) = 0$ may seem to contradict the Heisenberg uncertainty principle. However, the contradiction is resolved as the application of the local constant-crossed field approximation implies the inclusion of contributions from within the whole formation region around ϕ_k, such that the true initial position is blurred on the scale set by the formation region.

Note that the integration in ϕ in Eq. (1.89) exactly expresses the Heisenberg uncertainty relation between the phase formation region and the number of laser photons absorbed in the process [Di+13].

2.8. Numerical results for the differential pair-creation probability

To verify the applicability of the local constant-crossed field approximation [see Eq. (2.95)], we compare the result now with a full numerical calculation. As shown in Sec. 1.6.7, the calculation of the Fourier-transformed master integrals with respect to the parameter w reduces to a root-finding problem [see Eq. (1.101)]. Correspondingly, the master integrals can be evaluated for different values of w in parallel by using only a *single* fast Fourier transform (FFT). Therefore, this approach reduces the computation costs substantially, as usually a highly-oscillating integral must be computed for each value of w.

Since $\mathfrak{S}'_\Gamma(t_1, t_2; \phi_{\tilde{x}}) > 0$ on the real axis [see Eq. (2.90)], one could equivalently perform the change of variable $\mathfrak{S}_\Gamma(w, t_1, t_2; \phi_{\tilde{x}}) = \tilde{x}$ in Eq. (1.89) and evaluate the master integrals directly via FFT. This approach has been applied in [DHK09] to the analogous problem of nonlinear Thomson scattering.

For the numerical calculations the pulse shape $\psi'(\phi) = \sin^2[\phi/(2N)] \sin(\phi + \phi_0)$ [see Eq. (1.23)] has been used and the numerical values of the parameters are given in the captions of the figures.

2.8.1. Validity of the constant-crossed field approximation

As demonstrated in Fig. 19, the local constant-crossed field approximation reproduces all features of the spectrum, including the interference pattern [if applied
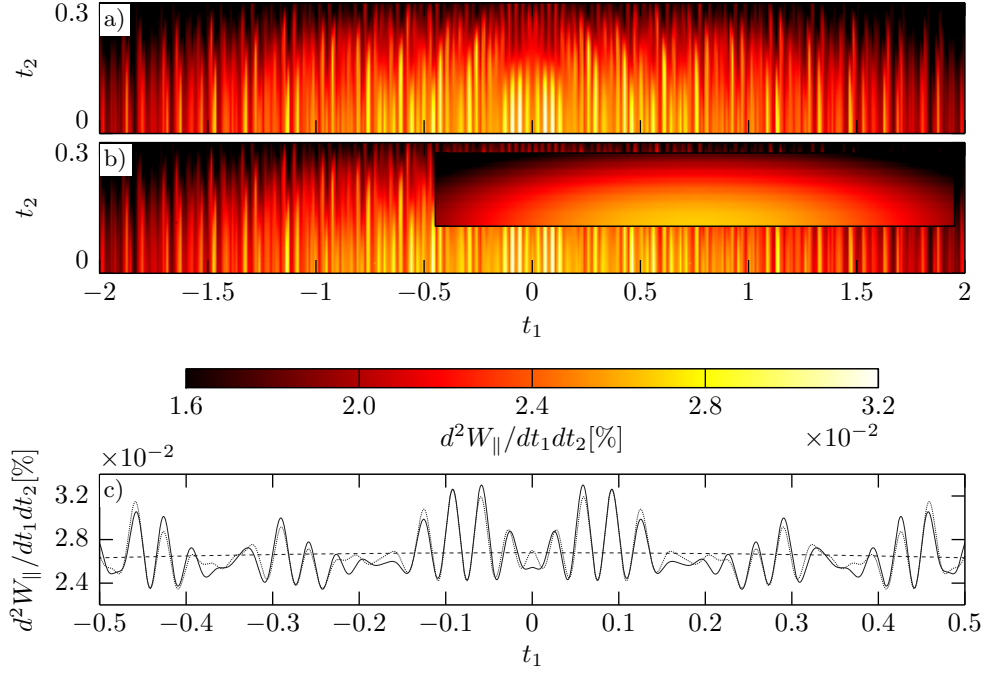
Fig. 19: Momentum distribution for the created electron-positron pair [see Eq. (2.78)] for the parameters $\chi = 1$, $\xi = 5$, $N = 5$ and $\phi_0 = \pi/2$ (the longitudinal momentum characterized by R is integrated). The parameters $\xi = 5$ and $\chi = 1$ could be obtained by colliding photons with an energy of $17\,\text{GeV}$ head-on with an optical ($\omega = 1.55\,\text{eV}$) laser pulses having an intensity of $10^{20}\,\text{W/cm}^2$ (note that few-cycle laser pulses are envisaged e.g. at the PFS in Garching [Ahm+09]). **a)** Full numerical calculation of the spectrum [see Eq. (1.101)]. **b)** Local constant-crossed field approximation applied on the amplitude level [see Eq. (2.95)]. The inset shows that the interference pattern is lost if the local constant-crossed field approximation is applied on the probability level. **c)** Outline for $t_2 = 0$. Solid line: full numerical calculation; dotted (dashed) line: local constant-crossed field approximation applied on the amplitude (probability) level.
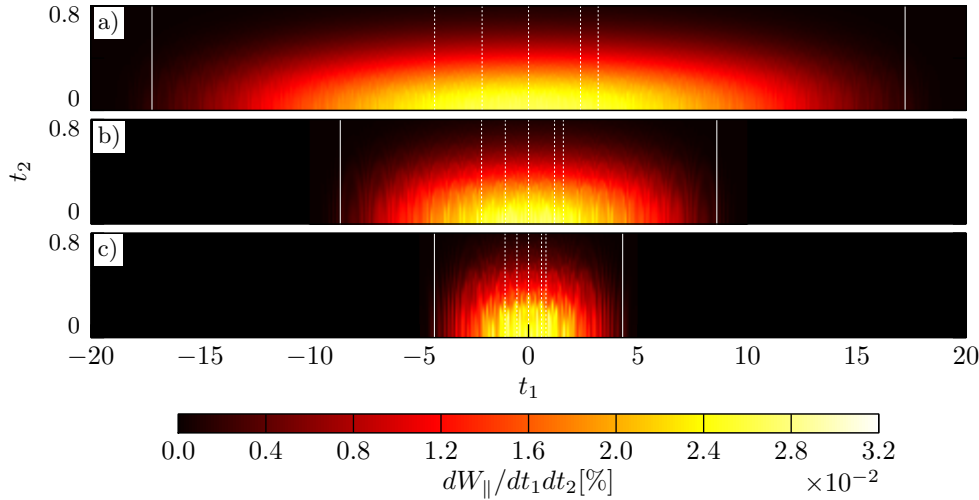
Fig. 20: Numerically calculated differential pair-creation probability as a function of the transversal momentum parameters t_1 and t_2 (the longitudinal momentum characterized by R is integrated out). As the spectrum is symmetric with respect to $t_2 \leftrightarrow -t_2$, it is plotted only for $t_2 \geq 0$. Here, the incoming photon has parallel polarization, $N = 5$, $\chi = 1$ and $\phi_0 = \pi/2$. To verify that the maximum achievable transversal momentum t_1 scales proportional to ξ, we compared the values $\xi = 20$ (**a**), 10 (**b**) and 5 (**c**). The solid white line confines the phase-space region where the pair can be created at a phase ϕ with $|\psi'(\phi)| \geq 0.5$ and the dashed white lines indicate the transverse momenta for which the pair can be created at a local field peak (only strong peaks are indicated). For the total pair-creation probability $W_\parallel$ we obtain 0.44%, 0.22% and 0.11%, respectively.

on the level of the master integrals, see Eq. (2.95)]. The interference fringes are lost, however, if the contribution of each stationary point is taken into account by simply adding the corresponding spectra and neglecting the phase factor (inset).

From Eq. (1.89) we conclude that the oscillation frequency of the interference fringes scales as $\sim \xi^3$ for w, $\sim \xi^2$ for t_1 and $\sim \xi$ for t_2. Correspondingly, we used for $\xi = 10$ a grid with $\sim 10^5 \times 10^4 \times 10^3 = 10^{12}$ (w, t_1, t_2) data points to resolve it. As a cross-check we ensured that the total probability obtained here by integrating numerically over the phase space agrees with the one calculated using the optical theorem in Sec. 2.5.

2.8.2. Scaling of the transverse momentum

From the classical equations of motion [see Eq. (2.97)] we expect that the extend of the spectrum in t_1 should be proportional to ξ. In Fig. 20 this is verified numerically. The semiclassical description fully accounts for all qualitative features of the spectrum in t_1, i.e. its extend and the position of the maxima. Correspondingly, the linear increase of the total pair-creation probability as a function of ξ in the regime $\xi \gg 1$ (see Sec. 2.5) is a pure kinematic effect (size of the available phase space).
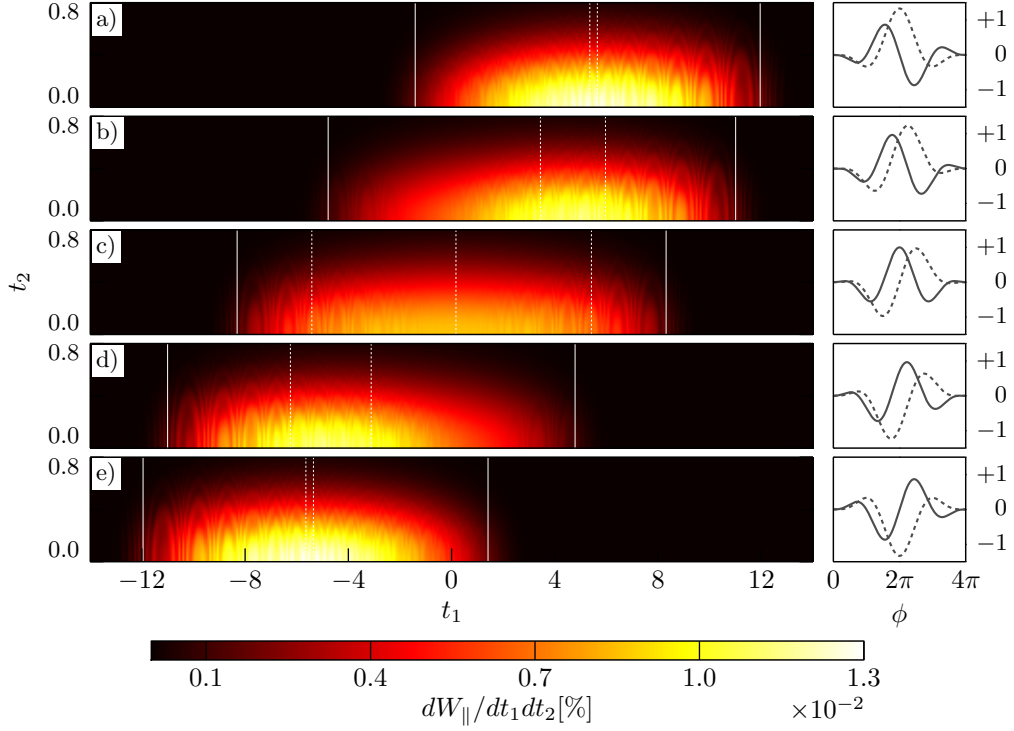
Fig. 21: Left side: Numerically calculated differential pair-creation probability as a function of the transversal momentum parameters t_1 and t_2 (the longitudinal momentum characterized by R is integrated out). As the spectrum is symmetric with respect to $t_2 \leftrightarrow -t_2$, it is plotted only for $t_2 \geq 0$. Here, the incoming photon has parallel polarization, $\chi = 1$, $\xi = 10$, $N = 2$ and $\phi_0 = \pi$ (**a**), $3\pi/4$ (**b**), $\pi/2$ (**c**), $\pi/4$ (**d**) and 0 (**e**). The solid white line confines the phase-space region where the pair can be created at a phase ϕ with $|\psi'(\phi)| \geq 0.5$ and the dashed white lines indicate the transverse momenta for which the pair can be created at a local field peak (only strong peaks are indicated). The interference pattern arises as for given values of t_1 and t_2 the pair can in general be created at more than just one laser phase. After integrating over t_1 and t_2 we obtain $W_\parallel = 0.09\,\%$ for the total pair-creation probability (up to this precision it is independent of the CEP). **Right side**: Plot of the laser pulse shape (solid line: ψ', dashed line: ψ).

2.8.3. Dependence on the CEP

In Ref. [KK12a] a strong dependence of the spectrum on the carrier-envelope phase (CEP) ϕ_0 was reported. As shown in Fig. 21, this can be explained completely by the fact that the classical acceleration of the created particles has a preferred direction (see the plot of ψ, which determines the stationary points). However, very short laser pulses are needed to detect the asymmetry. Already for $N \geq 3$ the effect is less profound (see Fig. 22), as most pairs experience several cycles before leaving the laser pulse.

2.8.4. Spectrum for the constants of motion

In contrary to t_1, the two other parameters R and t_2 are constants of motion (for a linearly polarized background field with $F^{\mu\nu} \sim f_1^{\mu\nu}$) and the associated probability distributions are not changed by the subsequent classical evolution of the produced
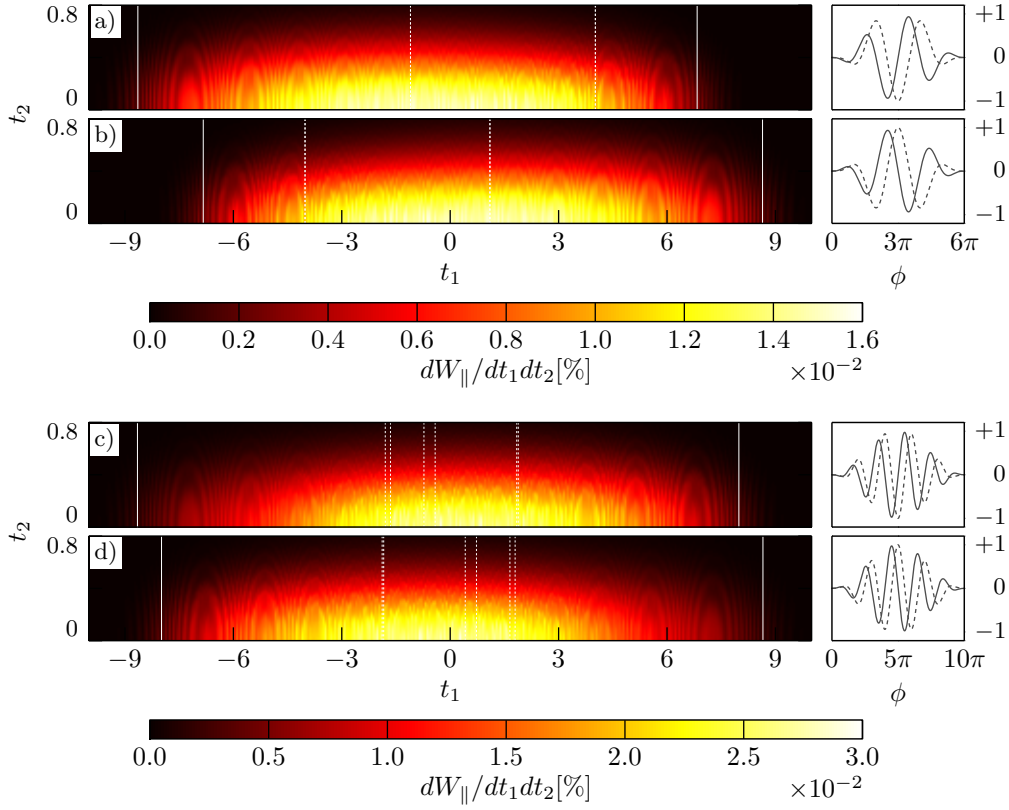
Fig. 22: Left side: Numerically calculated differential pair-creation probability (see Fig. 21 for more details). Already for $N = 3$ cycles (plot **a** and **b**) the CEP-dependence of the transverse momentum is less severe (compare with Fig. 21) and decreases further for $N = 5$ (plot **c** and **d**) [$\chi = 1$, $\xi = 10$ and $\phi_0 = \pi$ (**a,c**), $\phi_0 = 0$ (**b,d**)]. The total pair-creation probability is given by $W_\parallel = 0.13\,\%$ ($N = 3$) and $W_\parallel = 0.22\%$ ($N = 5$), up to this precision the total probability is independent of the CEP. **Right side**: Plot of the laser pulse shape (solid line: ψ', dashed line: ψ).
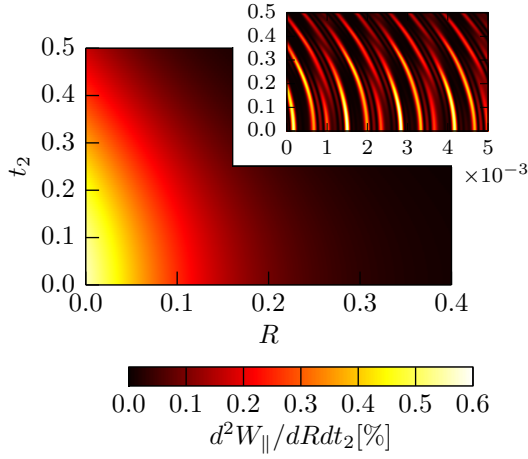
Fig. 23: Differential probability with respect to the parameters t_2 and R for $\chi = 1$, $\xi = 10$, $N = 5$ and $\phi_0 = \pi/2$ (full numerical calculation, t_1 is integrated). The inset shows $d^3 W_\parallel / dR dt_1 dt_2$ for $t_1 = 0$ (in arb. units). The pronounced interference pattern vanishes after the integral in t_1 is taken. Note that the differential probability does not depend on the sign of R and t_2.

particles. This is demonstrated in Fig. 23. We point out that after the parameter t_1 is integrated out, the spectrum corresponds very closely to the one obtained in a constant-crossed field (averaged over the pulse shape). This may not be expected at first sight, as for a fixed value of t_1 the differential spectrum has a rich interference structure (shown in the inset of Fig. 23).

3 Polarization operator for plane-wave laser fields

According to classical electrodynamics two light waves should not interact with each other. QED, however, predicts a nonvanishing coupling between different photons via intermediate charged particles, always present in the form of quantum fluctuations. The simplest Feynman diagram, which mediates photon-photon interactions inside an electromagnetic background field, is shown in Fig. 24. It represents the leading-order contribution to the polarization operator, which determines the properties of an external photon inside an electromagnetic background field via the Schwinger-Dyson equation (see Sec. 2.3). As a consequence, a plane-wave field acts like a medium in which external photons have a nontrivial dispersion relation (e.g., they obtain a mass) [BR13; Di+12; MS06]. Furthermore, the imaginary part of the polarization operator is related to the total electron-positron photoproduction probability due to the unitarity of the S-matrix (see Sec. 2.2) and leads to an exponential decay of the exact photon wave function (see Sec. 2.3). As we will show in Chap. 4, the polarization operator also describes laser-induced recollision processes of photoproduced electron-positron pairs.

The first calculation of the leading-order contribution to the polarization operator was published independently by Baier, Milstein, and Strakhovenko [BMS76] and by Becker and Mitter [BM75]. Here, we provide an alternative derivation based on the direct evaluation of the vertex- and momentum integrals obtained from the Feynman rules (see Sec. 3.2). This approach, published in Ref. [3], has the appealing feature that it is very similar to calculation techniques commonly used in vacuum QED.

Furthermore, we prove the validity of the Ward-Takahashi identity [Tak57; War50] for general loop diagrams in a plane-wave background field (see Sec. 3.1). The Ward-Takahashi identity is a consequence of the gauge-symmetry of the QED Lagrangian and restricts the tensor structure of the polarization operator (see Sec. 3.2.3). The absence of an anomalous contribution to the Ward-Takahashi
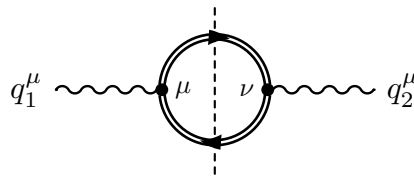
Fig. 24: The Feynman diagram corresponding to the leading-order contribution to the polarization operator $\mathcal{P}^{\mu\nu}(q_1, q_2)$ in a plane-wave background field (sign convention: q_1^μ is incoming, q_2^μ outgoing). The double lines represent the Volkov propagators for the fermions, which take the external field exactly into account [see Eq. (1.59)]. Due to the unitarity of the S-matrix the vertical dashed line links the polarization operator to the nonlinear Breit-Wheeler pair-creation diagram (see Chap. 2).

identity for the polarization operator is shown explicitly in Chap. 6, where the axial-vector current and the associated Adler-Bell-Jackiw (ABJ) anomaly [Adl69; BJ69] are investigated.

This chapter is organized as follows. In Sec. 3.2 a triple-integral representation for the leading-order contribution to the polarization operator is derived. It is manifestly symmetric with respect to the external photon four-momenta q_1^μ and q_2^μ [see Eq. (3.56)]. In particular, its equivalence to the triple-integral representation given in Ref. [BMS76] is demonstrated (see Sec. 3.2.7). Afterwards, the special cases of a constant-crossed field (see Sec. 3.3.1), a linearly polarized plane-wave field in the quasistatic approximation[1] (see Sec. 3.3.2), and a circularly polarized, monochromatic plane-wave field (see Sec. 3.3.3) are considered in more detail.

In the second part of this chapter, which was published in Ref. [4], a double-integral representation for the polarization operator in terms of the laser phases at the creation and the annihilation vertex is obtained [see Eq. (3.132)]. It serves as the starting point for the investigation of electron-positron recollisions carried out subsequently in Chap. 4.

Finally, we note that the polarization operator has recently also been considered by other authors for various field configurations [Din+14a; Din+14b; GKS14; GR11; Kar+12; Kar13]. A more detailed summary of the existing literature can be found in the review articles [BR13; Di+12; MS06].

3.1. Ward-Takahashi identity for loop diagrams

The Ward-Takahashi identity [Tak57; War50] is a direct consequence of the gauge invariance of QED, which becomes particularly transparent in the Feynman path integral approach [Col84; Wei95]. Diagrammatically, it is a functional relation for Feynman diagrams (in momentum space), where the polarization four-vector of an external photon leg is replaced by the corresponding momentum four-vector. In Ref. [PS95] a perturbative proof of the Ward-Takahashi identity in vacuum QED is given. Now, we will extend this derivation to electron-positron loops inside a plane-wave background field.

The starting point for the proof of the Ward-Takahashi identity is the algebraic identity for the dressed vertex given in Eq. (1.73)

$$q_\rho \Gamma^\rho(p', q, p) = (\not{p}' - m)I(p', q, p) - I(p', q, p)(\not{p} - m). \tag{3.1}$$

In the following, we apply it to a closed electron-positron loop which contains n dressed vertices and propagators (see Fig. 25). The ith propagator of such a loop together with its adjacent vertices is given by

$$\cdots \Gamma^{\mu_i}(p_{i-1}, q_i, p_i) \frac{1}{\not{p}_i - m} \Gamma^{\mu_{i+1}}(p_i, q_{i+1}, p_{i+1}) \cdots \tag{3.2}$$

(the electron four-momenta p_i^μ are integrated out). If we insert now a vertex (contracted with its photon four-momentum) at this propagator, we ob-

---

[1]Note that the quasistatic approximation is called quasi-classical approximation in Ref. [3].
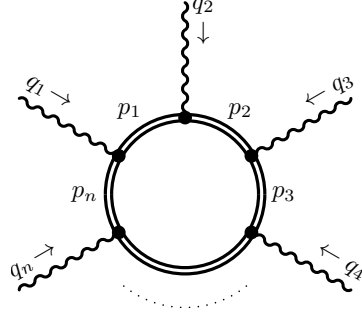
Fig. 25: Closed electron (positron) loop with n dressed vertices.

tain

$$\cdots \Gamma^{\mu_i}(p_{i-1}, q_i, p_i) \frac{1}{\not{p}_i - m} q_\mu \Gamma^\mu(p_i, q, p') \frac{1}{\not{p}' - m} \Gamma^{\mu_{i+1}}(p', q_{i+1}, p_{i+1}) \cdots . \quad (3.3)$$

Using the above identity and [see Eq. (1.77)]

$$\int \frac{d^4 p''}{(2\pi)^4} I(p, q', p'') \Gamma^\mu(p'', q, p') = -ie\Gamma^\mu(p, q + q', p'),$$

$$\int \frac{d^4 p''}{(2\pi)^4} \Gamma^\mu(p, q, p'') I(p'', q', p') = -ie\Gamma^\mu(p, q + q', p'), \quad (3.4)$$

we find that Eq. (3.3) is equivalent to

$$\cdots \Gamma^{\mu_i}(p_{i-1}, q_i + q, p_i) \frac{1}{\not{p}_i - m} \Gamma^{\mu_{i+1}}(p_i, q_{i+1}, p_{i+1}) \cdots$$

$$- \cdots \Gamma^{\mu_i}(p_{i-1}, q_i, p_i) \frac{1}{\not{p}_i - m} \Gamma^{\mu_{i+1}}(p_i, q_{i+1} + q, p_{i+1}) \cdots \quad (3.5)$$

(in the first line, we have changed the name of the integration variable from p'^μ to p_i^μ). Thus, the insertion splits the diagram into the sum of twice the original diagram with the additional four-momentum q^μ added once at the adjacent vertex before and after the insertion. If we sum now over all possible insertion points of the loop, we obtain zero, since all contributions cancel pairwise (as in the vacuum case [PS95]).

We point out that the above derivation relies on the fact that different terms cancel each other. Therefore, the proof can fail if the intermediate expressions are divergent. This possibility is discussed in Chap. 6. By using a suitable regularization procedure, it is shown there that the Ward-Takahashi identity for the axial-vector current obtains an additional anomalous contribution, in agreement with the Adler-Bell-Jackiw (ABJ) anomaly [Adl69; BJ69]. For the polarization operator, however, such subtleties are absent and the above derivation is applicable.

3.2. Calculation of the leading-order contribution

In this section a triple-integral representation for the leading-order contribution to the polarization operator shown in Fig. 24 is derived. After the Feynman rules summarized in Sec. 1.5.3 are applied, the momentum-dependence of the Dirac trace is simplified by introducing source terms to the phase and appropriate derivatives. Subsequently, most of the initially present integrals can be calculated analytically (see Sec. 3.2.2). Finally, the result given in Eq. (3.56) is obtained by evaluating the derivatives with respect to the sources (see Sec. 3.2.4). As shown in Sec. 3.2.7, the representation derived here is equivalent to the Baier-Milstein-Strakhovenko representation given in [BMS76].

3.2.1. General expression

The leading-order contribution to the polarization operator $\mathcal{P}^{\mu\nu}(q_1, q_2)$ for plane-wave background fields (see Ref. [LL82], Sec. 104) is determined by the diagram in Fig. 24. This diagram corresponds to the following expression

$$T^{\mu\nu}(q_1, q_2) = \int \frac{d^4p \, d^4p'}{(2\pi)^8} \, \mathbf{tr} \, \Gamma^\mu(p', q_1, p)$$
$$\times \frac{(\not{p} + m)}{p^2 - m^2 + i0} \Gamma^\nu(p, -q_2, p') \frac{(\not{p}' + m)}{p'^2 - m^2 + i0} \quad (3.6)$$

and $T^{\mu\nu} = i\mathcal{P}^{\mu\nu}$ (see Ref. [LL82], Sec. 115; [BKS75]). We note that $T^{\mu\nu}(q_1, q_2)$ is divergent, but if we write

$$T^{\mu\nu}(q_1, q_2) = \left[T^{\mu\nu}(q_1, q_2) - T^{\mu\nu}_{\mathfrak{F}=0}(q_1, q_2)\right] + T^{\mu\nu}_{\mathfrak{F}=0}(q_1, q_2), \quad (3.7)$$

the contribution in square brackets is finite [BMS76], and the regularization of the vacuum contribution is well known [LL82; Wei95]. In the following, we will focus on the tensor in square brackets, which contains only the corrections induced by the external background field.

To simplify the expression in Eq. (3.6), we have to insert the dressed vertex given in Eq. (1.68) [we will denote the vertex integrals associated with $\Gamma^\mu(p', q_1, p)$ and $\Gamma^\nu(p, -q_2, p')$ by d^4x and d^4y, respectively]. Then, we obtain

$$T^{\mu\nu}(q_1, q_2) = 4\,(-ie)^2 \int \frac{d^4p \, d^4p'}{(2\pi)^8} \int d^4x d^4y$$
$$\times \frac{\frac{1}{4}\,\mathbf{tr}\,[\cdots]^{\mu\nu}}{(p^2 - m^2 + i0)(p'^2 - m^2 + i0)} e^{iS_T} \quad (3.8)$$

(the prefactor $1/4$ in front of the trace is included explicitly for later convenience), where the phase reads [see Eq. (1.68)]

$$iS_T = i(p' - p - q_1)x + i(p - p' + q_2)y$$
$$+ i \int\limits_{ky}^{kx} d\phi' \left[\frac{ep_\mu p'_\nu \mathfrak{F}^{\mu\nu}}{(kp)(kp')} + \frac{e^2(kp - kp')}{2(kp)^2(kp')^2} p_\mu p'_\nu \mathfrak{F}^{2\mu\nu}\right] \quad (3.9)$$

and $\frac{1}{4}\,\mathbf{tr}\,[\cdots]^{\mu\nu}$ in Eq. (3.8) is given by (it can be calculated using the relations in App. D)

$$
\begin{aligned}
\frac{1}{4}\,&\mathbf{tr}\,\left[\gamma_\alpha a^{\alpha\mu} + i\gamma_\alpha\gamma^5 b^{\alpha\mu}\right](\not{p}+m)\left[\gamma_\beta c^{\beta\nu} + i\gamma_\beta\gamma^5 d^{\beta\nu}\right](\not{p}'+m)\\
&= m^2[(a^{\alpha\mu}c_\alpha{}^\nu) + (b^{\alpha\mu}d_\alpha{}^\nu)] + (pp')(b^{\alpha\mu}d_\alpha{}^\nu) - (pp')(a^{\alpha\mu}c_\alpha{}^\nu)\\
&\quad + (p_\alpha a^{\alpha\mu})(p'_\beta c^{\beta\nu}) + (p'_\alpha a^{\alpha\mu})(p_\beta c^{\beta\nu}) - (p_\alpha b^{\alpha\mu})(p'_\beta d^{\beta\nu})\\
&\quad - (p'_\alpha b^{\alpha\mu})(p_\beta d^{\beta\nu}) - \epsilon_{\rho\sigma\alpha\beta}p^\rho p'^\sigma(a^{\alpha\mu}d^{\beta\nu} + b^{\alpha\mu}c^{\beta\nu}).
\end{aligned}
\tag{3.10}
$$

Here,

$$
\begin{aligned}
a^{\alpha\mu} &= G^{\alpha\mu}(kp', kp; kx), \quad c^{\beta\nu} = G^{\beta\nu}(kp, kp'; ky),\\
b^{\alpha\mu} &= G_5^{\alpha\mu}(kp', kp; kx), \quad d^{\beta\nu} = G_5^{\beta\nu}(kp, kp'; ky).
\end{aligned}
\tag{3.11}
$$

3.2.2. Evaluation of the integrals

Working in light-cone coordinates (see Sec. 1.4) we can take all space-time integrals except of those in dx^- and dy^- and obtain the momentum-conserving delta functions

$$
(2\pi)^6\delta^{(-,\perp)}(p' - p - q)\,\delta^{(-,\perp)}(q_1 - q_2).
\tag{3.12}
$$

Here and in the following, we write q^μ if q_1^μ and q_2^μ can be used interchangeably due to the above delta functions. Successively, we can take the integrals in dp'^- and $dp'^\perp$ (for simplicity we will continue writing p'^μ and identify $p'^\mu = p^\mu + q^\mu$ for the components $-, \perp$).

It is now convenient to introduce the two four-vectors [see Eq. (1.48)]

$$
\Lambda_1^\mu = \frac{f_1^{\mu\nu}q_\nu}{kq\sqrt{-a_1^2}}, \quad \Lambda_2^\mu = \frac{f_2^{\mu\nu}q_\nu}{kq\sqrt{-a_2^2}},
\tag{3.13}
$$

which obey $\Lambda_i\Lambda_j = -\delta_{ij}$, $k\Lambda_i = q_i\Lambda_j = 0$ and

$$
f_1^{\mu\nu}\Lambda_{1\nu} = -\frac{m}{e}k^\mu\xi_1, \quad f_2^{\mu\nu}\Lambda_{2\nu} = -\frac{m}{e}k^\mu\xi_2.
\tag{3.14}
$$

They allow us to write the remaining phase as

$$
iS_T = i(p' - p - q_1)^+x^- + i(p - p' + q_2)^+y^- + ip\lambda + i\Lambda,
\tag{3.15}
$$

where we defined

$$
\begin{aligned}
\lambda^\mu &= -\frac{m(kq)}{(kp)(kp')}\sum_{i=1,2}\xi_i\Lambda_i^\mu\int_{ky}^{kx}d\phi'\,\psi_i(\phi'),\\
\Lambda &= -\frac{m^2(kq)}{2(kp)(kp')}\sum_{i=1,2}\xi_i^2\int_{ky}^{kx}d\phi'\,\psi_i^2(\phi').
\end{aligned}
\tag{3.16}
$$

Due to the appearance of Λ_i^μ in λ^μ, it is more convenient to use the canonical

light-cone coordinates[2] discussed in Sec. 1.4.3. In canonical light-cone coordinates we obtain the relations

$$p\lambda = -p^\perp \lambda^\perp, \quad q^\perp = 0, \quad p'^\perp = p^\perp, \tag{3.17}$$

which simplify the algebra considerably.

If the preexponent would not depend on p^+ and p'^+, both integrals could now be taken. Therefore, we introduce the proper-time representation of the scalar propagators [DG00; Sch51]

$$\frac{1}{p^2 - m^2 + i0} \frac{1}{p'^2 - m^2 + i0} = (-i)^2 \int\limits_0^\infty ds\, dt$$
$$\times \exp\left[i(p^2 - m^2 + i0)s + i(p'^2 - m^2 + i0)t\right]. \tag{3.18}$$

In the following we will drop the pole prescriptions $i0$ and keep the replacement $m^2 \to m^2 - i0$ in mind. Furthermore, we add the source terms $ip_\mu j^\mu + ip'_\mu j'^\mu$ to the phase, which allow for the replacement

$$\not{p} \longrightarrow (-i)\not{\partial}_j, \quad \not{p}' \longrightarrow (-i)\not{\partial}_{j'} \tag{3.19}$$

in the trace. Now, the preexponent depends only on p^- (through kp and kp'). Taking the derivatives with respect to the sources out of the integrals, we can take the integrals in dp^+, dp'^+, which results in the delta functions,

$$(2\pi)\delta\left[y^- - x^- - \frac{1}{s+t}(2stq^- - tj^- + sj'^-)\right]$$
$$\times (2\pi)\delta[2p^-(s+t) + 2q^-t + j^- + j'^-]. \tag{3.20}$$

Successively, these delta functions can be used to take also the integrals in dy^- and dp^-. To this end we rewrite (since $s + t \geq 0$)

$$\delta[2p^-(s+t) + 2q^-t + j^- + j'^-] = \frac{1}{2(s+t)}\delta\left[p^- + \frac{1}{2(s+t)}(2q^-t + j^- + j'^-)\right] \tag{3.21}$$

(for simplicity we keep writing y^- and p^-). In particular, we obtain the identities

$$kp = -\frac{1}{s+t}\left[tkq + \frac{1}{2}(kj + kj')\right], \quad kp' = +\frac{1}{s+t}\left[skq - \frac{1}{2}(kj + kj')\right],$$
$$ky = kx + \frac{1}{s+t}(2stkq - tkj + skj'). \tag{3.22}$$

---

[2]In Ref. [3] the canonical light-cone coordinates are called modified light-cone coordinates. Due to the equivalence between different light-cone coordinates the calculation so far is independent of this choice, see Sec. 1.4.2.

For $j^\mu = j'^\mu = 0$ they imply

$$G_1 = \frac{e}{2kq} \frac{(s-t)(s+t)}{st} = \frac{e}{2kq} \frac{v\tau}{\mu},$$

$$G_2 = -\frac{e^2}{2(kq)^2} \frac{(s+t)^2}{st} = -\frac{e^2}{2(kq)^2} \frac{\tau}{\mu}, \qquad (3.23)$$

$$G_3 = -\frac{e}{2kq} \frac{(s+t)^2}{st} = -\frac{e}{2kq} \frac{\tau}{\mu},$$

where we defined [BMS76]

$$\tau = s + t, \quad v = \frac{s-t}{s+t}, \quad \mu = \frac{st}{s+t} = \frac{1}{4}\tau(1-v^2) \qquad (3.24)$$

[the motivation for these definitions becomes clear in Eq. (3.41)].

The remaining part of the phase structure (including the part coming from the propagators and the sources) is now given by

$$iS'_T = i\Big[(q_2^+ - q_1^+)x^- + \frac{st}{s+t}q_2^2 - \frac{1}{s+t}(t\,q_2 j - s\,q_2 j') - (p^\perp p^\perp + m^2)(s+t)$$
$$- \frac{1}{2(s+t)}(j^+ + j'^+)(j^- + j'^-) - (j^\perp + j'^\perp + \lambda^\perp)p^\perp + \Lambda\Big]. \quad (3.25)$$

Taking the Gaussian integrals in p^{I} and p^{II}, we obtain the prefactor $\pi/[i(s+t)]$, and the final phase is given by

$$iS'_T = i\Big[(q_2^+ - q_1^+)x^- - m^2(s+t) + \frac{st}{s+t}q_2^2 - \frac{1}{s+t}(t\,q_2 j - s\,q_2 j')$$
$$- \frac{1}{4(s+t)}(j+j')^2 - \frac{1}{2(s+t)}(j+j')\lambda - \frac{1}{4(s+t)}\lambda^2 + \Lambda\Big]. \quad (3.26)$$

For zero sources ($j^\mu = j'^\mu = 0$) we obtain

$$iS'_T = i\Big[(q_2^+ - q_1^+)x^- + \mu q_2^2 - \tau m^2 + \tau m^2 \sum_{i=1,2} \xi_i^2(I_i^2 - J_i)\Big], \qquad (3.27)$$

where we defined

$$I_i = -\frac{1}{2kq\mu} \int\limits_{ky}^{kx} d\phi'\, \psi_i(\phi'), \quad J_i = -\frac{1}{2kq\mu} \int\limits_{ky}^{kx} d\phi'\, \psi_i^2(\phi') \qquad (3.28)$$

(the prefactor is chosen such that $I_i = J_i = 1$ if $j^\mu = j'^\mu = 0$ and $\psi_i = 1$). Finally, we can write the tensor $T^{\mu\nu}$ as

$$T^{\mu\nu}(q_1, q_2) = -2i\pi e^2\, \delta^{(-,\perp)}(q_1 - q_2) \int\limits_0^\infty \frac{ds\,dt}{(s+t)^2} \int\limits_{-\infty}^{+\infty} dx^-\, \frac{1}{4}\,\mathbf{tr}\,[\ldots]^{\mu\nu}\, e^{iS'_T}\Big|_{j=j'=0}, \qquad (3.29)$$

where the expression for $\frac{1}{4}\,\mathbf{tr}\,[\ldots]^{\mu\nu}$ is given in Eq. (3.10) with the replacement

in Eq. (3.19) and where the sources are set to zero after the derivatives are taken.

We point out that the two four-momenta q_1^μ and q_2^μ appear asymmetrically in the final expression [see Eq. (3.27)]. To remove this asymmetry, we shift the x^- integration by defining

$$z^- = x^- + \mu q^-. \tag{3.30}$$

After this shift, the phase contains $q_1 q_2$ since

$$(q_2^+ - q_1^+)x^- + \mu q_2^2 = (q_2^+ - q_1^+)z^- + \mu q_1 q_2. \tag{3.31}$$

Furthermore, we obtain (for $j^\mu = j'^\mu = 0$) symmetric representations for the functions defined in Eq. (3.28)

$$I_i = \frac{1}{2} \int\limits_{-1}^{+1} d\lambda \, \psi_i(kz - \lambda \mu kq), \quad J_i = \frac{1}{2} \int\limits_{-1}^{+1} d\lambda \, \psi_i^2(kz - \lambda \mu kq), \tag{3.32}$$

since

$$kx = kz - \mu kq, \quad ky = kz + \mu kq + \frac{1}{s+t}(skj' - tkj). \tag{3.33}$$

3.2.3. Tensor structure

In principle, the only remaining task is to evaluate the two derivatives with respect to j^μ and j'^μ and then set $j^\mu = j'^\mu = 0$. Despite being elementary, this is the most tedious part of the calculation, since the sources appear in many places in the final expression. The work is considerably reduced if we expand the polarization operator in a convenient basis [BMS76]. To this end we note that

$$q_{1\mu} T^{\mu\nu}(q_1, q_2) = 0, \quad T^{\mu\nu}(q_1, q_2)q_{2\nu} = 0 \tag{3.34}$$

due to the Ward-Takahashi identity (see Sec. 3.1).

Since the four-vectors Λ_i^μ appear in the phase [see Eq. (3.15)] and $q_i \Lambda_j = 0$, it is natural to introduce the two complete sets q_1^μ, $\mathcal{Q}_1^\mu$, Λ_1^μ, Λ_2^μ and q_2^ν, $\mathcal{Q}_2^\nu$, Λ_1^ν, Λ_2^ν, where

$$\mathcal{Q}_1^\mu = \frac{k^\mu q_1^2 - q_1^\mu kq}{kq}, \quad \mathcal{Q}_2^\mu = \frac{k^\mu q_2^2 - q_2^\mu kq}{kq} \tag{3.35}$$

($\mathcal{Q}_1^2 = -q_1^2$, $\mathcal{Q}_2^2 = -q_2^2$, $\mathcal{Q}_i \Lambda_j = 0$, $q_i \mathcal{Q}_i = 0$). Using the set including q_1^μ for the index μ and the set including q_2^ν for the index ν, seven of 16 coefficients vanish due to the Ward-Takahashi identity, and we can decompose $T^{\mu\nu}(q_1, q_2)$ as follows [BMS76]

$$\begin{aligned} T^{\mu\nu} = c_1 \Lambda_1^\mu \Lambda_2^\nu &+ c_2 \Lambda_2^\mu \Lambda_1^\nu + c_3 \Lambda_1^\mu \Lambda_1^\nu + c_4 \Lambda_2^\mu \Lambda_2^\nu + c_5 \mathcal{Q}_1^\mu \mathcal{Q}_2^\nu \\ &+ c_6 \mathcal{Q}_1^\mu \Lambda_1^\nu + c_7 \mathcal{Q}_1^\mu \Lambda_2^\nu + c_8 \Lambda_1^\mu \mathcal{Q}_2^\nu + c_9 \Lambda_2^\mu \mathcal{Q}_2^\nu. \end{aligned} \tag{3.36}$$

It turns out that also the coefficients $c_6 - c_9$ vanish. If analyzed perturbatively (with respect to the external field coupling) this can be understood from Furry's theorem [BM75; BMS76]. Since a closed fermion loop with an odd number of vertices does not contribute to the final amplitude, only diagrams with an even number of external field couplings (eA^μ) contribute to $T^{\mu\nu}$. Due to gauge invariance and the fact that $T^{\mu\nu}$ is a tensor, the external field can enter only as $\mathfrak{F}^{\mu\nu}$ (which is linear in A^μ). Since it is not possible to construct a scalar linear in $\mathfrak{F}^{\mu\nu}$ using only the four-vectors q_1^μ, q_2^μ and k^μ, the tensor structure cannot involve an odd number of the tensor $\mathfrak{F}^{\mu\nu}$ (note that $q_1 \mathfrak{F} q_2 = q \mathfrak{F} q = 0$). As a consequence, the coefficients $c_6 - c_9$ (which are linear in Λ_i^μ and thus in the external field) should vanish. We will later see that this is indeed the case.

The coefficients c_i in Eq. (3.36) can be determined by contracting $T^{\mu\nu}(q_1, q_2)$ with the appropriate four-vectors. Especially, using again the Ward-Takahashi identity, we obtain

$$\mathcal{Q}_{1\mu} T^{\mu\nu} = \frac{q_1^2}{kq} k_\mu T^{\mu\nu}, \quad T^{\mu\nu} \mathcal{Q}_{2\nu} = \frac{q_2^2}{kq} T^{\mu\nu} k_\nu. \tag{3.37}$$

Thus, effectively, we need to determine the contractions of $T^{\mu\nu}(q_1, q_2)$ with the four-vectors k^μ and Λ_i^μ to determine the coefficients c_i, i.e. we need to calculate the $(-, \perp)$-components of $T^{\mu\nu}(q_1, q_2)$ in canonical light-cone coordinates. Since k^μ has only a +-component, the evaluation of the derivatives is now considerably simplified. Leaving the term proportional to pp' aside, we see that all derivatives which act on kj or kj' can be ignored. They would result in the replacement of p^μ or p'^μ by k^μ. Since $k_\mu \mathfrak{F}^{\mu\nu} = k_\mu \mathfrak{F}^{2\mu\nu} = k_\mu \mathfrak{F}^{*\mu\nu} = 0$ and $k^2 = k\Lambda_i = 0$, we do not need to consider those terms. The derivatives acting on kj or kj' are therefore only important to determine the term proportional to pp'. However, this is achieved more easily if the calculation presented in Sec. 3.2.2 is repeated with a scalar source term $\mathcal{J}pp'$ in the exponent (see Sec. 3.2.5).

To calculate the preexponent of the polarization operator, we must now insert the explicit expressions given in Eq. (1.70) into the trace in Eq. (3.10). Many terms of the trace, e.g., the terms proportional to $\mathfrak{F}^{\mu\nu}$, $\mathfrak{F}^{2\mu\nu}$, $\mathfrak{F}^{2\mu\rho}p_\rho$ vanish, as they are contracted with k^μ or Λ_i^μ from each side. Using the relations in App. C, we can show that Eq. (3.10) can be substituted by the following expression

$$
\begin{aligned}
m^2 g^{\mu\nu} &+ p^\mu p'^\nu + p'^\mu p^\nu + g^{\mu\nu} [G_3 p \mathfrak{F}_y p' + G_3 p \mathfrak{F}_x p' - 2G_3^2 (p \mathfrak{F}_{xy}^2 p') - (pp')] \\
&- G_3 [(\mathfrak{F}_y p')^\mu p^\nu - (\mathfrak{F}_y p)^\mu p'^\nu + p^\mu (\mathfrak{F}_x p')^\nu - p'^\mu (\mathfrak{F}_x p)^\nu] \\
&- G_1 [p^\mu (\mathfrak{F}_y p')^\nu + p'^\mu (\mathfrak{F}_y p)^\nu + (\mathfrak{F}_x p)^\mu p'^\nu + (\mathfrak{F}_x p')^\mu p^\nu] \\
&+ G_1^2 [(\mathfrak{F}_x p)^\mu (\mathfrak{F}_y p')^\nu + (\mathfrak{F}_x p')^\mu (\mathfrak{F}_y p)^\nu] \\
&\qquad\qquad - G_3^2 [(\mathfrak{F}_y p)^\mu (\mathfrak{F}_x p')^\nu + (\mathfrak{F}_y p')^\mu (\mathfrak{F}_x p)^\nu], \quad (3.38)
\end{aligned}
$$

where $\mathfrak{F}_{xy}^{2\mu\nu} = \mathfrak{F}^{\mu\rho}(kx) \mathfrak{F}_\rho{}^\nu(ky) = \mathfrak{F}^{\mu\rho}(ky) \mathfrak{F}_\rho{}^\nu(kx)$ [here the replacement $p^\mu \longrightarrow (-i)\partial_j^\mu$ and $p'^\mu \longrightarrow (-i)\partial_{j'}^\mu$ is understood if the trace is inserted in Eq. (3.29); see Eq. (3.19)]. Since the term proportional to pp' enters as $g^{\mu\nu}$, it modifies only the diagonal coefficients c_3 and c_4.

3.2.4. Evaluation of the derivatives

Leaving the term proportional to pp' aside, we can ignore derivatives acting on kj and kj' as discussed above [this implies that the derivatives do not act on kp, kp', and ky; see Eq. (3.22)]. The remaining nontrivial source-dependent part of the phase is given by [see Eq. (3.26)]

$$-\frac{i}{s+t}\Big[t\,q_2 j - s\,q_2 j' + \frac{1}{4}(j+j')^2 + \frac{1}{2}(j+j')\lambda\Big]. \tag{3.39}$$

The squared term contributes only if both derivatives act on it, which results in the replacement

$$p^\alpha p'^\beta \longrightarrow (-i)^2 \partial_j^\alpha \partial_{j'}^\beta \longrightarrow \frac{i}{2(s+t)}g^{\alpha\beta} \tag{3.40a}$$

and the only nonzero contribution arises from the first three terms in Eq. (3.38). If the derivatives act on the other source terms, we obtain the replacement

$$p^\alpha p'^\beta \longrightarrow (-i)^2 \partial_j^\alpha \partial_{j'}^\beta \longrightarrow -\frac{1}{(s+t)^2}\Big(tq_2^\alpha + \frac{1}{2}\lambda^\alpha\Big)\Big(sq_2^\beta - \frac{1}{2}\lambda^\beta\Big). \tag{3.40b}$$

After these replacements are applied to Eq. (3.38) and the sources are set to zero, we obtain (effectively) the following expression for Eq. (3.38)

$$\begin{aligned}
g^{\mu\nu}\Big[&m^2 + \frac{i}{\tau} - \frac{e}{4kq}\frac{}{\mu}(q\mathfrak{F}_y\lambda + q\mathfrak{F}_x\lambda) + \frac{e^2}{2(kq)^2}\frac{\tau}{\mu}q\mathfrak{F}_{xy}^2 q - pp'\Big] \\
&- 2\frac{\mu}{\tau}q_2^\mu q_2^\nu - \frac{v}{2\tau}(q_2^\mu\lambda^\nu + \lambda^\mu q_2^\nu) + \frac{1}{2\tau^2}\lambda^\mu\lambda^\nu + \frac{e}{kq}v\big[q_2^\mu(\mathfrak{F}_y q)^\nu + (\mathfrak{F}_x q)^\mu q_2^\nu\big] \\
&\quad - \frac{e}{4kq}\frac{1}{\mu}\big[(\mathfrak{F}_y q)^\mu\lambda^\nu + \lambda^\mu(\mathfrak{F}_x q)^\nu\big] + \frac{e}{4kq}\frac{v^2}{\mu}\big[\lambda^\mu(\mathfrak{F}_y q)^\nu + (\mathfrak{F}_x q)^\mu\lambda^\nu\big] \\
&\qquad\qquad + \frac{e^2}{2(kq)^2}\frac{\tau}{\mu}\big[(\mathfrak{F}_y q)^\mu(\mathfrak{F}_x q)^\nu - v^2(\mathfrak{F}_x q)^\mu(\mathfrak{F}_y q)^\nu\big] \quad (3.41)
\end{aligned}$$

[note that terms proportional to $(\mathfrak{F}\lambda)^\mu$, $(\mathfrak{F}\lambda)^\nu$ can be omitted]. By changing the proper-time integrations from s, t to τ, v [BMS76],

$$\int\limits_0^\infty ds\,dt\,f(s,t) = \frac{1}{2}\int\limits_{-1}^{+1}dv \int\limits_0^\infty d\tau\,\tau\,\tilde{f}(\tau, v) \tag{3.42}$$

we see that the terms linear in v vanish. Those terms determine the coefficients $c_6 - c_9$, which are therefore zero (as already anticipated from Furry's theorem).

3.2.5. Scalar term

To determine the term proportional to pp', we add the scalar source term $i\mathcal{J}pp'$ to the phase (instead of $ip_\mu j^\mu + ip'_\mu j'^\mu$) and repeat the calculation presented in Sec. 3.2.2. The propagators are represented in the same way [see Eq. (3.18)], and we replace pp' by $-i\frac{\partial}{\partial\mathcal{J}}$. Then, we take the integrals in dx^+, $dx^\perp$, dy^+, $dy^\perp$, dp'^-, $dp'^\perp$,

dp'^+, and dp^+. Instead of Eq. (3.20), we obtain now

$$(2\pi)\delta\Big[y^- - x^- - \frac{4st - \mathcal{J}^2}{2(s + t + \mathcal{J})}q^-\Big]\,(2\pi)\delta[2(s + t + \mathcal{J})p^- + (2t + \mathcal{J})q^-]. \quad (3.43)$$

The remaining part of the phase (including the part from the propagator) can be written as

$$iS'_T = i[q_2^+ y^- - q_1^+ x^- - p^\perp p^\perp \mathcal{J} + (-p^\perp p^\perp - m^2)(s + t) - p^\perp \lambda^\perp + \Lambda]. \quad (3.44)$$

Now, it is convenient to shift the proper-time integrations

$$s \longrightarrow s - \frac{1}{2}\mathcal{J}, \quad t \longrightarrow t - \frac{1}{2}\mathcal{J}. \quad (3.45)$$

Due to this shift, also the integral boundaries of the proper-time integrations depend on the source. However, if the derivative acts on the integral boundaries, either s or t is set to zero or to infinity. The resulting terms do not depend on the external field since $s = 0$ or $t = 0$ implies $\mu = 0$, $ky = kx$ and thus $\lambda^\mu = 0$ and $\Lambda = 0$. On the other hand, the terms at $s \to \infty$ or $t \to \infty$ do not contribute because the field-dependent part of the integral is convergent. Since we want to calculate only the field-dependent part of the polarization operator [see Eq. (3.56)], we will ignore the source dependence of the integral boundaries.

After the shift in Eq. (3.45) the delta functions read

$$(2\pi)\delta[y^- - x^- - (2\mu - \mathcal{J})q^-]\,(2\pi)\delta[2p^-(s + t) + 2q^- t] \quad (3.46)$$

and the phase is given by

$$iS'_T = i\Big[(q_2^+ - q_1^+)x^- + \Big(\mu - \frac{1}{2}\mathcal{J}\Big)q_2^2 - m^2(s + t - \mathcal{J})$$
$$- p^\perp p^\perp(s + t) - p^\perp \lambda^\perp + \Lambda\Big]. \quad (3.47)$$

We can now use the delta functions to take the integrals in dy^- and dp^- (we keep writing y^- and p^- for convenience) and obtain the identities

$$kp = -\frac{t}{s + t}kq, \quad kp' = \frac{s}{s + t}kq, \quad ky = kx + (2\mu - \mathcal{J})kq \quad (3.48)$$

[for $\mathcal{J} = 0$ this agrees with Eq. (3.22)]. The shift in the proper-time integrals has the advantage that kp and kp' are now independent of $\mathcal{J}$. We could have proceeded similarly also in the calculation of the other terms. However, since we ignored sources contracted with k^μ, this was not necessary.

Taking now the Gaussian integrals in dp^I, dp^II, we obtain the prefactor $\pi/[i(s + t)]$, and the final phase is given by

$$iS'_T = i\Big[(q_2^+ - q_1^+)x^- + \Big(\mu - \frac{1}{2}\mathcal{J}\Big)q_2^2 - m^2(\tau - \mathcal{J}) + \tau m^2 \sum_{i=1,2} \xi_i^2(I_i^2 - J_i)\Big], \quad (3.49)$$

where I_i and J_i are defined in Eq. (3.28) [for zero sources Eq. (3.49) agrees with

Eq. (3.27)]. Since pp' in the preexponent is only multiplied by $g^{\mu\nu}$ [see Eq. (3.41)], the evaluation of the derivative is not very cumbersome, and we obtain the replacement

$$pp' \longrightarrow (-i)\frac{\partial}{\partial \mathcal{J}} \longrightarrow -\frac{1}{2}q_2^2 + m^2 + m^2\frac{\tau}{2\mu}\sum_{i=1,2}\xi_i^2[\psi_i^2(ky) - 2I_i\psi_i(ky)] \quad (3.50)$$

after $\mathcal{J}$ is set to zero (as explained above, we have ignored the source dependence of the proper-time integral boundaries).

To symmetrize the final expression, we change the x^--integration by defining [see Eq. (3.30)]

$$\tilde{z}^- = x^- + \left(\mu - \frac{1}{2}\mathcal{J}\right)q^- \quad (3.51)$$

($\tilde{z}^- = z^-$ for $\mathcal{J} = 0$), which implies

$$kx = k\tilde{z} - \left(\mu - \frac{1}{2}\mathcal{J}\right)kq, \quad ky = k\tilde{z} + \left(\mu - \frac{1}{2}\mathcal{J}\right)kq \quad (3.52)$$

and

$$(q_2^+ - q_1^+)x^- + \left(\mu - \frac{1}{2}\mathcal{J}\right)q_2^2 = (q_2^+ - q_1^+)\tilde{z}^- + \left(\mu - \frac{1}{2}\mathcal{J}\right)q_1q_2. \quad (3.53)$$

Finally, we obtain the symmetric replacement

$$pp' \longrightarrow (-i)\frac{\partial}{\partial \mathcal{J}} \longrightarrow -\frac{1}{2}q_1q_2 + m^2 + m^2\frac{\tau}{2\mu}\sum_{i=1,2}\xi_i^2$$
$$\times \left[\frac{1}{2}\psi_i^2(kx) + \frac{1}{2}\psi_i^2(ky) - I_i\psi_i(kx) - I_i\psi_i(ky)\right] \quad (3.54)$$

(we assume that at $x^- = \pm\infty$ the external field vanishes, and therefore the derivative does not act on the integral boundaries, which now also depend on the source).

3.2.6. Final result

To determine the nonvanishing coefficients $c_1 - c_5$ of the polarization operator [see Eq. (3.36)], we combine now Eqs. (3.29), (3.30), (3.41), and (3.54). Furthermore, we define the following functions

$$X_{ij} = [I_i - \psi_i(ky)][I_j - \psi_j(kx)], \quad Z_i = \frac{1}{2}[\psi_i(kx) - \psi_i(ky)]^2. \quad (3.55)$$

Finally, using the relations summarized in App. C, we obtain the following expression for the field-dependent part of the tensor $T^{\mu\nu}$

$$T^{\mu\nu}(q_1, q_2) - T^{\mu\nu}_{\mathfrak{F}=0}(q_1, q_2) = -i\pi e^2\,\delta^{(-,\perp)}(q_1 - q_2)\int_{-1}^{+1}dv\int_0^\infty\frac{d\tau}{\tau}\int_{-\infty}^{+\infty}dz^-$$
$$\times\left[b_1\Lambda_1^\mu\Lambda_2^\nu + b_2\Lambda_2^\mu\Lambda_1^\nu + b_3\Lambda_1^\mu\Lambda_1^\nu + b_4\Lambda_2^\mu\Lambda_2^\nu + b_5\mathcal{Q}_1^\mu\mathcal{Q}_2^\nu\right]e^{i\Phi}, \quad (3.56)$$

where the field-independent phase reads [see Eqs. (3.27) and (3.31)]

$$e^{i\Phi} = \exp\left\{i\left[(q_2^+ - q_1^+)z^- + \mu q_1 q_2 - \tau m^2\right]\right\} \tag{3.57}$$

$[\mu = \frac{1}{4}\tau(1-v^2);$ see Eq. (3.24)] and

$$b_1 = 2m^2\xi_1\xi_2\left(\frac{\tau}{4\mu}X_{12} - \frac{\tau v^2}{4\mu}X_{21}\right)e^{i\tau\beta},$$

$$b_2 = 2m^2\xi_1\xi_2\left(\frac{\tau}{4\mu}X_{21} - \frac{\tau v^2}{4\mu}X_{12}\right)e^{i\tau\beta},$$

$$b_3 = -\left(\frac{i}{\tau} + \frac{q_1 q_2}{2}\right)\left(e^{i\tau\beta} - 1\right) + 2m^2\left[\frac{\tau}{4\mu}\left(\xi_1^2 Z_1 + \xi_2^2 Z_2\right) + \xi_1^2 X_{11}\right]e^{i\tau\beta},$$

$$b_4 = -\left(\frac{i}{\tau} + \frac{q_1 q_2}{2}\right)\left(e^{i\tau\beta} - 1\right) + 2m^2\left[\frac{\tau}{4\mu}\left(\xi_1^2 Z_1 + \xi_2^2 Z_2\right) + \xi_2^2 X_{22}\right]e^{i\tau\beta},$$

$$b_5 = -\frac{2\mu}{\tau}\left(e^{i\tau\beta} - 1\right). \tag{3.58}$$

The field-dependent phase is given by [see Eq. (3.27)]

$$e^{i\tau\beta} = \exp\left[i\tau m^2 \sum_{i=1,2} \xi_i^2(I_i^2 - J_i)\right], \tag{3.59}$$

where [see Eq. (3.32)]

$$I_i = \frac{1}{2}\int_{-1}^{+1} d\lambda\,\psi_i(kz - \lambda\mu kq), \quad J_i = \frac{1}{2}\int_{-1}^{+1} d\lambda\,\psi_i^2(kz - \lambda\mu kq) \tag{3.60}$$

and [see Eq. (3.55)]

$$X_{ij} = [I_i - \psi_i(kz + \mu kq)]\,[I_j - \psi_j(kz - \mu kq)],$$
$$Z_i = \frac{1}{2}[\psi_i(kz - \mu kq) - \psi_i(kz + \mu kq)]^2. \tag{3.61}$$

We note that, using the metric tensor $g^{\mu\nu}$, we can construct the following projection tensor [BM75]

$$G^{\mu\nu} = q_2^\mu q_1^\nu - q_1 q_2\, g^{\mu\nu}, \tag{3.62}$$

which obeys

$$q_{1\mu}G^{\mu\nu} = G^{\mu\nu}q_{2\nu} = 0 \tag{3.63}$$

and can be decomposed as

$$G^{\mu\nu} = q_1 q_2\left(\Lambda_1^\mu\Lambda_1^\nu + \Lambda_2^\mu\Lambda_2^\nu\right) + \mathcal{Q}_1^\mu\mathcal{Q}_2^\nu. \tag{3.64}$$

This shows that the decomposition given in Eq. (3.56) has the structure claimed in Ref. [BM75].

3.2.7. Derivation of the BMS representation

The expression we obtained for the field-dependent part of $T^{\mu\nu}$ in Eq. (3.56) is manifestly symmetric in q_1^μ and q_2^μ. Now, we will show how the Baier-Milstein-Strakhovenko (BMS) representation found in Ref. [BMS76] can be derived from our calculation (see also Sec. 3.4.3). To this end we do not apply the shift in Eqs. (3.30) and (3.51), which means that we have to use the replacement given in Eq. (3.50) [rather than Eq. (3.54)] for the pp' term in Eq. (3.41). This modifies the coefficients b_3 and b_4. Furthermore, we apply the change of variables $z^- \to y^-$ [see Eq. (3.22)]

$$y^- = x^- + 2\mu q^- = z^- + \mu q^-, \tag{3.65}$$

which allows us to write [see Eq. (3.31)]

$$(q_2^+ - q_1^+)x^- + \mu q_2^2 = (q_2^+ - q_1^+)z^- + \mu q_1 q_2 = (q_2^+ - q_1^+)y^- + \mu q_1^2. \tag{3.66}$$

(here and in the remaining subsection we assume that all sources are set to zero). Thus, we obtain the following representation [see Eq. (3.28)]

$$I_i = \int_0^1 d\lambda\, \psi_i(ky - 2kq\mu\lambda), \quad J_i = \int_0^1 d\lambda\, \psi_i^2(ky - 2kq\mu\lambda), \tag{3.67}$$

$$I_i^2 - J_i = \left[\int_0^1 d\lambda\, \Delta_i(\mu\lambda)\right]^2 - \int_0^1 d\lambda\, \Delta_i^2(\mu\lambda), \tag{3.68}$$

where we introduced [BMS76]

$$\Delta_i(r) = \psi_i(ky - 2kqr) - \psi_i(ky). \tag{3.69}$$

Furthermore, it is useful to define [compare with Eq. (3.55)]

$$X_{ij} = [I_i - \psi_i(ky)]\,[I_j - \psi_j(kx)], \quad Y_i = [I_i - \psi_i(ky)]\,[\psi_i(kx) - \psi_i(ky)] \tag{3.70}$$

which can be written as

$$X_{ij} = \left[\int_0^1 d\lambda\, \Delta_i(\mu\lambda)\right]\left[\int_0^1 d\lambda\, \Delta_j(\mu\lambda) - \Delta_j(\mu)\right], \quad Y_i = \left[\int_0^1 d\lambda\, \Delta_i(\mu\lambda)\right]\Delta_i(\mu). \tag{3.71}$$

Finally, we obtain the following alternative representation for the field-dependent part of $T^{\mu\nu}$

$$T^{\mu\nu}(q_1, q_2) - T_{\mathfrak{F}=0}^{\mu\nu}(q_1, q_2) = -i\pi e^2\, \delta^{(-,\perp)}(q_1 - q_2) \int_{-1}^{+1} dv \int_0^\infty \frac{d\tau}{\tau} \int_{-\infty}^{+\infty} dy^-$$

$$\times\; [b_1\Lambda_1^\mu\Lambda_2^\nu + b_2\Lambda_2^\mu\Lambda_1^\nu + b_3'\Lambda_1^\mu\Lambda_1^\nu + b_4'\Lambda_2^\mu\Lambda_2^\nu + b_5\mathcal{Q}_1^\mu\mathcal{Q}_2^\nu]e^{i\Phi} \tag{3.72}$$

with the coefficients

$$b_1 = 2m^2\xi_1\xi_2\Big(\frac{\tau}{4\mu}X_{12} - \frac{\tau v^2}{4\mu}X_{21}\Big)e^{i\tau\beta},$$

$$b_2 = 2m^2\xi_1\xi_2\Big(\frac{\tau}{4\mu}X_{21} - \frac{\tau v^2}{4\mu}X_{12}\Big)e^{i\tau\beta},$$

$$b_3' = -\Big(\frac{i}{\tau} + \frac{q_2^2}{2}\Big)\left(e^{i\tau\beta} - 1\right) + 2m^2\Big[\frac{\tau}{4\mu}\left(\xi_1^2 Y_1 + \xi_2^2 Y_2\right) + \xi_1^2 X_{11}\Big]e^{i\tau\beta},$$

$$b_4' = -\Big(\frac{i}{\tau} + \frac{q_2^2}{2}\Big)\left(e^{i\tau\beta} - 1\right) + 2m^2\Big[\frac{\tau}{4\mu}\left(\xi_1^2 Y_1 + \xi_2^2 Y_2\right) + \xi_2^2 X_{22}\Big]e^{i\tau\beta},$$

$$b_5 = -\frac{2\mu}{\tau}\left(e^{i\tau\beta} - 1\right) \tag{3.73}$$

and phases

$$
\begin{aligned}
e^{i\Phi} &= \exp\left\{i\left[(q_2^+ - q_1^+)y^- + \mu q_1^2 - \tau m^2\right]\right\}, \\
e^{i\tau\beta} &= \exp\left[i\tau m^2 \sum_{i=1,2} \xi_i^2(I_i^2 - J_i)\right].
\end{aligned}
\tag{3.74}
$$

This representation coincides with Eq. (2.27) in Ref. [BMS76].

3.3. Special field configurations

The triple-integral representation given in Eq. (3.56) holds for an arbitrary plane-wave background field (arbitrary polarization and pulse shape). In this section we consider three important external field configurations for which the general result simplifies considerably.

3.3.1. Constant-crossed field

The polarization operator for a constant-crossed field was first obtained in Refs. [BS68; Nar69] (see also Refs. [BS71; Rit72a; Rit85]). We show now how this result can be obtained from the expression in Eq. (3.56).

A constant-crossed field is characterized by

$$\psi_1(\phi) = \phi, \quad \psi_2(\phi) = 0 \tag{3.75}$$

(the latter condition corresponds to $\xi_2 = 0$, and we will write $\xi = \xi_1$ in this paragraph). The field tensor and its square are then given by [see Eq. (1.17)]

$$F^{\mu\nu} = f_1^{\mu\nu}, \quad F^{2\mu\nu} = \frac{m^2\xi^2}{e^2}k^\mu k^\nu. \tag{3.76}$$

For a constant-crossed field, we obtain

$$
\begin{aligned}
I_1 &= kz, \quad J_1 = (kz)^2 + \frac{1}{3}(\mu kq)^2, \quad I_2 = J_2 = 0, \\
X_{11} &= -(\mu kq)^2, \quad Z_1 = 2(\mu kq)^2, \quad Z_2 = X_{12} = X_{21} = X_{22} = 0.
\end{aligned}
\tag{3.77}
$$

After inserting these expressions into Eq. (3.56), we can take the integral in dz^- and obtain a fourth delta function $2\pi\,\delta^{(+)}(q_1 - q_2) = 2\pi\,\delta(q_1^+ - q_2^+)$, which implies that the polarization tensor for a constant-crossed field is diagonal in the external photon four-momenta. Therefore, we define the four-vectors [see Eq. (3.35)]

$$q^\mu = q_1^\mu = q_2^\mu, \quad \mathcal{Q}^\mu = \mathcal{Q}_1^\mu = \mathcal{Q}_2^\mu = \frac{k^\mu q^2 - q^\mu kq}{kq}. \tag{3.78}$$

They obey

$$k\mathcal{Q} = -kq, \quad q\mathcal{Q} = 0, \quad \mathcal{Q}^2 = -q^2. \tag{3.79}$$

The four-vectors q^μ, $\mathcal{Q}^\mu$, Λ_1^μ, and Λ_2^μ form a complete set, and we obtain the following representation of the metric tensor

$$g^{\mu\nu} = \frac{1}{q^2}\left(q^\mu q^\nu - \mathcal{Q}^\mu \mathcal{Q}^\nu\right) - \Lambda_1^\mu \Lambda_1^\nu - \Lambda_2^\mu \Lambda_2^\nu. \tag{3.80}$$

Accordingly, the field-dependent part of $T^{\mu\nu}$ is in a constant-crossed field [see Eq. (3.75)] given by [see Eq. (3.56)]

$$T^{\mu\nu}(q_1, q_2) - T_{\mathfrak{F}=0}^{\mu\nu}(q_1, q_2) = -2i\pi^2 e^2\,\delta^4(q_1 - q_2)\int\limits_{-1}^{+1} dv \int\limits_0^\infty \frac{d\tau}{\tau}$$
$$\times\,[b_3\Lambda_1^\mu\Lambda_1^\nu + b_4\Lambda_2^\mu\Lambda_2^\nu + b_5\mathcal{Q}^\mu\mathcal{Q}^\nu]e^{i\Phi}, \tag{3.81}$$

where

$$b_3 = -\left(\frac{i}{\tau} + \frac{q^2}{2}\right)\left(e^{i\tau\beta} - 1\right) + m^6\chi^2\tau^2\frac{1}{4}(1 - v^2)\left[1 - \frac{1}{2}(1 - v^2)\right]e^{i\tau\beta},$$
$$b_4 = -\left(\frac{i}{\tau} + \frac{q^2}{2}\right)\left(e^{i\tau\beta} - 1\right) + m^6\chi^2\tau^2\frac{1}{4}(1 - v^2)e^{i\tau\beta},$$
$$b_5 = -\frac{1}{2}(1 - v^2)\left(e^{i\tau\beta} - 1\right) \tag{3.82}$$

and the phases are given by

$$i\Phi = -i\tau a, \quad a = m^2\left[1 - \frac{1}{4}(1 - v^2)\frac{q^2}{m^2}\right],$$
$$i\tau\beta = -\frac{i}{3}\tau^3 b, \quad b = m^6\chi^2\left[\frac{1}{4}(1 - v^2)\right]^2 \tag{3.83}$$

(in the following, we will make the change of variables $\tau \to t$, where $\tau^3 b = t^3$ and $\rho = a/\sqrt[3]{b}$). Here, we have introduced the quantum nonlinearity parameter [see Eq. (1.21)]

$$\chi = \frac{|e|\sqrt{qF^2q}}{m^3} = \xi\frac{\sqrt{(kq)^2}}{m^2} \tag{3.84}$$

(κ in Refs. [Nar69; Rit72a]).

Now, we use the identities

$$\Lambda_1^\mu \Lambda_1^\nu = -\frac{(Fq)^\mu (Fq)^\nu}{(Fq)^2}, \quad \Lambda_2^\mu \Lambda_2^\nu = -\frac{(F^*q)^\mu (F^*q)^\nu}{(F^*q)^2}, \tag{3.85}$$

where

$$(F^*q)^2 = (Fq)^2 = -\frac{m^2 \xi^2}{e^2}(kq)^2 \tag{3.86}$$

and [see Eq. (3.62)]

$$G^{\mu\nu} = q^\mu q^\nu - q^2\, g^{\mu\nu} = q^2\,(\Lambda_1^\mu \Lambda_1^\nu + \Lambda_2^\mu \Lambda_2^\nu) + \mathcal{Q}^\mu \mathcal{Q}^\nu. \tag{3.87}$$

Note that $G^{\mu\nu}$ obeys the following relations

$$q_\rho G^{\rho\nu} = G^{\mu\rho} q_\rho = 0, \quad k_\rho G^{\rho\mu} = G^{\mu\rho} k_\rho = -kq\mathcal{Q}^\mu,$$

$$G^{\mu\rho} F_{\rho\sigma}^2 G^{\sigma\nu} = \frac{m^2}{e^2}\xi^2 (kq)^2 \mathcal{Q}^\mu \mathcal{Q}^\nu. \tag{3.88}$$

To obtain the representation given in Refs. [Rit72a; Rit85], we pass over to different basis tensors

$$b_3 \Lambda_1^\mu \Lambda_1^\nu + b_4 \Lambda_2^\mu \Lambda_2^\nu + b_5 \mathcal{Q}^\mu \mathcal{Q}^\nu = (q^2 b_5 - b_3)\frac{(Fq)^\mu (Fq)^\nu}{(Fq)^2}$$
$$+ (q^2 b_5 - b_4)\frac{(F^*q)^\mu (F^*q)^\nu}{(F^*q)^2} + b_5 G^{\mu\nu} \tag{3.89}$$

and define the following functions (see App. F for more details)

$$f(x) = i\int_0^\infty dt \exp\left[-i\left(tx + \frac{1}{3}t^3\right)\right] = \pi\,\mathrm{Gi}(x) + i\pi\,\mathrm{Ai}(x), \tag{3.90}$$

$$f'(x) = \int_0^\infty t dt \exp\left[-i\left(tx + \frac{1}{3}t^3\right)\right], \tag{3.91}$$

$$f_1(x) = \int_0^\infty \frac{dt}{t} \exp(-itx)\left[\exp\left(-\frac{i}{3}t^3\right) - 1\right], \tag{3.92}$$

where Ai and Gi denote the Airy and Scorer function, respectively [Olv+10]. They obey the following differential equations

$$f''(x) = xf(x) - 1, \quad f_1'(x) = \frac{1}{x} - f(x) = -\frac{1}{x}f''(x). \tag{3.93}$$

Using the latter, we can replace the function $f_1(x)$ by $f'(x)$ in the following way (if all boundary terms vanish)

$$\int_{-1}^{+1} dv\, g(v) f_1[\rho(v)] = -\int_{-1}^{+1} dv \left[\frac{G(v)}{\rho(v)}\right]' f'[\rho(v)], \quad G'(v) = g(v). \tag{3.94}$$

Using the above notation, it is possible to represent the field-dependent part of the tensor $T^{\mu\nu}$ for a constant-crossed field [see Eq. (3.81)] by

$$T^{\mu\nu}(q_1, q_2) - T^{\mu\nu}_{\mathfrak{F}=0}(q_1, q_2) = i(2\pi)^4 \delta^4(q_1 - q_2)$$
$$\times \left[\pi_1 \frac{(Fq)^\mu (Fq)^\nu}{(Fq)^2} + \pi_2 \frac{(F^*q)^\mu (F^*q)^\nu}{(F^*q)^2} - \frac{\pi_3}{q^2} G^{\mu\nu} \right], \quad (3.95)$$

where

$$\pi_1 = \alpha \frac{m^2}{3\pi} \int\limits_{-1}^{+1} dv\, (w-1) \left(\frac{\chi}{w}\right)^{2/3} f'(\rho), \quad \pi_2 = \alpha \frac{m^2}{3\pi} \int\limits_{-1}^{+1} dv\, (w+2) \left(\frac{\chi}{w}\right)^{2/3} f'(\rho),$$

$$\pi_3 = -\alpha \frac{q^2}{\pi} \int\limits_{-1}^{+1} dv\, \frac{f_1(\rho)}{w}$$

$$(3.96)$$

$[\frac{1}{w} = \frac{1}{4}(1-v^2),\ \rho = (w/\chi)^{2/3}(1 - \frac{q^2}{m^2}\frac{1}{w})]$. Since all nonvanishing functions are even in v, we can now apply the following change of variables

$$\int\limits_{-1}^{+1} dv = 2 \int\limits_{0}^{1} dv = \int\limits_{4}^{\infty} dw\, \frac{4}{w\sqrt{w(w-4)}}, \quad (3.97)$$

which shows that the result in Eq. (3.95) is equivalent to the one given in Refs. [Rit72a; Rit85].

3.3.2. Quasistatic limit

We consider now a linearly polarized plane-wave field

$$\psi_1(\phi) = \psi(\phi), \quad \psi_2(\phi) = 0 \quad (3.98)$$

(we will set $\xi = \xi_1$ and $f^{\mu\nu} = f_1^{\mu\nu}$ in this paragraph) in the quasistatic limit defined by $\xi \to \infty$ while [see Eq. (3.84)]

$$\chi = \frac{|e|\sqrt{q f^2 q}}{m^3} = \xi \frac{\sqrt{(kq)^2}}{m^2} \quad (3.99)$$

is kept constant. In the optical regime (photon energy $\omega_0 \sim 1\,\text{eV}$), $\chi \gtrsim 1$ requires $\xi \gg 1$ (unless the incoming photon energy exceeds the threshold of about 1 TeV), which means that the quasistatic limit is sufficient to analyze most of the upcoming strong-field experiments with optical lasers (one notable exception are recollision processes, see Chap. 4).

By employing the identity $|kq| = m^2\chi/\xi$, we can expand all functions depending on μkq

$$I_1^2 - J_1 = -(1/3)(\mu kq)^2 [\psi'(kz)]^2 + \mathcal{O}(\mu kq)^3,$$

$$Z_1 = 2(\mu kq)^2 [\psi'(kz)]^2 + \mathcal{O}(\mu kq)^3, \quad X_{11} = -(\mu kq)^2 [\psi'(kz)]^2 + \mathcal{O}(\mu kq)^3 \tag{3.100}$$

($X_{12} = X_{21} = X_{22} = Z_2 = I_2 = J_2 = 0$ for linear polarization). Thus, if multiplied by ξ^2, only the leading-order terms are independent of ξ, and all others are suppressed. In the limit $\xi \to \infty$, the expressions in Eq. (3.100) correspond to those in Eq. (3.77) with the replacement $\chi \to \chi(kz) = \chi\psi'(kz)$. The remaining calculation is therefore similar to the one in the constant-crossed field case, and the final result in Eq. (3.102) corresponds essentially to Eq. (3.95) with the above replacement. Using [see Eq. (3.85)]

$$\Lambda_1^\mu \Lambda_1^\nu = -\frac{(fq)^\mu (fq)^\nu}{(fq)^2}, \quad \Lambda_2^\mu \Lambda_2^\nu = -\frac{(f^*q)^\mu (f^*q)^\nu}{(f^*q)^2} \tag{3.101}$$

and Eq. (3.64), we obtain for a linearly polarized plane-wave field in the quasistatic approximation the following representation for the field-dependent part of the tensor $T^{\mu\nu}$ [see Eq. (3.56)]

$$T^{\mu\nu}(q_1, q_2) - T_{\mathfrak{F}=0}^{\mu\nu}(q_1, q_2) = i(2\pi)^4 \delta^{(-,\perp)}(q_1 - q_2) \frac{1}{2\pi} \int_{-\infty}^{+\infty} dz^- \, e^{i(q_2^+ - q_1^+)z^-}$$
$$\times \left[\pi_1' \frac{(fq)^\mu (fq)^\nu}{(fq)^2} + \pi_2' \frac{(f^*q)^\mu (f^*q)^\nu}{(f^*q)^2} - \frac{\pi_3'}{q_1 q_2} G^{\mu\nu} \right], \tag{3.102}$$

where [see Eq. (3.96)]

$$\pi_1' = \alpha \frac{m^2}{3\pi} \int_{-1}^{+1} dv \, (w - 1) \left[\frac{|\chi(kz)|}{w} \right]^{2/3} f'(\rho),$$

$$\pi_2' = \alpha \frac{m^2}{3\pi} \int_{-1}^{+1} dv \, (w + 2) \left[\frac{|\chi(kz)|}{w} \right]^{2/3} f'(\rho),$$

$$\pi_3' = -\alpha \frac{q_1 q_2}{\pi} \int_{-1}^{+1} dv \, \frac{f_1(\rho)}{w} \tag{3.103}$$

with $\frac{1}{w} = \frac{1}{4}(1 - v^2)$, $\rho = [w/|\chi(kz)|]^{2/3}(1 - \frac{q_1 q_2}{m^2} \frac{1}{w})$ and $G^{\mu\nu} = q_2^\mu q_1^\nu - q_1 q_2 \, g^{\mu\nu}$ [see Eq. (3.62)].

3.3.3. Circular polarization

The general result in Eq. (3.56) also simplifies considerably if the plane wave is circularly polarized and monochromatic,

$$\psi_1(\phi) = \Re e^{i\phi}, \quad \psi_2(\phi) = \Im e^{i\phi}, \quad \xi_1 = \xi_2 = \xi. \tag{3.104}$$

Then, we obtain

$$I_1 = \mathrm{sinc}(\mu kq)\Re e^{ikz}, \quad I_2 = \mathrm{sinc}(\mu kq)\Im e^{ikz},$$

$$J_1 + J_2 = 1, \quad Z_1 + Z_2 = 2\sin^2(\mu kq), \tag{3.105}$$

$$
\begin{aligned}
I_1 - \psi_1(kz + \mu kq) = \Re A, \quad I_2 - \psi_2(kz + \mu kq) = \Im A, \\
I_1 - \psi_1(kz - \mu kq) = \Re B, \quad I_2 - \psi_2(kz - \mu kq) = \Im B,
\end{aligned}
\tag{3.106}
$$

where

$$
\begin{aligned}
A &= e^{ikz}\left[\operatorname{sinc}(\mu kq) - \cos(\mu kq) - i\sin(\mu kq)\right], \\
B &= e^{ikz}\left[\operatorname{sinc}(\mu kq) - \cos(\mu kq) + i\sin(\mu kq)\right]
\end{aligned}
\tag{3.107}
$$

[we define $\operatorname{sinc} x = (\sin x)/x$]. Thus,

$$
\begin{aligned}
X_{12} - X_{21} = \Im A^* B, \quad X_{11} - X_{22} = \Re AB, \\
X_{12} + X_{21} = \Im AB, \quad\ \ X_{11} + X_{22} = \Re A^* B,
\end{aligned}
\tag{3.108}
$$

where

$$
\begin{aligned}
A^* B &= \operatorname{sinc}^2(\mu kq) + \cos(2\mu kq) - 2\operatorname{sinc}(2\mu kq) \\
&\quad + i\left[-\sin(2\mu kq) + 2\operatorname{sinc}(\mu kq)\sin(\mu kq)\right], \\
AB &= e^{2ikz}\left[\operatorname{sinc}^2(\mu kq) - 2\operatorname{sinc}(2\mu kq) + 1\right].
\end{aligned}
\tag{3.109}
$$

Thus, we can write the field-dependent part of the tensor $T^{\mu\nu}$ for a circularly polarized plane wave as [see Eq. (3.56)]

$$
\begin{aligned}
T^{\mu\nu}(q_1, q_2) - T^{\mu\nu}_{\mathfrak{F}=0}(q_1, q_2) &= -i\pi e^2\, \delta^{(-,\perp)}(q_1 - q_2) \int\limits_{-1}^{+1} dv \int\limits_{0}^{\infty} \frac{d\tau}{\tau} \int\limits_{-\infty}^{+\infty} dz^- \\
&\times \Big[b_+\Lambda_+^\mu\Lambda_+^\nu + b_-\Lambda_-^\mu\Lambda_-^\nu + \frac{1}{2}(b_1 - b_2)(\Lambda_1^\mu\Lambda_2^\nu - \Lambda_2^\mu\Lambda_1^\nu) \\
&\quad + \frac{1}{2}(b_3 + b_4)(\Lambda_1^\mu\Lambda_1^\nu + \Lambda_2^\mu\Lambda_2^\nu) + b_5\mathcal{Q}_1^\mu\mathcal{Q}_2^\nu \Big] e^{i\Phi}, \quad (3.110)
\end{aligned}
$$

where we defined $\Lambda_\pm^\mu = \Lambda_1^\mu \pm i\Lambda_2^\mu$. Furthermore, the coefficients are given by

$$
\begin{aligned}
b_\pm &= \frac{1}{4}\left[(b_3 - b_4) \mp i(b_1 + b_2)\right] \\
&= \frac{1}{2}m^2\xi^2\left[\operatorname{sinc}^2(\mu kq) - 2\operatorname{sinc}(2\mu kq) + 1\right]e^{\mp 2ikz + i\tau\beta}, \quad (3.111\text{a})
\end{aligned}
$$

$$\frac{1}{2}(b_1 - b_2) = m^2\xi^2\frac{(1 + v^2)}{(1 - v^2)}\left[-\sin(2\mu kq) + 2\operatorname{sinc}(\mu kq)\sin(\mu kq)\right]e^{i\tau\beta}, \quad (3.111\text{b})$$

$$
\begin{aligned}
\frac{1}{2}(b_3 + b_4) &= -\left(\frac{i}{\tau} + \frac{q_1 q_2}{2}\right)\left(e^{i\tau\beta} - 1\right) + m^2\xi^2\Big[2\frac{(1 + v^2)}{(1 - v^2)}\sin^2(\mu kq) \\
&\quad + \operatorname{sinc}^2(\mu kq) - 2\operatorname{sinc}(2\mu kq) + 1\Big]e^{i\tau\beta}, \quad (3.111\text{c})
\end{aligned}
$$

$$b_5 = -\frac{2\mu}{\tau}\left(e^{i\tau\beta} - 1\right) \tag{3.111d}$$

and the phases read

$$i\tau\beta = i\tau m^2\xi^2\left[\operatorname{sinc}^2(\mu k q) - 1\right],$$
$$i\Phi = i\left[(q_2^+ - q_1^+)z^- + \mu q_1 q_2 - \tau m^2\right] \tag{3.112}$$

$[\mu = \frac{1}{4}\tau(1 - v^2)]$. Finally, the integral in dz^- can be taken and we obtain the following expression for the field-dependent part of $T^{\mu\nu}(q_1, q_2)$ for a monochromatic, circularly polarized plane-wave laser field

$$T^{\mu\nu}(q_1, q_2) - T^{\mu\nu}_{\mathfrak{F}=0}(q_1, q_2) = -\frac{i(2\pi)^4 e^2}{8\pi^2}\int\limits_{-1}^{+1}dv\int\limits_{0}^{\infty}\frac{d\tau}{\tau}\,e^{i\Phi_{\mathrm{cp}}}$$
$$\times\;\left[T_0^{\mu\nu}\delta^4(q_1 - q_2) + T_+^{\mu\nu}\delta^4(q_1 - q_2 + 2k) + T_-^{\mu\nu}\delta^4(q_1 - q_2 - 2k)\right], \tag{3.113}$$

where

$$i\Phi_{\mathrm{cp}} = -i\tau m^2\{1 + \xi^2[1 - \operatorname{sinc}^2(\mu k q)]\} + i\mu q_1 q_2, \tag{3.114}$$

$$T_0^{\mu\nu} = \tau_1(\Lambda_1^\mu\Lambda_2^\nu - \Lambda_2^\mu\Lambda_1^\nu) + \tau_2(\Lambda_1^\mu\Lambda_1^\nu + \Lambda_2^\mu\Lambda_2^\nu) + \tau_3\mathcal{Q}_1^\mu\mathcal{Q}_2^\nu,$$
$$T_\pm^{\mu\nu} = \frac{1}{2}m^2\xi^2\left[\operatorname{sinc}^2(\mu k q) - 2\operatorname{sinc}(2\mu k q) + 1\right]\Lambda_\pm^\mu\Lambda_\pm^\nu \tag{3.115}$$

and

$$\tau_1 = m^2\xi^2\frac{(1 + v^2)}{(1 - v^2)}\left[2\sin^2(\mu k q)/(\mu k q) - \sin(2\mu k q)\right],$$
$$\tau_2 = 2m^2\xi^2\frac{(1 + v^2)}{(1 - v^2)}\sin^2(\mu k q) + \left[\left(\frac{\mu}{\tau} - \frac{1}{2}\right)q_1 q_2 - m^2\right]\left(1 - e^{-i\tau\beta}\right), \tag{3.116}$$
$$\tau_3 = -\frac{2\mu}{\tau}\left(1 - e^{-i\tau\beta}\right).$$

This result agrees with Eq. (2.34) in Ref. [BMS76]. The terms described by $T_\pm^{\mu\nu}$ can be interpreted as describing processes where two photons from the background field are absorbed or emitted, respectively (since the external field is not quantized, this interpretation relies only on the momentum-conserving delta function).

In order to obtain Eq. (3.113) from Eq. (3.110), we have used the identity

$$\int\limits_{0}^{\infty}\frac{d\tau}{\tau}e^{i\Phi}\,m^2\xi^2\left[\operatorname{sinc}^2(\mu k q) - 2\operatorname{sinc}(2\mu k q) + 1\right]e^{i\tau\beta}$$
$$= \int\limits_{0}^{\infty}\frac{d\tau}{\tau}e^{i\Phi}\left[\frac{i}{\tau} + \frac{\mu}{\tau}q_1 q_2 - m^2\right]\left(e^{i\tau\beta} - 1\right), \tag{3.117}$$

which follows from

$$i\frac{d}{d\tau}\big(e^{i\tau\beta}-1\big) = i\frac{d}{d\tau}e^{i\tau\beta} = m^2\xi^2\big[\operatorname{sinc}^2(\mu kq) - 2\operatorname{sinc}(2\mu kq) + 1\big]e^{i\tau\beta} \qquad (3.118)$$

via integration by parts.

3.4. Double-integral representation for the leading-order result

In Sec. 3.3 we investigated several important special field configurations and derived compact expressions for the associated polarization operators. Now, we return to the general triple-integral expression given in Eq. (3.56) and show how one more integral can be solved analytically without any assumption about the background field[3]. To this end we clarify the physical meaning of the remaining integration variables (see Sec. 3.4.1). More specifically, we show that after an appropriate change of variables two of them are related to the laser phase of the creation and the annihilation vertex, respectively, and one determines the momentum propagating in the loop. The latter integral can be expressed analytically in terms of Hankel functions, for which very efficient numerical calculation schemes are known (see Sec. 3.4.2).

As the incoming and the outgoing photon momentum must differ only by a multiple of the plane-wave four-momentum k^μ, the dependence of the polarization operator on the momenta of the external photons can be expressed in terms of different scalar products (e.g., q_1^2, q_2^2 or $q_1 q_2$; see Sec. 3.4.3). Choosing $q_1 q_2$ and kq as independent variables as in Eq. (3.56) ensures that the symmetry between the incoming and the outgoing photon is manifest. For the calculations presented in Chap. 2 and Chap. 4, however, the incoming photon is to a good approximation on shell ($q_1^2 = 0$), which implies that the combination q_1^2 and kq is more convenient. Such a representation is finally derived in Sec. 3.4.4 (for other double-integral representations see [BM75; Din+14b]).

Naturally, the remaining two integrals over the laser phases of the two vertices depend nontrivially on the shape of the laser field and can in general only be solved numerically or by applying approximations. As the integrals are highly oscillatory (at least for $\xi \gg 1$), a full numerical calculation is by itself a challenging task (this problem is addressed in Chap. 4, see Sec. 4.5).

3.4.1. Physical interpretation of the integration variables

The triple-integral representation for the leading-order contribution to the polarization operator given in Eq. (3.56) is expressed in terms of the integration variables $kz = z^-$, τ and v. To understand the physical meaning of τ and v [which originate from the proper-time integrals in s and t, see Eq. (3.18) and Eq. (3.24)], the delta functions obtained in Sec. 3.2.2 must be analyzed.

As the phases of the creation and the annihilation vertex are given by $kx = kz - \varrho$ and $ky = kz + \varrho$, respectively [see Eq. (3.22) and Eq. (3.30)], the change of variables

---

[3]Note that the results obtained in Sec. 3.3 and the analysis carried out here are complementary, as different integrals are considered. In the quasistatic limit (see Sec. 3.3.2) one of the integrals in the laser phases is solved approximately (for a constant-crossed field even both) but the momentum integral remains. Here, the momentum integral is solved exactly. For reasons explained in Sec. 3.4.4, a simple combination of both approaches is not feasible.

from τ to ϱ is useful

$$\tau = \mu w = \frac{\varrho w}{kq}, \quad \varrho = \mu kq, \quad \mu = \frac{1}{4}\tau(1 - v^2), \quad \frac{1}{w} = \frac{1}{4}(1 - v^2). \qquad (3.119)$$

Furthermore, it is convenient to integrate over w instead of v. The variable w is related to the momenta p_1^μ and p_2^μ of the created electron and positron, respectively, by[4] $w = (kq)^2/(kp_1 kp_2)$ [see Eq. (3.22)]. Assuming that the integrand is an even function of v, we obtain [see Eq. (3.97)]

$$\int_{-1}^{+1} dv \int_0^\infty \frac{d\tau}{\tau} \int_{-\infty}^{+\infty} dz^- = \int_4^\infty dw \frac{4}{w\sqrt{w(w-4)}} \int_0^{\sigma\infty} \frac{d\varrho}{\varrho} \int_{-\infty}^{+\infty} dz^-, \qquad (3.120)$$

where $\sigma = \operatorname{sign}(kq)$.

In terms of the new variables the phases [see Eq. (3.57) and Eq. (3.59)] can be written as

$$\begin{aligned}
\Phi &= (q_2^+ - q_1^+)z^- + \varrho(q_1 q_2/kq) - w\,(m^2/kq)\,\varrho, \\
\Phi_1 &= (q_2^+ - q_1^+)z^- + \varrho\,(q_1 q_2/kq) - w\,(m^2/kq)\,\mathcal{D}(\varrho, kz),
\end{aligned} \qquad (3.121)$$

where $\Phi_1 = \Phi + \tau\beta$ and we defined [see Eq. (3.28)]

$$\mathcal{D}(\varrho, kz) = \varrho\left[1 + \sum_{i=1,2} \xi_i^2\left(J_i - I_i^2\right)\right],$$

$$I_i = \frac{1}{2\varrho} \int_{kz-\varrho}^{kz+\varrho} d\phi\,\psi_i(\phi), \quad J_i = \frac{1}{2\varrho} \int_{kz-\varrho}^{kz+\varrho} d\phi\,\psi_i^2(\phi). \qquad (3.122)$$

3.4.2. Analytical calculation of the momentum integral

After the change of variables given in Eq. (3.120), the phases have a very simple dependence on w [see Eq. (3.121)] and the integral in w can be calculated analytically. To this end we define the functions $\mathcal{W}_l(x)$ [$l = 0, 1, 2$, $x \geq 0$, see Eq. (G.2) and Fig. 41]

$$\int_4^\infty dw \frac{4}{w^l\sqrt{w(w-4)}}\,e^{-iwx} = e^{-i4x}\,\mathcal{W}_l(x), \qquad (3.123)$$

which are non-oscillatory and scale asymptotically as [see Eq. (G.4)]

$$\mathcal{W}_l(x) \sim -\frac{2\sqrt{\pi}i}{4^l}\,e^{i\pi/4}\frac{1}{\sqrt{x}} \qquad (3.124)$$

---

[4]Note that the definition used here for w (see Sec. 3.3.1) agrees with the one introduced in Eq. (1.84) for the dressed vertex. Due to the sign convention adopted for the dressed vertex, the momenta p'^μ and p^μ appearing in the polarization operator are related to the momenta p_1^μ and p_2^μ of the created electron and positron, respectively, by $p'^\mu = p_1^\mu$ and $p^\mu = -p_2^\mu$, see Sec. 1.6.

[note that $\mathcal{W}_0(x)$ has a logarithmic singularity at $x = 0$]. As shown in App. G, they can be expressed in terms of Hankel functions [see Eq. (G.19)]

$$
\begin{aligned}
\mathcal{W}_0(x) &= (-2\pi i)\, e^{i2x}\, \mathrm{H}_0^{(2)}(2x), \\
\mathcal{W}_1(x) &= (-2\pi x)\, e^{i2x} \left[\mathrm{H}_0^{(2)}(2x) + i\, \mathrm{H}_1^{(2)}(2x) \right], \\
\mathcal{W}_2(x) &= \frac{\pi x}{3}\, e^{i2x} \left[4ix\, \mathrm{H}_0^{(2)}(2x) - (4x + i)\, \mathrm{H}_1^{(2)}(2x) \right].
\end{aligned}
\tag{3.125}
$$

3.4.3. Different representations for the polarization operator

The representation given for the polarization operator in Eq. (3.56) depends on the external photon momenta via the scalar $q_1 q_2$. As already mentioned in the introduction, for a real incoming or a real outgoing photon it is more convenient to use a representation which depends only on q_1^2 or q_2^2, respectively. To obtain such a representation, we use the fact that momentum is conserved and write

$$
q_2^\mu = q_1^\mu + nk^\mu, \quad n = q_2^+ - q_1^+, \quad q_1 q_2 = q_1^2 + nkq = q_2^2 - nkq, \tag{3.126}
$$

where n is in general not an integer and denotes the amount of four-momentum k^μ exchanged with the background field ($n > 0$ corresponds to absorption, $n < 0$ to emission). Thus, the integral in z^- represents a Fourier transform that determines the probability amplitude to absorb nk^μ four-momentum from the background field. Using the relations above, the phases can be rewritten as [see Eq. (3.121)]

$$
(q_2^+ - q_1^+)z^- + \varrho \frac{q_1 q_2}{kq} = nkz + \varrho \frac{q_1 q_2}{kq} = nky + \varrho \frac{q_1^2}{kq} = nkx + \varrho \frac{q_2^2}{kq}. \tag{3.127}
$$

By changing now the integration variable from z^- to either x^- (real outgoing photon) or y^- (real incoming photon), the phase of the polarization operator simplifies in these cases. Depending on this choice one of the following representations for the functions I_i and J_i defined in Eq. (3.28) is particularly convenient [see Eq. (3.122)]

$$
\begin{aligned}
I_i &= \int_0^1 d\lambda\, \psi_i(ky - 2\varrho\lambda) = \int_0^1 d\lambda\, \psi_i(kx + 2\varrho\lambda), \\
J_i &= \int_0^1 d\lambda\, \psi_i^2(ky - 2\varrho\lambda) = \int_0^1 d\lambda\, \psi_i^2(kx + 2\varrho\lambda).
\end{aligned}
\tag{3.128}
$$

Similarly, we can rewrite the preexponent using the following identity

$$
\frac{nkq}{2} \int_{-\infty}^{+\infty} dz^-\, e^{i\Phi} \left(e^{i\tau\beta} - 1 \right) = (-i)\frac{kq}{2} \int_{-\infty}^{+\infty} dz^- \left(e^{i\tau\beta} - 1 \right) \frac{\partial}{\partial z^-} e^{i\Phi}
$$

$$
= 2m^2 \frac{\tau}{4\mu} \int_{-\infty}^{+\infty} dz^-\, e^{i\Phi} e^{i\tau\beta} \sum_{i=1,2} \xi_i^2 \left(Y_i - Z_i \right), \tag{3.129}
$$

where [see Eq. (3.70)]

$$Y_i = [I_i - \psi_i(ky)] [\psi_i(kx) - \psi_i(ky)]. \tag{3.130}$$

To prove Eq. (3.129) we used integration by parts and

$$
\begin{aligned}
\frac{\partial I_i(\varrho, kz)}{\partial z^-} &= -\frac{1}{2\varrho} [\psi_i(kz - \varrho) - \psi_i(kz + \varrho)], \\
\frac{\partial J_i(\varrho, kz)}{\partial z^-} &= -\frac{1}{2\varrho} \left[\psi_i^2(kz - \varrho) - \psi_i^2(kz + \varrho) \right].
\end{aligned} \tag{3.131}
$$

Furthermore, it is useful to define $V_i = 2Z_i - Y_i$.

By applying the above relations to the symmetric representation for the polarization operator given in Eq. (3.56), we immediately obtain the BMS-representation [see Eq. (3.72)], which has been derived differently in Sec. 3.2.7.

3.4.4. Final result

After combining the results discussed above, we obtain the following double-integral representation for the field-dependent part of the polarization operator inside a plane-wave background field

$$
\begin{aligned}
i\mathcal{P}^{\mu\nu}(q_1, q_2) - i\mathcal{P}^{\mu\nu}_{\mathfrak{F}=0}(q_1, q_2) = &-i(2\pi)^3 \, \delta^{(-,\perp)}(q_1 - q_2) \frac{\alpha}{2\pi} \int\limits_0^{\sigma\infty} \frac{d\varrho}{\varrho} \int\limits_{-\infty}^{+\infty} dy^- \\
&\times [P_{12}\Lambda_1^\mu\Lambda_2^\nu + P_{21}\Lambda_2^\mu\Lambda_1^\nu + P_{11}\Lambda_1^\mu\Lambda_1^\nu + P_{22}\Lambda_2^\mu\Lambda_2^\nu + P_Q\mathcal{Q}_1^\mu\mathcal{Q}_2^\nu], \quad (3.132)
\end{aligned}
$$

$\sigma = \mathrm{sign}(kq)$, where the coefficients are given by

$$
\begin{aligned}
P_{12} &= \frac{m^2\xi_1\xi_2}{2} \{\mathcal{W}_0(x_1)X_{12} + [4\mathcal{W}_1(x_1) - \mathcal{W}_0(x_1)]X_{21}\}e^{i\widetilde{\Phi}_1}, \\
P_{21} &= \frac{m^2\xi_1\xi_2}{2} \{\mathcal{W}_0(x_1)X_{21} + [4\mathcal{W}_1(x_1) - \mathcal{W}_0(x_1)]X_{12}\}e^{i\widetilde{\Phi}_1}, \\
P_{11} &= -m^2 \left[\frac{i}{\varrho}\frac{kq}{m^2}\mathcal{W}_2(x_1) + \frac{q_1^2}{2m^2}\mathcal{W}_1(x_1)\right]e^{i\widetilde{\Phi}_1} \\
&\quad + m^2 \left[\frac{i}{\varrho}\frac{kq}{m^2}\mathcal{W}_2(x_0) + \frac{q_1^2}{2m^2}\mathcal{W}_1(x_0)\right]e^{i\widetilde{\Phi}_0} \\
&\quad + m^2 \left[\frac{1}{2}\left(\xi_1^2 V_1 + \xi_2^2 V_2\right)\mathcal{W}_0(x_1) + 2\xi_1^2 X_{11}\mathcal{W}_1(x_1)\right]e^{i\widetilde{\Phi}_1}, \\
P_{22} &= -m^2 \left[\frac{i}{\varrho}\frac{kq}{m^2}\mathcal{W}_2(x_1) + \frac{q_1^2}{2m^2}\mathcal{W}_1(x_1)\right]e^{i\widetilde{\Phi}_1} \\
&\quad + m^2 \left[\frac{i}{\varrho}\frac{kq}{m^2}\mathcal{W}_2(x_0) + \frac{q_1^2}{2m^2}\mathcal{W}_1(x_0)\right]e^{i\widetilde{\Phi}_0} \\
&\quad + m^2 \left[\frac{1}{2}\left(\xi_1^2 V_1 + \xi_2^2 V_2\right)\mathcal{W}_0(x_1) + 2\xi_2^2 X_{22}\mathcal{W}_1(x_1)\right]e^{i\widetilde{\Phi}_1}, \\
P_Q &= -2 \left[\mathcal{W}_2(x_1)e^{i\widetilde{\Phi}_1} - \mathcal{W}_2(x_0)e^{i\widetilde{\Phi}_0}\right]
\end{aligned} \tag{3.133}
$$

and the phases read [see Eq. (3.121)]

$$\widetilde{\Phi}_0 = (q_2^+ - q_1^+)y^- + \varrho(q_1^2/kq) - 4x_0,$$
$$\widetilde{\Phi}_1 = (q_2^+ - q_1^+)y^- + \varrho\,(q_1^2/kq) - 4x_1. \tag{3.134}$$

Here, we have introduced

$$x_0 = (m^2/kq)\,\varrho, \quad x_1 = (m^2/kq)\,\mathcal{D}(\varrho, ky), \tag{3.135}$$

where [see Eq. (3.122) and Eq. (3.128)]

$$\mathcal{D}(\varrho, ky) = \varrho\left[1 + \sum_{i=1,2} \xi_i^2(J_i - I_i^2)\right],$$
$$I_i = \int_0^1 d\lambda\,\psi_i(ky - 2\varrho\lambda), \quad J_i = \int_0^1 d\lambda\,\psi_i^2(ky - 2\varrho\lambda). \tag{3.136}$$

Furthermore, [see Eq. (3.55)]

$$X_{ij} = [I_i - \psi_i(ky)]\,[I_j - \psi_j(ky - 2\varrho)],$$
$$V_i = [I_i - \psi_i(ky - 2\varrho)]\,[\psi_i(ky) - \psi_i(ky - 2\varrho)] \tag{3.137}$$

and the functions $\mathcal{W}_l(x)$ are defined in Eq. (G.1).

Having taken the w-integral analytically, we are left with the integrals in $y^- = ky$ and ϱ. To evaluate these integrals, the precise shape of the background field has to be known and it is therefore reasonable to use numerical methods (see Chap. 4 for more details).

Finally, we note that the quasistatic approximation [see Eq. (3.102)] was obtained from the triple-integral representation given in Eq. (3.56) using suitable approximations. It is tempting to apply them also to the double-integral representation in Eq. (3.132). However, this is not possible because the functions $\mathcal{W}_i$ change over the formation region ($\mathcal{W}_0$ even has a logarithmic singularity at the origin).

3.5. Mass dressing in the laser field

To conclude this chapter, we want to show that the nonlinear phase of the polarization operator can be interpreted in terms of the so-called mass dressing in the laser field.

It is well known that inside a linearly polarized, monochromatic field the square of the dressed electron (positron) mass is given by [Rit85]

$$m_*^2 = m^2(1 + \xi^2/2), \tag{3.138}$$

which corresponds to the square of the average (classical) electron four-momentum. This definition of the dressed mass may be generalized to an arbitrary plane-wave field by noting that the classical four-momentum of an electron (charge e and mass

m) is given by [see Eq. (A.13)]

$$P^\mu(\phi) = P_0^\mu + \frac{e\mathfrak{F}^\mu{}_\nu(\phi,\phi_0)P_0^\nu}{kP_0} + \frac{e^2\mathfrak{F}^{2\mu}{}_\nu(\phi,\phi_0)P_0^\nu}{2(kP_0)^2}, \tag{3.139}$$

where $P_0^\mu = P^\mu(\phi_0)$ and [see Eq. (1.17)]

$$\mathfrak{F}^{\mu\nu}(\phi,\phi_0) = \int_{\phi_0}^{\phi} d\phi'\, F^{\mu\nu}(\phi') = \sum_{i=1,2} f_i^{\mu\nu}[\psi_i(\phi) - \psi_i(\phi_0)]. \tag{3.140}$$

For an electron which propagates from ϕ_0 to ϕ we define the dressed momentum by [LL82]

$$Q^\mu(\phi,\phi_0) = \frac{1}{(\phi-\phi_0)} \int_{\phi_0}^{\phi} d\phi'\, P^\mu(\phi'). \tag{3.141}$$

Correspondingly, the square of the dress mass is in general given by [Mit75]

$$m_*^2(ky,kx) = Q^2(ky,kx) = m^2\Big[1 + \sum_{i=1,2} \xi_i^2(J_i - I_i^2)\Big], \tag{3.142}$$

where I_i and J_i are defined in Eq. (3.122). As it depends only on e^2, the positron has the same dressed mass. For $\psi_1(\phi) = \sin(\phi)$, $\psi_2 = 0$, $kx = 0$, $ky = 2\pi$ we obtain the above monochromatic result.

Thus, the nonlinear phase of the polarization operator [see Eq. (3.121)] can be interpreted in terms of the mass dressing in the laser field [BM75; Din+14b].

4 Recollision processes of electron-positron pairs

In was shown in Chap. 2 that for strong background fields many aspects of the nonlinear Beit-Wheeler pair-production process can be understood from the classical time evolution of the created particles in the laser field. The developed semiclassical description (valid for $\xi \gg 1$) provides an intuitive understanding for several characteristic features of the asymptotic electron (positron) momentum distribution like its extend, the regions of highest probability and interference effects (see Sec. 2.7 for more details).

A closer analysis of the classical propagation of the pair inside a linearly polarized laser field reveals that the electron and the positron could experience a laser-induced recollision after roughly one laser half-cycle (for certain initial conditions, see Fig. 32) [HMK06; Kuc07]. In this chapter, which was partly published in Ref. [5], we rigorously prove the feasibility for electron-positron recollisions after photoproduction by showing that these processes – characterized by a separation of the creation and the annihilation vertex on the scale set by the laser wavelength – contribute to the laser-dressed polarization operator (see Chap. 3 and Fig. 26).

Recollision processes are responsible for a variety of phenomena, which have been investigated especially in the realm of atomic and molecular physics. After an atom (or a molecule) is ionized by a linearly polarized laser field, the electron is accelerated and possibly brought to a recollision with the parent ion. The energy that the electron absorbs between the ionization and the recollision can be released in different ways: as a high-energy photon after recombination [high-harmonic generation (HHG)] or by striking out another electron (nonsequential double ionization), see, e.g., [Bec+02; Di+12; JKP12; Koh+12; Sal+99]. The maximal energy absorbed by the recolliding ionized electron in a laser field with
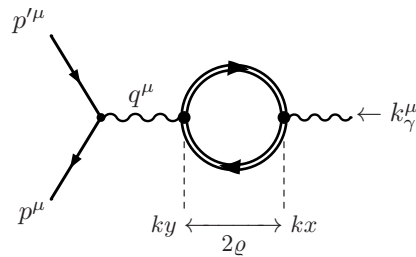
Fig. 26: Depending on the distance 2ϱ of the two polarization-operator vertices, this Feynman diagram describes either radiative corrections to the photon propagator or laser-induced recollision processes. The wavy lines denote photons, the double lines the laser-dressed electron (positron) propagators, and the straight solid lines indicate the particles produced in the secondary reaction. The meaning of the other symbols is explained in the text (time increases from right to left).

peak-electric field strength E_0 and mean angular frequency ω is found to be about $3.17\,U_p$, where $U_p = e^2 E_0^2/(4m\omega^2)$ is the ponderomotive potential, with $e < 0$ and m being the electron charge and mass, respectively [BLM90; Cor93; KI09; Kuc87; Sch+93]. Recently, applications of recollisions in nuclear physics have been discussed as well [Cor+13; LM14].

Recollision processes also play an important role in high-energy physics as originating, for example, from an electron and a positron initially bound in a positronium atom, which may annihilate during a recollision and create other particles, analogously as in an ordinary collider experiment [HHK04; HMK06; MHK08]. Moreover, the electron and the positron inducing the high-energy recollision process can also be created from vacuum in an ultrastrong laser field, e.g., in the presence of a laser field and a nucleus [Kuc07]. In both mentioned cases, classical considerations show that the available energy in the recollision, which happens after the particles propagated for approximately one laser wavelength, is of the order of $mc^2\xi^2 = 4U_p$, where $\xi = |e|E_0/(m\omega c)$ is the classical intensity parameter [see Eq. (1.20)]. This explains why the ultrarelativistic regime $\xi \gg 1$ is of relevance in high-energy recollision physics.

From a pictorial point of view, recollisions are expected to be described by loop diagrams in the realm of quantum field theory. The simplest Feynman diagram, which contains an electron-positron loop, is the polarization operator; see Fig. 26. Since the seminal work of Baier, Milstein, and Strakhovenko [BMS76] and Becker and Mitter [BM75], the polarization operator in a plane-wave field has been investigated in many publications (see Chap. 3). Surprisingly, no high-energy recollisions have been identified so far. To explain this, we note that the leading-order contribution to the polarization operator in $1/\xi$ permits only the net exchange of a few laser photons [Di+13]. This so-called quasistatic approximation (see Sec. 3.3.2) describes electron-positron pairs annihilating within the coherence length λ/ξ of pair production, which is much smaller than the laser wavelength $\lambda = 2\pi c/\omega$.

In this chapter, we consider high-energy recollisions experienced by an electron-positron pair which is created by pure light in the collision of a gamma photon and an intense laser field (see Fig. 26). It is shown for the first time that the polarization operator contains subleading contributions in $1/\xi$, which allow for the efficient absorption of up to $3.17\,\xi^3/\chi$ laser photons if $\chi \gtrsim 1$. For a head-on collision the quantum-nonlinearity parameter is given by $\chi = (2\hbar\omega_\gamma/mc^2)(E_0/E_{\rm cr})$ [see Eq. (1.21)], where $\hbar\omega_\gamma$ is the gamma photon energy and $E_{\rm cr} = m^2c^3/(|e|\hbar) = 1.3 \times 10^{16}\,{\rm V/cm}$ the QED critical field. Contrary to the leading-order quasistatic approximation considered so far, the subleading contributions to the polarization operator derived in this chapter describe recollision processes. They are characterized by a separation of the creation and annihilation point of the electron-positron pair on the scale set by the laser wavelength. Correspondingly, it is possible to absorb much more energy from the laser field (for $\chi \gtrsim 1$ the Heisenberg uncertainty relation is not violated, as even real e^+e^- photoproduction is energetically allowed [Di+12; Rit85; RVX10]). Experimentally, the regime $\chi \gtrsim 1$, $\xi \gg 1$ could be explored by colliding GeV photons (obtainable, e.g., via Compton backscattering) [ESL09; Kim+13; Lee+06; Lee+14; Mur+14; Phu+12; Pow+14; Wan+13] with strong optical laser pulses [CLF; ELI; XCELS; Yan+08].
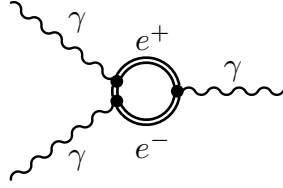
Fig. 27: Two-photon annihilation of the recolliding electron-positron pair. Like Bhabha scattering (see Fig. 28) this processes is always kinematically allowed. If the whole loop is contained within a single formation region, the process is called photon splitting [DMK07].

a) Annihilation channel   **b)** Scattering channel
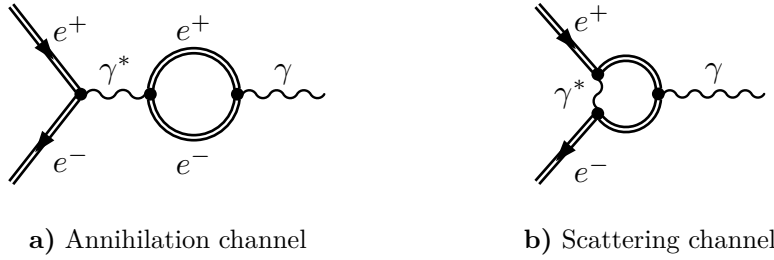
Fig. 28: During a recollision the photoproduced electron-positron pair could also experience Bhabha scattering. From a theoretical point of view this process is more complicated than the production of other lepton pairs (see Fig. 26), as both the annihilation and the scattering channel have to be taken into account.

4.1. Lepton pair production via electron-positron recollisions

Exemplarily, we consider now recollision processes where the virtual photon decays into a lepton pair (see Fig. 26). The generalization of the calculation to other secondary reactions (see, e.g., Fig. 27 and Fig. 28) is technically more involved but conceptually straightforward. To reduce the calculation to its essential part, we focus on the electron-positron loop and neglect the influence of the laser field on the final particles in Fig. 26. After applying the usual Feynman rules (see Chap. 1), the total recollision probability is given by

$$W(k_\gamma) = -\int\limits_{n_0}^{\infty} dn \, \frac{\epsilon_\mu \Pi^{\mu\nu}[\epsilon^\rho \Pi_{\rho\nu}]^*}{2kk_\gamma \alpha(2\pi)^2} \, \sigma_{\text{tot}}(q^2) \tag{4.1}$$

(for an electron-positron pair in the final state also the scattering channel and the laser dressing must be taken into account, see Fig. 28). In Eq. (4.1) $k^\mu = (\omega, \boldsymbol{k})$ ($k^2 = 0$) denotes the average four-momentum of the laser photons, $k_\gamma^\mu = (\omega_\gamma, \boldsymbol{k}_\gamma)$ ($k_\gamma^2 = 0$) and ϵ^μ the momentum and polarization four-vector of the incoming gamma photon, respectively, $\Pi^{\alpha\beta} = \Pi^{\alpha\beta}(k_\gamma, q)$ the nonsingular part of the polarization operator (after renormalization of the vacuum part, see Chap. 3) and $q^\mu = k_\gamma^\mu + nk^\mu$ the four-momentum of the intermediate virtual photon ($\sqrt{q^2} = \sqrt{2nkk_\gamma}$ is the center-of-mass energy of the laser-induced electron-positron recollision). Furthermore, $\sigma_{\text{tot}}(q^2)$ represents the total cross section for the secondary process,

e.g.,

$$\sigma_{\text{tot}}(q^2) = \frac{4\pi\alpha^2}{3q^2} \sqrt{1 - 4m_\mu^2/q^2} \left(1 + 2m_\mu^2/q^2\right) \tag{4.2}$$

for muon pair production [LL82; PS95] and n_0 a possible kinematic threshold [e.g. $n_0 = 2m_\mu^2/(kk_\gamma)$ for muon pair production, where m_μ is the muon mass].

4.2. Recollision contribution to the polarization operator

We show now analytically that recollision processes contribute to the polarization operator in a plane-wave laser field. To this end a stationary-phase analysis is applied to the double-integral representation for the polarization operator derived in Chap. 3. It turns out that recollisions are only possible if the laser is linearly polarized (see Sec. 4.4 for a semiclassical explanation). Therefore, we set $\psi_2(\phi) = 0$ [$\psi_1(\phi) = \psi(\phi)$] throughout this chapter. For the numerical calculations the pulse shape $\psi'(\phi) = \sin^2[\phi/(2N)] \sin(\phi + \phi_0)$ [see Eq. (1.23)] is employed, with $N = 5$ cycles and $\phi_0 = 0$ for the CEP.

For a linearly-polarized laser, the field-dependent part of the polarization operator is given by [see Eq. (3.132)]

$$\Pi^{\mu\nu}(k_\gamma, q) - \Pi^{\mu\nu}_{\mathfrak{F}=0}(k_\gamma, q)$$
$$= - \int\limits_{-\infty}^{+\infty} dky \int\limits_{0}^{\infty} \frac{d\varrho}{\varrho} \frac{\alpha}{2\pi} \left[P_{11}\Lambda_1^\mu\Lambda_1^\nu + P_{22}\Lambda_2^\mu\Lambda_2^\nu + P_Q\mathcal{Q}_1^\mu\mathcal{Q}_2^\nu \right], \quad (4.3)$$

where $\varrho = (ky - kx)/2$ and kx and ky denote the laser phase when the pair is created and annihilated, respectively (see Fig. 26). It is shown in App. E that the polarization four-vector ϵ^μ of the incoming photon can be chosen as $\epsilon_\parallel^\mu = \Lambda_1^\mu$ (polarization parallel to the electric field of the laser) and $\epsilon_\perp^\mu = \Lambda_2^\mu$ (polarization perpendicular to the electric field of the laser), respectively, whereas the last term on the right-hand side of Eq. (4.3) does not contribute. Thus,

$$\left| \int P_{\perp,\parallel} \right|^2 = \left| \int\limits_{-\infty}^{+\infty} dky \int\limits_{0}^{\infty} \frac{d\varrho}{\varrho} P_{\perp,\parallel} \right|^2, \quad P_\parallel = P_{11}, \quad P_\perp = P_{22} \tag{4.4}$$

determines the recollision probability for the corresponding photon polarization [see Eq. (4.1)] and will be calculated in the following.

4.2.1. Stationary phase analysis

For strong laser fields ($\xi \gg 1$) the polarization-operator integrals over the laser phases kx and ky [see Eq. (4.3) and Eq. (3.132)] are highly oscillatory and a stationary-phase analysis is applicable (see also Sec. 2.7, where the pair-creation matrix element is analyzed in a similar way).

For the subsequent analysis it is sufficient to note that the coefficients $P_{11} = P_\parallel$ and $P_{22} = P_\perp$ contain the oscillatory phase factor $\exp[i\varphi(\varrho, ky)]$ [see Eq. (3.134)],

Fig. 29: Combinations of creation (kx) and annihilation (ky) laser phases for which a recollision is possible [see Eq. (4.8)]. The color depicts the quantity n proportional to the energy absorbed (classically) by the electron-positron pair in the laser field [see Eq. (4.16)]. The solid black line illustrates the absolute value of the laser-envelope function $\psi'(kx)$ in arbitrary units.
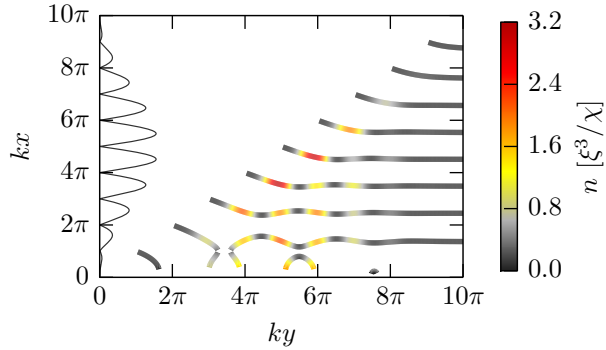
where

$$\varphi(\varrho, ky) = nky - 4\,(\xi/\chi)\,[\varrho + \xi^2 D(\varrho, ky)], \tag{4.5}$$

with $D(\varrho, ky) = \varrho(J - I^2)$ and [see Eq. (3.136)]

$$I = \int_0^1 dl\,\psi(ky - 2\varrho l), \quad J = \int_0^1 dl\,\psi^2(ky - 2\varrho l). \tag{4.6}$$

We first investigate the integral in ϱ for a fixed value of ky. For $\xi \gg 1$ and at fixed χ the phase factor $\exp\left[-4i\,(\xi^3/\chi)\,D(\varrho, ky)\right]$ is highly oscillating and we can apply a stationary-phase analysis. The stationary points ϱ_k are determined by the condition[1]

$$D'(\varrho_k, ky) = [\psi(ky - 2\varrho_k) - I(\varrho_k, ky)]^2 = 0, \tag{4.7}$$

which implies

$$(ky - kx)\psi(kx) = \int_{kx}^{ky} d\phi\,\psi(\phi) \tag{4.8}$$

(for D, the prime denotes the partial derivative with respect to ϱ). Equation (4.8) links the creation ($kx = ky - 2\varrho$) and the annihilation (ky) phases (see Fig. 29). It is shown in Sec. 4.4 that it exactly corresponds to the condition that the classical coordinates of the electron and the positron coincide again at a later phase $\phi_r = ky$ [see Eq. (4.24)].

4.2.2. Physical interpretation of the stationary points

The stationary-phase equation $D'(\varrho_k, ky) = 0$ always admits the solution $\varrho_0 = 0$, independently of the shape of the background field. The contribution of this stationary point is formed for values of ϱ in the region $0 \leq \varrho \lesssim 1/\xi$, where the phase $4\,(\xi^3/\chi)\,D(\varrho, ky)$ is less than or of the order of unity. Thus, this contribution

---

[1]Note that by definition ϱ_k is a stationary point of the highly-oscillating part of the polarization-operator phase. Even if the total phase function $\mathcal{D}(\varrho, ky) = \varrho + \xi^2 D(\varrho, ky)$ has no real stationary points [see Eq. (4.43)], the (quasi-) stationary points ϱ_k determine the regions which dominate the integral for $\xi \gg 1$ [see also App. H and Eq. (4.9)].
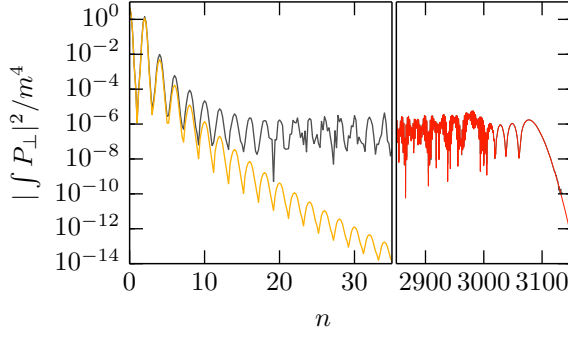
Fig. 30: *Left side*: Comparison of the quasistatic contribution (lower yellow curve) with the full numerical calculation (upper gray curve). *Right side*: Plateau-region, analytical (red curve) and numerical calculation coincide [$\chi = 1$, $\xi = 10$, $N = 5$, $\phi_0 = 0$, see Eq. (4.3)].

describes the immediate annihilation of the created electron-positron pair within a distance of the order of λ/ξ inside an (effectively) constant-crossed field (quasistatic limit). The compensation of the large parameter ξ^3/χ in the phase occurring at $\rho \lesssim 1/\xi$ explains why the stationary point ρ_0 provides the leading contribution to the polarization operator and, at the same time, why it allows for a net exchange of only a few laser photons [Di+13]. On the other hand, laser-induced recollision processes are described by the contributions to the integral in ϱ close to the nonvanishing stationary points ϱ_k, $k = 1, 2, \ldots$, with $\varrho_k \gtrsim \pi \gg 1/\xi$ (see Fig. 29). As we will see below, these contributions are formed in the regions $|\varrho - \varrho_k| \lesssim 1/\xi$, where the phase $4 \, (\xi^3/\chi) \, D(\varrho, ky)$ remains of the order of ξ^3/χ. Thus, although such contributions are suppressed with respect to the one from ϱ_0, they are essential to understand the high-energy plateau region of the photon-absorption spectrum [see Fig. 30 (left side)].

In order to determine the contribution from the recollision processes, we expand the function $D(\varrho, ky)$ around ϱ_k up to the third order

$$D'(\varrho_k, ky) = D''(\varrho_k, ky) = 0, \quad D'''(\varrho_k \neq 0, ky) = 8\big[\psi'(ky - 2\varrho_k)\big]^2. \qquad (4.9)$$

Since the third-order term of the expansion scales as $(\varrho - \varrho_k)^3 \xi^3/\chi$, the contribution is formed in the region $|\varrho - \varrho_k| \lesssim 1/\xi$ and also the linear term in ξ in $\varphi(\varrho, ky)$ must be taken into account. All higher-order terms can be neglected. On the other hand, the preexponent functions in $P_{\perp,\parallel}$ vanish at ϱ_k and it is necessary to expand them up to linear terms in $\varrho - \varrho_k$.

Next, we apply the change of variable from ϱ to t

$$\varrho - \varrho_k = [r\chi/(4\xi)]t, \quad r = [2/\chi(\varrho_k, ky)]^{2/3}, \quad \chi(\varrho, ky) = \chi \, |\psi'(ky - 2\varrho)|. \quad (4.10)$$

Here, $\chi(\varrho, ky)$ denotes the quantum-nonlinearity parameter at the pair-production vertex. Then, the phase $\varphi(\varrho, ky)$ can be approximated by [see Eq. (4.5)]

$$\varphi(\varrho, ky) \approx \varphi(\varrho_k, ky) - (tr + t^3/3). \qquad (4.11)$$

After extending the integration boundaries in the new variable t to $\pm\infty$, the contribution to the integral from the region around the stationary point $\varrho_k \neq 0$

Fig. 31: Numerically calculated photon absorption spectra for $\chi = 1$, $N = 5$, $\phi_0 = 0$ and $\xi = 10^{2/3} \approx 4.6$ (upper two), $\xi = 10$ (middle two), $\xi = 10^{4/3} \approx 21.5$ (lower two). Of each pair the upper (lower) spectrum corresponds to perpendicular (parallel) polarization.
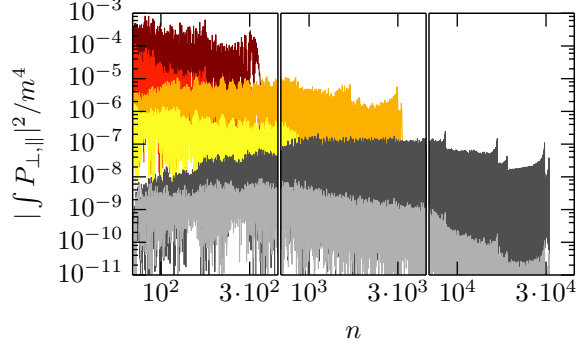
reads (see App. F)

$$\int\limits_{0}^{\infty} d\varrho \, g(\varrho) e^{i\varphi(\varrho, ky)} \approx e^{i\varphi(\varrho_k, ky)} \frac{\pi\chi}{2\xi} \left[g(\varrho_k) \, r \, \mathrm{Ai}(r) + ig'(\varrho_k) \, \mathrm{Ai}'(r) \frac{r^2\chi}{4\xi} \right], \quad (4.12)$$

where $g(\varrho)$ is an arbitrary, slowly varying function and Ai is the Airy function [Olv+10]. As expected, at $\chi \ll 1$ the above contribution features an exponential suppression $\sim \exp\{-4/[3\chi(\varrho_k, ky)]\}$, i.e. as the electron-positron pair-production amplitude inside a (locally) constant-crossed field (see Chap. 2).

By applying Eq. (4.12) to Eq. (4.3) we obtain

$$\int\limits_{0}^{\infty} \frac{d\varrho}{\varrho} \, P_{\perp} \approx im^2 \, e^{i\varphi(\varrho_k, ky)} \frac{\pi\chi^2}{2} \left\{ \psi'(ky - 2\varrho_k) M(\varrho_k, ky) \mathcal{W}_0[x_1(\varrho_k, ky)] \right.$$

$$\left. \times \frac{r^2 \, \mathrm{Ai}'(r)}{4\varrho_k} - \mathcal{W}_2[x_1(\varrho_k, ky)] \frac{r \, \mathrm{Ai}(r)}{\varrho_k^2 \xi^2} \right\} \quad (4.13a)$$

and

$$\int\limits_{0}^{\infty} \frac{d\varrho}{\varrho} \, P_{\|} \approx -im^2 \, e^{i\varphi(\varrho_k, ky)} \, \psi'(ky - 2\varrho_k) M(\varrho_k, ky)$$

$$\times \mathcal{W}_1[x_1(\varrho_k, ky)] \, r^2 \, \mathrm{Ai}'(r) \frac{\pi\chi^2}{2\varrho_k} + \int\limits_{0}^{\infty} \frac{d\varrho}{\varrho} \, P_{\perp}, \quad (4.13b)$$

where the functions $\mathcal{W}_i$ are defined in Eq. (G.1), $x_1(\varrho, ky) = (\xi/\chi) \left[\varrho + \xi^2 D(\varrho, ky) \right]$ [see Eq. (3.135)] and

$$M(\varrho, ky) = \psi(ky) - \psi(ky - 2\varrho). \quad (4.14)$$

4.2.3. Number of absorbed laser photons

Now, we proceed to determine the stationary points of the integral in ky. To this end we have to solve the equation $\varphi'(ky) = 0$, where $\varphi(ky) = \varphi[\varrho_k(ky), ky]$ [see

Eq. (4.12)]. The stationary-phase condition reads

$$n = \frac{\xi^3}{\chi}\left[2M^2(\varrho_k, ky) + \frac{2}{\xi^2} - \frac{1}{\xi^2}\frac{M(\varrho_k, ky)}{\varrho_k\psi'(ky - 2\varrho_k)}\right],\qquad(4.15)$$

where $\varrho_k = \varrho_k(ky)$ [note that for $\psi'(ky - 2\varrho) \to 0$ the pair-production probability is exponentially suppressed]. The leading-order contribution with $n \approx 2M^2(\varrho_k, ky)\xi^3/\chi$ corresponds to the four-momentum

$$k'^\mu = nk^\mu = 2\frac{\xi^3}{\chi}[\psi(ky) - \psi(kx)]^2\, k^\mu \qquad(4.16)$$

that the electron-positron pair has classically absorbed from the laser field [see Eq. (4.31) and Fig. 32]. For a monochromatic field pairs created after the peak ($\phi \approx \pi/10$) have the highest recollision energy (see Sec. 4.4) and we obtain the cutoff $n_c = 3.17\,\xi^3/\chi$, which corresponds to the result $3.17\,U_p$ obtained in atomic HHG ($U_p = m\xi^2/4$) [BLM90; Cor93; Di+12; Kuc87; Sch+93]. The ξ^3/χ scaling of the cutoff is confirmed by a full numerical calculation in Fig. 31.

Now, the approximate contribution of the stationary point ky_s, solution of Eq. (4.15), is given by

$$\int\limits_{-\infty}^{+\infty} dky\, h(ky)\, e^{i\varphi(ky)} \approx h_s\, e^{i(\sigma\pi/4+\varphi_s)}\sqrt{\frac{2\pi}{|\varphi''_s|}},\qquad(4.17)$$

where $h(ky)$ is an arbitrary, slowly-varying function, $h_s = h(ky_s)$, $\varphi_s = \varphi(ky_s)$, $\varphi''_s = \varphi''(ky_s)$, $\sigma = \text{sign}(\varphi''_s)$, and

$$\varphi''(ky) = -4\frac{\xi^3}{\chi}\left[M(\varrho_k, ky)\psi'(ky) - \frac{M^2(\varrho, ky)}{2\varrho_k} + \frac{\varrho''_k}{\xi^2}\right],\qquad(4.18)$$

where $\varrho''_k = \varrho''_k(ky)$. If two stationary points coalesce, the Airy uniform approximation must be used instead of Eq. (4.17) (see App. H).

The validity of the stationary-phase approximation is demonstrated in Fig. 30 (right side), where the recollision contribution was calculated analytically as outlined above and compared with a full numerical calculation (see Sec. 4.5). For large photon numbers both results agree already for $\xi = 10$.

Combining Eqs. (4.13) and (4.17), we conclude that the recollision contribution to $|\int P_\perp|^2$ scales as $\xi^{-6}\chi^{10/3}$ at $\chi \gtrsim 1$ [$\mathcal{W}_i(x) \sim x^{-1/2}$, see Eq. (G.4)], while the quasistatic contribution is independent of ξ (see Sec. 3.3.2). The ξ^{-6}-scaling of the recollision contribution is confirmed numerically in Fig. 31.

4.3. Recollision probability

In order to determine the efficiency of the "vacuum electron-positron collider", we consider the ratio R between the recollision probability $W(k_\gamma)$ and the pair-production probability $W_{e^+e^-}(k_\gamma)$. Using Eq. (4.1) we can estimate the ξ scaling of R. Since $n \sim \xi^3$, $\epsilon_\mu\Pi^{\mu\nu}[\epsilon^\rho\Pi_{\rho\nu}]^* \sim m^4\xi^{-6}$, and $W_{e^+e^-}(k_\gamma) \sim \xi$ (see Chap. 2), we

obtain

$$R = \frac{W(k_\gamma)}{W_{e^+e^-}(k_\gamma)} \sim \xi^{-3} m^2 \sigma_{\text{tot}}, \quad \sigma_{\text{tot}} \sim \sigma_{\text{tot}}(q^2 = m^2 \xi^2). \qquad (4.19)$$

An intuitive explanation of this scaling is based on the wave packet spreading of the electron-positron pair between the production and the recollision as in [HMK06; Kuc07]. In fact, in the frame, where the recollision is head-on and along the polarization direction of the laser, one obtains $R \sim \sigma_{\text{tot}}/\mathcal{A}$ [PS95], where $\mathcal{A} = \Delta L_b \Delta L_k$, with $\Delta L_b \sim \xi/m$ and $\Delta L_k \sim \xi^2/m$ being the spread of the particles along the direction of the magnetic field and along the propagation direction, respectively (see Sec. 4.4). Note that the initial conditions assumed in [Kuc07] for the classical propagation do not correspond to the most probable ones employed here, which explains the different scaling of the quantity R there.

4.3.1. Probability for muon pair production

As the tree-level production of $\mu^+\mu^-$ pairs is exponentially suppressed $[\exp(-8/3\chi_\mu),$ with $\chi_\mu \sim 10^{-7}\chi]$, their observation would unambiguously prove the existence of recollision processes. For a pulse with 5 cycles, $\chi = 1$ and $\xi = 200 \approx m_\mu/m$ (kinematic threshold) we obtain to leading order a probability of 2×10^{-20} per incoming gamma photon. However, for $\xi \gtrsim 200$ the emission of additional photons within the electron-positron loop should be taken into account. In fact, $N_\gamma \approx \pi\alpha\xi$ photons are emitted on average by each particle in the loop (integrating the total emission probability yields $N_\gamma = 4.5$) [Di+12]. Taking the corresponding exponential decay of the electron (positron) wave function into account (see Chap. 5), the probability for $\mu^+\mu^-$ pair production without the emission of additional photons is $\sim 10^{-24}$. We stress that this is a lower bound for the exact probability, as the emission of additional soft photons does not prevent the recollision.

4.3.2. Probability for electron-positron scattering

Finally, we consider the case of an e^+e^- pair in the final state. Because of the ξ^{-6} scaling of the plateau (see Fig. 31) much higher recollision probabilities are now obtained in the regime $\chi = 1$, $\xi = 10$. From Eq. (4.1) we expect $\sim 10^{-13}$ recollision events per incoming gamma photon for a 5-cycle pulse. Furthermore, in this case $N_\gamma < 1$ and still the absorption of $\sim 10^3$ laser photons is possible. As shown in Chap. 2, photoproduced electron-positron pairs with $t_2 > 1$ are exponentially suppressed (mt_1 and mt_2 denote the momentum component along the direction of the laser electric and magnetic field, respectively; $t_1 \lesssim \xi$). After the recollision, however, also t_2 spans up to ξ. Therefore, in comparison with tree-level e^+e^- photoproduction, recollision-produced e^+e^- pairs cover a much wider phase-space region, such that these channels are, in principle, distinguishable.

4.4. Semiclassical description of the recollision process

In the previous section an ab initio derivation of the recollision contribution to the polarization operator valid in the important strong-field regime $\xi \gg 1$ was given. Now, we will show that the obtained results are in agreement with the following intuitive three-step model, which is a natural generalization of the well established three-step description of atomic recollision processes[2] [BLM90; Cor93; KI09; Kuc87; Sch+93]:

❶ Pair creation inside an effectively constant-crossed field

❷ Acceleration of the pair by the laser field

❸ Recollision after one or more laser (half-)cycles

To this end the classical trajectories of the created electron-positron pair are considered (see App. A.3). As we have already found the appropriate initial conditions for the classical propagation in Chap. 2, the determination of the recollision condition (see Sec. 4.4.1) and the recollision energy (see Sec. 4.4.2) is straightforward. Finally, recollisions with finite impact parameters are considered (see Sec. 4.4.3). By identifying how the impact parameter depends on the laser intensity, an intuitive explanation for the scaling laws given in Sec. 4.2 is obtained.

4.4.1. Classical recollision condition

According to QED the electron and the positron are created at the same space-time point x_0^μ with possibly different initial four-momenta p_1^μ and p_2^μ (see Fig. 26). As for $\xi \gg 1$ the formation region is small in comparison with the scale set by the laser wavelength, we assume in the following that both particles are always real ($p_i^2 = m^2$). Correspondingly, their trajectories are given by [see Eq. (A.15)]

$$x_i^\mu(\phi_i) = x_0^\mu + \int_{\phi_0}^{\phi_i} d\phi' \, \frac{p_i^\mu(\phi')}{kp_i}, \tag{4.20}$$

where $\phi_i = kx_i$ and the classical four-momenta read [see Eq. (A.13)]

$$\begin{aligned}
p_1^\mu(\phi_1) &= p_1^\mu + \frac{e\mathfrak{F}^{\mu\nu}(\phi_1,\phi_0)p_{1\nu}}{kp_1} + \frac{e^2\mathfrak{F}^{2\mu\nu}(\phi_1,\phi_0)p_{1\nu}}{2(kp_1)^2}, \\
p_2^\mu(\phi_2) &= p_2^\mu - \frac{e\mathfrak{F}^{\mu\nu}(\phi_2,\phi_0)p_{2\nu}}{kp_2} + \frac{e^2\mathfrak{F}^{2\mu\nu}(\phi_2,\phi_0)p_{2\nu}}{2(kp_2)^2}.
\end{aligned} \tag{4.21}$$

To obtain compact expressions, we denote here the initial four-momentum by $p_i^\mu = p_i^\mu(\phi_0)$ and the corresponding classical evolution by $p_i^\mu(\phi_i)$. Note that this notation (which is employed throughout Sec. 4.4) differs from the one used for S-matrix

---

[2]Kuchiev [Kuc07] was the first who suggested that this model should also apply to electron-positron pairs produced in combined laser and Coulomb fields (e.g., during the collision of a relativistic nucleus with a strong laser pulse). Note, however, that the initial conditions for the classical propagation used in [Kuc07] are not very likely.

elements, where the four-momenta p_i^μ always denote the initial/final asymptotic values at $\phi = \pm\infty$. As $p_1^\mu \neq p_2^\mu$ implies $x_1^0(\phi) \neq x_2^0(\phi)$, the two particles encounter the same laser phase at different times (in general).

Classically, a perfect recollision is obtained if the trajectory of the electron and the positron intersect again at a later time, i.e. if $x_1^\mu = x_2^\mu$. Before considering recollisions with a finite impact parameter, we focus on this important special case. A necessary condition for a recollision with zero impact parameter is the requirement that the laser phases of the electron and the positron are the same at the recollision point ($\phi_1 = \phi_2 = \phi_r$). Therefore, a recollision with zero impact parameter is possible if the integral equation

$$\int\limits_{\phi_0}^{\phi_r} d\phi' \, \frac{p_1^\mu(\phi')}{kp_1} = \int\limits_{\phi_0}^{\phi_r} d\phi' \, \frac{p_2^\mu(\phi')}{kp_2} \tag{4.22}$$

has a nontrivial solution $\phi_r \neq \phi_0$. If the initial momenta of the electron and the positron are equal ($p_1^\mu = p_2^\mu = p_0^\mu$), their trajectories are symmetric and the analysis simplifies considerably. In this case the recollision condition given in Eq. (4.22) becomes

$$\int\limits_{\phi_0}^{\phi_r} d\phi' \, \mathfrak{F}^{\mu\nu}(\phi', \phi_0) p_{0\nu} = 0. \tag{4.23}$$

Correspondingly, a recollision is only feasible if the laser is linearly polarized [$\psi(\phi) = \psi_1(\phi), \psi_2(\phi) = 0, \xi = \xi_1$] and we obtain [see Eq. (1.30)]

$$(\phi_r - \phi_0) \, \psi(\phi_0) = \int\limits_{\phi_0}^{\phi_r} d\phi' \, \psi(\phi') \tag{4.24}$$

in this case. The result given in Eq. (4.24) corresponds exactly to the stationary-point condition encountered during the quantum calculation [see Eq. (4.8)].

4.4.2. Recollision energy

After expanding in the canonical light-cone basis associated with the momentum four-vector $q^\mu = k_\gamma^\mu$ ($q^2 = 0$) of the incoming photon [see Eqs. (1.85), (1.93) and (A.17)], the classical momenta of the electron and the positron are given by [see Eq. (4.21)]

$$\begin{aligned} p_1^\mu(\phi) &= r'q^\mu + s'(\phi)k^\mu + t_1(\phi)\, m\Lambda_1^\mu + t_2(\phi)\, m\Lambda_2^\mu, \\ -p_2^\mu(\phi) &= rq^\mu + s(\phi)k^\mu + t_1(\phi)\, m\Lambda_1^\mu + t_2(\phi)\, m\Lambda_2^\mu, \end{aligned} \tag{4.25}$$

where $r' = r + 1$ (momentum conservation; r and r' are constants of motion) and $t_2(\phi) = t_2$ (linearly polarized background field). Correspondingly,

$$\begin{aligned} p_1^\mu(\phi) + p_2^\mu(\phi) &= q^\mu + Nk^\mu, \\ p_1^\mu(\phi) - p_2^\mu(\phi) &= \frac{\bar{w}}{w}[q^\mu - Nk^\mu] + 2m(T_1\Lambda_1^\mu + T_2\Lambda_2^\mu). \end{aligned} \tag{4.26}$$

Here, the classical transverse momentum parameters are introduced [see Eq. (1.83) and Eq. (A.19)]

$$T_i = t_i(\phi) = -\frac{1}{m}\Lambda_i^\mu[p_1(\phi)]_\mu = \frac{1}{m}\Lambda_i^\mu[p_2(\phi)]_\mu, \qquad (4.27)$$

the amount of classically absorbed laser four-momentum is given by [see Eq. (1.95)]

$$N = n(\phi) = s'(\phi) - s(\phi) = \frac{1}{2}w\frac{m^2}{kq}[1 + t_1^2(\phi) + t_2^2(\phi)] \qquad (4.28)$$

and [see Eq. (1.84) and Eq. (1.86)]

$$w = \frac{(kq)^2}{(kp_1)(kp_2)} = -\frac{1}{rr'}, \quad \bar{w} = \frac{(kp_1 - kp_2)}{kq}\, w = -\frac{(r + r')}{rr'} \qquad (4.29)$$

are both constants of motion. For a linearly polarized laser field $[t_2(\phi) = t_2]$, the nontrivial time evolution of the particles is completely specified by [see Eq. (A.19)]

$$T_1 = t_1(\phi) = t_1 - \xi[\psi(\phi) - \psi(\phi_0)], \quad t_1 = t_1(\phi_0). \qquad (4.30)$$

In the following, we will call the plane spanned by k^μ and q^μ the longitudinal and the plane spanned by Λ_i^μ $(i = 1, 2)$ the transverse plane.

From Eq. (4.28) and Eq. (4.30) we conclude that the four-momentum k'^μ absorbed from the laser field during the propagation from the creation to the annihilation point is given by[3]

$$k'^\mu = n_r k^\mu = 2\frac{m^2}{kq}\xi^2[\psi(\phi_r) - \psi(\phi_0)]^2 k^\mu, \qquad (4.31)$$

where the initial conditions $t_i = t_i(\phi_0) = 0$ and $w = 4$ are used, as required by the recollision condition for zero impact parameter [see Eq. (4.23)]. This result coincides with the leading-order expression obtained from the quantum calculation [see Eq. (4.16)]. In Fig. 32 the four-momentum gain n_r is plotted for different trajectories.

4.4.3. Impact parameter

To obtain an intuitive understanding of the scaling law for the recollision probability derived in Sec. 4.2 (see in particular Fig. 31), we consider now recollision processes with a finite impact parameter (see App. B). To this end we introduce two four-vectors B_1^μ and B_2^μ, which obey the relations given in Eq. (B.6) [with the replacement $p_1^\mu \to p_1^\mu(\phi_r)$ and $p_2^\mu \to p_2^\mu(\phi_r)$, where $p_i^\mu(\phi_r)$ are the momenta of the two colliding particles at the recollision point, see Eq. (4.21)].

According to Eq. (4.26) the three four-vectors Λ_i^μ and $q^\mu - Nk^\mu$ are orthogonal to $(p_1 + p_2)^\mu(\phi)$ and among them we must find two linear combinations which are also orthogonal to $(p_1 - p_2)^\mu(\phi)$. One of this two four-vectors may be chosen

---

[3]Note that we have dropped here the constant term $2\frac{m^2}{kq}$ as in Eq. (4.16).

Fig. 32: Classical trajectories for the electron $[X_1(\phi)$, see Eq. (A.20)] and the positron $[-X_1(\phi) = \Lambda_1^\mu x_\mu(\phi)]$ for equal initial momenta $(p_1^\mu = p_2^\mu = p_0^\mu)$ and $X_1(\phi_0) = 0$ but different values for ϕ_0 [monochromatic background, $\psi'(\phi) = \cos(\phi)$]. The recollision phase ϕ_r is determined by Eq. (4.24), the color depicts the absorbed laser four-momentum at the recollision point [see Eq. (4.31)]. The highest four-momentum gain $n_c = 3.17\,\xi^3/\chi$ is obtained for $\phi_0 \approx 0.31$.
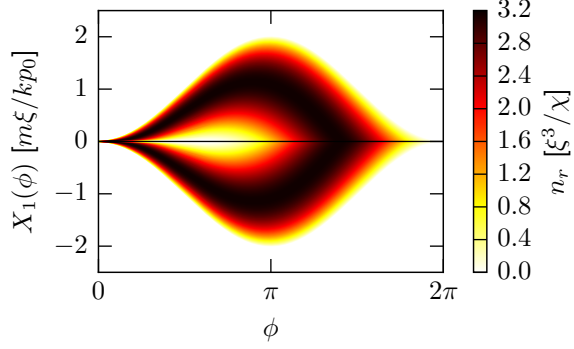
completely transverse

$$B_1^\mu = \frac{T_1 \Lambda_2^\mu - T_2 \Lambda_1^\mu}{\sqrt{T_1^2 + T_2^2}}, \quad B_1^2 = -1. \tag{4.32}$$

The second four-vector is mostly longitudinal (i.e. proportional to $q^\mu - Nk^\mu$), with a small transverse component (proportional to $T_1\Lambda_1^\mu + T_2\Lambda_2^\mu$)

$$B_2^\mu = \mathcal{B}\left[2m(T_1^2 + T_2^2)(q^\mu - Nk^\mu) - 2Nkq\frac{\bar{w}}{w}(T_1\Lambda_1^\mu + T_2\Lambda_2^\mu)\right] \tag{4.33}$$

$(B_2^2 = -1)$, the normalization constant is given by

$$\mathcal{B} = \left[(T_1^2 + T_2^2)2Nkq(2Nkq - 4m^2)\right]^{-1/2}. \tag{4.34}$$

We assume now that the recollision condition in Eq. (4.24) admits for a given ϕ_0 a nontrivial solution ϕ_r. Thus, the classical trajectories intersect for the initial conditions $p_1^\mu = p_2^\mu$, i.e. for $t_1 = t_2 = \bar{w} = 0$ [see Eq. (4.26)]. The collision still takes place if this assumption is slightly relaxed ($t_1 \approx t_2 \approx \bar{w} \approx 0$), but with finite impact parameters

$$b_i(\phi_r) = d^\mu(\phi_r)B_{i\mu}(\phi_r), \quad d^\mu(\phi) = [x_1(\phi) - x_2(\phi)]^\mu. \tag{4.35}$$

Due to the smallness of the relevant cross sections, only very small impact parameters lead to a scattering event. Therefore, the momentum of the electron $p_1^\mu(\phi_{r,1})$ and the positron $p_2^\mu(\phi_{r,2})$ at the recollision point are to a good approximation given by $p_1^\mu(\phi_r)$ and $p_2^\mu(\phi_r)$, respectively (note that we can specify the position of the two particles at different times in the above formula). Even if in general $\phi_{r,1} \neq \phi_{r,2} \neq \phi_r$, we call ϕ_r the recollision phase.

As the electron and the positron are created at the same space-time point, the four-position difference at the recollision phase is given by [see Eqs. (4.20)

and (A.15)]

$$d^\mu(\phi) = \int\limits_{\phi_0}^{\phi_r} d\phi' \left[\frac{p_1^\mu(\phi')}{kp_1} - \frac{p_2^\mu(\phi')}{kp_2} \right]. \tag{4.36}$$

Using the recollision condition [see Eq. (4.23)], we obtain from Eq. (A.13)

$$d^\mu(\phi_r) = (\phi_r - \phi_0) \left[\frac{p_1^\mu}{kp_1} - \frac{p_2^\mu}{kp_2} \right] + \lambda(\phi_r)\, e^2 f^{2\mu\nu} \left[\frac{p_{1\nu}}{(kp_1)^3} - \frac{p_{2\nu}}{(kp_2)^3} \right], \tag{4.37}$$

where

$$\lambda(\phi_r) = \frac{1}{2} \int\limits_{\phi_0}^{\phi_r} d\phi' \left[\psi(\phi') - \psi(\phi_0) \right]^2. \tag{4.38}$$

To determine the impact parameter we note that [see Eq. (4.25)]

$$k_\mu \left[\frac{p_1^\mu}{kp_1} - \frac{p_2^\mu}{kp_2} \right] = 0, \quad q_\mu \left[\frac{p_1^\mu}{kp_1} - \frac{p_2^\mu}{kp_2} \right] = -\bar{w}n, \quad \Lambda_{i\mu} \left[\frac{p_1^\mu}{kp_1} - \frac{p_2^\mu}{kp_2} \right] = \frac{m}{kq} wt_i \tag{4.39a}$$

and

$$e^2 f^{2\mu\nu} \left[\frac{p_{1\nu}}{(kp_1)^3} - \frac{p_{2\nu}}{(kp_2)^3} \right] = -k^\mu \frac{m^2 \xi^2}{(kq)^2} \bar{w}w. \tag{4.39b}$$

After combining everything, we obtain

$$b_1 = B_1^\mu d_\mu(\phi_r) = \frac{1}{m} \frac{m^2}{kq} wt_2 \frac{\xi}{\sqrt{T_1^2 + T_2^2}} (\phi_r - \phi_0)[\psi(\phi_r) - \psi(\phi_0)],$$

$$b_2 = B_2^\mu d_\mu(\phi_r) = -\frac{2}{m} \frac{m^2}{kq} \xi^2 \bar{w}w(T_1^2 + T_2^2)\lambda(\phi_r)\, m^2 \mathcal{B}$$
$$+ \frac{2}{m} \bar{w} \left[N(T_1 t_1 + T_2 t_2) - n(T_1^2 + T_2^2) \right] (\phi_r - \phi_0)\, m^2 \mathcal{B}. \tag{4.40}$$

To analyze the scaling laws for the impact parameters we note that a significant pair-creation probability is only obtained if the initial parameters t_1, t_2 and $\bar{w}$ are all of order one and $T_1 \lesssim \xi$ (see Chap. 2). Correspondingly, $\xi/(T_1^2 + T_2^2)^{1/2} \sim 1$, $m^2 \mathcal{B} \sim \xi^{-3}$ and

$$b_1 \sim \frac{1}{m} \xi t_2, \quad b_2 \sim \frac{1}{m} \xi^2 \bar{w} \tag{4.41}$$

(note that $w \geq 4 \sim 1$). Therefore, both t_2 and $\bar{w}$ must actually be much smaller than unity to match the impact parameter with a typical QED cross section, while t_1 is not constrained. In the limit $t_2, \bar{w} \to 0$ the differential pair-creation probability in a constant-crossed field (see Chap. 2) becomes constant and the effective beam area (at the recollision point) scales as $\mathcal{A} \sim b_1 \times b_2 \sim \xi^3/m^2$ [see

Eq. (4.19)].

4.5. Numerical calculation of the polarization-operator spectrum

In order to verify that the stationary-phase analysis presented in Sec. 4.2 is applicable for strong background fields ($\xi \gg 1$), we also calculated the polarization-operator integrals in ϱ and $y^- = ky$ [see Eq. (4.3) and Eq. (3.132)] fully numerically without any approximation (see Fig. 30 and Fig. 31). As the absolute magnitude of the leading-order contribution to the polarization operator is several orders of magnitude larger than the recollision contribution (see Fig. 30), the numerical evaluation of the highly-oscillating integral in ϱ must be carried out with a relative accuracy of at least $8 - 10$ digits already for $\xi \sim 10$, which is a challenging task. In the following, we explain how it can be accomplished.

4.5.1. Transformation to a regularly oscillating integral

Due to the appearance of the field-dependent function [see Eq. (3.136) and Eq. (4.5), we consider only linear polarization]

$$\mathcal{D}(\varrho, ky) = \varrho \left[1 + \xi^2 (J - I^2) \right] = \varrho + \xi^2 D(\varrho, ky), \tag{4.42}$$

the phase $\widetilde{\Phi}_1$ is nonlinear [see Eq. (3.134)] and the integral in ϱ oscillates irregularly. In order to use the Chebyshev methods presented in App. I, we first apply a change of variables to transform it into a regularly oscillating integral. This is possible, because the derivative [see Eq. (4.7)]

$$\mathcal{D}'(\varrho, ky) = 1 + \xi^2 [\psi(ky - 2\varrho) - I(\varrho, ky)]^2 \tag{4.43}$$

is always positive (this has also been observed in [Din+14b]; the prime denotes the partial derivative with respect to ϱ). Therefore, the change of variables $u = \mathcal{D}(\varrho)$ is uniquely defined and can be applied to obtain an regularly oscillating integral [Eva94], suitable for a standard treatment

$$\int\limits_0^\infty \frac{d\varrho}{\varrho} g(\varrho) e^{-i4(m^2/kq)\mathcal{D}(\varrho)} = \int\limits_0^\infty \frac{du}{\mathcal{D}'(\varrho)} \frac{g(\varrho)}{\varrho} e^{-i4(m^2/kq)u}. \tag{4.44}$$

Here, the inverse function $\varrho = \mathcal{D}^{-1}(u)$ is calculated numerically using a root-finding algorithm [due to $\mathcal{D}'(\varrho) > 0$ the map is one-to-one].

4.5.2. Splitting of the integration range

Having transformed the integral in ϱ to a regularly oscillating one [see Eq. (4.44)], we can calculate it numerically using a Chebyshev series expansion of the preexponent (see App. I). However, as the stationary points ϱ_k [$\mathcal{D}'(\varrho_k, ky) = 1$] lead to delta-like peaks (see Fig. 33), the convergence of the Chebyshev series is rather poor. To circumvent this problem, we note that around a stationary point ϱ_k the preexponent is rapidly varying over a single oscillation cycle of the phase. Correspondingly, it is possible to employ an ordinary integration routine for the integration of the peaks. Between two peaks the situation is reversed, the preexponent varies only slightly
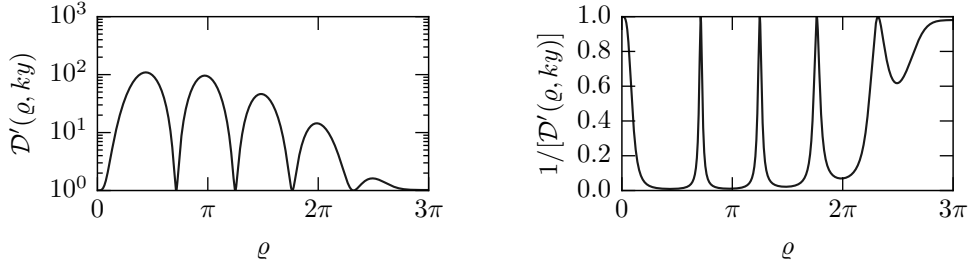
Fig. 33: In the regime $\xi \gg 1$ the phase of the polarization-operator integrals [see Eq. (4.5)] is highly oscillating (parameters used in the plot: $\xi = 10$, $N = 5$, $\phi_0 = 0$, $ky = 6\pi$). As discussed in Sec. 4.2, the main contribution to the integral in ϱ arises from the regions around the stationary points ϱ_k defined by $D'(\varrho_k, ky) = 0$ [see Eq. (4.7)], where $\mathcal{D}'(\varrho_k, ky) = 1$ has a global minimum (**left side**). After the change of variables in Eq. (4.44), the stationary points define the location of the delta-like peaks in the preexponent (**right side**).

over one oscillation cycle and the Chebyshev expansion converges fast. Therefore, we split the total integral in the following way

$$\sum_{k=0}^{n} \int_{\varrho_k^a}^{\varrho_k^b} d\varrho + \sum_{k=0}^{n-1} \int_{\varrho_k^b}^{\varrho_{k+1}^a} d\varrho + \int_{\varrho_n^b}^{\infty} d\varrho. \tag{4.45}$$

Here, $[\varrho_k^a, \varrho_k^b]$ represents a small interval around the stationary point ϱ_k, which contains only a few oscillation cycles of the phase. The integrals over these regions are calculated with, e.g, the QAG algorithm from the GSL [GSL; Pie+83]. The integrals over the intermediate regions $[\varrho_k^b, \varrho_{k+1}^a]$ are calculated using Chebyshev integration, if necessary they are further divided into subintervals (see App. I). To minimize the numerical error caused by cancellations among different integrals, the points ϱ_k^a and ϱ_k^b should be chosen such that each integral in the above decomposition covers an integer number of oscillation cycles (with respect to the new integration variable u).

Finally, the remaining integral from ϱ_n^b to infinity is calculated using standard algorithms like the one introduced by Longman [Lon56] or the QAWF algorithm from the GSL [GSL; Pie+83]. If theses algorithms fail to achieve convergence, a finite part of the integral must be split off first and integrated separately using, e.g., Chebyshev methods

$$\int_{\varrho_n^b}^{\infty} d\varrho = \int_{\varrho_n^b}^{\varrho_n^c} d\varrho + \int_{\varrho_n^c}^{\infty} d\varrho. \tag{4.46}$$

The outlined algorithm is fast and achieves a high numerical precision. To minimize the adaptive splitting of the integration range into smaller subintervals, Chebyshev series expansions with $\sim 10^3$ coefficients have been used. Their calculation using fast Fourier transform in combination with Olver's algorithm for the integral moments turns out to be very efficient.

5 Vacuum-induced electron spin rotations

The first evidence for physics beyond the Dirac equation was found by Lamb and Retherford [LR47]. Their measurement revealed a finite gap ("Lamb shift") between the energy levels $2S^{1/2}$ and $2P^{1/2}$ of atomic hydrogen, not explainable within relativistic quantum mechanics [Dir27; Dir28; Dir30]. This observation triggered the development of renormalization techniques, which are needed to handle the infinities appearing in quantum-field theory calculations beyond tree level. Finally, a consistent covariant description of QED was jointly established by Dyson [Dys49a; Dys49b], Feynman [Fey48a; Fey48b; Fey49a; Fey49b; Fey50; Fey51] Schwinger [Sch48a; Sch48b; Sch49a; Sch49b; Sch49c; Sch51] and Tomonaga [TO48; Tom46].

According to QED, an electron bound to a nucleus interacts also with the quantum vacuum. The continuous emission and absorption of virtual photons changes the effective Coulomb potential and is responsible for the Lamb shift (the first nonrelativistic calculation was carried out by Bethe [Bet47]). Closely related to the Lamb shift is the anomalous magnetic dipole moment of the electron ($g = 2 + \alpha/\pi$ at one-loop) [Sch48a; Sch51].

An analogous situation is encountered for electrons interacting with a plane-wave laser field. According to the Dirac equation, the asymptotic electron spin polarization is not changed by the propagation through a plane-wave laser pulse. Even if the spin precesses around the magnetic field inside the pulse, the original orientation is restored again afterwards (see Sec. 5.1). Quantum fluctuations, however, change this prediction. For an electron, they are described by the mass operator (see Fig. 34) and taken into account by solving the Schwinger-Dirac equation for the exact electron wave function (see Fig. 35). Note that similar spin effects could also be observed if an electron interacts with a non-coherent state of the photon field (see, e.g., Refs. [Ber69; SFK13]).

In this chapter, we give an alternative derivation of the exact electron wave function inside a plane-wave background field (see Sec. 5.2; it was first considered
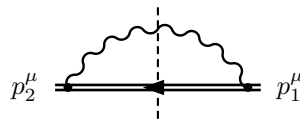
Fig. 34: The Feynman diagram corresponding to the leading-order contribution to the mass operator $\mathsf{M}(p_2, p_1)$ in a plane-wave background field (sign convention: p_1^μ is incoming, p_2^μ outgoing). The double lines represent the Volkov propagators/wave functions for the fermion, which takes the external field exactly into account [see Eq. (1.59)]. Due to the unitarity of the S-matrix the vertical dashed line links the mass operator to the nonlinear Compton scattering diagram (see Fig. 7).

in Ref. [Meu10] using an operator approach, see also Ref. [BM76]). The calculation is very similar to the one carried out in Chap. 2 for the exact photon wave function (see Sec. 2.3). Subsequently, it is shown that the real part of the mass operator induces a nontrivial electron spin dynamics in analogy to birefringence for photons, which is caused by the real part of the polarization operator (see Sec. 5.3). Even if the magnetic field of the laser oscillates, the nonlinear dependence of the anomalous magnetic moment of the electron on the field strength leads to a nonvanishing spin-flip probability for ultra-short laser pulses. The calculated spin-flip asymmetries depend strongly on the CEP of the pulse and vanish in the monochromatic limit (these findings were reported in Refs. [1] and [2]).

5.1. Spin dynamics predicted by the Dirac equation

Before discussing the influence of quantum fluctuations on the electron spin dynamics, we briefly review the definition of the spin four-vector ζ^μ and its time evolution inside a plane-wave laser field.

5.1.1. Electron density matrix

Any measurable quantity related to an electron (positron) depends on its Dirac spinor u_p (v_p) [see Eq. (1.57)] only through the density matrices

$$\rho_u = u_p \bar{u}_p, \quad \rho_v = v_p \bar{v}_p. \tag{5.1}$$

Like any other matrix in spinor space, the density matrices can be decomposed into five fundamental terms (see App. D). For the electron we obtain [IZ05; Lea01; MW55; Sre07]

$$\rho_u = u_p \bar{u}_p = \mathbf{1}\frac{m}{2} + \gamma^\mu \frac{p_\mu}{2} + i\gamma^\mu \gamma^5 (-i)\frac{m}{2}\zeta_\mu + i\sigma^{\mu\nu}\frac{1}{4}\epsilon_{\mu\nu\rho\sigma}\zeta^\rho p^\sigma$$
$$= \frac{1}{2}(m + \not{p})(\mathbf{1} + \not{\zeta}\gamma^5), \tag{5.2}$$

where we defined the spin four-vector[1]

$$\zeta^\mu = \frac{1}{2m}\bar{u}_p \gamma^5 \gamma^\mu u_p; \quad \zeta^2 = -1, \quad \zeta^\mu p_\mu = 0. \tag{5.3}$$

Using the standard representation for the Dirac spinors [LL82]

$$u_p = \begin{pmatrix} \sqrt{\epsilon + m}\,\omega \\ \sqrt{\epsilon - m}\,(\hat{\boldsymbol{p}}\boldsymbol{\sigma})\,\omega \end{pmatrix}, \quad v_p = \begin{pmatrix} \sqrt{\epsilon - m}\,(\hat{\boldsymbol{p}}\boldsymbol{\sigma})\,\omega' \\ \sqrt{\epsilon + m}\,\omega' \end{pmatrix} \tag{5.4}$$

$(\hat{\boldsymbol{p}} = \boldsymbol{p}/|\boldsymbol{p}|)$ and the standard representation for the Dirac gamma matrices [LL82]

$$\gamma^0 = \begin{pmatrix} 1 & 0 \\ 0 & -1 \end{pmatrix}, \quad \gamma^i = \begin{pmatrix} 0 & \sigma^i \\ -\sigma^i & 0 \end{pmatrix}, \quad \gamma^5 = \begin{pmatrix} 0 & -1 \\ -1 & 0 \end{pmatrix}, \tag{5.5}$$

---

[1]Note that ζ^μ is actually a pseudo four-vector.

we obtain [LL82; Tol56]

$$\zeta^\mu = \left(\frac{\boldsymbol{p}\boldsymbol{\zeta}}{m}, \boldsymbol{\zeta} + \frac{\boldsymbol{p}(\boldsymbol{p}\boldsymbol{\zeta})}{m(\epsilon+m)}\right), \quad \zeta^i = \omega^\dagger \sigma^i \omega, \tag{5.6}$$

(note that, unfortunately, $\zeta^i \neq \boldsymbol{\zeta}^i$). Here, $\sigma^i = \sigma_i$ [$\boldsymbol{\sigma} = (\sigma^1, \sigma^2, \sigma^3)$] denote the Pauli matrices [LL82]

$$\sigma_1 = \begin{pmatrix} 0 & 1 \\ 1 & 0 \end{pmatrix}, \quad \sigma_2 = \begin{pmatrix} 0 & -i \\ i & 0 \end{pmatrix}, \quad \sigma_3 = \begin{pmatrix} 1 & 0 \\ 0 & -1 \end{pmatrix} \tag{5.7}$$

and ω an arbitrary two component spinor with normalization $\omega^\dagger \omega = 1$. Correspondingly, the free spinor u_p is described completely by its momentum $\boldsymbol{p}$ and its spin polarization $\boldsymbol{\zeta}$ in the rest frame (i.e. we should actually write $u_{\boldsymbol{p},\boldsymbol{\zeta}}$ instead of u_p).

In (nonrelativistic) quantum mechanics the spin operator $\boldsymbol{S}$ and the spin polarization vector $\boldsymbol{P}$ are defined by [LL81; Mer98; PS95]

$$\boldsymbol{S} = \frac{1}{2}\boldsymbol{\sigma}, \quad \boldsymbol{P} = \langle \boldsymbol{S} \rangle = \omega^\dagger \boldsymbol{S} \omega = \frac{1}{2}\boldsymbol{\zeta}. \tag{5.8}$$

They are related to the magnetic moment $\boldsymbol{\mu}$ of the electron as follows

$$\boldsymbol{\mu} = -\mu_{\text{BM}}\, g \, \langle \boldsymbol{S} \rangle = -\mu_{\text{BM}}\, g\frac{1}{2}\boldsymbol{\zeta}, \quad \mu_{\text{BM}} = \frac{|e|}{2m} \tag{5.9}$$

where μ_{BM} is called the Bohr magneton and $g \approx 2$ the electron g-factor.

5.1.2. Evolution of the spin four-vector in a plane-wave laser field

To analyze the spin dynamics predicted by the Dirac equation, we consider the Volkov solution [see Eq. (1.54)]

$$\Psi^V_{\boldsymbol{p},\boldsymbol{\zeta}}(x) = E_p(x)u_{\boldsymbol{p},\boldsymbol{\zeta}} \tag{5.10}$$

and calculate the expectation value of the spin four-vector

$$\zeta^\mu(\phi) = \frac{\bar{\Psi}^V_{\boldsymbol{p},\boldsymbol{\zeta}}(x)\gamma^5\gamma^\mu\Psi^V_{\boldsymbol{p},\boldsymbol{\zeta}}(x)}{\bar{\Psi}^V_{\boldsymbol{p},\boldsymbol{\zeta}}(x)\Psi^V_{\boldsymbol{p},\boldsymbol{\zeta}}(x)} = \zeta^\mu + \frac{e\mathfrak{F}^{\mu\nu}(\phi)\zeta_\nu}{pk} + \frac{e^2\mathfrak{F}^{2\mu\nu}(\phi)\zeta_\nu}{2(pk)^2}, \tag{5.11}$$

where $\zeta^\mu = \zeta^\mu(-\infty)$ and $\phi = kx$. Interestingly, the result given in Eq. (5.11) (which corresponds to an exact solution of the Dirac equation) also obeys the Bargmann-Michel-Telegdi (BMT) equation [BMT59; LL82]

$$\frac{d\zeta^\mu(\tau)}{d\tau} = \frac{e}{m}F^{\mu\nu}\zeta_\nu(\tau), \tag{5.12}$$

which describes the evolution of the spin four-vector $\zeta^\mu(\tau)$ semiclassically [in Eq. (5.12) we neglected the anomalous magnetic moment].

Note that the spin continuously changes its orientation while the electron propagates through a plane-wave field. However, the Volkov solution predicts that
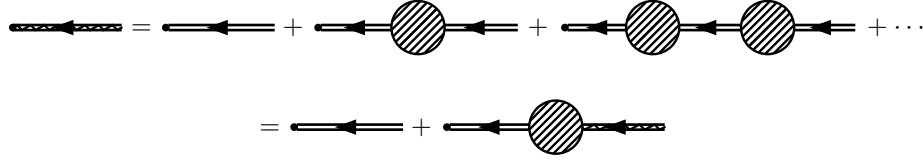
a) Exact electron wave function
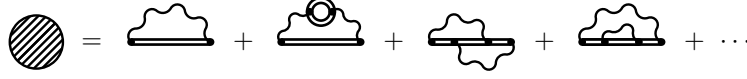
b) One-particle irreducible diagrams

Fig. 35: a) The exact electron wave function (double zigzag line) can be defined either implicitly or by an geometric expansion. **b)** One-particle irreducible (1PI) contributions to the mass operator (see Sec. 5.2.3).

the initial spin configuration is recovered again after the electron has left the laser field $[\zeta^\mu(+\infty) = \zeta^\mu(-\infty)]$. We will show later that this is no longer the case if nonlinear QED corrections are taken into account.

5.1.3. Canonical spin quantization axis

If the background field is linearly polarized $[F^{\mu\nu} = f^{\mu\nu}\psi'(\phi)$, see Eq. (1.17)], the direction of the magnetic field does not change. Therefore, the following (pseudo) four-vector represents a good quantization axis for the electron spin [Rit72a; Rit85]

$$s^\mu = \frac{|e|}{m^3\chi}f^{*\mu\nu}p_\nu, \quad s^2 = -1, \quad ps = 0, \quad ks = 0, \tag{5.13}$$

where

$$\chi = \frac{|e|\sqrt{pf^2p}}{m^3} = \xi\frac{\sqrt{(kp)^2}}{m^2} \tag{5.14}$$

denotes the quantum-nonlinearity parameter of the electron with four-momentum p^μ [this notation is used throughout this chapter; it differs from Eq. (1.21)].

In agreement with Eq. (5.2) we define the following spin operator

$$\Sigma = \slashed{s}\gamma^5 = \frac{|e|}{m^3\chi}\gamma^5 pf^*\gamma, \quad (\slashed{s}\gamma^5)^2 = \mathbf{1} \tag{5.15}$$

and construct the corresponding spin projectors

$$P_s^\pm = \frac{1}{2}(\mathbf{1} \pm \slashed{s}\gamma^5), \quad (P_s^\pm)^2 = P_s^\pm, \quad P_s^+ P_s^- = 0. \tag{5.16}$$

126

5.2. Exact electron wave function

In Chap. 2 we considered the exact photon wave function (see Sec. 2.3). There, we showed that the inclusion of quantum fluctuations guarantees a unitary time evolution and leads to a birefringent quantum vacuum. Here, we will obtain a similar result for the exact electron (positron) wave function (see Fig. 35). On the one hand, the imaginary part of the mass operator (see Fig. 34) causes an exponential wave-function decay [dressed states are unstable, as an electron (positron) radiates inside the background field]. On the other hand, the real part of the mass operator induces a nontrivial spin dynamics even for particles which propagate through the pulse without emitting photons.

5.2.1. Schwinger-Dirac equation

In the following we consider exemplarily the exact wave function of an incoming electron $\Psi_p^E(x)$ (see Fig. 35). To leading order it coincides with the Volkov solution $\Psi_p^V(x)$ of the Dirac equation [see Eq. (1.54)], which reduces to a momentum eigenstate $\psi_p(x)$ in the absence of the background field

$$\Psi_p^V(x) = E_p(x)u_p, \quad \psi_p(x) = e^{-ipx}u_p \tag{5.17}$$

[for simplicity we drop the spin labels, see Eq. (5.10)]. Therefore, we require the same boundary condition also for the exact electron wave function [$\Psi_p^E(x) \to \psi_p(x)$ if $kx \to -\infty$ with a suitable choice of u_p].

To define the exact electron wave function we introduce the position-space mass operator $M(x, y)$ (see Ref. [LL82], Sec. 105) such that $-iM(x, y)$ denotes the set of all one-particle irreducible diagrams (see Fig. 35; we use the convention that electrons propagate from y to x). Correspondingly,

$$\begin{aligned}
\Psi_p^E(x) &= \Psi_p^V(x) + \int d^4y d^4z\, G(x, y)M(y, z)\Psi_p^V(z) + \dots \\
&= \Psi_p^V(x) + \int d^4y d^4z\, G(x, y)M(y, z)\Psi_p^E(z), \quad (5.18)
\end{aligned}$$

where $G(x, y)$ is the Green's function in the background field [see Eq. (1.59)]

$$\begin{aligned}
\left[i\slashed{\partial}_x - e\slashed{A}(x) - m\right]G(x, y) &= \delta^4(x - y), \\
\left[i\slashed{\partial}_x - e\slashed{A}(x) - m\right]\Psi_p^V(x) &= 0
\end{aligned} \tag{5.19}$$

(the index x indicates that the derivative ∂_x^μ acts solely on x). Therefore, the exact electron wave function obeys the following so-called Schwinger-Dirac equation [Sch51]

$$\left[i\slashed{\partial}_x - e\slashed{A}(x) - m\right]\Psi_p^E(x) = \int d^4y\, M(x, y)\Psi_p^E(y). \tag{5.20}$$

For a plane-wave background field, which depends nontrivially only on $\phi = kx$, we can write the exact wave function in the following way

$$\Psi_p^E(x) = E_p(x)U_p^E(kx), \tag{5.21}$$

where $U_p^E(kx) \to u_p$ for $kx \to -\infty$. Using $\bar{E}_{p,x} E_{p,x} = \mathbf{1}$ [see Eq. (1.56)], $\not{k} E_p(x) = E_p(x) \not{k}$ and

$$[i\not{\partial}_x - e\not{A}(kx)]E_p(x) = E_p(x)\not{p} \tag{5.22}$$

[if the derivative acts solely on $E_p(x)$, see Eq. (1.60)], we obtain

$$i\not{k}U_p'^E(kx) + (\not{p} - m)U_p^E(kx) = \int d^4y\, \bar{E}_p(x)\mathsf{M}(x,y)E_p(y)\, U_p^E(ky). \tag{5.23}$$

Finally, after defining the quantity (see Sec. 1.4 for the definition of light-cone coordinates)

$$\mathsf{M}(kx, ky; p) = \int dy^+ dy^\perp\, \bar{E}_p(x)\mathsf{M}(x,y)E_p(y), \tag{5.24}$$

we obtain the following integro-differential equation

$$i\not{k}U_p'^E(\phi) + (\not{p} - m)U_p^E(\phi) = \int d\phi'\, \mathsf{M}(\phi, \phi'; p)\, U_p^E(\phi'). \tag{5.25}$$

Note that due to momentum conservation the function $\mathsf{M}(kx, ky; p)$ depends only on $kx = x^-$, even if this is not manifest in the definition.

5.2.2. Quasistatic approximation

For strong background fields ($\xi \gg 1$) the formation region for the integral in $d\phi'$ in Eq. (5.25) is small and we may apply the replacement $U_p^E(\phi') \to U_p^E(\phi)$, which transforms the Schwinger-Dirac equation into an ordinary differential equation[2]

$$i\not{k}U_p'^E(\phi) + (\not{p} - m)U_p^E(\phi) = \mathsf{M}_p(\phi)\, U_p^E(\phi), \tag{5.26}$$

where now [see Eq. (5.24)]

$$\mathsf{M}_p(kx) = \int d^4y\, \bar{E}_p(x)\mathsf{M}(x,y)E_p(y). \tag{5.27}$$

Using the completeness relation for the Ritus matrices [see Eq. (1.61)], we obtain the following relation

$$\mathsf{M}_p(kx) = \int d^4z d^4y\, \bar{E}_p(x)\delta^4(x-z)\mathsf{M}(z,y)E_p(y)$$
$$= \int \frac{d^4p'}{(2\pi)^4}\, \bar{E}_p(x)E_{p'}(x)\mathsf{M}(p',p), \tag{5.28}$$

---

[2]Effectively, $\mathsf{M}(\phi, \phi'; p) = \delta(\phi - \phi')\mathsf{M}_p(\phi)$ [see Eq. (5.25)] in the quasistatic approximation, which was used in Ref. [1] to obtain Eq. (5.26).

where we defined the mass operator in momentum space[3] (see Fig. 34)

$$\mathsf{M}(p', p) = \int d^4z' d^4z \, \bar{E}_{p'}(z') \mathsf{M}(z', z) E_p(z) \tag{5.29}$$

$[p^\mu$ is incoming, p'^μ is outgoing].

For $\xi \gg 1$ (i.e. in the quasistatic approximation) we can use the mass operator inside a constant-crossed field [see Eq. (5.35)] for $\mathsf{M}(p', p)$ if the field tensor $F^{\mu\nu}$ of the constant-crossed field is replaced by the local value of the wave field $[F^{\mu\nu} \to f^{\mu\nu}\psi'(kx)]$. The mass operator for a constant-crossed field is diagonal [see Eq. (5.32)]

$$\mathsf{M}_{\mathrm{cc}}(p', p) = (2\pi)^4 \delta^4(p' - p) \mathsf{M}_{\mathrm{cc}}(p). \tag{5.30}$$

Therefore, we obtain in the quasistatic approximation [see Eq. (5.28)]

$$\mathsf{M}_p(\phi) \longrightarrow \mathsf{M}_p^{\mathrm{qs}}(\phi) = \mathsf{M}_{\mathrm{cc}}[p; F \to f\psi'(\phi)]. \tag{5.31}$$

5.2.3. Mass operator for a constant-crossed field

For a constant-crossed field with field tensor $F^{\mu\nu}$, the mass operator was first calculated by Ritus [Rit70a; Rit70b; Rit85]; it is diagonal in the E_p-representation [see Eq. (5.29)]

$$\mathsf{M}_{\mathrm{cc}}(p', p) = \int d^4z' d^4z \, \bar{E}_{p'}(z') \mathsf{M}_{\mathrm{cc}}(z', z) E_p(z) = (2\pi)^4 \delta^4(p' - p) \mathsf{M}_{\mathrm{cc}}(p). \tag{5.32}$$

To renormalize the mass operator, we apply the same renormalization conditions as in ordinary QED [Bai+76; BKS75; Bro02; PS95; Rit85]

$$\mathsf{M}_{\mathrm{cc}}^R(p; F = 0, \slashed{p} = m) = 0, \quad \left. \frac{d}{d\slashed{p}} \mathsf{M}_{\mathrm{cc}}^R(p; F = 0) \right|_{\slashed{p}=m} = 0. \tag{5.33}$$

Correspondingly, the renormalized mass operator is defined by

$$\mathsf{M}_{\mathrm{cc}}^R(p) = \mathsf{M}_{\mathrm{cc}}(p) - \mathsf{M}_{\mathrm{cc}}(p; F = 0, \slashed{p} = m) - (\slashed{p} - m) \left. \frac{d\mathsf{M}_{\mathrm{cc}}(p; F = 0)}{d\slashed{p}} \right|_{\slashed{p}=m}. \tag{5.34}$$

---

[3]Note that the order of the arguments differs between mass and polarization operator, see Eq. (3.6). Furthermore, the mass operator in position $[\mathsf{M}(x, y)]$ and momentum space $[\mathsf{M}(p', p)]$ is denoted by the same symbol, even if it is not the same object.

Finally, the field-dependent part of the renormalized mass operator inside a constant-crossed background field is given by [Rit70a; Rit70b; Rit85]

$$
\mathrm{M}_{\mathrm{cc}}^{R}(p) - \mathrm{M}_{\mathrm{cc}}^{R}(p; F = 0) = \frac{\alpha}{2\pi} \int\limits_{0}^{\infty} \frac{dw}{(1+w)^2} \left[\left(2m - \frac{\not{p}}{1+w} \right) f_1(z) \right.
$$
$$
+ e \left(\frac{2+w}{1+w} \gamma^5 p F^* \gamma + im\, \gamma F \gamma \right) \frac{1}{m^2 \chi} \left(\frac{\chi}{w} \right)^{1/3} f(z)
$$
$$
\left. + 2e^2 \frac{(1+w/3)}{m^4 \chi^2} \left(\frac{\chi}{w} \right)^{2/3} p F^2 \gamma\, f'(z) \right], \quad (5.35)
$$

where $z = (w/\chi)^{2/3} \left[1 + (1-\nu)/w \right]$ and $\nu = p^2/m^2$.

For a numerical evaluation it is convenient to eliminate the function f_1. To this end we note the following identities, which hold for $z = (w/\chi)^{2/3}$ (i.e. if $p^2 = m^2$) and can be proven via integration by parts

$$
\int\limits_{0}^{\infty} dw\, \frac{1+2w}{(1+w)^3} f_1(z) = - \int\limits_{0}^{\infty} dw\, \frac{1+w-3w^2}{3z(1+w)^3} f'(z), \quad (5.36a)
$$

$$
\int\limits_{0}^{\infty} \frac{dw}{(1+w)^2} \left[f_1(z) + \frac{2+2w+w^2}{1+w} \frac{f'(z)}{z} \right] = \int\limits_{0}^{\infty} dw\, \frac{f'(z)}{z} \frac{5+7w+5w^2}{3(1+w)^3}. \quad (5.36b)
$$

5.2.4. Exact electron wave function for strong background fields

As shown in Sec. 5.2.2, the Schwinger-Dirac equation reduces to [see Eqs. (5.26) and (5.31)]

$$
i\not{k} U_p'^{E}(\phi) + (\not{p} - m) U_p^{E}(\phi) = \mathrm{M}_p^{\mathrm{qs}}(\phi)\, U_p^{E}(\phi) \quad (5.37)
$$

for strong background fields ($\xi \gg 1$). Here, $\mathrm{M}_p^{\mathrm{qs}}(\phi) = \mathrm{M}_{\mathrm{cc}}[p; F \to f\psi'(\phi)]$ [see Eq. (5.31)] corresponds to the mass operator inside a constant-crossed field [see Eq. (5.35)]. Therefore, Eq. (5.37) has the following spinor structure [see Eq. (5.35) and App. D]

$$
\begin{array}{ccccc}
\mathbf{1} & \gamma^5 & \gamma^\mu & i\gamma^\mu\gamma^5 & i\sigma^{\mu\nu} \\
\mathbf{1} & - & \not{p}, \not{k} & \not{s}\gamma^5 & \gamma f \gamma
\end{array} \quad (5.38)
$$

As the Ritus matrices contain the terms $\mathbf{1}$ and $\gamma f \gamma$ [see Eq. (1.55)], we use the following expansion for the exact electron wave function [see Eq. (5.21)]

$$
\Psi_{p,\sigma}^{E}(x) = E_p(x) U_{p,\sigma}^{E}(kx), \quad U_{p,\sigma}^{E}(kx) = e^{iA(kx)} \left[\mathbf{1} + B(kx) \gamma f \gamma \right] u_{p,\sigma}, \quad (5.39)
$$

where the constant four-spinor $u_{p,\sigma}$ is chosen such that it is an eigenstate of the spin operator

$$
\not{s}\gamma^5\, u_{p,\sigma} = \sigma u_{p,\sigma}, \quad (\not{p} - m) u_{p,\sigma} = 0, \quad \bar{u}_{p,\sigma} u_{p,\sigma} = 2m \quad (5.40)
$$

($\sigma = \pm 1$). In order to show that the exact electron wave function has the spinor structure assumed in Eq. (5.39), we note that the spin operator commutes with all other operators in Eq. (5.38)

$$[\slashed{f}\gamma^5, \slashed{p}] = 0, \quad [\slashed{f}\gamma^5, \slashed{k}] = 0, \quad [\slashed{f}\gamma^5, \gamma f \gamma] = 0. \tag{5.41}$$

Correspondingly, $U_{p,\sigma}^E(kx)$ is also an eigenspinor of $\slashed{f}\gamma^5$ [see Eq. (5.40)]. Furthermore, we can use the relations

$$\slashed{k} = \frac{i}{2}\frac{e(kp)}{\chi m^3}\gamma f \gamma(\slashed{f}\gamma^5), \quad \gamma f^2 p = \frac{i}{2}\frac{\chi m^3}{e}\gamma f \gamma(\slashed{f}\gamma^5) \tag{5.42}$$

to express $\slashed{k}$ and $\gamma f^2 p$ using $\gamma f \gamma$ and

$$\{\slashed{p}, \gamma f \gamma\} = -4i\frac{m^3\chi}{e}\slashed{f}\gamma^5 \tag{5.43}$$

to eliminate $\slashed{p}$. After some algebra [note that only terms to leading-order in α are taken into account for both $A(kx)$ and $B(kx)$], we obtain the following result [Meu10]

$$\Psi_{p,\sigma}^E(x) = \left[\mathbf{1} + \frac{e}{kp}\gamma f \gamma \, \psi(kx) - \frac{i}{4\xi}\frac{e}{kp}\gamma f \gamma \, \mu_B(\phi)\right] e^{iS_{p,\sigma}^E(x)} u_{p,\sigma}, \tag{5.44}$$

where the new phase is given by

$$S_{p,\sigma}^E(x) = -px - \int\limits_{-\infty}^{kx} d\phi' \left[\frac{e\,pA(\phi')}{kp} - \frac{e^2 A^2(\phi')}{2\,kp} + \frac{m^2}{kp}\mu_A(\phi')\right]. \tag{5.45}$$

Here, we defined the following coefficients related to the mass operator [see Eq. (5.35)]

$$\mu_A(\phi) = \frac{\alpha}{2\pi}\int\limits_0^\infty \frac{dw}{(1+w)^3}\left[\frac{5+7w+5w^2}{3z}f'(z) + \sigma\chi(\phi)zf(z)\right], \tag{5.46a}$$

$$\mu_B(\phi) = \frac{\alpha}{2\pi}\int\limits_0^\infty \frac{dw}{(1+w)^3}\left[(2+w)\frac{f(z)}{\sqrt{z}} + \sigma\frac{1+w-3w^2}{3z}f'(z)\right], \tag{5.46b}$$

where $z = [w/\chi(\phi)]^{2/3}$, $\chi(\phi) = \chi\psi'(\phi)$ and the Ritus functions are defined in Eq. (F.1). Note that $p^2 = m^2$, as it denotes the asymptotic (on-shell) four-momentum of the incoming electron.

5.2.5. Exponential wave-function decay

In Chap. 2 we discussed the exponential decay of the exact photon wave function due to pair creation (see Sec. 2.3). Similarly, the optical theorem (see Sec. 2.2) ensures for electrons that the total probability for photon emission corresponds to the imaginary part of the mass operator.

From the square of the exact electron wave function [see Eq. (5.44)], we conclude

that the probability for no photon emission is given by

$$W_{p,\sigma}^{\mathrm{s}} = \exp\left\{ \frac{m^2}{kp} \int\limits_{-\infty}^{+\infty} d\phi' \, \Im \, 2\mu_A(\phi') \right\}, \tag{5.47}$$

where [see Eq. (5.46) and App. F]

$$\Im \, 2\mu_A(\phi) = \alpha \int\limits_{0}^{\infty} \frac{dw}{(1+w)^3} \left[\frac{5 + 7w + 5w^2}{3z} \, \mathrm{Ai}'(z) + \sigma\chi(\phi)z \, \mathrm{Ai}(z) \right], \tag{5.48}$$

$z = [w/\chi(\phi)]^{2/3}$, $\chi(\phi) = \chi\psi'(\phi)$ and Ai denotes the Airy function [Olv+10].

To verify this result, we compare it with the total photon emission rate inside a constant-crossed field calculated by Ritus [Rit70b; Rit72a; Rit85]. To obtain a rate, we transform the integral in the laser phase $\phi = kx$ into an integral over time

$$\frac{dx^\mu}{dt} = \frac{p^\mu}{\epsilon}, \quad \frac{1}{kp}\frac{d\phi}{dt} = \frac{1}{\epsilon}. \tag{5.49}$$

Using the following relation for the decay probability

$$W_{p,\sigma}^{\mathrm{d}} = 1 - W_{p,\sigma}^{\mathrm{s}} = 1 - \exp[-W_{p,\sigma}] \approx W_{p,\sigma} \tag{5.50}$$

(the last relation holds if $W_{p,\sigma}$ is much smaller than unity), we conclude that Eq. (5.47) agrees with the results previously published.

5.3. Nonlinear QED modifications of the electron spin dynamics

As the phase of the exact electron wave function depends on the spin quantum number σ [see Eq. (5.44)], the two spin states have a different quasi-energy inside the laser pulse. Nevertheless, the difference does not play a role for long pulses. Since it is proportional to $\psi'(\phi)$ (which continuously changes its sign), the total accumulated phase[4]

$$\Phi_{\mathrm{tot}} = -\frac{m^2}{kp} \int\limits_{-\infty}^{+\infty} d\phi' \, \mu_A(\phi') = \Phi_0 + \sigma\Phi_{\mathrm{s}} \tag{5.51}$$

is independent of σ in the monochromatic limit. However, the spin-dependent contribution Φ_{s} is a nonlinear function of the laser intensity. Therefore, its average over an asymmetric pulse profile does not necessarily vanish. We will show in the following that $\Phi_{\mathrm{s}} \neq 0$ is possible for ultra-short laser pulses.

5.3.1. Evolution of the spin polarization vector

For definiteness, we consider now the head-on collision between an electron with fixed spin orientation and initial four-momentum $p^\mu = (\epsilon, 0, 0, -p_z)$ and a laser pulse linearly polarized along the x-direction with peak electric field amplitude

---

[4]Note that in Refs. [1] and [2] a different sign convention is used for the phase.

E_0 and angular frequency ω [$k^\mu = \omega(1,0,0,1)$ and $a^\mu = (0, E_0/\omega, 0, 0)$]. After the interaction, we measure the orientation of the spin polarization vector $\boldsymbol{\zeta}^i = \omega^\dagger \sigma^i \omega$ [see Eq. (5.6)] to detect possible changes.

The most general initial spin state is given by[5]

$$|\chi_i\rangle = c_1 |\uparrow_z\rangle + c_2 |\downarrow_z\rangle = \begin{pmatrix} c_1 \\ c_2 \end{pmatrix}, \quad |c_1|^2 + |c_2|^2 = 1, \tag{5.52}$$

with the following spin polarization vector [see Eq. (5.6)]

$$\boldsymbol{\zeta}^x = c_1^* c_2 + c_1 c_2^*, \quad \boldsymbol{\zeta}^y = i(c_1 c_2^* - c_1^* c_2), \quad \boldsymbol{\zeta}^z = |c_1|^2 - |c_2|^2. \tag{5.53}$$

As the magnetic field of the laser points along the y-direction, we have to use this axis as the quantization axis during the propagation. The corresponding eigenspinors of σ_2 are given by

$$
\begin{aligned}
|\uparrow_y\rangle &= \frac{1}{\sqrt{2}} \left(|\uparrow_z\rangle + i |\downarrow_z\rangle \right) = \frac{1}{\sqrt{2}} \begin{pmatrix} 1 \\ i \end{pmatrix}, \\
|\downarrow_y\rangle &= \frac{1}{\sqrt{2}} \left(i |\uparrow_z\rangle + |\downarrow_z\rangle \right) = \frac{1}{\sqrt{2}} \begin{pmatrix} i \\ 1 \end{pmatrix}.
\end{aligned}
\tag{5.54}
$$

For completeness, we also note the eigenstates of σ_1

$$
\begin{aligned}
|\uparrow_x\rangle &= \frac{1}{\sqrt{2}} \left(|\uparrow_z\rangle + |\downarrow_z\rangle \right) = \frac{1}{\sqrt{2}} \begin{pmatrix} 1 \\ 1 \end{pmatrix}, \\
|\downarrow_x\rangle &= \frac{1}{\sqrt{2}} \left(|\uparrow_z\rangle - |\downarrow_z\rangle \right) = \frac{1}{\sqrt{2}} \begin{pmatrix} 1 \\ -1 \end{pmatrix}.
\end{aligned}
\tag{5.55}
$$

Hence, a measurement of the initial spin polarization along one of the coordinate axes would show the following probability distributions

$$
\begin{aligned}
|\langle \uparrow_x | \chi_i \rangle|^2 &= \frac{1}{2}(1 + \boldsymbol{\zeta}^x), \quad |\langle \downarrow_x | \chi_i \rangle|^2 = \frac{1}{2}(1 - \boldsymbol{\zeta}^x), \\
|\langle \uparrow_y | \chi_i \rangle|^2 &= \frac{1}{2}(1 + \boldsymbol{\zeta}^y), \quad |\langle \downarrow_y | \chi_i \rangle|^2 = \frac{1}{2}(1 - \boldsymbol{\zeta}^y), \\
|\langle \uparrow_z | \chi_i \rangle|^2 &= \frac{1}{2}(1 + \boldsymbol{\zeta}^z), \quad |\langle \downarrow_z | \chi_i \rangle|^2 = \frac{1}{2}(1 - \boldsymbol{\zeta}^z).
\end{aligned}
\tag{5.56}
$$

Inside the laser pulse, the states $|\uparrow_y\rangle$ ($\sigma = +1$) and $|\downarrow_y\rangle$ ($\sigma = -1$) acquire the

---

[5]Here and in the following we use the notation

$$|\uparrow_z\rangle = \begin{pmatrix} 1 \\ 0 \end{pmatrix}, \quad |\downarrow_z\rangle = \begin{pmatrix} 0 \\ 1 \end{pmatrix},$$

where $\uparrow$ and $\downarrow$ corresponds to the eigenvalue $+1$ and -1, respectively. Furthermore,

$$\langle \chi_i | = c_1^* \langle \uparrow_z | + c_2^* \langle \downarrow_z | = \begin{pmatrix} c_1^* & c_2^* \end{pmatrix}.$$

following phases [see Eq. (5.51)]

$$|\uparrow_y\rangle \longrightarrow e^{i(\Phi_0 + \Phi_s)} |\uparrow_y\rangle, \quad |\downarrow_y\rangle \longrightarrow e^{i(\Phi_0 - \Phi_s)} |\downarrow_y\rangle. \tag{5.57}$$

Expanding the initial state [see Eq. (5.52)] in the y-basis [see Eq. (5.54)], we obtain

$$|\chi_i\rangle = \frac{c_1 - ic_2}{\sqrt{2}} |\uparrow_y\rangle + \frac{c_2 - ic_1}{\sqrt{2}} |\downarrow_y\rangle. \tag{5.58}$$

Using Eq. (5.57), we can now calculate the time evolution of the initial state

$$|\chi_i\rangle \longrightarrow |\chi_f\rangle \tag{5.59}$$

and obtain the following transition probabilities [see Eq. (5.53)]

$$\mathcal{P}_\uparrow = |\langle \uparrow_z |\chi_f\rangle|^2 = e^{-2\Im\Phi_0} \left\{ \frac{1}{4}(1 + \zeta^y)e^{-2\Im\Phi_s} + \frac{1}{4}(1 - \zeta^y)e^{2\Im\Phi_s} \right.$$
$$\left. + \frac{1}{2} \left[\zeta^z \cos(2\Re\Phi_s) + \zeta^x \sin(2\Re\Phi_s) \right] \right\}, \tag{5.60a}$$

$$\mathcal{P}_\downarrow = |\langle \downarrow_z |\chi_f\rangle|^2 = e^{-2\Im\Phi_0} \left\{ \frac{1}{4}(1 + \zeta^y)e^{-2\Im\Phi_s} + \frac{1}{4}(1 - \zeta^y)e^{2\Im\Phi_s} \right.$$
$$\left. - \frac{1}{2} \left[\zeta^z \cos(2\Re\Phi_s) + \zeta^x \sin(2\Re\Phi_s) \right] \right\}. \tag{5.60b}$$

The first contribution to $\mathcal{P}_{\uparrow\downarrow}$ represents a change in the polarization induced by the life-time difference of the two spin states (imaginary part of the mass operator). It can be controlled by reducing the total emission probability, i.e. by using short laser pulses.

The second contribution to $\mathcal{P}_{\uparrow\downarrow}$ is a spin rotation analogous to birefringence for photons. As the dispersion relation (real part of the mass operator) depends on the spin orientation, the propagation induces a rotation of the spin polarization along the axis of the magnetic field. For $\Im\Phi_s = 0$ we obtain

$$|\langle \uparrow_z |\chi_f\rangle|^2 = e^{-2\Im\Phi_0} \frac{1}{2}(1 + \zeta'^z), \quad |\langle \downarrow_z |\chi_f\rangle|^2 = e^{-2\Im\Phi_0} \frac{1}{2}(1 - \zeta'^z), \tag{5.61}$$

where the new polarization along the z-axis is given by

$$\zeta'^z = \zeta^z \cos(2\Re\Phi_s) + \zeta^x \sin(2\Re\Phi_s). \tag{5.62}$$

5.3.2. Spin asymmetry

For possible experimental measurements the following spin asymmetry is a convenient observable

$$\mathcal{A} = \frac{\mathcal{P}_\uparrow - \mathcal{P}_\downarrow}{\mathcal{P}_\uparrow + \mathcal{P}_\downarrow}. \tag{5.63}$$

Here, the difference

$$\mathcal{P}_\uparrow - \mathcal{P}_\downarrow = e^{-2\Im\Phi_0} \left[\zeta^z \cos\left(2\Re\Phi_s\right) + \zeta^x \sin\left(2\Re\Phi_s\right) \right] \tag{5.64}$$

measures the vacuum-induced spin rotation and the sum

$$\mathcal{P}_\uparrow + \mathcal{P}_\downarrow = e^{-2\Im\Phi_0} \left[\frac{1}{2}(1 + \zeta^y)e^{-2\Im\Phi_s} + \frac{1}{2}(1 - \zeta^y)e^{2\Im\Phi_s} \right] \tag{5.65}$$

represents the total probability for the emission of zero photons [note that the two spin states have a different decay exponent; see Eqs. (5.51) and (5.56)].

Due to the expansions

$$\cos(\phi) \approx 1 - \frac{1}{2}\phi^2, \quad \sin(\phi) \approx \phi, \tag{5.66}$$

it is much easier to detect the spin rotation if the electron is initially polarized transversely along the x direction [$\boldsymbol{\zeta} = (1, 0, 0)$]. Therefore, we focus on this case in the following, where the asymmetry is given by

$$\mathcal{A} = \frac{\mathcal{P}_\uparrow - \mathcal{P}_\downarrow}{\mathcal{P}_\uparrow + \mathcal{P}_\downarrow} = \frac{\sin\left(2\Re\Phi_s\right)}{\cosh\left(2\Im\Phi_s\right)}. \tag{5.67}$$

As aforementioned, the Volkov states predict no relative phase between two different spin states and thus $\mathcal{A} = 0$ (see Sec. 5.1). Measuring a nonzero asymmetry would therefore be a clear signature for nonlinear QED contributions to the electron's spin dynamics.

5.3.3. Numerical results

Since for long pulses a relatively large amount of electrons will decay by radiating, it is convenient to employ rather short pulses (furthermore, the asymmetry becomes insensitive to the CEP for longer pulses). In Fig. 36 we show the asymmetry $\mathcal{A}$ as a function of the laser intensity I and of the laser carrier-envelope phase (CEP) ϕ_0 for a pulse with $N = 2$ and $N = 3$ cycles, respectively. Note that phase-stabilized laser pulses with $\tau \sim 5\,\mathrm{fs}$ and $I \gtrsim 10^{22}\,\mathrm{W/cm^2}$ are experimentally envisaged at the PFS in Garching [Ahm+09; Kar+08]. At an intensity of $I \sim 5 \times 10^{22}\,\mathrm{W/cm^2}$, for example, we find $\exp[-2\Im(\Phi_0)] \sim 10^{-3}$ (for $N = 3$) and a maximal asymmetry $\mathcal{A}_0 \sim 1\,\%$ (see Fig. 36). An asymmetry of this order of magnitude has already been measured experimentally [Esc+05]. Furthermore, polarized ultra-relativistic electron beams with $\mathcal{N} \approx 10^{10}$ electrons, a spot area $\approx 1.7\,\mathrm{\mu m} \times 0.75\,\mathrm{\mu m}$ and a length l_e of about $0.5\,\mathrm{mm}$ have been produced [SLAC376; SLAC9961]. Assuming a Gaussian laser beam focused to one wavelength (spot radius $w_0 = \lambda$ and Rayleigh
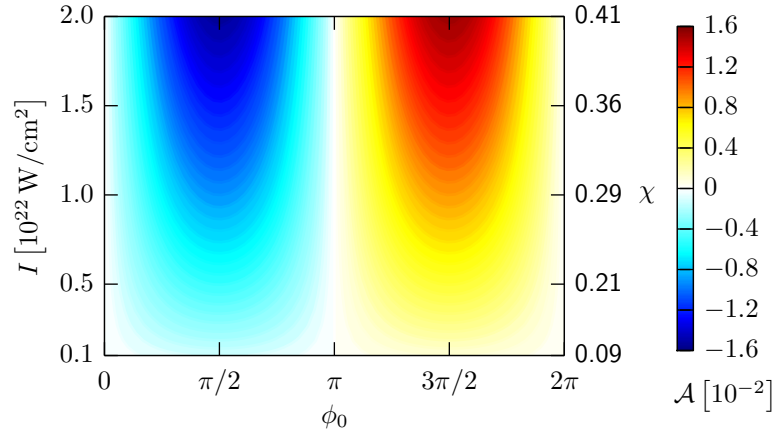
a) Laser pulse with $N = 2$ cycles ($\tau = 2\pi N/\omega \approx 5\,\text{fs}$)
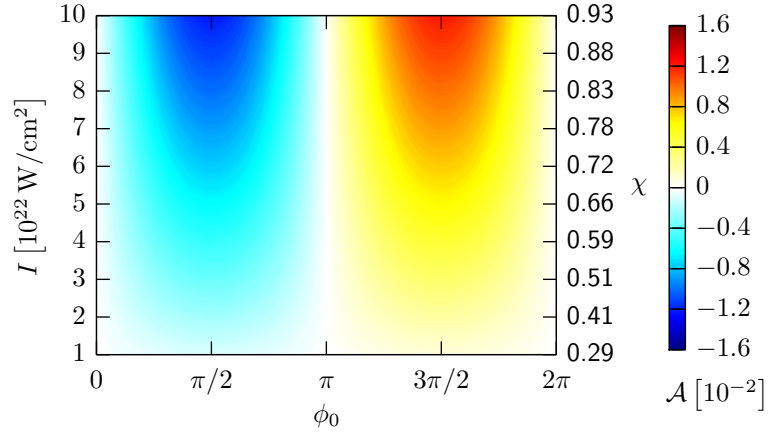
b) Laser pulse with $N = 3$ cycles ($\tau = 2\pi N/\omega \approx 8\,\text{fs}$)

Fig. 36: Expected spin asymmetry $\mathcal{A}$ [see Eq. (5.67)] as a function of the laser peak intensity I and the laser carrier-envelope phase (CEP) ϕ_0. The optical laser pulse ($\omega = 1.55\,\text{eV}$) is described by $\psi'(\phi) = \sin^2(\phi/2N)\sin(\phi + \phi_0)$ if $\phi \in [0, 2\pi N]$ and zero otherwise [see Eq. (1.23)]. The electrons collide head-on with an energy $\epsilon = 500\,\text{MeV}$ (corresponding to $\gamma \approx 1000$). The peak intensity I and the peak value for χ are related by $\chi = \gamma(1 + \beta)\sqrt{I/I_{\text{cr}}}$ ($I_{\text{cr}} = 4.6 \times 10^{29}\,\text{W/cm}^2$).

length $l_r = \pi w_0^2/\lambda = \pi\lambda$) [ST07], about $\mathcal{N}^* \sim \mathcal{N} \times \exp[-2\Im(\Phi_0)] \times 2l_r/l_e \sim 10^5$ electrons pass through the strong-field region without radiating. Thus, the absolute difference of the expected electrons with opposite spin is $\sim \mathcal{A}_0 \times \mathcal{N}^* \sim 10^3$. Note also that in the above example the transverse excursion of an electron in the field is approximately $\lambda m\xi/\epsilon \sim 0.1\,\lambda$, i.e. much smaller than w_0 [LL87]. Finally, the relatively weak dependence of the asymmetry on the laser intensity at $I \gtrsim 5 \times 10^{22}\,\text{W/cm}^2$ renders our results sufficiently insensitive to possible fluctuations of the laser intensity. Thus, we conclude that a spin asymmetry due to the electron's self-interaction is, in principle, measurable with presently available technology.

6 Neutrino-photon coupling inside strong laser pulses

As different neutrino mass eigenstates exist [AEE08; Bil10; BP87; GK07; Kay03; MP04; RPP14], only the lowest one is stable and all others can, in principle, decay radiatively [BPP77; LS77; MS77; Pet77; PW82; Shr82]. However, due to the smallness of the available phase space and the Glashow-Iliopoulos-Maiani (GIM) suppression mechanism (i.e. cancellations between contributions from different fermion generations) [GIM70; PW82] the neutrino life time is much larger than the age of the universe (the electromagnetic properties of neutrinos in vacuum are discussed in Refs. [BGS12; DS04a; DS04c; GS09; Nie82; Shr82]).

Nevertheless, a neutrino can emit photons inside strong electromagnetic background fields, which catalyze the decay. For example, strong magnetic fields encountered in various astrophysical situations substantially reduce the neutrino life time [AM13; GMV92; GMV97; IR97; KW97; TE14; ZEG96] (see also [GMV94b], where the Coulomb field has been investigated). Inside background fields also the production of electron-positron pairs – which is not possible in vacuum due to energy-momentum conservation – is feasible under certain circumstances [BTZ93; CI69; DRT07; KM97; KMR00; KMR02; Tin05].

Moreover, neutrino properties like their mass and their magnetic moment are modified by electromagnetic background fields [DMN13; Erd09; Kuz+06]. Implications for neutrino oscillations have been studied in Refs. [DS01; DS04b; ELS00; LS01] and the possibility for spin light has been pointed out in Refs. [LS03; ST05].

The presence of electromagnetic background fields could also be exploited to create neutrinos, e.g., via photon splitting [DMD76; KMV98; Sko76], scattering [CM02; KMR03; Sha98] or the trident process [Tit+11] (for a review of electroweak processes in electromagnetic background fields see the Refs. [KM03; KM13]).

It is an interesting question whether the emission of photons by neutrinos or other processes like electron-positron pair production could be investigated in a laboratory experiment using high-power lasers (see Fig. 37). To shed light on the feasibility of this idea, the special case of a circularly polarized, monochromatic plane-wave laser field has been analyzed in [GMV93; GMV94a; GMV96] (see also [Sko91]). As laser fields are naturally produced with linear polarization and the highest intensities can only be achieved by using short laser pulses, it is desirable to generalize these results accordingly. In this chapter we will therefore consider a plane-wave laser field with arbitrary polarization and pulse shape.

Inside plane-wave laser fields the probability for a neutrino process depends primarily on the laser intensity and the neutrino energy. A convenient gauge- and Lorentz-invariant measure for the laser field strength is given by the parameter

$\xi = |e|E_0/(m\omega c)$ [see Eq. (1.20)], where E_0 is the electric field amplitude and ω the central angular frequency of the laser. In the regime $\xi \gtrsim 1$ the interaction between the background field and the electron and the positron, must be taken into account exactly by solving the Dirac equation in the presence of the background field (see Chap. 1). For a plane-wave field this is possible analytically and one obtains the Volkov states as single-particle states [LL82; Vol35]. Working in momentum space, the only necessary modification of the Feynman rules (for QED) is the replacement of the free vertex $-ie\gamma^\mu$ by the dressed vertex Γ^μ [see Eq. (1.67)]. Unlike in vacuum, four-momentum is conserved only up to a multiple of the laser four-momentum at the dressed vertex, which changes the kinematics of the processes.

It is well known that for $\xi \gg 1$ the formation region for single-vertex processes primed by the laser field is much smaller than the laser wavelength, such that the local constant-crossed field approximation is applicable [Di+12; Rit85]. Therefore, the case of a constant-crossed background field (studied, e.g., in [BKM99; BTZ93; GMV96; GN72]) is particularly interesting and provides the order of magnitude for the expected probabilities. Inside a constant-crossed field the probability depends nontrivially only on the quantum-nonlinearity parameter $\chi = (2E_\nu/mc^2)(E_0/E_{\rm cr})$ [see Eqs. (1.21) and (6.72)], where E_ν denotes the energy of the incoming neutrino and $E_{\rm cr} = m^2c^3/(\hbar|e|) = 1.3 \times 10^{16}\,\mathrm{V/cm}$ the critical field strength of QED [HE36; Sau31; Sch51] (the expression for χ given here assumes a head-on collision and neglects the neutrino mass).

As the nonlinear-quantum parameter is inversely proportional to the cube of the electron (positron) mass ($\chi \sim m^{-3}$), nonlinear quantum effects caused by muon or tau leptons are strongly suppressed for reasonable parameters and ignored here.

a) Photon emission   **b**) Pair production

c) Optical theorem for pair production
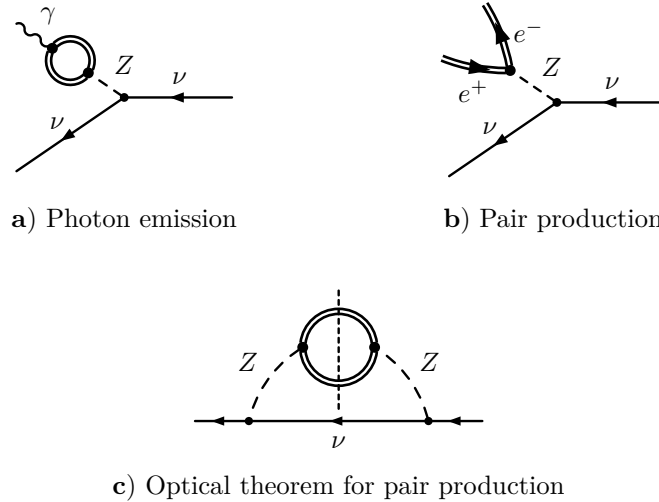
Fig. 37: a) Photon emission and **b**) trident electron-positron pair production by a neutrino inside a strong, plane-wave laser field (mediated by the neutral current, i.e. Z boson exchange). For an electron neutrino also the charged current must be taken into account (W boson exchange, see Fig. 40). **c**) The total trident pair-production probability is related to the imaginary part of the neutrino self-energy diagram (see, e.g., [BTZ93] for details). The double lines denote here electron and positron states, which are dressed by the laser field (time axis from right to left).

a) Current-coupling tensor $T_5^{\mu\nu}(q_1, q_2)$

b) Polarization tensor $T^{\mu\nu}(q_1, q_2)$
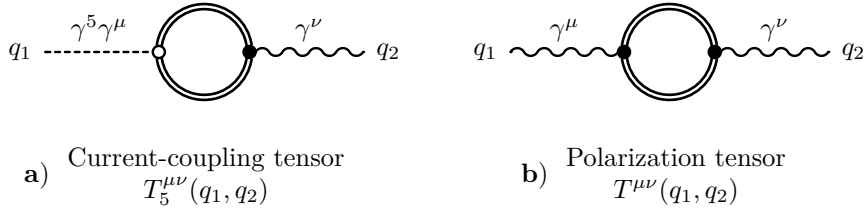
Fig. 38: a) The leading-order Feynman diagram for the coupling between the vector current (γ^μ-vertex) and the axial-vector current ($\gamma^5\gamma^\mu$-vertex), see Eq. (6.8). **b**) The current-coupling tensor $T_5^{\mu\nu}(q_1, q_2)$ is closely related to the polarization tensor $T^{\mu\nu}(q_1, q_2)$ [see Chap. 3 and Eq. (3.6)]. Solid lines indicate fermions, double lines Volkov states (which take the plane-wave background field exactly into account), wiggly lines photons and dashed lines the axial-vector current.

Correspondingly, the symmetry between different lepton generations is broken and the GIM mechanism does not apply. Furthermore, the laser provides additional energy and momentum to the reaction, which enlarges the available phase space. Due to these two reasons, the probability for photon emission by neutrinos inside a plane-wave field is strongly enhanced in comparison with the vacuum case (note that the laser field also affects tree-level processes like the decay of a muon [Dic+09; Far+09]). Nevertheless, the enhancement is primed by an electromagnetic exchange of photons between an electron/positron loop and the laser. Therefore, we expect that the probabilities for nonlinear neutrino processes inside laser fields still contain the suppression factor $(m/M_{Z,W})^4 \sim 10^{-20}$ which renders an experimental observation challenging ($M_Z \approx 91\,\text{GeV}$ and $M_W \approx 80\,\text{GeV}$ denote the mass of the Z and the W boson, respectively [RPP14]).

By combining accelerator-based neutrino beams with energies in the GeV range [Ban+09; Ber+06; Bog+14; Gee12; Gee98; IDS; ISS; Kap14; MAP; The+09] and strong optical lasers ($\xi \sim 10^{2-3}$) [CLF; ELI; XCELS; Yan+08], the nonlinear quantum regime $\chi \gtrsim 1$ could be entered, where also the production of real electron-positron pairs via the trident process becomes feasible [BTZ93; CI69; DRT07; KM97; KMR00; KMR02; Tin05]. As the energy and momentum required to bring the electron-positron pair on shell are provided by the laser field, the probability for trident pair production even exceeds the one for photon emission if $\chi \gtrsim 1$ (the corresponding Feynman diagram contains only two interaction vertices, see Fig. 37).

In order to calculate the probability for neutrino photon emission or trident pair production (via the optical theorem), the coupling between the vector current (γ^μ-vertex) and the axial-vector current ($\gamma^5\gamma^\mu$-vertex) described by the tensor $T_5^{\mu\nu}(q_1, q_2)$ must be determined (see Fig. 38). For a constant background field it has been investigated in [BG03; GS00a; GS00b; GS01; Nie03; Sch00a; Sch00b; Sha00]. In the present paper an arbitrary plane-wave laser field is considered as background field (see Sec. 1.3) and a triple-integral representation for $T_5^{\mu\nu}(q_1, q_2)$ is derived, which can be transformed into a double-integral representation using the relations given in Chap. 3. Special attention is payed to the Ward-Takahashi identity, which contains a contribution due to the Adler-Bell-Jackiw (ABJ) anomaly (see Fig. 39) [Adl69; BJ69]. The anomalous term is calculated here explicitly by applying a suitable regularization procedure.

a) Anomalous triangle diagram

b) Leading-order expansion in the external field
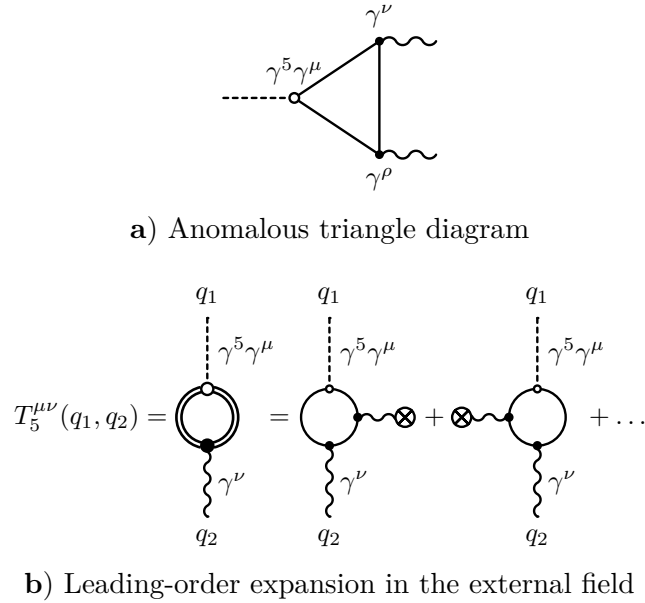
Fig. 39: a) The axial-vector anomaly in vacuum QED is caused by the triangle diagram. **b**) As for weak external fields $A^\mu(\phi)$ (denoted by $\otimes$) the leading-order field-dependent contribution to the current-coupling tensor $T_5^{\mu\nu}(q_1, q_2)$ [see Eq. (6.8)] corresponds to the triangle diagram, one also expects an anomalous term in the Ward-Takahashi identity for $T_5^{\mu\nu}(q_1, q_2)$ [see Eq. (6.38)]. Here, solid lines indicate the vacuum states and double lines dressed Volkov states for the charged fermions, wiggly lines photons and dashed lines the axial-vector current.

This chapter is organized as follows: In Sec. 6.1 the interaction between neutrinos and photons inside a plane-wave background field is considered and it is shown how the axial-vector–vector current-coupling tensor $T_5^{\mu\nu}(q_1, q_2)$ (see Fig. 38) appears naturally in the electroweak sector of the standard model if plane-wave background fields are taken into account. The calculation of $T_5^{\mu\nu}(q_1, q_2)$ is then presented in Sec. 6.2, followed by a detailed discussion of the ABJ anomaly in Sec. 6.3. Subsequently, various important special cases like a constant-crossed and a circularly polarized, monochromatic field are considered in Sec. 6.4 and compared with known expressions from the literature.

6.1. Nonlinear neutrino-photon interactions

As neutrinos are neutral particles, their interaction with photons must be mediated by loop diagrams which contain electrically charged particles (see Fig. 40). At the loop level the quantization of the electroweak sector of the standard model involves "unphysical" degrees of freedom, i.e. particles which appear only in loops but not as free, asymptotic states [BP99; DGH94]. These are the unphysical scalar Higgs particles, present if the calculation is performed in a renormalizable gauge (from the Higgs doublet, which consists of four scalar fields, only one degree of freedom corresponds to the physically observable Higgs particle) and the Feynman-Faddeev-Popov ghosts, which appear in the quantization of a nonabelian gauge theory [CL82; Pok00]. Therefore, the complete set of Feynman rules for the electroweak sector of the standard model after symmetry breaking is rather large [Aok+82;

a) Z boson exchange

b) W boson exchange

c) Local limit (Fermi description)
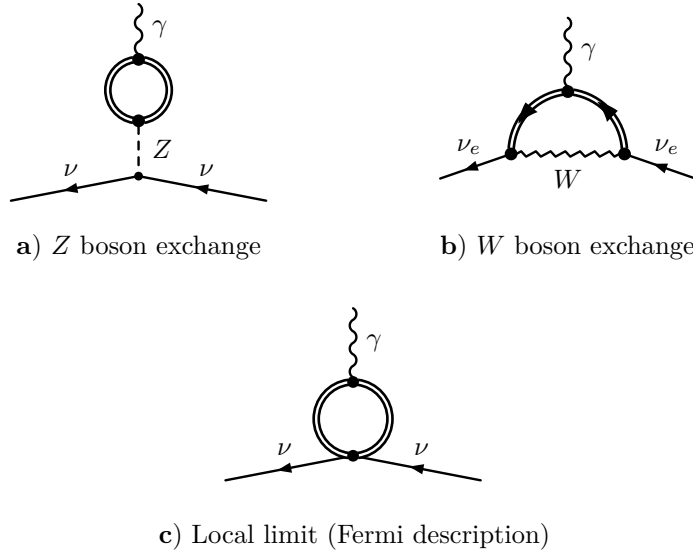
Fig. 40: Neutrino-photon interaction vertex. **a**) The electron-positron loop interacts via the neutral current with all neutrino flavor states. **b**) Electron neutrinos also couple via the charged current to electrons and positrons. **c**) In the local limit (exchanged momentum much smaller than the weak gauge-boson mass) the effective four-point Fermi interaction is obtained. The double lines denote dressed electron and positron states which take the laser field exactly into account (time axis from right to left).

BSH86; Den93; Hol90]. Fortunately, the leading-order contribution (with respect to the electroweak mass scale) to the neutrino-photon coupling inside a plane-wave background field is given by only two diagrams, which are shown in Fig. 40 (see also [DS04a; GMV96]).

Due to the existence of neutrino oscillations we know that neutrinos have a finite mass [AEE08; Bil10; BP87; GK07; Kay03; Kay81; MP04; RPP14]. The left-handed neutrino mass eigenstates ν_{rL} ($r = 1, 2, 3$) are related by the unitary Pontecorvo-Maki-Nakagawa-Sakata (PMNS) matrix $\mathbf{U}_{\alpha r}$ (which is also simply called neutrino mixing matrix) $\nu_{\alpha L} = \mathbf{U}_{\alpha r} \nu_{rL}$ [MNS62; Pon57; Pon58; RPP14] to the left-handed flavor neutrino eigenstates $\nu_{\alpha L}$ ($\alpha = e, \mu, \tau$). As neutrinos are produced via the charged current as left-handed flavor eigenstates, the nature of their right-handed component (required for the construction of a mass term in the Lagrangian) is not determined so far, i.e. the neutrino could be either a Dirac or a Majorana particle. At high energies, however, the neutrino mass can usually be neglected and with a reasonable experimental precision it is not possible to distinguish between Dirac and Majorana neutrinos. Correspondingly, we can assume in the following that the neutrino is a massless, left-handed Dirac particle as originally postulated in the standard model.

6.1.1. Lagrangian density

After electroweak-symmetry breaking the Lagrangian density, which describes the interaction between the photon field $\mathcal{A}^\mu$ and the various fermion fields ψ_f, is given

by [DGH94; RPP14]

$$\mathcal{L}_L^{EM} = e\mathcal{A}_\mu J_{EM}^\mu, \quad J_{EM}^\mu = -\bar{\psi}_e\gamma^\mu\psi_e + \frac{2}{3}\bar{\psi}_u\gamma^\mu\psi_u - \frac{1}{3}\bar{\psi}_d\gamma^\mu\psi_d + \dots \quad (6.1)$$

[the index $f = e, \mu, \tau, \dots$ labels the type of fermion field (quarks and leptons), Dirac spinor indices are suppressed (note that we use the convention $e < 0$)]. Correspondingly, we obtain

$$\mathcal{L}_L^Z = -\frac{g}{2\cos\theta_W}Z_\mu J_Z^\mu, \quad J_Z^\mu = \bar{\psi}_f[g_v^{(f)}\gamma^\mu + g_a^{(f)}\gamma^\mu\gamma^5]\psi_f \quad (6.2)$$

for the interaction with the Z boson field Z^μ. Here $g = g_2$ and $g' = g_1 = g\tan\theta_W$ are the fundamental coupling constants for weak isospin and hypercharge, respectively, which are (after symmetry breaking) related to the electron charge e and the Fermi constant G_F by $-e = g\sin\theta_W$ and $G_F = (g^2\sqrt{2})/(8M_W^2) \approx 1.17 \times 10^{-5}\,\text{GeV}^{-2}$, respectively (at tree level the gauge-boson masses obey $M_W = M_Z\cos\theta_W$, θ_W is called the weak mixing or Weinberg angle). The constants $g_v^{(f)}$ and $g_a^{(f)}$ depend on the type of fermion. For the charged leptons we obtain $g_v^{(e,\mu,\tau)} = -1/2 + 2\sin^2\theta_W$ and $g_a^{(e,\mu,\tau)} = -1/2$, for the (massless) neutrinos $g_v^{(\nu_e,\nu_\mu,\nu_\tau)} = g_a^{(\nu_e,\nu_\mu,\nu_\tau)} = 1/2$ and for the quarks $g_v^{(u,c,t)} = 1/2 - (4/3)\sin^2\theta_W$ $g_v^{(d,s,b)} = -1/2 + (2/3)\sin^2\theta_W$, $g_a^{(u,c,t)} = -g_a^{(d,s,b)} = 1/2$ [note that we use the same notation for γ^5 as in [LL82] and [DGH94], i.e. the projection operators P_L for the left-handed and P_R for the right-handed component are given by $P_L = (\mathbf{1} + \gamma^5)/2$ and $P_R = (\mathbf{1} - \gamma^5)/2$, respectively].

Finally, the Lagrangian density, which describes the interaction between the complex W boson field W_μ^+ [the plus is part of the symbol name, we also define $W_\mu^- = (W_\mu^+)^\dagger$] and the first lepton generation can be written as

$$\mathcal{L}_e^W = -\frac{g}{2\sqrt{2}}[W_\mu^+ J_{W,e}^\mu + W_\mu^-(J_{W,e}^\mu)^\dagger], \quad J_{W,e}^\mu = \bar{\psi}_{\nu_e}\gamma^\mu(\mathbf{1} + \gamma^5)\psi_e. \quad (6.3)$$

From Eqs. (6.1)-(6.3) one obtains the interaction vertices between the fermions and the electroweak gauge fields of the standard model [Aok+82; DGH94]; they contain both vector (γ^μ) and axial-vector ($\gamma^\mu\gamma^5$) couplings.

After quantization the propagators for the weak gauge bosons are (in position space and Feynman gauge) given by [DGH94]

$$iG_{Z,W}^{\mu\nu}(x - y) = \int \frac{d^4p}{(2\pi)^4} \frac{-ig^{\mu\nu}}{p^2 - M_{Z,W}^2 + i0} e^{-ip(x-y)}. \quad (6.4)$$

If the exchanged momenta are much smaller than the weak mass scale $M_{Z,W} \sim 100\,\text{GeV}$, one can neglect the momentum dependence in the denominator in Eq. (6.4) (local limit). After taking the momentum integrals, the propagators are then given by

$$iG_{Z,W}^{\mu\nu}(x - y) = i\frac{g^{\mu\nu}}{M_{Z,W}^2}\delta^4(x - y) \quad (6.5)$$

(see Fig. 40, c). Physically, this means that the Z and the W boson are too heavy

to propagate a significant distance and we obtain essentially Fermi's description for the weak force [Fer34a; Fer34b].

6.1.2. Z boson exchange

In the local limit, the matrix element for the emission of a photon with four-momentum q^μ and polarization four-vector ϵ^μ by a neutrino due to Z boson exchange (see Fig. 40, a) is given by [IR97]

$$i\mathfrak{M}_Z(p', q; p) = \frac{2G_F}{\sqrt{2}}\, \bar{u}_{\nu,p'}\gamma_\mu P_L u_{\nu,p} \frac{1}{e}\Big[g_v^{(e)}T^{\mu\nu}(p - p', q) + g_a^{(e)}T_5^{\mu\nu}(p - p', q)\Big]\epsilon_\nu^* \tag{6.6}$$

(we use the same conventions for matrix elements as in Chap. 2). Here, $u_{\nu,p}$ and $u_{\nu,p'}$ are the Dirac spinors for the incoming neutrino with four-momentum p^μ and the outgoing neutrino with four-momentum p'^μ, respectively. Furthermore, $T^{\mu\nu}(q_1, q_2)$ denotes the polarization tensor [see Fig. 38 and Eq. (3.6)]

$$T^{\mu\nu}(q_1, q_2) = \int \frac{d^4p\, d^4p'}{(2\pi)^8}\, \mathbf{tr}\ \Gamma^\mu(p', q_1, p)$$
$$\times \frac{\slashed{p} + m}{p^2 - m^2 + i0}\, \Gamma^\nu(p, -q_2, p')\frac{\slashed{p}' + m}{p'^2 - m^2 + i0} \tag{6.7}$$

and $T_5^{\mu\nu}(q_1, q_2)$ the axial-vector–vector current-coupling tensor

$$T_5^{\mu\nu}(q_1, q_2) = \int \frac{d^4p\, d^4p'}{(2\pi)^8}\, \mathbf{tr}\ \Gamma^\mu(p', q_1, p)\gamma^5$$
$$\times \frac{\slashed{p} + m}{p^2 - m^2 + i0}\, \Gamma^\nu(p, -q_2, p')\frac{\slashed{p}' + m}{p'^2 - m^2 + i0}, \tag{6.8}$$

which will be calculated in Sec. 6.2 [the final result is given in Eq. (6.51); for the definition of the dressed vertex Γ^μ see Eq. (1.67)]. Note that $T_5^{\mu\nu}(q_1, q_2)$ is actually a pseudo-tensor and that in our definition the electron charge e is taken as the coupling constant for both vertices [this is the reason for the prefactor $1/e$ appearing in Eq. (6.6)]. Furthermore, the appearance of $g_v^{(e)}$ and $g_a^{(e)}$ in Eq. (6.6) is related to the electron-positron loop and is independent of the neutrino species which interacts with the photon.

Despite the fact that the electron and the positron are the lightest charged fermions, also the muon, the tau and the various quarks contribute to the loop which couples the photon with the Z boson (see Fig. 40, a). To calculate the contribution of the other charged fermions to this loop, the electron (positron) mass and charge appearing in $\frac{1}{e}T^{\mu\nu}(q_1, q_2)$ and $\frac{1}{e}T_5^{\mu\nu}(q_1, q_2)$ must be replaced accordingly and the Z boson coupling constants $g_{v,a}^{(e)} \to g_{v,a}^{(f)}$ adjusted. As discussed in the introduction, the nonlinear interaction with the background field can be neglected for fermions with a mass well above the electron (positron) scale (for reasonable field strengths of the background field). However, the contribution of all fermions in each generation is needed for the cancellation of the axial-vector anomaly. As the anomalous contribution to $\frac{1}{e}T_5^{\mu\nu}(q_1, q_2)$ is independent of the

fermion mass and proportional to the square of the electric charge [at one loop in the presence of a plane-wave, see Eq. (6.48)], this cancellation (for each fermion generation) can be seen from the relation

$$\frac{1}{2}\big[-(-1)^2 + 3\,(2/3)^2 - 3\,(-1/3)^2\,\big] = 0 \tag{6.9}$$

(all gauge-symmetry anomalies must cancel in the standard model, otherwise it would be nonrenormalizable [GJ72]).

6.1.3. W boson exchange

For electron neutrinos also the exchange of a W boson contributes to the photon-emission matrix element (see Fig. 40, b). Applying the local limit for the W boson propagator, we obtain the following expression for the matrix element

$$i\mathfrak{M}_W(p',q;p) = \frac{4G_F}{\sqrt{2}} \int \frac{dp_1^4 dp_2^4}{(2\pi)^8} \int d^4x\, e^{-i(p-p')x}$$
$$\times \bar{u}_{\nu,p'}\gamma^\rho P_L\, M^\nu(p_1,p_2,q;x)\epsilon^*_\nu\,\gamma_\rho P_L u_{\nu,p}, \tag{6.10}$$

where

$$M^\nu(p_1,p_2,q;x) = iE_{p_1,x}\frac{\not{p}_1+m}{p_1^2-m^2+i0}\Gamma^\nu(p_1,-q,p_2)\frac{\not{p}_2+m}{p_2^2-m^2+i0}\bar{E}_{p_2,x}. \tag{6.11}$$

Using the identities given in App. D for an arbitrary 4×4 matrix Γ in spinor space, we obtain

$$\gamma^\rho P_L\Gamma\gamma_\rho P_L = -2r_\mu\gamma^\mu P_L, \tag{6.12}$$

where

$$r_\mu = \tfrac{1}{2}\,\mathbf{tr}\,P_R\gamma_\mu\Gamma = \tfrac{1}{2}\,\mathbf{tr}\,\gamma_\mu P_L\Gamma. \tag{6.13}$$

Therefore, we can write the matrix element for the W boson exchange diagram as [see Eq. (6.10)] [IR97]

$$i\mathfrak{M}_W(p',q;p) = \frac{2G_F}{\sqrt{2}}\,\bar{u}_{\nu,p'}\gamma_\mu P_L u_{\nu,p}\,\frac{1}{e}\Big[T^{\mu\nu}(p-p',q) + T_5^{\mu\nu}(p-p',q)\Big]\epsilon^*_\nu \tag{6.14}$$

(note that it only contributes for electron neutrinos). In the local limit it has the same structure as the one for the Z boson exchange given in Eq. (6.6). The anomaly, however, must drop also for this diagram if one first performs the calculations by employing the full W boson propagator in Eq. (6.4) [IR97].

6.2. Current-coupling tensor

In the previous section it was shown how the axial-vector–vector current-coupling tensor $T_5^{\mu\nu}(q_1,q_2)$ (see Fig. 38) arises in the calculation of neutrino-photon interactions inside strong laser fields. Now, we will examine $T_5^{\mu\nu}(q_1,q_2)$ closer and derive a compact triple-integral representation for it. After applying the Feynman rules

[DG00; Di+12; FGS91; Mit75; Rit85], we obtain the following expression [see Eq. (6.8)]

$$T_5^{\mu\nu}(q_1, q_2) = \int \frac{d^4 p \, d^4 p'}{(2\pi)^8} \, \mathbf{tr} \, \Gamma^\mu(p', q_1, p)\gamma^5$$

$$\times \frac{\not{p} + m}{p^2 - m^2 + i0} \Gamma^\nu(p, -q_2, p') \frac{\not{p}' + m}{p'^2 - m^2 + i0} \quad (6.15)$$

[for the definition of the dressed vertex Γ^ρ see Eq. (1.67)]. Note that $T_5^{\mu\nu}(q_1, q_2)$ is equivalent to the tensor

$$\widetilde{T}_5^{\mu\nu}(q_1, q_2) = \int \frac{d^4 p \, d^4 p'}{(2\pi)^8} \, \mathbf{tr} \, \Gamma^\mu(p', q_1, p)$$

$$\times \frac{\not{p} + m}{p^2 - m^2 + i0} \Gamma^\nu(p, -q_2, p')\gamma^5 \frac{\not{p}' + m}{p'^2 - m^2 + i0}, \quad (6.16)$$

which is obtained by interchanging the vector- and the axial-vector current vertex $[\widetilde{T}_5^{\mu\nu}(q_1, q_2) = T_5^{\nu\mu}(-q_2, -q_1)]$.

The current-coupling tensor $T_5^{\mu\nu}(q_1, q_2)$, which we consider here, differs from the polarization tensor $T^{\mu\nu}(q_1, q_2)$ [see Eq. (6.7)] only by the insertion of γ^5 (i.e. by the trace). Hence, the calculation of $T_5^{\mu\nu}(q_1, q_2)$ is related to the one of $T^{\mu\nu}(q_1, q_2)$ carried out in Chap. 3 and we will focus in this chapter mainly on the differences between both derivations. At first sight one may think that the small modification of the trace should only affect the technical details of the calculation. However, it is responsible for several important qualitative changes like the appearance of the ABJ anomaly in $T_5^{\mu\nu}(q_1, q_2)$, which we will discuss now in detail.

An important consequence of the additional γ^5 in the trace of $T_5^{\mu\nu}(q_1, q_2)$ is the fact that only an odd number of couplings to the background field are allowed if the background field is treated perturbatively (this follows from a generalization of Furry's theorem, see, e.g., [Nis51]; for the polarization tensor only an even number of couplings is possible). Accordingly, the tensor structure of $T_5^{\mu\nu}(q_1, q_2)$ is different from that of $T^{\mu\nu}(q_1, q_2)$ [see Eq. (6.47)] and the vacuum contribution to $T_5^{\mu\nu}(q_1, q_2)$ vanishes (see Fig. 39). Furthermore, we will see that no infinities are encountered and $T_5^{\mu\nu}(q_1, q_2)$ does not need to be regularized.

In order to determine $T_5^{\mu\nu}(q_1, q_2)$ we insert the dressed vertex [see Eq. (1.67)] into Eq. (6.8) [we will denote the vertex integrals associated with $\Gamma^\mu(p', q_1, p)$ and $\Gamma^\nu(p, -q_2, p')$ by $d^4 x$ and $d^4 y$, respectively] and obtain

$$T_5^{\mu\nu}(q_1, q_2) = 4 \, (-ie)^2 \int \frac{d^4 p \, d^4 p'}{(2\pi)^8} \int d^4 x d^4 y$$

$$\times \frac{\frac{1}{4} \, \mathbf{tr} \, [\cdots]_5^{\mu\nu}}{(p^2 - m^2 + i0)(p'^2 - m^2 + i0)} e^{iS_T}, \quad (6.17)$$

where [see Eq. (3.9)]

$$
iS_T = i(p' - p - q_1)x + i(p - p' + q_2)y
$$

$$
+ i \int\limits_{ky}^{kx} d\phi' \left[\frac{e p_\mu p'_\nu \mathfrak{F}^{\mu\nu}(\phi')}{(kp)(kp')} + \frac{e^2(kp - kp')}{2(kp)^2(kp')^2} p_\mu p'_\nu \mathfrak{F}^{2\mu\nu}(\phi') \right] \quad (6.18)
$$

and the trace $\frac{1}{4} \mathbf{tr} \left[\cdots \right]_5^{\mu\nu}$ in Eq. (6.17) is given by

$$
\frac{1}{4} \mathbf{tr} \left[\gamma_\alpha a^{\alpha\mu} + i\gamma_\alpha \gamma^5 b^{\alpha\mu} \right] \gamma^5 (\not{p} + m) \left[\gamma_\beta c^{\beta\nu} + i\gamma_\beta \gamma^5 d^{\beta\nu} \right] (\not{p}' + m)
$$

$$
= im^2 [(b^{\alpha\mu} c_\alpha{}^\nu) - (a^{\alpha\mu} d_\alpha{}^\nu)] - i(pp')[(a^{\alpha\mu} d_\alpha{}^\nu) + (b^{\alpha\mu} c_\alpha{}^\nu)]
$$

$$
+ i(p_\alpha p'_\beta + p_\beta p'_\alpha)(b^{\alpha\mu} c^{\beta\nu} + a^{\alpha\mu} d^{\beta\nu}) \quad (6.19)
$$

$$
- i\epsilon_{\rho\sigma\alpha\beta} p^\rho p'^\sigma (b^{\alpha\mu} d^{\beta\nu} - a^{\alpha\mu} c^{\beta\nu}),
$$

where

$$
a^{\alpha\mu} = G^{\alpha\mu}(kp', kp; kx), \quad c^{\beta\nu} = G^{\beta\nu}(kp, kp'; ky),
$$

$$
b^{\alpha\mu} = G_5^{\alpha\mu}(kp', kp; kx), \quad d^{\beta\nu} = G_5^{\beta\nu}(kp, kp'; ky) \quad (6.20)
$$

[the additional γ^5 in Eq. (6.19) exchanges the vector and the axial-vector current in comparison with the polarization tensor].

Next, we employ the following proper-time parametrization for the propagators [see Eq. (3.18)]

$$
\frac{1}{p^2 - m^2 + i0} \frac{1}{p'^2 - m^2 + i0} = (-i)^2 \int\limits_0^\infty ds\, dt
$$

$$
\times \exp \left[i(p^2 - m^2 + i0)s + i(p'^2 - m^2 + i0)t \right] \quad (6.21)
$$

(the pole prescription $i0$ will be dropped in the exponents and can be restored by substituting $m^2 \to m^2 - i0$). In the final representation we change the proper-time integrals in the following way [see Eq. (3.42)]

$$
\int\limits_0^\infty ds\, dt\, f(s, t) = \frac{1}{2} \int\limits_{-1}^{+1} dv \int\limits_0^\infty d\tau\, \tau \tilde{f}(\tau, v) \quad (6.22)
$$

(note that terms odd in v in the resulting function $\tilde{f}(\tau, v)$ can be dropped), where [see Eq. (6.23)]

$$
\tau = s + t, \quad v = \frac{s - t}{s + t}, \quad \mu = \frac{st}{s + t} = \frac{1}{4}\tau(1 - v^2). \quad (6.23)
$$

After using the parametrization from Eq. (6.21) also in Eq. (6.17) and by adding the source terms $ip_\mu j^\mu + ip'_\mu j'^\mu$ to the resulting phase in the same equation, we

apply the replacements

$$p^\mu \longrightarrow (-i)\partial_j^\mu, \quad p'^\mu \longrightarrow (-i)\partial_{j'}^\mu \qquad (6.24)$$

to the trace given in Eq. (6.19), use canonical light-cone coordinates (see Sec. 1.4.3) and define [see Eqs. (3.16) and (6.26)]

$$\lambda^\mu = -\frac{m(kq)}{(kp)(kp')}\sum_{i=1,2}\xi_i\Lambda_i^\mu\int\limits_{ky}^{kx}d\phi'\,\psi_i(\phi'),$$

$$\Lambda = -\frac{m^2(kq)}{2(kp)(kp')}\sum_{i=1,2}\xi_i^2\int\limits_{ky}^{kx}d\phi'\,\psi_i^2(\phi'), \qquad (6.25)$$

$$I_i = -\frac{1}{2kq\mu}\int\limits_{ky}^{kx}d\phi'\,\psi_i(\phi'), \quad J_i = -\frac{1}{2kq\mu}\int\limits_{ky}^{kx}d\phi'\,\psi_i^2(\phi') \qquad (6.26)$$

(see App. C for more details). Finally, we obtain the following structure for the current-coupling tensor

$$T_5^{\mu\nu}(q_1, q_2) = 4(-ie)^2\int\frac{d^4p\,d^4p'}{(2\pi)^8}\int d^4x d^4y\,(-i)^2\int\limits_0^\infty ds dt\,\frac{1}{4}\,\mathbf{tr}[\cdots]_5^{\mu\nu}e^{iS_T'}, \qquad (6.27)$$

where the full phase including the proper-time exponents and the source terms is given by [see Eq. (3.25)]

$$S_T' = \tilde{S}_T + p_\mu j^\mu + p'_\mu j'^\mu, \quad \tilde{S}_T = (p^2 - m^2)s + (p'^2 - m^2)t + S_T \qquad (6.28)$$

(if no explicit argument is present, the prime is a part of the symbol name and does not indicate a derivative). After taking most of the integrals, we obtain the result [see Eq. (3.29)]

$$T_5^{\mu\nu}(q_1, q_2) = -2i\pi e^2\,\delta^{(-,\perp)}(q_1 - q_2)\int\limits_0^\infty ds\,dt\int\limits_{-\infty}^{+\infty}dx^-$$

$$\times\,\frac{1}{(s+t)^2}\frac{1}{4}\,\mathbf{tr}\left[\cdots\right]_5^{\mu\nu}e^{iS_T'}\Big|_{j=j'=0}, \qquad (6.29)$$

where $x^- = kx = \phi$ and the trace is given in Eq. (6.19) with the replacement in Eq. (6.24) and [see Eq. (3.26)]

$$iS_T' = i\Big[(q_2^+ - q_1^+)x^- - m^2(s+t) + \frac{st}{s+t}q_2^2 - \frac{1}{s+t}(t\,q_2 j - s\,q_2 j')$$

$$-\,\frac{1}{4(s+t)}(j+j')^2 - \frac{1}{2(s+t)}(j+j')\lambda - \frac{1}{4(s+t)}\lambda^2 + \Lambda\Big] \qquad (6.30)$$

[note that, since no confusion can arise, we use the same symbol for the phase

before and after the mentioned integrals are taken, see Eqs. (6.27) and (6.28) and Eqs. (6.29) and (6.30)].

Due to the momentum-conserving delta functions in Eq. (6.29), we will simply write q^μ whenever q_1^μ and q_2^μ can be used interchangeably as in Chap. 3.

To obtain a symmetric expression with respect to the external momenta q_1^μ and q_2^μ, we will perform below the shift [see Eq. (3.30)]

$$z^- = x^- + \mu q^- \tag{6.31}$$

and use z^- as integration variable.

6.2.1. Ward-Takahashi identity

According to Noether's theorem the gauge invariance of the QED Lagrangian implies electric charge conservation. More specifically, if the spinor field $\psi(x)$ obeys the Dirac equation

$$[i\slashed{\partial} - e\slashed{A}(x) - m]\psi(x) = 0 \tag{6.32}$$

[here, $A^\mu(x)$ denotes the classical background field], the vector current is conserved

$$\partial_\mu j^\mu(x) = 0, \quad j^\mu(x) = \bar{\psi}(x)\gamma^\mu\psi(x). \tag{6.33}$$

After changing to momentum space, the current conservation law is expressed by

$$\int d^4x\, e^{-iqx}[\partial_\mu j^\mu(x)] = iq_\mu j_q^\mu = 0, \quad j_q^\mu = \int d^4x\, e^{-iqx} j^\mu(x). \tag{6.34}$$

Therefore, one expects that the polarization tensor $T^{\mu\nu}(q_1, q_2)$ obeys the following homogeneous Ward-Takahashi identity

$$q_{1\mu}T^{\mu\nu}(q_1, q_2) = 0, \quad T^{\mu\nu}(q_1, q_2)q_{2\nu} = 0, \tag{6.35}$$

which is indeed the case (see Chap. 3).

Similarly, the divergence of the axial-vector current

$$j_5^\mu(x) = \bar{\psi}(x)\gamma^\mu\gamma^5\psi(x) \tag{6.36}$$

should be given by

$$\partial_\mu j_5^\mu(x) = 2mi\,\bar{\psi}(x)\gamma^5\psi(x). \tag{6.37}$$

After applying Eq. (1.73) to the definition of $T_5^{\mu\nu}(q_1, q_2)$ [see Eq. (6.8)], we obtain the following Ward-Takahashi identity for the tensor $T_5^{\mu\nu}(q_1, q_2)$

$$q_{1\mu}T_5^{\mu\nu}(q_1, q_2) = T_5^\nu(q_1, q_2) + \mathfrak{T}_5^\nu(q_1, q_2), \quad T_5^{\mu\nu}(q_1, q_2)q_{2\nu} = -\mathfrak{T}_5^\mu(-q_2, -q_1), \tag{6.38}$$

where we defined

$$T_5^\nu(q_1, q_2) = 2m \int \frac{d^4p\, d^4p'}{(2\pi)^8}\, \mathbf{tr}\, I(p', q_1, p)\gamma^5$$
$$\times \frac{\slashed{p} + m}{p^2 - m^2 + i0}\, \Gamma^\nu(p, -q_2, p') \frac{\slashed{p}' + m}{p'^2 - m^2 + i0} \quad (6.39)$$

and the so-called anomalous contribution

$$\mathfrak{T}_5^\nu(q_1, q_2) = \int \frac{d^4p\, d^4p'}{(2\pi)^8} \Big[\mathbf{tr}\, \Gamma^\nu(p, -q_2, p')I(p', q_1, p)\gamma^5 \frac{\slashed{p} + m}{p^2 - m^2 + i0}$$
$$- \mathbf{tr}\, I(p', q_1, p)\Gamma^\nu(p, -q_2, p')\gamma^5 \frac{\slashed{p}' + m}{p'^2 - m^2 + i0} \Big]. \quad (6.40)$$

Furthermore, we introduced the dressed scalar vertex $I(p', q, p)$ [see Eq. (1.74)].

Based on Eq. (6.37), one expects that the anomalous contribution to the Ward-Takahashi identity vanishes. If the relations given in Eq. (1.77) are formally applied to Eq. (6.40) as in Sec. 3.1, it looks like this is really the case. However, a closer analysis reveals that the intermediate expressions are divergent and the required formal manipulations cannot be justified. In fact, as shown in Sec. 6.3, the anomalous contribution does not vanish and is given by

$$\mathfrak{T}_5^\nu(q_1, q_2) = -i\pi e^2 \delta^{(-,\perp)}(q_1 - q_2)\, 4e \int\limits_{-\infty}^{+\infty} dx^-\, e^{i(q_2^+ - q_1^+)x^-}\, q_\mu F^{*\mu\nu}(kx). \quad (6.41)$$

The phenomenon that quantum fluctuations can spoil the results expected from the classical symmetries of the Lagrangian has first been observed in Refs. [Adl69; BJ69] and, as we have mentioned, is known as ABJ anomaly (see also Refs. [AB69; Bar69; JJ69], Ref. [Fuj79] for a discussion using the Feynman path integral and, e.g., Refs. [DG00; PS95; Wei96] for a textbook discussion).

The calculation of $T_5^\nu(q_1, q_2)$ [see Eq. (6.39)] is much less involved. Due to the identity [see Eq. (1.74)]

$$I(p', q, p)\gamma^5 = -ie \int d^4x \Big(\gamma^5 - \frac{1}{2}G_3\mathfrak{F}_x^{*\rho\sigma}i\sigma_{\rho\sigma}\Big)e^{iS_\Gamma(p', q, p; x)} \quad (6.42)$$

we only have to change the trace $\frac{1}{4}\mathbf{tr}\,[\cdots]_5^\nu$ in Eq. (6.19) to

$$\frac{1}{4}\mathbf{tr}\, 2m\big(\gamma^5 - \frac{1}{2}G_3\mathfrak{F}_x^{*\rho\sigma}i\sigma_{\rho\sigma}\big)(\slashed{p} + m)(\gamma_\beta c^{\beta\nu} + i\gamma_\beta\gamma^5 d^{\beta\nu})(\slashed{p}' + m)$$
$$= 2im^2\big[(p - p')_\beta d^{\beta\nu} + G_3(p - p')^\alpha \mathfrak{F}_{x\alpha\beta}^* c^{\beta\nu} - G_3(p + p')^\alpha \mathfrak{F}_{x\alpha\beta} d^{\beta\nu}\big]. \quad (6.43)$$

Since the action of the derivatives on kj and kj' gives no contribution, we obtain the replacement rules [see Eq. (6.24)]

$$p^\mu \longrightarrow (-i)\partial_j^\mu \longrightarrow -\frac{1}{s+t}\Big(tq_2^\mu + \frac{1}{2}\lambda^\mu\Big),$$
$$p'^\mu \longrightarrow (-i)\partial_{j'}^\mu \longrightarrow \frac{1}{s+t}\Big(sq_2^\mu - \frac{1}{2}\lambda^\mu\Big), \quad (6.44)$$

implying

$$(p - p')^\mu \longrightarrow -q_2^\mu, \quad (p + p')^\mu \longrightarrow vq_2^\mu - \frac{1}{\tau}\lambda^\mu. \tag{6.45}$$

After applying them and noting that terms linear in v do not contribute [see Eq. (6.22)], we can replace the trace in Eq. (6.43) by

$$\frac{1}{4}\,\mathbf{tr}\left[\cdots\right]_5^\nu \longrightarrow 2im^2G_3\big[(\mathfrak{F}_x^*q)^\nu - (\mathfrak{F}_y^*q)^\nu\big] \tag{6.46}$$

for the calculation of $T_5^\nu(q_1, q_2)$ [see Eq. (6.39)].

6.2.2. Tensor structure

Due to the inhomogeneous Ward-Takahashi identity [see Eq. (6.38)], the tensor structure of $T_5^{\mu\nu}(q_1, q_2)$ is more complicated than that of the polarization tensor $T^{\mu\nu}(q_1, q_2)$. Using the complete sets $q_1^\mu, \mathcal{Q}_1^\mu, \Lambda_1^{*\mu}, \Lambda_2^{*\mu}$ and $q_2^\nu, \mathcal{Q}_2^\nu, \Lambda_1^{*\nu}, \Lambda_2^{*\nu}$ (see App. C for more details) we obtain the following expansion

$$\begin{aligned}
T_5^{\mu\nu} = \mathfrak{T}_5^{\mu\nu} &+ d_1\Lambda_1^{*\mu}\Lambda_2^{*\nu} + d_2\Lambda_2^{*\mu}\Lambda_1^{*\nu} + d_3\Lambda_1^{*\mu}\Lambda_1^{*\nu} + d_4\Lambda_2^{*\mu}\Lambda_2^{*\nu} \\
&+ d_5\mathcal{Q}_1^\mu\mathcal{Q}_2^\nu + d_6\mathcal{Q}_1^\mu\Lambda_1^{*\nu} + d_7\mathcal{Q}_1^\mu\Lambda_2^{*\nu} + d_8\Lambda_1^{*\mu}\mathcal{Q}_2^\nu \\
&+ d_9\Lambda_2^{*\mu}\mathcal{Q}_2^\nu + d_{10}q_1^\mu\Lambda_1^{*\nu} + d_{11}q_1^\mu\Lambda_2^{*\nu} + d_{12}q_1^\mu\mathcal{Q}_2^\nu,
\end{aligned} \tag{6.47}$$

where $\mathfrak{T}_5^{\mu\nu}(q_1, q_2)$ contains the contribution from the anomaly, i.e. [see Eq. (6.41)]

$$\begin{aligned}
\mathfrak{T}_5^{\mu\nu}(q_1, q_2) = -i\pi e^2\delta^{(-,\perp)}(q_1 - q_2)\,4e\int\limits_{-\infty}^{+\infty}dx^- \\
\times\, e^{i(q_2^+ - q_1^+)x^-}\frac{1}{kq}\big[k^\mu(qF^*)^\nu(kx) + (qF^*)^\mu(kx)k^\nu\big].
\end{aligned} \tag{6.48}$$

As expected from Furry's theorem [Nis51], the coefficients $d_1 - d_5$ and d_{12} (which contain an even power of the external field tensors $f_i^{\mu\nu}$) vanish and only $d_6 - d_{11}$ are different from zero.

6.2.3. Determination of the coefficients

Having determined the contraction of $T_5^{\mu\nu}(q_1, q_2)$ with q_1^μ and q_2^μ explicitly, we can restrict us to the contraction from the set $k^\mu, \Lambda_1^{*\mu}$ and $\Lambda_2^{*\mu}$ (or alternatively k^μ, Λ_1^μ and Λ_2^μ, see App. C) if we analyze the general trace given in Eq. (6.19). This means that, in order to complete the calculation of $T_5^{\mu\nu}(q_1, q_2)$, we can ignore the action of the derivatives on kj and kj' and also terms in the trace which are, e.g., proportional to $\mathfrak{F}^{\mu\nu}, \mathfrak{F}^{*\mu\nu}, \mathfrak{F}^{2\mu\nu}, (\mathfrak{F}\mathfrak{F}^*)^{\mu\nu}, (\mathfrak{F}^*\mathfrak{F})^{\mu\nu}, \mathfrak{F}^{2\mu\rho}v_\rho, v_\rho\mathfrak{F}^{2\rho\nu}$, where v^μ is an arbitrary four-vector. In particular, we see that the terms $a^{\alpha\mu}d_\alpha{}^\nu$ and $b^{\alpha\mu}c_\alpha{}^\nu$ can be ignored and therefore also the action of the derivatives on the term in the exponent which is quadratic in the sources. If the derivatives act on the non-quadratic source-terms in the exponent, we obtain the replacement

rules

$$p^\alpha p'^\beta + p^\beta p'^\alpha \quad \longrightarrow \quad -\frac{2\mu}{\tau} q_2^\alpha q_2^\beta + \frac{1}{2\tau^2}\lambda^\alpha \lambda^\beta - \frac{v}{2\tau}(q_2^\alpha \lambda^\beta + \lambda^\alpha q_2^\beta),$$

$$p^\alpha p'^\beta - p^\beta p'^\alpha \quad \longrightarrow \quad \frac{1}{2\tau}(q_2^\alpha \lambda^\beta - q_2^\beta \lambda^\alpha). \tag{6.49}$$

Finally, we can replace the trace given in Eq. (6.19) by (terms linear in v do not contrubute after the integration)

$$\frac{1}{4}\,\mathbf{tr}\left[\cdots\right]_5^{\mu\nu} \longrightarrow i\left\{\frac{e}{kq}\left[q_2^\mu(\mathfrak{F}_y^* q)^\nu - (\mathfrak{F}_x^* q)^\mu q_2^\nu\right] + \frac{1}{2\tau}\epsilon^{\mu\nu\rho\sigma} q_{2\rho}\lambda_\sigma\right\} \tag{6.50}$$

[as long as only contractions with k^μ and $\Lambda_i^\mu/\Lambda_i^{*\mu}$ are considered, which also means that the anomaly does not contribute, see Eq. (6.41)].

6.2.4. Final result

Using the relations given in App. C we obtain the following representation for the tensor $T_5^{\mu\nu}(q_1, q_2)$

$$T_5^{\mu\nu}(q_1, q_2) = \mathfrak{T}_5^{\mu\nu}(q_1, q_2) - i\pi e^2\, \delta^{(-,\perp)}(q_1 - q_2) \int\limits_{-1}^{+1} dv \int\limits_{0}^{\infty} \frac{d\tau}{\tau} \int\limits_{-\infty}^{+\infty} dz^- \left[a_6 \mathcal{Q}_1^\mu \Lambda_1^{*\nu}\right.$$

$$\left. + a_7 \mathcal{Q}_1^\mu \Lambda_2^{*\nu} + a_8 \Lambda_1^{*\mu} \mathcal{Q}_2^\nu + a_9 \Lambda_2^{*\mu} \mathcal{Q}_2^\nu + a_{10} q_1^\mu \Lambda_1^{*\nu} + a_{11} q_1^\mu \Lambda_2^{*\nu}\right]e^{i\Phi}, \tag{6.51}$$

where the anomalous contribution $\mathfrak{T}_5^{\mu\nu}(q_1, q_2)$ is given in Eq. (6.48) and the coefficients read

$$a_6 = im\xi_1\left[W_1 + U_1\frac{m^2}{q_1^2}\frac{\tau}{\mu}\right]e^{i\tau\beta},$$

$$a_7 = im\xi_2\left[W_2 + U_2\frac{m^2}{q_1^2}\frac{\tau}{\mu}\right]e^{i\tau\beta},$$

$$a_8 = -im\xi_1 V_1 e^{i\tau\beta}, \quad a_{10} = im\xi_1 U_1\frac{m^2}{q_1^2}\frac{\tau}{\mu}e^{i\tau\beta}, \tag{6.52}$$

$$a_9 = -im\xi_2 V_2 e^{i\tau\beta}, \quad a_{11} = im\xi_2 U_2\frac{m^2}{q_1^2}\frac{\tau}{\mu}e^{i\tau\beta}.$$

Here, the phases are given by [see Eq. (3.57)]

$$e^{i\Phi} = \exp\left\{i\left[(q_2^+ - q_1^+)z^- + \mu q_1 q_2 - \tau m^2\right]\right\}, \tag{6.53}$$

$$e^{i\tau\beta} = \exp\left[i\tau m^2 \sum_{i=1,2}\xi_i^2(I_i^2 - J_i)\right], \tag{6.54}$$

where [see Eq. (6.26)]

$$I_i = \frac{1}{2}\int\limits_{-1}^{+1} d\lambda\,\psi_i(kz - \lambda\mu kq), \quad J_i = \frac{1}{2}\int\limits_{-1}^{+1} d\lambda\,\psi_i^2(kz - \lambda\mu kq). \tag{6.55}$$

151

In the preexponent we have introduced the following symbols

$$U_i = \psi_i(kx) - \psi_i(ky), \quad V_i = \psi_i(kx) - I_i, \quad W_i = \psi_i(ky) - I_i, \tag{6.56}$$

where $kx = kz - \mu kq$, $ky = kz + \mu kq$ and $\mu = \frac{1}{4}\tau(1-v^2)$.

Alternatively, the result in Eq. (6.51) can be written as

$$T_5^{\mu\nu}(q_1, q_2) = \mathfrak{T}_5^{\mu\nu}(q_1, q_2) - i\pi e^2 \, \delta^{(-,\perp)}(q_1 - q_2) \int\limits_{-1}^{+1} dv \int\limits_{0}^{\infty} \frac{d\tau}{\tau} \int\limits_{-\infty}^{+\infty} dz^- \left[a_6' \mathcal{Q}_1^\mu \Lambda_1^{*\nu} \right.$$
$$\left. + a_7' \mathcal{Q}_1^\mu \Lambda_2^{*\nu} + a_8 \Lambda_1^{*\mu} \mathcal{Q}_2^\nu + a_9 \Lambda_2^{*\mu} \mathcal{Q}_2^\nu + a_{10}' k^\mu \Lambda_1^{*\nu} + a_{11}' k^\mu \Lambda_2^{*\nu} \right] e^{i\Phi}, \tag{6.57}$$

where

$$a_6' = im\xi_1 W_1 e^{i\tau\beta}, \quad a_8 = -im\xi_1 V_1 e^{i\tau\beta}, \quad a_{10}' = im\xi_1 U_1 \frac{m^2}{kq}\frac{\tau}{\mu} e^{i\tau\beta},$$
$$a_7' = im\xi_2 W_2 e^{i\tau\beta}, \quad a_9 = -im\xi_2 V_2 e^{i\tau\beta}, \quad a_{11}' = im\xi_2 U_2 \frac{m^2}{kq}\frac{\tau}{\mu} e^{i\tau\beta}. \tag{6.58}$$

The last two terms (a_{10}' and a_{11}') are responsible for the inhomogeneous contribution to the Ward-Takahashi identity [see Eq. (6.38) and Eq. (6.39)].

6.3. Adler-Bell-Jackiw anomaly

We will show now explicitly that the anomalous contribution to the Ward-Takahashi identity $\mathfrak{T}_5^\nu(q_1, q_2)$ [see Eq. (6.40)] of the current-coupling tensor $T_5^{\mu\nu}(q_1, q_2)$ [see Eq. (6.38)] is different from zero.

As pointed out in Sec. 6.2.1, the formal application of the relations given in Eq. (1.77) to Eq. (6.40) would prove that $\mathfrak{T}_5^\nu(q_1, q_2) = 0$. However, this procedure leads to divergent expressions and a more careful analysis reveals that the obtained result would be incorrect. To determine the anomalous contribution we rewrite Eq. (6.40) as

$$\mathfrak{T}_5^\nu(q_1, q_2) = \lim_{\epsilon \to 0} 4(-ie)^2 \int \frac{d^4p \, d^4p'}{(2\pi)^8} \int d^4x d^4y \, (-i) \int\limits_0^\infty ds$$
$$\times \Big[\underbrace{\frac{1}{4}\,\mathbf{tr}[\cdots]_{5A}^\nu e^{i\tilde{S}_T}}_{t=\epsilon} - \underbrace{\frac{1}{4}\,\mathbf{tr}[\cdots]_{5B}^\nu e^{i\tilde{S}_T}}_{s=\epsilon, t=s} \Big], \tag{6.59}$$

where the phase $\tilde{S}_T$ is defined in Eq. (6.28) and the traces are given by

$$\frac{1}{4}\,\mathbf{tr}[\cdots]_{5A}^\nu = iG_3 \big[(p_\mu \mathfrak{F}_x^{*\mu\nu} - p_\mu \mathfrak{F}_y^{*\mu\nu}) + G_1 \, p^\rho \mathfrak{F}_{x\rho\mu}^* \mathfrak{F}_y^{\mu\nu} + G_3 \, p^\rho \mathfrak{F}_{x\rho\mu} \mathfrak{F}_y^{*\mu\nu} \big], \tag{6.60a}$$

and

$$\frac{1}{4}\,\mathbf{tr}[\cdots]_{5B}^\nu = iG_3 \big[(p_\mu' \mathfrak{F}_x^{*\mu\nu} - p_\mu' \mathfrak{F}_y^{*\mu\nu}) + G_1 \, p'^\rho \mathfrak{F}_{x\rho\mu}^* \mathfrak{F}_y^{\mu\nu} - G_3 \, p'^\rho \mathfrak{F}_{x\rho\mu} \mathfrak{F}_y^{*\mu\nu} \big], \tag{6.60b}$$

with $G_i = G_i(kp', kp)$.

Although we need to exponentiate here only one scalar propagator [see Eq. (6.40)], we artificially add a second term in the exponent (multiplied by a quantity ϵ which will be later sent to zero), in order to recover exactly the same structure as in Eq. (6.28). Also note that the traces in Eq. (6.60a) and Eq. (6.60b) can be formally obtained from Eq. (6.43) by setting $p'^\mu = 0$ and $p^\mu = 0$, respectively, and by dividing by $2m^2$ and $-2m^2$, respectively. To match the first and the second contribution in Eq. (6.59), we changed the name of the integration variable $t \to s$ (after the replacement $s \to \epsilon$) in the second expression.

In order to determine the first and the second contribution to Eq. (6.59), respectively, we need to apply the following replacements to Eq. (6.27)

$$
\begin{aligned}
(-i) \int_0^\infty dt \to \mathbf{1}, \quad t \to \epsilon, \quad \mathbf{tr}[\cdots]_5^{\mu\nu} \to \mathbf{tr}[\cdots]_{5A}^\nu, \\
(-i) \int_0^\infty ds \to \mathbf{1}, \quad \begin{matrix} s \to \epsilon, \\ t \to s, \end{matrix} \quad \mathbf{tr}[\cdots]_5^{\mu\nu} \to \mathbf{tr}[\cdots]_{5B}^\nu.
\end{aligned}
\tag{6.61}
$$

In this way, the final result can then be obtained from Eq. (6.29).

The replacements given in Eq. (6.61) imply that $\tau = s+t$ and $\mu = st/(s+t)$ are mapped to the same quantity in both expressions, but $v = (s-t)/(s+t)$ changes its sign

$$
\begin{aligned}
\tau(t \to \epsilon) &= \tau(s \to \epsilon, t \to s) = s + \epsilon, \\
\mu(t \to \epsilon) &= \mu(s \to \epsilon, t \to s) = \frac{s\epsilon}{s + \epsilon}, \\
v(t \to \epsilon) &= -v(s \to \epsilon, t \to s) = \frac{s - \epsilon}{s + \epsilon}.
\end{aligned}
\tag{6.62}
$$

We note that due to the relation $ky = kx + 2\mu kq$ [see Eq. (3.22)] the distance (here in phase) between the two vertices tends to zero as $\epsilon \to 0$. A similar regularization procedure for the axial-vector vertex is also commonly used in the calculation of the vacuum amplitude (see, e.g., Chap. 19 of [PS95] for a textbook discussion).

To use Eq. (6.29), we have to apply the replacement rules given in Eq. (6.44). Firstly, we note that λ^μ does not contribute, as it would only give a non-vanishing contribution after contraction with the first line of each trace in Eq. (6.60), which then cancel pairwise. Correspondingly, we can focus on the contribution due to q_2^μ. As the second and the third line of each trace cancel both pairwise, we focus on the first line. Using the following representation for the delta function

$$
\lim_{\epsilon \to 0} \int_0^\infty dx \, \frac{\epsilon \, g(x)}{(x + \epsilon)^2} = \lim_{\epsilon \to 0} \int_0^\infty dy \, \frac{g(\epsilon y)}{(y + 1)^2} = g(0)
\tag{6.63}
$$

[$g(x)$ is assumed to be sufficiently regular], we finally obtain the result given in Eq. (6.41).

Concluding, we note that the adaptation of the presented calculation to the

polarization operator proves that the results obtained in Sec. 3.1 using formal manipulations are correct.

6.4. Special field configurations

In this section the general expression given in Eqs. (6.51) and (6.57) is used to derive compact representations for the current-coupling tensor $T_5^{\mu\nu}(q_1, q_2)$ for three important special field configurations: a constant-crossed field, a relativistically strong, linearly polarized plane-wave background field (quasistatic limit) and a monochromatic, circularly polarized plane-wave background field. When possible, the result is compared with existing representations from the literature.

6.4.1. Constant-crossed field

From Eq. (6.51) we can derive the result for a constant-crossed field, which is characterized by [see Eq. (3.75)]

$$\psi_1(\phi) = \phi, \quad \psi_2 = 0, \tag{6.64}$$

(the latter condition corresponds to $\xi_2 = 0$ and we will write $\xi = \xi_1$ in the following). For a constant-crossed field the field tensor is given by

$$F^{\mu\nu} = f_1^{\mu\nu} = f^{\mu\nu}. \tag{6.65}$$

As $\psi_2 = 0$, the following functions vanish

$$I_2 = J_2 = U_2 = V_2 = W_2 = 0 \tag{6.66}$$

and due to the simple form of ψ_1

$$I_1 = kx + \mu kq, \quad J_1 = (kx + \mu kq)^2 + \frac{1}{3}(\mu kq)^2,$$
$$U_1 = -2\mu kq, \quad V_1 = -\mu kq, \quad W_1 = \mu kq. \tag{6.67}$$

Finally, we obtain the following explicit expression for the tensor $T_5^{\mu\nu}(q_1, q_2)$ in a constant-crossed field

$$T_5^{\mu\nu}(q_1, q_2) = \mathfrak{T}_5^{\mu\nu}(q_1, q_2) - 2i\pi^2 e^2 \, \delta^4(q_1 - q_2) \int\limits_{-1}^{+1} dv \int\limits_{0}^{\infty} \frac{d\tau}{\tau}$$
$$\times \, [\tilde{b}_6^c \mathcal{Q}^\mu \Lambda_1^{*\nu} + \tilde{b}_8^c \Lambda_1^{*\mu} \mathcal{Q}^\nu + \tilde{b}_{10}^c q^\mu \Lambda_1^{*\nu}] e^{i\Phi_c}, \tag{6.68}$$

where the coefficients are given by

$$\tilde{b}_6^c = i\xi mkq \left[\frac{1}{w} - \frac{2m^2}{q^2} \right] \tau e^{i\tau\beta_c}, \quad \tilde{b}_8^c = i\xi mkq \, \frac{1}{w} \tau e^{i\tau\beta_c},$$
$$\tilde{b}_{10}^c = i\xi mkq \left(-\frac{2m^2}{q^2} \right) \tau e^{i\tau\beta_c}, \tag{6.69}$$

the phases read

$$i\Phi_{\rm c} = -i\tau a, \qquad a = m^2\left[1 - \frac{1}{4}(1 - v^2)\frac{q^2}{m^2}\right],$$
$$i\tau\beta_{\rm c} = -\frac{i}{3}\tau^3 b, \quad b = m^6\chi^2\left[\frac{1}{4}(1 - v^2)\right]^2 \tag{6.70}$$

and the anomaly $\mathfrak{T}_5^{\mu\nu}(q_1, q_2)$ [see Eq. (6.48)] becomes

$$\mathfrak{T}_5^{\mu\nu}(q_1, q_2) = i(2\pi)^4\delta^4(q_1 - q_2)\left(-\frac{e^3}{8\pi^2 m^2}\right)4\frac{m^2}{kq}\left[k^\mu(qF^*)^\nu + (qF^*)^\mu k^\nu\right]. \tag{6.71}$$

Above, we introduced the quantum-nonlinearity parameter [see Eq. (1.21)]

$$\chi = -\frac{e\sqrt{qF^2q}}{m^3} = \xi\frac{\sqrt{(kq)^2}}{m^2}. \tag{6.72}$$

Due to the overall momentum-conserving delta function we define

$$q^\mu = q_1^\mu = q_2^\mu, \quad \mathcal{Q}^\mu = \mathcal{Q}_1^\mu = \mathcal{Q}_2^\mu = \frac{k^\mu q^2 - q^\mu kq}{kq}. \tag{6.73}$$

Using the relation

$$\tilde{b}_6^{\rm c}\mathcal{Q}^\mu\Lambda_1^{*\nu} + \tilde{b}_{10}^{\rm c}q^\mu\Lambda_1^{*\nu} = \frac{e}{\xi mkq}(\tilde{b}_6^{\rm c} - \tilde{b}_{10}^{\rm c})\,q^\mu(F^*q)^\nu - \frac{e}{\xi mkq}\frac{q^2}{kq}\tilde{b}_6^{\rm c}\,k^\mu(F^*q)^\nu \tag{6.74}$$

we can rewrite Eq. (6.68) as

$$T_5^{\mu\nu}(q_1, q_2) = \mathfrak{T}_5^{\mu\nu}(q_1, q_2) + i(2\pi)^4\delta^4(q_1 - q_2)$$
$$\times\left[\tilde{\tau}_1\mathcal{Q}^\mu(F^*q)^\nu + \tilde{\tau}_2 k^\mu(F^*q)^\nu + \tilde{\tau}_1(F^*q)^\mu\mathcal{Q}^\nu\right], \tag{6.75}$$

where

$$\tilde{\tau}_1 = \frac{e^3}{8\pi^2 m^2}\int\limits_{-1}^{+1}dv\,\frac{1}{w}\left(\frac{w}{\chi}\right)^{2/3}f(\rho), \quad \tilde{\tau}_2 = -\frac{e^3}{8\pi^2 m^2}\int\limits_{-1}^{+1}dv\,2\frac{m^2}{kq}\left(\frac{w}{\chi}\right)^{2/3}f(\rho) \tag{6.76}$$

$[\frac{1}{w} = \frac{1}{4}(1 - v^2), \rho = \left(\frac{w}{\chi}\right)^{2/3}(1 - \frac{q^2}{m^2}\frac{1}{w})]$ and the anomaly is given in Eq. (6.71). Furthermore, the Ritus functions are defined by (see App. F)

$$f(x) = i\int\limits_0^\infty dt\,\exp\left[-i(tx + t^3/3)\right] = \pi\,\mathrm{Gi}(x) + i\pi\,\mathrm{Ai}(x), \tag{6.77a}$$

$$f_1(x) = \int\limits_0^\infty \frac{dt}{t}\exp\left(-itx\right)\left[\exp\left(-it^3/3\right) - 1\right], \tag{6.77b}$$

where Ai and Gi are the Airy and Scorer function, respectively [Olv+10].

Since all nonvanishing functions are even in v, it is possible to apply the following

change of variables

$$\int\limits_{-1}^{+1} dv = 2 \int\limits_{0}^{1} dv = \int\limits_{4}^{\infty} dw \, \frac{4}{w\sqrt{w(w-4)}}. \tag{6.78}$$

The final result given in Eq. (6.75) coincides with the one given in Eq. (4.24) of [Sch00b], apart from the anomalous contribution in the vector index [see Eq. (6.38)], which automatically drops out by performing the calculations within the wordline formalism as in [Sch00b]. If evaluated on the mass shell (i.e. for $q^2 = 0$), it also agrees with Eq. (15) in [Sha00].

6.4.2. Linear polarization

We consider now a linearly polarized plane-wave field [see Eq. (3.98)]

$$\psi_1(\phi) = \psi(\phi), \quad \psi_2 = 0 \tag{6.79}$$

($\xi = \xi_1$, $f^{\mu\nu} = f_1^{\mu\nu}$) in the quasistatic limit defined by $\xi \to \infty$ while the quantum-nonlinearity parameter [see Eq. (6.72)]

$$\chi = -\frac{e\sqrt{qf^2q}}{m^3} = \xi \frac{\sqrt{(kq)^2}}{m^2} \tag{6.80}$$

is kept constant. In the optical regime (laser photon energy $\omega \sim 1\,\text{eV}$) the condition $\chi \gtrsim 1$ usually requires $\xi \gg 1$, which means that the quasistatic limit is in general sufficient to analyze strong-field experiments with optical lasers (it neglects the recollision contribution considered in Chap. 4, though).

For a linearly polarized background field we obtain

$$I_2 = J_2 = U_2 = V_2 = W_2 = 0 \tag{6.81}$$

and using the relation $|kq| = m^2\chi/\xi$ it is sufficient to consider the leading-order contribution to the following quantities

$$\begin{aligned}
I_1^2 - J_1 &= -(1/3)(\mu kq)^2 \left[\psi'(kz)\right]^2 + \mathcal{O}(\mu kq)^3, \\
U_1 &= -2\mu kq \psi'(kz) + \mathcal{O}(\mu kq)^2, \\
V_1 &= -\mu kq \psi'(kz) + \mathcal{O}(\mu kq)^2, \\
W_1 &= +\mu kq \psi'(kz) + \mathcal{O}(\mu kq)^2.
\end{aligned} \tag{6.82}$$

If we insert these relations into Eq. (6.57), the remaining calculation is very similar to the one for a constant-crossed field (see Sec. 6.4.1), the essential change is the replacement $\chi \to \chi(kz) = \chi |\psi'(kz)|$. The final result is given by

$$\begin{aligned}
T_5^{\mu\nu}(q_1, q_2) = \mathfrak{T}_5^{\mu\nu}(q_1, q_2) + i(2\pi)^4 \delta^{(-,\perp)}(q_1 - q_2) \frac{1}{2\pi} \int\limits_{-\infty}^{+\infty} dz^- e^{i(q_2^+ - q_1^+)z^-} \\
\times \psi'(kz) \left[\tau_1' \mathcal{Q}_1^\mu (f^*q)^\nu + \tau_1' (f^*q)^\mu \mathcal{Q}_2^\nu + \tau_2' k^\mu (f^*q)^\nu\right]
\end{aligned} \tag{6.83}$$

where

$$\tau_1' = +\frac{e^3}{8\pi^2 m^2} \int\limits_{-1}^{+1} dv \, \frac{1}{w} \left[\frac{w}{|\chi(kz)|}\right]^{2/3} f(\rho),$$

$$\tau_2' = -\frac{e^3}{8\pi^2 m^2} \int\limits_{-1}^{+1} dv \, \frac{2m^2}{kq} \left[\frac{w}{|\chi(kz)|}\right]^{2/3} f(\rho) \tag{6.84}$$

and $\frac{1}{w} = \frac{1}{4}(1 - v^2)$, $\rho = \left[\frac{w}{|\chi(kz)|}\right]^{2/3}(1 - \frac{q_1 q_2}{m^2}\frac{1}{w})$. Furthermore, the anomaly reads [see Eq. (6.48)]

$$\mathfrak{T}_5^{\mu\nu}(q_1, q_2) = i(2\pi)^4 \delta^{(-,\perp)}(q_1 - q_2) \frac{1}{2\pi} \int\limits_{-\infty}^{+\infty} dz^- \, e^{i(q_2^+ - q_1^+)z^-} \, \psi'(kz)$$

$$\times \left(-\frac{e^3}{8\pi^2 m^2}\right) 4\frac{m^2}{kq} \left[k^\mu (qf^*)^\nu + (qf^*)^\mu k^\nu\right]. \tag{6.85}$$

Note that for $\psi'(\phi) = 1$ the result given in Eq. (6.83) coincides (as required) with the one for a constant-crossed field [see Eq. (6.75)].

6.4.3. Circular polarization

Also for a circularly polarized, monochromatic background field

$$\psi_1(\phi) = \Re e^{i\phi}, \quad \psi_2(\phi) = \Im e^{i\phi}, \quad \xi_1 = \xi_2 = \xi \tag{6.86}$$

the result given in Eq. (6.57) simplifies considerably and we obtain

$$T_5^{\mu\nu}(q_1, q_2) = \mathfrak{T}_5^{\mu\nu}(q_1, q_2) - i\pi e^2 \, \delta^{(-,\perp)}(q_1 - q_2) \int\limits_{-1}^{+1} dv \int\limits_0^\infty \frac{d\tau}{\tau} \int\limits_{-\infty}^{+\infty} dz^- \, [a_1^+ \mathcal{Q}_1^\mu \widetilde{\Lambda}_+^\nu$$

$$+ a_1^- \mathcal{Q}_1^\mu \widetilde{\Lambda}_-^\nu + a_2^+ \widetilde{\Lambda}_+^\mu \mathcal{Q}_2^\nu + a_2^- \widetilde{\Lambda}_-^\mu \mathcal{Q}_2^\nu + a_3^+ k^\mu \widetilde{\Lambda}_+^\nu + a_3^- k^\mu \widetilde{\Lambda}_-^\nu] e^{i\Phi}, \tag{6.87}$$

where the anomaly is given in Eq. (6.48) and

$$a_1^+ = \frac{1}{2}(a_6' - ia_7') = \frac{1}{2}im\xi(W_1 - iW_2)e^{i\tau\beta},$$

$$a_1^- = \frac{1}{2}(a_6' + ia_7') = \frac{1}{2}im\xi(W_1 + iW_2)e^{i\tau\beta},$$

$$a_2^+ = \frac{1}{2}(a_8 - ia_9) = -\frac{1}{2}im\xi(V_1 - iV_2)e^{i\tau\beta},$$

$$a_2^- = \frac{1}{2}(a_8 + ia_9) = -\frac{1}{2}im\xi(V_1 + iV_2)e^{i\tau\beta}, \tag{6.88}$$

$$a_3^+ = \frac{1}{2}(a_{10}' - ia_{11}') = \frac{1}{2}im\xi\frac{\tau m^2}{\mu kq}(U_1 - iU_2)e^{i\tau\beta},$$

$$a_3^- = \frac{1}{2}(a_{10}' + ia_{11}') = \frac{1}{2}im\xi\frac{\tau m^2}{\mu kq}(U_1 + iU_2)e^{i\tau\beta},$$

$$i\tau\beta = i\tau m^2 \xi^2 \left[\text{sinc}^2(\mu kq) - 1\right],$$
$$i\Phi = i\left[(q_2^+ - q_1^+)z^- + \mu q_1 q_2 - \tau m^2\right] \tag{6.89}$$

and

$$\widetilde{\Lambda}_\pm^\mu = \Lambda_1^{*\mu} \pm i\Lambda_2^{*\mu} \tag{6.90}$$

(the star is part of the symbol, both $\Lambda_1^{*\mu}$ and $\Lambda_2^{*\mu}$ are real four-vectors). Furthermore,

$$W_1 + iW_2 = -A, \quad W_1 - iW_2 = -A^*,$$
$$V_1 + iV_2 = -B, \quad V_1 - iV_2 = -B^*, \tag{6.91}$$
$$U_1 + iU_2 = -C, \quad U_1 - iU_2 = -C^*$$

where

$$A = e^{ikz}\left[\text{sinc}(\mu kq) - \cos(\mu kq) - i\sin(\mu kq)\right],$$
$$B = e^{ikz}\left[\text{sinc}(\mu kq) - \cos(\mu kq) + i\sin(\mu kq)\right], \tag{6.92}$$
$$C = e^{ikz}\, 2i\sin(\mu kq)$$

and therefore

$$-W_1 = I_1 - \psi_1(kz + \mu kq) = \Re A,$$
$$-W_2 = I_2 - \psi_2(kz + \mu kq) = \Im A,$$
$$-V_1 = I_1 - \psi_1(kz - \mu kq) = \Re B,$$
$$-V_2 = I_2 - \psi_2(kz - \mu kq) = \Im B,$$
$$-U_1 = \psi_1(kz + \mu kq) - \psi_1(kz - \mu kq) = \Re C,$$
$$-U_2 = \psi_2(kz + \mu kq) - \psi_2(kz - \mu kq) = \Im C. \tag{6.93}$$

We can now take the integral in dz^- and obtain

$$T_5^{\mu\nu}(q_1, q_2) = \mathfrak{T}_5^{\mu\nu}(q_1, q_2) - i(2\pi)^4 \frac{e^2}{8\pi^2} \int\limits_{-1}^{+1} dv \int\limits_0^\infty \frac{d\tau}{\tau}$$
$$\times \left[T_{5+}^{\mu\nu}\,\delta(q_1 - q_2 + k) + T_{5-}^{\mu\nu}\,\delta(q_1 - q_2 - k)\right]e^{i\Phi_{\text{cp}}}, \tag{6.94}$$

where

$$i\Phi_{\text{cp}} = -i\tau m^2\{1 + \xi^2[1 - \text{sinc}^2(\mu kq)]\} + i\mu q_1 q_2, \tag{6.95}$$

$$T_{5\pm}^{\mu\nu} = (\lambda_1^\pm \mathcal{Q}_1^\mu + \lambda_3^\pm k^\mu)\widetilde{\Lambda}_\pm^\nu + \lambda_2^\pm \widetilde{\Lambda}_\pm^\mu \mathcal{Q}_2^\nu \tag{6.96}$$

and

$$\lambda_1^\pm = -\frac{1}{2}im\xi \left[\mathrm{sinc}(\mu kq) - \cos(\mu kq) \pm i\sin(\mu kq)\right],$$
$$\lambda_2^\pm = +\frac{1}{2}im\xi \left[\mathrm{sinc}(\mu kq) - \cos(\mu kq) \mp i\sin(\mu kq)\right], \qquad (6.97)$$
$$\lambda_3^\pm = \mp m\xi\,\tau m^2\,\mathrm{sinc}(\mu kq).$$

Correspondingly, the result is in agreement with the one obtained in [GMV93; GMV94a; GMV96].

Conclusion and outlook

In the present thesis several nonlinear processes have been examined, whose feasibility necessitates ultra-strong electromagnetic background fields. Throughout, we focused on genuine quantum effects not explainable using classical electrodynamics alone. Particularly appealing is the conversion of pure light into matter, hitherto unobserved in a laboratory. By thoroughly studying the nonlinear generalization of the Breit-Wheeler process, we substantiated its suitability for an experimental realization of a light-to-matter transformation with presently existing technology. Moreover, our investigation indicates that for next-generation laser parameters the pair-creation probability is sufficient to observe two other remarkable phenomena. On the one hand, the back reaction of pair creation on the photon wave function leads to an exponential decay, which modifies the measured probabilities. Correspondingly, also the momentum distribution of the created electron-positron pair is expected to change with respect to tree-level predictions in this regime, as the impinging high-energy photon effectively experiences a modified laser pulse shape. For a consistent description, also the radiative energy loss of the created charged particles and possible cascade reactions must be taken into account, which is an exciting challenge for future investigations. On the other hand, a large flux of photoproduced electron-positron pairs renders the detection of high-energy recollision processes feasible. By proving that in the framework of strong-field QED electron-positron recollisions are consistently described by loop Feynman diagrams, we established a new field of research in this thesis. Apparently, an exhaustive survey of all conceivable secondary recollision reactions requires further investigations. Even though a definite confirmation demands these calculations, one can expect that recollision processes impress distinguished signatures on measurable observables like the transverse electron-positron momentum along the direction of the magnetic field or the probability for the coincidental emission of two high-energy gamma photons.

The influence of quantum fluctuations constitutes another topic that is central for this thesis. In particular, we considered the emission and absorption of virtual light quanta by electrons. In close analogy to vacuum birefringence experienced by photons, the electron dispersion relation becomes spin-dependent due to these fluctuations in the radiation field. Our numerical calculations demonstrate the measurability of this effect if few-cycle laser pulses and spin-polarized electron beams are employed. The next step would be the examination of radiative corrections for pair production and nonlinear Compton scattering. This is desirable, as also for strong-field experiments the achievable experimental precision continuously improves. In the calculation of the polarization operator and in the derivation of the exact photon/electron wave function we demonstrated the suitability of

our framework for this venture. Concurrently, a more realistic description of the experimentally employed laser pulses is eligible, in particular the inclusion of focusing effects also in space.

Besides, the present thesis also considered the weak force. Whereas the coupling between electrons, positrons and photons is only slightly affected by quantum fluctuations, they are essential for neutrino-photon interactions. So far, many questions related to the nature and the properties of neutrinos remain open. Therefore, their coupling to the photon field could also afford surprises and should be tested experimentally. As the probabilities for neutrino interactions are generally small, a laboratory investigation requires considerable efforts. Nonetheless, our calculation constitutes the first step towards a realistic description of possible future neutrino-laser experiments. A different application of the derived current-coupling tensor are parity-violating contributions to the fundamental QED processes pair creation and Compton scattering.

Appendix

A. Classical electrodynamics

This appendix summarizes those results from classical electrodynamics which are important for this thesis. For more details see, e.g., [Jac98; LL87].

A.1. Field tensor

The electric E and the magentic field B are jointly described by the anti-symmetric electromagnetic field tensor

$$F^{\mu\nu} = \partial^\mu A^\nu - \partial^\nu A^\mu, \tag{A.1}$$

where $A^\mu = (\phi, \boldsymbol{A})$ denotes the four-potential[1]. The components of the field tensor and its dual $F^{*\mu\nu}$ are given by

$$F^{0i} = -\boldsymbol{E}^i, \quad F^{ij} = -\epsilon^{ijk}\boldsymbol{B}^k, \quad F^{*0i} = -\boldsymbol{B}^i, \quad F^{*ij} = \epsilon^{ijk}\boldsymbol{E}^k. \tag{A.2}$$

In matrix notation we obtain

$$F^{\mu\nu} = \begin{pmatrix} 0 & -\boldsymbol{E}^1 & -\boldsymbol{E}^2 & -\boldsymbol{E}^3 \\ \boldsymbol{E}^1 & 0 & -\boldsymbol{B}^3 & \boldsymbol{B}^2 \\ \boldsymbol{E}^2 & \boldsymbol{B}^3 & 0 & -\boldsymbol{B}^1 \\ \boldsymbol{E}^3 & -\boldsymbol{B}^2 & \boldsymbol{B}^1 & 0 \end{pmatrix}, \quad F^{*\mu\nu} = \begin{pmatrix} 0 & -\boldsymbol{B}^1 & -\boldsymbol{B}^2 & -\boldsymbol{B}^3 \\ \boldsymbol{B}^1 & 0 & \boldsymbol{E}^3 & -\boldsymbol{E}^2 \\ \boldsymbol{B}^2 & -\boldsymbol{E}^3 & 0 & \boldsymbol{E}^1 \\ \boldsymbol{B}^3 & \boldsymbol{E}^2 & -\boldsymbol{E}^1 & 0 \end{pmatrix}. \tag{A.3}$$

A.2. Equations of motion for a charged particle

The four-velocity of a classical particle is defined by

$$u^\mu = \frac{dx^\mu}{ds} = \gamma\frac{dx^\mu}{dt} = \gamma\,(1, \boldsymbol{v})^\mu, \quad \boldsymbol{v} = \frac{d\boldsymbol{x}}{dt}, \quad \gamma = \frac{1}{\sqrt{1 - \boldsymbol{v}^2}}, \tag{A.4}$$

where $s = \tau$ denotes the proper time ($dt = \gamma ds$) and γ is called the relativistic gamma factor. Correspondingly, we also introduce the four-acceleration[2]

$$a^\mu = \frac{d^2 x^\mu}{ds^2} = \frac{du^\mu}{ds}, \quad u^2 = 1, \quad ua = 0 \tag{A.5}$$

(the last relation follows from differentiating $u^2 = 1$). Using the mass m of the particle, we define its four-momentum by

$$p^\mu = (\epsilon_{\boldsymbol{p}}, \boldsymbol{p}) = \gamma m\,(1, \boldsymbol{v}) = mu^\mu. \tag{A.6}$$

Finally, the Lorenz force acting on the particle is given by

$$\frac{dp^\mu}{ds} = \frac{q}{m}F^{\mu\nu}p_\nu, \tag{A.7}$$

---

[1]Note that the zero component of the four-potential is denoted here by the same symbol which is normally used for the laser phase. The field tensor is also called field-strength tensor.

[2]Note that the four-acceleration is denoted here by the same symbol which is normally used for the constant plane-wave four-potential.

where q denotes the charge of the particle and $F^{\mu\nu}$ the field tensor of the background field [see Eq. (A.1)].

A.3. Classical dynamics in a plane-wave field

For a plane-wave background field [$F^{\mu\nu} = F^{\mu\nu}(\phi)$, $\phi = kx$; see Sec. 1.3] the classical equations of motion for a particle with charge q and mass m [see Eq. (A.7)] can be solved analytically [Di+12; Mey71; SS70]. To this end we note that $k_\mu F^{\mu\nu} = 0$ implies $d(kp)/d\tau = 0$ for a plane-wave field. Correspondingly, $kp = kp_0$ is conserved [$p_0^\mu = p^\mu(\phi_0)$ denotes the initial four-momentum of the particle].

As we assume that the field tensor depends only on the laser phase $\phi = kx$, it is useful to parametrize the trajectory of the charge by the laser phase rather than the proper time. To this end we note that [see Eq. (A.6)]

$$\frac{d\phi}{d\tau} = \frac{d(kx)}{d\tau} = \frac{kp_0}{m}, \quad \frac{d}{d\tau} = \frac{kp_0}{m}\frac{d}{d\phi}. \tag{A.8}$$

Thus, the equation of motion [see Eq. (A.7)] can be written as

$$\frac{dp^\mu(\phi)}{d\phi} = \frac{q}{kp_0}F^{\mu\nu}(\phi)p_\nu(\phi). \tag{A.9}$$

We will express the solution to this equation in terms of the integrated field strength tensor [see Eq. (1.29)]

$$\mathfrak{F}^{\mu\nu}(\phi, \phi_0) = \int\limits_{\phi_0}^{\phi} d\phi' \, F^{\mu\nu}(\phi'), \quad \frac{\partial\mathfrak{F}^{\mu\nu}(\phi, \phi_0)}{\partial\phi} = F^{\mu\nu}(\phi). \tag{A.10}$$

The most general (integrated) field tensor for a plane-wave field is given by [see Eq. (1.17) and Eq. (1.29)]

$$F^{\mu\nu}(\phi) = \sum_{i=1,2} f_i^{\mu\nu}\psi_i'(\phi), \quad \mathfrak{F}^{\mu\nu}(\phi, \phi_0) = \sum_{i=1,2} f_i^{\mu\nu}[\psi_i(\phi) - \psi_i(\phi_0)], \tag{A.11}$$

which implies the following commutation relation

$$F^{\mu\nu}(\phi)\mathfrak{F}_{\nu\rho}(\phi, \phi_0) = \mathfrak{F}^{\mu\nu}(\phi, \phi_0)F_{\nu\rho}(\phi). \tag{A.12}$$

Therefore, the solution of Eq. (A.9) is given by [Di+12; Mey71; SS70]

$$p^\mu(\phi) = p_0^\mu + \frac{q\mathfrak{F}^{\mu\nu}(\phi, \phi_0)p_{0\nu}}{kp_0} + \frac{q^2\mathfrak{F}^{2\mu\nu}(\phi, \phi_0)p_{0\nu}}{2(kp_0)^2}, \tag{A.13}$$

where $p_0^\mu = p^\mu(\phi_0)$ denotes the initial four-momentum. After inserting the above representation for the integrated field tensor [see Eq. (1.30)] the result

reads

$$p^\mu(\phi) = p_0^\mu + \sum_{i=1,2} \left\{ \frac{q}{kp_0} f_i^{\mu\nu} p_{0\nu} \left[\psi_i(\phi) - \psi_i(\phi_0) \right] \right.$$

$$\left. + \frac{q^2}{2(kp_0)^2} f_i^{2\mu\nu} p_{0\nu} [\psi_i(\phi) - \psi_i(\phi_0)]^2 \right\}. \quad \text{(A.14)}$$

Note that for a laser field without dc component [i.e. $\psi_i(\pm\infty) = 0$] the initial and final asymptotic momenta are the same $[p^\mu(\infty) = p^\mu(-\infty)]$. This result is in agreement with the Lawson-Woodward theorem [Law79; WL48], which states that a plane-wave laser field cannot accelerate particles.

Finally, we obtain the classical trajectory $x^\mu(\phi)$ by integrating Eq. (A.13)

$$x^\mu(\phi) = x_0^\mu + \int_{\phi_0}^{\phi} d\phi' \frac{p^\mu(\phi')}{kp_0}, \quad \text{(A.15)}$$

where $x_0^\mu = x^\mu(\phi_0)$ denotes the initial four-position.

A.4. Classical dynamics in light-cone coordinates

The classical evolution of the four-momentum $p^\mu(\phi)$ given in Eq. (A.13) becomes particularly transparent in light-cone coordinates. To this end we consider an electron with charge $q = e$ and assume that q^μ is a constant light-like four-momentum $[q^2 = 0, kq \neq 0, q^\mu \neq q^\mu(\phi)]$. Expanding in the canonical light-cone basis defined in Sec. 1.4.3 [see Eq. (1.48)]

$$\Lambda_1^\mu = \frac{f_1^{\mu\nu} q_\nu}{kq \sqrt{-a_1^2}}, \quad \Lambda_2^\mu = \frac{f_2^{\mu\nu} q_\nu}{kq \sqrt{-a_2^2}}, \quad \text{(A.16)}$$

we obtain [see Eq. (1.49)]

$$p^\mu(\phi) = r(\phi)q^\mu + s(\phi)k^\mu + t_1(\phi)m\Lambda_1^\mu + t_2(\phi)m\Lambda_2^\mu, \quad \text{(A.17a)}$$

where

$$s(\phi) = \frac{qp(\phi)}{kq}, \quad r(\phi) = \frac{kp(\phi)}{kq}, \quad t_i(\phi) = -\frac{\Lambda_i p(\phi)}{m}. \quad \text{(A.17b)}$$

As $kp(\phi) = kp(\phi_0) = kp_0$ implies $r(\phi) = r(\phi_0)$ and

$$s(\phi) = \frac{1}{2} \frac{m^2}{kp_0} \left[1 + t_1^2(\phi) + t_2^2(\phi) \right] \quad \text{(A.18)}$$

is determined by the on-shell condition $p^2(\phi) = m^2$ [see Eq. (1.50)], the nontrivial dynamic is entirely described by [see Eq. (A.14) and App. C]

$$t_i(\phi) = t_i(\phi_0) - \xi_i[\psi_i(\phi) - \psi_i(\phi_0)]. \quad \text{(A.19)}$$

Note that also $t_2(\phi) = t_2(\phi_0)$ is conserved if the background field is linearly polarized $[\psi_2(\phi) = 0]$.

To obtain the trajectory we combine Eq. (A.15) and Eq. (A.17). As $\phi = kx(\phi)$, we only have to consider the components

$$X_i(\phi) = -\Lambda_i^\mu x_\mu(\phi) = X_i(\phi_0) + \frac{1}{m}\frac{m^2}{kp_0}\int\limits_{\phi_0}^{\phi} d\phi'\, t_i(\phi') \tag{A.20}$$

and

$$X_Q(\phi) = q^\mu x_\mu(\phi) = X_Q(\phi_0) + \frac{1}{2}\frac{kq}{m^2}\left(\frac{m^2}{kp_0}\right)^2\int\limits_{\phi_0}^{\phi} d\phi'\, [1 + t_1^2(\phi') + t_2^2(\phi')]. \tag{A.21}$$

B. Two-particle collision kinematics

Normally, scattering experiments involve two beams with many incoherent particles and the probability for a collision is related to a cross section [PS95; Tay72]. To describe recollision processes of coherently produced electron-positron pairs, the impact parameter for a two-particle collision must be considered.

B.1. Impact parameter

In this Appendix we derive an invariant expression for the impact parameter, which can be evaluated in an arbitrary Lorentz frame. To this end we consider first the rest frame of particle one, where the second particle moves along the trajectory $\boldsymbol{x}_2(t_2) + (t - t_2)\boldsymbol{v}_2$ (we assume that the momentum of each particle is constant during the interaction). In this frame the impact parameter b is defined as the minimal distance between the two particles, it is given by the following expression

$$b = \frac{\sqrt{d^2 v_2^2 - (dv_2)^2}}{|\boldsymbol{v}_2|}, \quad b = |\boldsymbol{b}|, \quad \boldsymbol{b} = \boldsymbol{d} \times \boldsymbol{v}_2/|\boldsymbol{v}_2|, \tag{B.1}$$

with $\boldsymbol{d} = \boldsymbol{x}_2 - \boldsymbol{x}_1$. Note that b depends only on the direction of $\boldsymbol{v}_2$ and the replacement $\boldsymbol{v}_2 \to \boldsymbol{p}_2$ is applicable. Furthermore, the position $\boldsymbol{x}_2$ may be evaluated at an arbitrary time, as long as we can assume that the momentum of the particle remains constant during the collision.

As the impact parameter is defined in the rest frame of a particle, it represents by definition a Lorentz invariant quantity. To obtain a manifestly covariant representation, we introduce the four-vector

$$b^\mu = \epsilon^{\mu\nu\rho\sigma}(x_2 - x_1)_\nu p_{1\rho} p_{2\sigma} [(p_1 p_2)^2 - m_1^2 m_2^2]^{-1/2}. \tag{B.2}$$

In the rest frame of particle one $b^\mu = (0, \boldsymbol{b})$, as $p_1^\mu = (m_1, 0, 0, 0)$, $p_2^\mu = (\epsilon_2, \boldsymbol{p}_2)$, $x_1^\mu = (t_1, \boldsymbol{x}_1)$ and $x_2^\mu = (t_2, \boldsymbol{x}_2)$. Thus, $b = \sqrt{-b^\mu b_\mu}$ is the desired expression, which holds in an arbitrary Lorentz frame.

B.2. Scattering plane

The plane, which passes through the origin where particle one is at rest, and which is orthogonal to the velocity vector $\boldsymbol{v}_2$ of the second particle, is called the scattering plane. Correspondingly, the impact parameter b describes the radial distance to the trajectory of the second particle within the scattering plane. In general, we are not only interested in the radial distance but in both coordinates of the intersection. To this end we have to specify two vectors $\boldsymbol{B}_1$ and $\boldsymbol{B}_2$, which are orthonormal and orthogonal to the velocity $\boldsymbol{v}_2$

$$|\boldsymbol{B}_i| = 1, \quad \boldsymbol{B}_1 \boldsymbol{B}_2 = 0, \quad \boldsymbol{B}_i \boldsymbol{v}_2 = 0. \tag{B.3}$$

They define a coordinate system within the scattering plane and we can decompose the distance vector as follows

$$\boldsymbol{d} = b_1 \boldsymbol{B}_1 + b_2 \boldsymbol{B}_2 + \frac{(\boldsymbol{d}\boldsymbol{v}_2)}{\boldsymbol{v}_2^2} \boldsymbol{v}_2. \tag{B.4}$$

Thus, the scattering is more precisely described by the two coordinates

$$b_1 = \boldsymbol{d}\boldsymbol{B}_1, \quad b_2 = \boldsymbol{d}\boldsymbol{B}_2; \quad b = \sqrt{b_1^2 + b_2^2}. \tag{B.5}$$

The two vectors $\boldsymbol{B}_1$ and $\boldsymbol{B}_2$ must depend on $\boldsymbol{v}_2$. In general, also their absolute orientation may change if we change $\boldsymbol{v}_2$ (i.e. the coordinate system is rotated within the scattering plane). To fix the absolute orientation, we would need another vector (e.g. the spin vector of one of the particles), which defines a preferred direction within the scattering plane. If such a vector does not exist, the problem must be spherical symmetric and a rotation within the scattering plane cannot play a role.

To obtain covariant expressions, we search for two four-vectors B_1^μ and B_2^μ, which obey

$$B_i p_1 = B_i p_2 = 0, \quad B_1 B_2 = 0, \quad B_1^2 = B_2^2 = -1. \tag{B.6}$$

In the rest frame of particle one we obtain $B_i^\mu = (0, \boldsymbol{B}_i)$, where the two vectors $\boldsymbol{B}_i$ obey the relations given in Eq. (B.3). Using B_i^μ, the scattering process is described by the two coordinates $b_i = (x_2 - x_1)^\mu B_{i\mu}$.

C. Tensor identities

After a summary of generally important tensor identities many useful properties of the four-vectors and tensors related to plane-wave background fields are listed.

C.1. General relations

To simplify products or contractions of the totally antisymmetric tensor $\epsilon^{\alpha\beta\gamma\delta}$ we note the following identities [LL87]

$$
\begin{aligned}
&\epsilon^{\alpha\beta\gamma\delta}\epsilon_{\alpha\beta\gamma\delta} = -24,\\
&\epsilon^{\alpha\beta\gamma\mu}\epsilon_{\alpha\beta\gamma\nu} = -6\delta^{\mu}_{\nu},\\
&\epsilon^{\alpha\beta\mu\nu}\epsilon_{\alpha\beta\rho\sigma} = -2(\delta^{\mu}_{\rho}\delta^{\nu}_{\sigma} - \delta^{\mu}_{\sigma}\delta^{\nu}_{\rho}),\\
&\epsilon^{\mu\nu\rho\sigma}\epsilon_{\alpha\beta\gamma\sigma} = -(\delta^{\mu}_{\alpha}\delta^{\nu}_{\beta}\delta^{\rho}_{\gamma} - \delta^{\mu}_{\alpha}\delta^{\nu}_{\gamma}\delta^{\rho}_{\beta} + \delta^{\mu}_{\gamma}\delta^{\nu}_{\alpha}\delta^{\rho}_{\beta} - \delta^{\mu}_{\gamma}\delta^{\nu}_{\beta}\delta^{\rho}_{\alpha} + \delta^{\mu}_{\beta}\delta^{\nu}_{\gamma}\delta^{\rho}_{\alpha} - \delta^{\mu}_{\beta}\delta^{\nu}_{\alpha}\delta^{\rho}_{\gamma}),\\
&-\epsilon^{\mu\nu\rho\sigma}\epsilon_{\alpha\beta\gamma\delta} = \det\begin{pmatrix} \delta^{\mu}_{\alpha} & \delta^{\mu}_{\beta} & \delta^{\mu}_{\gamma} & \delta^{\mu}_{\delta} \\ \delta^{\nu}_{\alpha} & \delta^{\nu}_{\beta} & \delta^{\nu}_{\gamma} & \delta^{\nu}_{\delta} \\ \delta^{\rho}_{\alpha} & \delta^{\rho}_{\beta} & \delta^{\rho}_{\gamma} & \delta^{\rho}_{\delta} \\ \delta^{\sigma}_{\alpha} & \delta^{\sigma}_{\beta} & \delta^{\sigma}_{\gamma} & \delta^{\sigma}_{\delta} \end{pmatrix}.
\end{aligned}
\tag{C.1}
$$

Furthermore, antisymmetric tensors $T^{\mu\nu}$, $T_1^{\mu\nu}$, and $T_2^{\alpha\beta}$ obey

$$
\begin{aligned}
T_1^{*\mu\nu}T_2^{*\alpha\beta} = \frac{1}{2}(g^{\mu\beta}g^{\nu\alpha} - g^{\mu\alpha}g^{\nu\beta})T_{1\rho\sigma}T_2^{\rho\sigma} - T_1^{\alpha\beta}T_2^{\mu\nu}\\
+ g^{\nu\alpha}(T_1T_2)^{\beta\mu} - g^{\mu\alpha}(T_1T_2)^{\beta\nu} - g^{\nu\beta}(T_1T_2)^{\alpha\mu} + g^{\mu\beta}(T_1T_2)^{\alpha\nu},
\end{aligned}
\tag{C.2}
$$

$$
\begin{aligned}
(T_1^*T_2^*)^{\mu\nu} = \frac{1}{2}g^{\mu\nu}T_{1\alpha\beta}T_2^{\alpha\beta} + (T_1T_2)^{\nu\mu}, \qquad T_{1\mu\nu}^*T_2^{*\mu\nu} = -T_{1\mu\nu}T_2^{\mu\nu},\\
\epsilon^{\mu\nu\rho\sigma}T_{\sigma\alpha}^* = \delta^{\mu}_{\alpha}T^{\nu\rho} - \delta^{\nu}_{\alpha}T^{\mu\rho} + \delta^{\rho}_{\alpha}T^{\mu\nu}, \qquad \frac{1}{2}\epsilon_{\mu\nu\rho\sigma}T^{*\rho\sigma} = -T_{\mu\nu}.
\end{aligned}
\tag{C.3}
$$

C.2. Lambda four-vectors

We consider the two sets of four-vectors Λ_i^{μ} and $\Lambda_i^{*\mu}$ (the star is part of the symbol)

$$
\begin{aligned}
\Lambda_1^{\mu} = \frac{f_1^{\mu\nu}q_{\nu}}{kq\sqrt{-a_1^2}}, \quad \Lambda_2^{\mu} = \frac{f_2^{\mu\nu}q_{\nu}}{kq\sqrt{-a_2^2}},\\
\Lambda_1^{*\mu} = \frac{f_1^{*\mu\nu}q_{\nu}}{kq\sqrt{-a_1^2}}, \quad \Lambda_2^{*\mu} = \frac{f_2^{*\mu\nu}q_{\nu}}{kq\sqrt{-a_2^2}}
\end{aligned}
\tag{C.4}
$$

($f_i^{*\mu\nu}$ denotes the dual tensor). Here, q^{μ} is an arbitrary four-vector (we only assume that $kq \neq 0$) and [see Eq. (1.18)]

$$
f_i^{\mu\nu} = k^{\mu}a_i^{\nu} - k^{\nu}a_i^{\mu}.
\tag{C.5}
$$

We obtain the following properties [see Eq. (C.4)]

$$\Lambda_i \Lambda_j = \Lambda_i^* \Lambda_j^* = -\delta_{ij}, \quad k\Lambda_i = q\Lambda_i = 0, \quad k\Lambda_i^* = q\Lambda_i^* = 0. \tag{C.6}$$

Furthermore, we define

$$\Lambda_5^\mu = \epsilon^{\mu\nu\rho\sigma} k_\nu \Lambda_{1\rho} \Lambda_{2\sigma} = \epsilon^{\mu\nu\rho\sigma} k_\nu a_{1\rho} a_{2\sigma} \left(a_1^2 a_2^2\right)^{-1/2} \tag{C.7}$$

with the properties

$$\Lambda_5^2 = \Lambda_5 k = \Lambda_5 \Lambda_1 = \Lambda_5 \Lambda_2 = 0, \quad (q\Lambda_5)^2 = (kq)^2, \quad \frac{q\Lambda_5}{kq} = \frac{kq}{q\Lambda_5}. \tag{C.8}$$

Beside being a pseudo-vector, Λ_5^μ is proportional to k^μ, i.e. we obtain

$$\Lambda_5^\mu = \frac{q\Lambda_5}{kq} k^\mu. \tag{C.9}$$

Furthermore, we note the identities

$$\Lambda_1^\mu = \frac{q\Lambda_5}{kq} \Lambda_2^{*\mu}, \quad \Lambda_2^\mu = -\frac{q\Lambda_5}{kq} \Lambda_1^{*\mu} \tag{C.10}$$

and correspondingly

$$\Lambda_1^* \Lambda_2 = \frac{q\Lambda_5}{kq}, \quad \Lambda_1 \Lambda_2^* = -\frac{q\Lambda_5}{kq}. \tag{C.11}$$

Using this notation, we can represent the constant field tensors $f_i^{\mu\nu}$ as follows [see Eq. (1.20) for the definition of ξ_i]

$$e f_i^{\mu\nu} = m\xi_i (k^\mu \Lambda_i^\nu - k^\nu \Lambda_i^\mu). \tag{C.12a}$$

Correspondingly, we also obtain

$$e f_i^{*\mu\nu} = m\xi_i (k^\mu \Lambda_i^{*\nu} - k^\nu \Lambda_i^{*\mu}). \tag{C.12b}$$

This implies the relations

$$f_i^{\mu\nu} \Lambda_{j\nu} = -\delta_{ij} \frac{m\xi_i}{e} k^\mu, \quad f_1^{*\mu\nu} \Lambda_{2\nu} = \frac{m\xi_1}{e} \Lambda_5^\mu, \quad f_2^{*\mu\nu} \Lambda_{1\nu} = -\frac{m\xi_2}{e} \Lambda_5^\mu \tag{C.13}$$

and

$$f_i^{*\mu\nu} \Lambda_{j\nu}^* = -\delta_{ij} \frac{m\xi_i}{e} k^\mu, \quad f_1^{\mu\nu} \Lambda_{2\nu}^* = -\frac{m\xi_1}{e} \Lambda_5^\mu, \quad f_2^{\mu\nu} \Lambda_{1\nu}^* = \frac{m\xi_2}{e} \Lambda_5^\mu. \tag{C.14}$$

C.3. Tensor contraction identities

We note the following contraction identities for the constant field tensors

$$f_{i\,\rho}^\mu f_j^{\rho\nu} = f_{i\,\rho}^{*\mu} f_j^{*\rho\nu} = -\delta_{ij} a_i^2 \, k^\mu k^\nu,$$
$$f_i^{*\mu\rho} f_{i\rho\nu} = f_i^{\mu\rho} f_{i\rho\nu}^* = 0,$$
$$f_1^{\mu\rho} f_{2\rho}^{*\ \nu} = \sqrt{a_1^2 a_2^2} \, k^\mu \Lambda_5^\nu, \quad f_1^{*\mu\rho} f_{2\rho}^{\ \nu} = -\sqrt{a_1^2 a_2^2} \, \Lambda_5^\mu k^\nu,$$
$$f_2^{\mu\rho} f_{1\rho}^{*\ \nu} = -\sqrt{a_1^2 a_2^2} \, k^\mu \Lambda_5^\nu, \quad f_2^{*\mu\rho} f_{1\rho}^{\ \nu} = \sqrt{a_1^2 a_2^2} \, \Lambda_5^\mu k^\nu. \tag{C.15}$$

Therefore, the integrated field tensor obeys the relations

$$\mathfrak{F}^{\mu\nu}(\phi)\Lambda_{i\nu} = -\frac{m}{e}k^{\mu}\xi_i\psi_i(\phi),$$

$$\mathfrak{F}^{*\mu\nu}(\phi)\Lambda_{1\nu} = -\frac{m}{e}\Lambda_5^{\mu}\xi_2\psi_2(\phi), \quad \mathfrak{F}^{*\mu\nu}(\phi)\Lambda_{2\nu} = \frac{m}{e}\Lambda_5^{\mu}\xi_1\psi_1(\phi) \tag{C.16}$$

and

$$\mathfrak{F}^{*\mu\nu}(\phi)\Lambda_{i\nu}^* = -\frac{m}{e}k^{\mu}\xi_i\psi_i(\phi),$$

$$\mathfrak{F}^{\mu\nu}(\phi)\Lambda_{1\nu}^* = \frac{m}{e}\frac{q\Lambda_5}{kq}k^{\mu}\xi_2\psi_2(\phi), \quad \mathfrak{F}^{\mu\nu}(\phi)\Lambda_{2\nu}^* = -\frac{m}{e}\frac{q\Lambda_5}{kq}k^{\mu}\xi_1\psi_1(\phi). \tag{C.17}$$

Correspondingly, it is natural to expand $\mathfrak{F}$ using the four-vectors Λ_i and $\mathfrak{F}^*$ using the four-vectors Λ_i^*. Furthermore,

$$\mathfrak{F}_x^{\mu\rho}\mathfrak{F}_{y\rho\nu} = \frac{m^2}{e^2}k^{\mu}k_{\nu}\sum_{i=1,2}\xi_i^2\psi_i(kx)\psi_i(ky),$$

$$\mathfrak{F}_x^{*\mu\rho}\mathfrak{F}_{y\rho\nu} = -\frac{m^2}{e^2}\xi_1\xi_2\,\Lambda_5^{\mu}k_{\nu}\left[\psi_1(kx)\psi_2(ky) - \psi_1(ky)\psi_2(kx)\right],$$

$$\mathfrak{F}_x^{\mu\rho}\mathfrak{F}_{y\rho\nu}^* = \frac{m^2}{e^2}\xi_1\xi_2\,k^{\mu}\Lambda_{5\nu}\left[\psi_1(kx)\psi_2(ky) - \psi_1(ky)\psi_2(kx)\right]. \tag{C.18}$$

In particular, we obtain

$$e\Lambda_{i\mu}\mathfrak{F}_x^{\mu\nu}q_{\nu} = m\,kq\,\xi_i\,\psi_i(kx),$$

$$e^2q\mathfrak{F}_{x,y}^2q = m^2(kq)^2\sum_{i=1,2}\xi_i^2\psi_i(kx)\psi_i(ky). \tag{C.19}$$

During the calculation of the polarization operator the four-vector [see Eq. (3.16)]

$$\lambda^{\mu} = -2m\tau\sum_{i=1,2}\Lambda_i^{\mu}\xi_iI_i \tag{C.20}$$

appears. It obeys the following contraction identities

$$\mathfrak{F}_x^{\mu\nu}\lambda_{\nu} = 2\frac{m^2}{e}\tau k^{\mu}\sum_{i=1,2}\xi_i^2\psi_i(kx)I_i,$$

$$\mathfrak{F}_x^{*\mu\nu}\lambda_{\nu} = -2\frac{m^2}{e}\tau\Lambda_5^{\mu}\xi_1\xi_2\left[\psi_1(kx)I_2 - \psi_2(kx)I_1\right], \tag{C.21a}$$

$$\Lambda_i\lambda = 2m\tau\xi_iI_i, \quad eq\mathfrak{F}_x\lambda = 2kq\,\tau m^2\sum_{i=1,2}\xi_i^2\psi_i(kx)I_i, \tag{C.21b}$$

$$\Lambda_{1\mu}^*\Lambda_{2\nu}^*\epsilon^{\mu\nu\rho\sigma}q_{\rho}\lambda_{\sigma} = \Lambda_{1\mu}\Lambda_{2\nu}\epsilon^{\mu\nu\rho\sigma}q_{\rho}\lambda_{\sigma} = 0, \tag{C.21c}$$

$$\begin{aligned}
\Lambda_{i\mu}^*k_{\nu}\epsilon^{\mu\nu\rho\sigma}q_{\rho}\lambda_{\sigma} &= 2m\tau\,kq\,\xi_iI_i, \\
\Lambda_{1\mu}k_{\nu}\epsilon^{\mu\nu\rho\sigma}q_{\rho}\lambda_{\sigma} &= 2m\tau\,q\Lambda_5\,\xi_2I_2, \\
\Lambda_{2\mu}k_{\nu}\epsilon^{\mu\nu\rho\sigma}q_{\rho}\lambda_{\sigma} &= -2m\tau\,q\Lambda_5\,\xi_1I_1.
\end{aligned} \tag{C.21d}$$

D. Gamma matrix algebra

The gamma matrices form a complete set in the sense that any matrix Γ_c in spinor space can be decomposed according to [Lea01]

$$\Gamma_c = c_{\mathbf{1}}\mathbf{1} + c_5\gamma^5 + c_\mu\gamma^\mu + c_{5\mu}i\gamma^\mu\gamma^5 + c_{\mu\nu}i\sigma^{\mu\nu}, \tag{D.1}$$

where we assume that $c_{\mu\nu} = -c_{\nu\mu}$. The fundamental terms have the following conjugation properties

$$\overline{\mathbf{1}} = \mathbf{1}, \quad \overline{\gamma^5} = -\gamma^5, \quad \overline{\gamma^\mu} = \gamma^\mu, \quad \overline{(i\gamma^\mu\gamma^5)} = -i\gamma^\mu\gamma^5, \quad \overline{(i\sigma^{\mu\nu})} = i\sigma^{\mu\nu}. \tag{D.2}$$

The coefficients in Eq. (D.1) can be calculated by using the following traces

$$\begin{aligned}
c_{\mathbf{1}} &= \tfrac{1}{4}\,\mathbf{tr}\,\mathbf{1}\Gamma_c, \quad c_5 = \tfrac{1}{4}\,\mathbf{tr}\,\gamma^5\Gamma_c, \quad c_\mu = \tfrac{1}{4}\,\mathbf{tr}\,\gamma_\mu\Gamma_c, \\
c_{5\mu} &= \tfrac{1}{4}\,\mathbf{tr}\,i\gamma_\mu\gamma^5\Gamma_c, \quad c_{\mu\nu} = \tfrac{1}{8}\,\mathbf{tr}\,i\sigma_{\mu\nu}\Gamma_c.
\end{aligned} \tag{D.3}$$

Instead of the vector and the axial-vector current one can also use the left- and the right-handed current

$$c_\mu\gamma^\mu + c_{5\mu}i\gamma^\mu\gamma^5 = l_\mu\gamma^\mu P_L + r_\mu\gamma^\mu P_R, \tag{D.4}$$

where the chirality projectors for the left and the right-handed component are given by

$$P_L = \frac{1}{2}(\mathbf{1} + \gamma^5), \quad P_R = \frac{1}{2}(\mathbf{1} - \gamma^5) \tag{D.5}$$

(note that we define $\gamma^5 = -i\gamma^0\gamma^1\gamma^2\gamma^3$ as in [LL82]). The coefficients c_μ, $c_{5\mu}$ and l_μ, r_μ are related via

$$l_\mu = c_\mu + ic_{5\mu}, \quad r_\mu = c_\mu - ic_{5\mu} \tag{D.6}$$

and

$$c_\mu = \frac{1}{2}(l_\mu + r_\mu), \quad c_{5\mu} = \frac{i}{2}(r_\mu - l_\mu). \tag{D.7}$$

Therefore, the coefficients for the left- and the right-handed current can be determined from the following traces

$$l_\mu = \frac{1}{2}\,\mathbf{tr}\,P_L\gamma_\mu\Gamma, \quad r_\mu = \frac{1}{2}\,\mathbf{tr}\,P_R\gamma_\mu\Gamma. \tag{D.8}$$

Due to the cyclic property of the trace, one can recursively calculate traces of arbitrary length without conceptual difficulties by permuting the first gamma matrix to the last position. For completeness we note the following relations

$$\begin{aligned}
\tfrac{1}{4}\,\mathbf{tr}\,\gamma^\mu\gamma^\nu &= g^{\mu\nu}, \\
\tfrac{1}{4}\,\mathbf{tr}\,\gamma^\mu\gamma^\nu\gamma^\rho\gamma^\sigma &= g^{\mu\sigma}\,g^{\nu\rho} - g^{\mu\rho}\,g^{\nu\sigma} + g^{\mu\nu}\,g^{\rho\sigma}, \\
\tfrac{1}{4}\,\mathbf{tr}\,\sigma^{\mu\nu}\gamma^\rho\gamma^\sigma &= g^{\mu\sigma}\,g^{\nu\rho} - g^{\mu\rho}\,g^{\nu\sigma}, \\
\tfrac{1}{4}\,\mathbf{tr}\,\gamma^\mu\gamma^\nu\gamma^\rho\gamma^\sigma\gamma^5 &= i\epsilon^{\mu\nu\rho\sigma}.
\end{aligned} \tag{D.9}$$

Thus, any identity involving gamma matrices can be proven by calculating the fundamental terms given in Eq. (D.1) for both sides of the equation. It is in

particular possible to map the gamma matrix algebra to a corresponding tensor algebra once the decomposition of the product of two arbitrary gamma matrix expressions $\Gamma_c = \Gamma_a \Gamma_b$ is known. Here, Γ_x is written as in Eq. (D.1) with the letter c replaced by the letter x appearing in the index. The coefficients of Γ_c are then given by

$$c_{\mathbf{1}} = a_{\mathbf{1}} b_{\mathbf{1}} + a_5 b_5 + a^\mu b_\mu + a_5^\mu b_{5\mu} + 2 a_{\mu\nu} b^{\mu\nu},$$

$$c_5 = (a_{\mathbf{1}} b_5 + a_5 b_{\mathbf{1}}) + (i a^\mu b_{5\mu} - i a_{5\mu} b^\mu) - i\epsilon^{\mu\nu\rho\sigma} a_{\mu\nu} b_{\rho\sigma},$$

$$\begin{aligned} c_\mu &= (a_{\mathbf{1}} b_\mu + a_\mu b_{\mathbf{1}}) + (i a_{5\mu} b_5 - i a_5 b_{5\mu}) \\ &\quad + 2\left(i a_{\mu\nu} b^\nu - i a^\nu b_{\mu\nu}\right) - i\epsilon_{\mu\nu\rho\sigma}\left(a_5^\nu b^{\rho\sigma} + a^{\rho\sigma} b_5^\nu\right), \end{aligned}$$

$$\begin{aligned} c_{5\mu} &= (a_{\mathbf{1}} b_{5\mu} + a_{5\mu} b_{\mathbf{1}}) + (i a_5 b_\mu - i a_\mu b_5) \\ &\quad + i\epsilon_{\mu\nu\rho\sigma}\left(a^\nu b^{\rho\sigma} + a^{\rho\sigma} b^\nu\right) + 2\left(i a_{\mu\nu} b_5^\nu - i a_5^\nu b_{\mu\nu}\right), \end{aligned}$$

$$\begin{aligned} c_{\mu\nu} &= (a_{\mathbf{1}} b_{\mu\nu} + a_{\mu\nu} b_{\mathbf{1}}) - \frac{i}{2}\epsilon_{\mu\nu\rho\sigma}\left(a^{\rho\sigma} b_5 + a_5 b^{\rho\sigma}\right) - \frac{i}{2}\left(a_\mu b_\nu - a_\nu b_\mu\right) \\ &\quad - \frac{i}{2}\epsilon_{\mu\nu\rho\sigma}\left(a^\rho b_5^\sigma + a_5^\sigma b^\rho\right) - \frac{i}{2}\left(a_{5\mu} b_{5\nu} - a_{5\nu} b_{5\mu}\right) + 2i(a_{\mu\rho} b^\rho{}_\nu - a_{\nu\rho} b^\rho{}_\mu). \end{aligned}$$

$$\text{(D.10)}$$

We point out that the trace of Γ_c is given by $c_{\mathbf{1}}$ [see Eq. (D.3)]. Therefore, Eq. (D.10) is also useful for the calculation of traces. Finally, we note the following contraction identities

$$\begin{aligned} &\gamma^\rho \mathbf{1} \gamma_\rho = 4, \quad \gamma^\rho \gamma^5 \gamma_\rho = -4\gamma^5, \quad \gamma^\rho \gamma^\mu \gamma_\rho = -2\gamma^\mu, \\ &\gamma^\rho (i\gamma^\mu \gamma^5)\gamma_\rho = 2(i\gamma^\mu \gamma^5), \quad \gamma^\rho (i\sigma^{\mu\nu})\gamma_\rho = 0. \end{aligned}$$

$$\text{(D.11)}$$

E. Photon polarization density matrix

The (complex) polarization four-vector ϵ^μ of a photon with four-momentum q^μ ($q^2 = 0$) must obey $\epsilon^{*\mu}\epsilon_\mu = -1$ and $q\epsilon = 0$. In the canonical light-cone basis k^μ, q^μ, Λ_i^μ (see Sec. 1.4.3) the polarization four-vector is given by

$$\epsilon^\mu = c_1 \Lambda_1^\mu + c_2 \Lambda_2^\mu + c_3 q^\mu, \quad c_1 = -(\epsilon\Lambda_1), \quad c_2 = -(\epsilon\Lambda_2), \quad c_3 = \frac{k\epsilon}{kq} \quad \text{(E.1)}$$

with the normalization condition $|c_1|^2 + |c_2|^2 = 1$. As the contraction of the matrix element with the four-momentum q^μ must vanish due to gauge symmetry, we can restrict us to the vectors Λ_i^μ and replace the density matrix by

$$\rho^{\mu\nu} = \epsilon^\mu \epsilon^{*\nu} \longrightarrow \sum_{i,j=1,2} \rho_{ij} \Lambda_i^\mu \Lambda_j^\nu, \quad \text{(E.2a)}$$

$$\rho_{11} = |c_1|^2, \quad \rho_{22} = |c_2|^2, \quad \rho_{12} = c_1 c_2^*, \quad \rho_{21} = c_1^* c_2. \quad \text{(E.2b)}$$

The 2×2 density matrix ρ_{ij} is Hermitian and has unit trace

$$\rho_{ij} = \Lambda_{i\mu}\Lambda_{j\nu}\rho^{\mu\nu}, \quad \rho_{ij}^\dagger = \rho_{ji}^* = \rho_{ij}, \quad \mathbf{tr}\,\rho = \sum_{i=1,2} \rho_{ii} = 1. \quad \text{(E.3)}$$

Any Hermitian 2×2 matrix can be expanded using the Pauli matrices σ^i and the identity $\mathbf{1}$ (with real parameters). Since $\mathbf{tr}\,\sigma^i = 0$, we obtain (see [LL82], Eq. 8.9)

$$\rho = \frac{1}{2}(\mathbf{1} + s_i\sigma^i) = \frac{1}{2}\begin{pmatrix} 1 + s_3 & s_1 - is_2 \\ s_1 + is_2 & 1 - s_3 \end{pmatrix} = \begin{pmatrix} |c_1|^2 & c_1 c_2^* \\ c_1^* c_2 & |c_2|^2 \end{pmatrix}, \quad \text{(E.4)}$$

where s_i are called Stokes parameters. The Stokes vector $\boldsymbol{s} = (s_1, s_2, s_3)$ is a unit vector, which can be seen from

$$\det\rho = 0 = \frac{1}{4}\left(1 - \boldsymbol{s}^2\right). \quad \text{(E.5)}$$

Correspondingly, it can be described by two Stokes angles

$$s_1 = \cos(\varphi)\sin(\theta), \quad s_2 = \sin(\varphi)\sin(\theta), \quad s_3 = \cos(\theta). \quad \text{(E.6)}$$

Using trigonometric identities we conclude that the complex coefficients c_1 and c_2 can be expressed in terms of the stokes angles as

$$c_1 = \cos(\theta/2)\,e^{-i\varphi/2}, \quad c_2 = \sin(\theta/2)\,e^{+i\varphi/2}, \quad \text{(E.7)}$$

implying the representations

$$|c_1|^2 = \cos^2(\theta/2), \quad |c_2|^2 = \sin^2(\theta/2), \quad \text{(E.8a)}$$

$$c_1 c_2^* = \frac{1}{2}\sin(\theta)\left[\cos(\varphi) - i\sin(\varphi)\right] \quad \text{(E.8b)}$$

[note that we can always multiply by a total phase in Eq. (E.7)].

F. Airy, Scorer and Ritus functions

The Ritus functions are defined by [Rit72a; Rit85]

$$f(x) = i \int_0^\infty dt \exp\left[-i(tx + t^3/3)\right] = \pi \operatorname{Gi}(x) + i\pi \operatorname{Ai}(x), \tag{F.1a}$$

$$f'(x) = \int_0^\infty t\,dt \exp\left[-i(tx + t^3/3)\right] = \pi \operatorname{Gi}'(x) + i\pi \operatorname{Ai}'(x), \tag{F.1b}$$

$$f_1(x) = \int_0^\infty \frac{dt}{t} \exp\left(-itx\right)\left[\exp\left(-it^3/3\right) - 1\right] \tag{F.1c}$$

and

$$f_2(x) = \int_0^\infty \frac{dt}{t^2} \exp\left(-itx\right)\left[\exp\left(-it^3/3\right) - 1\right] = -i\left[x f_1(x) + f'(x)\right], \tag{F.1d}$$

where Ai and Gi are the Airy and Scorer function, respectively [Olv+10]. Note that in Ritus' work the normalization of the Airy function is different and also changes (see [Rit85], App. C and [NR64b], Eq. B5). The functions defined in Eq. (F.1) obey the following differential equations [Olv+10; Rit85]

$$f''(x) = x f(x) - 1, \quad f_1'(x) = \frac{1}{x} - f(x) = -\frac{1}{x} f''(x). \tag{F.2}$$

Furthermore, for $x > 0$ we obtain [Rit85]

$$f_1(x) = \int_x^\infty dt\,[f(t) - 1/t] = \ln(x) + \frac{2}{3}\gamma + \frac{1}{3}\ln(3) + i\frac{\pi}{3} - \int_0^x dt\,f(t). \tag{F.3}$$

The integral converges, as [Olv+10]

$$\operatorname{Gi}(x) \sim \frac{1}{\pi x} \sum_{k=0}^\infty \frac{(3k)!}{k!3^k x^{3k}}. \tag{F.4}$$

The imaginary part of $f_1(x)$ is related to [VS04]

$$\operatorname{Ai}_1(x) = \int_x^\infty dt\,\operatorname{Ai}(t) = \pi\left[\operatorname{Ai}(x)\operatorname{Gi}'(x) - \operatorname{Ai}'(x)\operatorname{Gi}(x)\right] \tag{F.5}$$

for $x \geq 0$ and

$$\operatorname{Ai}_{1'}(x) = \int_{-\infty}^x dt\,\operatorname{Ai}(t) = \pi\left[\operatorname{Ai}(x)\operatorname{Hi}'(x) - \operatorname{Ai}'(x)\operatorname{Hi}(x)\right] \tag{F.6}$$

for $x \leq 0$. Here Hi denotes the second Scorer function [Olv+10].

For large values we obtain the following asymptotic series expansions for the

Airy function [Olv+10]

$$\text{Ai}(z) \sim \frac{e^{-\zeta}}{2\sqrt{\pi}z^{1/4}} \sum_{k=0}^{\infty} (-1)^k \frac{\Gamma(3k + \frac{1}{2})}{54^k k! \Gamma(k + \frac{1}{2})} \zeta^{-k} \tag{F.7}$$

and its derivative

$$\text{Ai}'(z) \sim -\frac{z^{1/4} e^{-\zeta}}{2\sqrt{\pi}} \sum_{k=0}^{\infty} (-1)^k \frac{6k + 1}{1 - 6k} \frac{\Gamma(3k + \frac{1}{2})}{54^k k! \Gamma(k + \frac{1}{2})} \zeta^{-k}, \tag{F.8}$$

where $\zeta \equiv \frac{2}{3} z^{3/2}$.

Finally, we note the following integral representations for the Airy function and its derivative, which are frequently encountered [see Eq. (F.1)]

$$F(x) = i \int_{-\infty}^{+\infty} dt \exp\left[-i(tx + t^3/3)\right] = 2\pi i \, \text{Ai}(x), \tag{F.9a}$$

$$F'(x) = \int_{-\infty}^{+\infty} t \, dt \exp\left[-i(tx + t^3/3)\right] = 2\pi i \, \text{Ai}'(x). \tag{F.9b}$$

G. Integrals expressible by Hankel functions

In this appendix we consider the functions

$$\mathcal{W}_l(x) = \int\limits_0^\infty dW \, \frac{4}{(W+4)^l \sqrt{(W+4)W}} \, e^{-iWx} \tag{G.1}$$

($l = 0, 1, 2$, $x \geq 0$), which appear in the following integrals related to the polarization operator

$$\int\limits_4^\infty dw \, \frac{4}{w^l \sqrt{w(w-4)}} \, e^{-iwx} = e^{-i4x} \, \mathcal{W}_l(x) \tag{G.2}$$

($w = W + 4$).

By rescaling the integration variable ($Wx = U$, assuming $x > 0$)

$$\mathcal{W}_l(x) = \int\limits_0^\infty dU \, \frac{4}{(U/x+4)^l \sqrt{(U+4x)U}} \, e^{-iU} \tag{G.3}$$

and noting that for $x \gg 1$ the integral is formed around $U = 0$, we obtain the leading-order behavior in the limit $x \to \infty$

$$\mathcal{W}_l(x) \sim -\frac{2\sqrt{\pi i}}{4^l} \, e^{i\pi/4} \frac{1}{\sqrt{x}}. \tag{G.4}$$

Here, we used

$$\int\limits_0^\infty dU \, \frac{1}{\sqrt{U}} \, e^{-iU} = \int\limits_{-\infty}^{+\infty} dV \, e^{-iV^2} = -i\sqrt{\pi} \, e^{i\pi/4} \tag{G.5}$$

($V = \sqrt{U}$). From Eq. (G.4) we conclude that the functions $\mathcal{W}_l$ are nonoscillatory and vanish for large arguments.

We note that the functions $\mathcal{W}_l$ can be represented using Hankel functions $\mathrm{H}_\nu^{(2)}(x) = \mathrm{J}_\nu(x) - i\,\mathrm{Y}_\nu(x)$ (J_ν and Y_ν denote the Bessel function of the first and the second kind, respectively) [Olv+10]. To this end we apply the change of variables $W = 2(\cosh t - 1)$, which yields together with

$$\cosh t + 1 = 2\cosh^2(t/2) \tag{G.6}$$

the alternative integral representation

$$\mathcal{W}_l(x) = e^{i2x} \int\limits_0^\infty dt \, \frac{4}{4^l \cosh^{2l}(t/2)} \, e^{-i2x \cosh t}. \tag{G.7}$$

For $l = 0$ we obtain, using the following integral representation for the Hankel functions [GR07]

$$\mathrm{H}_\nu^{(2)}(z) = i\frac{2}{\pi} e^{\nu\pi i/2} \int\limits_0^\infty dt \, e^{-iz \cosh t} \cosh(\nu t) \tag{G.8}$$

(valid for $-1 < \Re\nu < 1$, $z > 0$)

$$\mathcal{W}_0(x) = (-2\pi i)\, e^{i2x}\, \mathrm{H}_0^{(2)}(2x). \tag{G.9}$$

With the help of the asymptotic expansion of the Hankel functions [Olv+10]

$$\mathrm{H}_\nu^{(2)}(z) \sim \sqrt{\frac{2}{\pi z}}\, e^{-i(z - \frac{1}{2}\nu\pi - \frac{1}{4}\pi)} \sum_{k=0}^{\infty} (-i)^k \frac{a_k(\nu)}{z^k},$$

$$a_k(\nu) = \frac{(4\nu^2 - 1^2)(4\nu^2 - 3^2)\cdots[4\nu^2 - (2k-1)^2]}{k!\, 8^k}, \tag{G.10}$$

$a_0(\nu) = 1$, the leading asymptotic behavior given in Eq. (G.4) is verified for $\mathcal{W}_0$. We note that $\mathcal{W}_0(x)$ has a logarithmic singularity at $x = 0$ [Olv+10].

We point out that the integral in Eq. (G.7) converges also for $l > 0$. Therefore, we can use the replacement $x \to x - i\epsilon$ together with the limit $\epsilon \to 0$, which allows us to apply Eq. (G.8) also for $\nu = 1$. Using the identity

$$\cosh t - 1 = \tanh(t/2)\sinh t, \tag{G.11}$$

the integrals

$$\int dt\, \frac{1}{\cosh^2(t/2)} = 2\tanh(t/2),$$

$$\int dt\, \frac{1}{\cosh^4(t/2)} = \frac{2}{3}\tanh(t/2)\left[2 + \frac{1}{\cosh^2(t/2)}\right] \tag{G.12}$$

and integration by parts (due to the regularization the boundary terms vanish) we obtain

$$\mathcal{W}_1(x) = (-2\pi x)\, e^{i2x} \left[\mathrm{H}_0^{(2)}(2x) + i\,\mathrm{H}_1^{(2)}(2x)\right],$$

$$\mathcal{W}_2(x) = \frac{\pi x}{3}\, e^{i2x} \left[4ix\,\mathrm{H}_0^{(2)}(2x) - (4x + i)\,\mathrm{H}_1^{(2)}(2x)\right], \tag{G.13}$$

where

$$\mathrm{H}_0^{(2)}(2x) + i\,\mathrm{H}_1^{(2)}(2x) = \mathrm{J}_0(2x) + \mathrm{Y}_1(2x) + i\left[\mathrm{J}_1(2x) - \mathrm{Y}_0(2x)\right] \tag{G.14}$$

and

$$4ix\,\mathrm{H}_0^{(2)}(2x) - (4x + i)\,\mathrm{H}_1^{(2)}(2x) = 4x\,\mathrm{Y}_0(2x) - 4x\,\mathrm{J}_1(2x) - \mathrm{Y}_1(2x)$$
$$+ i\left[4x\,\mathrm{J}_0(2x) + 4x\,\mathrm{Y}_1(2x) - \mathrm{J}_1(2x)\right]. \tag{G.15}$$

In order to verify the final result in Eq. (G.13), we note that the asymptotic behavior given in Eq. (G.4) agrees with the one obtained from Eq. (G.13) by applying the asymptotic expansion of the Hankel function given in Eq. (G.10). Furthermore, for $x = 0$ the integrals in Eq. (G.7) can be solved using Eq. (G.12) and we obtain

$$\mathcal{W}_1(0) = 2, \quad \mathcal{W}_2 = 1/3. \tag{G.16}$$

These values are also obtained if the limit $x \to 0$ is considered in Eq. (G.13). Finally,
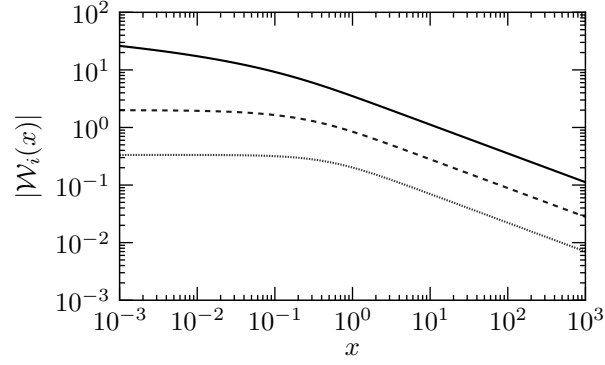
Fig. 41: The function $\mathcal{W}_0$ (solid line) has a logarithmic singularity at the origin, $\mathcal{W}_1$ (dashed line) and $\mathcal{W}_2$ (dotted line) are regular. For large values they behave as $\sim x^{-1/2}$.

the expressions in Eq. (G.13) also obey the differential equations

$$\frac{d}{dx}\mathcal{W}_1(x) = 4i\mathcal{W}_1(x) - i\mathcal{W}_0(x), \quad \frac{d}{dx}\mathcal{W}_2(x) = 4i\mathcal{W}_2(x) - i\mathcal{W}_1(x), \qquad \text{(G.17)}$$

obtained by differentiating Eq. (G.1) under the integral. This can be verified using the relations [Olv+10]

$$\frac{d}{dx}\,\mathrm{H}_0^{(2)}(x) = -\,\mathrm{H}_1^{(2)}(x), \quad \frac{d}{dx}\,\mathrm{H}_1^{(2)}(x) = \mathrm{H}_0^{(2)}(x) - \frac{1}{x}\,\mathrm{H}_1^{(2)}(x). \qquad \text{(G.18)}$$

Summarizing, we obtain (see Fig. 41)

$$\begin{aligned}
\mathcal{W}_0(x) &= (-2\pi i)\, e^{i2x}\, \mathrm{H}_0^{(2)}(2x), \\
\mathcal{W}_1(x) &= (-2\pi x)\, e^{i2x}\, \big[\, \mathrm{H}_0^{(2)}(2x) + i\, \mathrm{H}_1^{(2)}(2x) \big], \\
\mathcal{W}_2(x) &= \frac{\pi x}{3}\, e^{i2x}\, \big[4ix\, \mathrm{H}_0^{(2)}(2x) - (4x + i)\, \mathrm{H}_1^{(2)}(2x) \big].
\end{aligned} \qquad \text{(G.19)}$$

H. Oscillating integrals with coalescing stationary points

As long as all stationary points x_s $[f'(x_s) = 0]$ of the oscillatory integral

$$I = \int dx\, g(x) e^{i\lambda f(x)} \tag{H.1}$$

are well separated, the ordinary stationary-phase approximation can be used to take them into account [Won01]

$$I \approx g(x_s) \left[\frac{2\pi i}{\lambda f''(x_s)}\right]^{1/2} e^{i\lambda f(x_s)}, \quad \sqrt{\pm i} = e^{\pm i\pi/4}. \tag{H.2}$$

Sometimes, however, two stationary points x_1 and x_2 are located very close to each other ($x_1 \approx x_2$) or even coalesce ($x_1 = x_2$) and Eq. H.2 is not applicable anymore. Following the idea of [CFU57] (see also [OT94; VS04]), we consider both two (nearly) coalescing stationary points located on the real line and two (nearly) coalescing stationary points located close to the real line inside the complex plane.

H.1. Two nearly coalescing real stationary points

If two stationary points x_1 and x_2 are located very close to each other, they must be taken into account simultaneously. To this end we apply the change of variables $x \to y$, implicitly defined by

$$F(y) = \lambda f[x(y)] = a - b^2 y + y^3/3. \tag{H.3}$$

In terms of the new variable we obtain

$$I = \int dy\, G(y)\, e^{iF(y)}, \quad G(y) = g[x(y)]\frac{dx}{dy}. \tag{H.4}$$

The transformed phase has two real stationary points located at $\pm b$. We conclude from

$$F'(y) = \lambda f'[x(y)]\frac{dx}{dy} \tag{H.5}$$

that $-b = y(x_1)$ and $b = y(x_2)$, implying

$$\lambda f(x_1) = a + \frac{2}{3}b^3, \quad \lambda f(x_2) = a - \frac{2}{3}b^3. \tag{H.6}$$

Correspondingly, we obtain

$$a = \frac{\lambda}{2}\left[f(x_1) + f(x_2)\right], \quad b^3 = \frac{3\lambda}{4}\left[f(x_1) - f(x_2)\right]. \tag{H.7}$$

In the following we assume that $b \geq 0$, which we can always ensure by relabeling the two stationary points.

Having determined $F(y)$, we consider now $G(y)$ and approximate it by a linear function

$$G(y) = \frac{1}{2\pi}\left(r + isy\right). \tag{H.8}$$

As [see Eq. (F.9)]

$$2\pi \operatorname{Ai}(x) = \int\limits_{-\infty}^{+\infty} dt \exp\left[i(tx + \tfrac{1}{3}t^3)\right], \quad 2\pi \operatorname{Ai}'(x) = i \int\limits_{-\infty}^{+\infty} t\,dt \exp\left[i(tx + \tfrac{1}{3}t^3)\right],$$

$$\text{(H.9a)}$$

we obtain [see Eq. (H.1)]

$$I \approx e^{ia}\left[r \operatorname{Ai}(-b^2) + s \operatorname{Ai}'(-b^2)\right]. \tag{H.10}$$

In order to determine the two unknown coefficients, we require that the result of the ordinary stationary-phase approximation is obtained in the limit where both stationary points are sufficiently far away (i.e. for $b \gg 1$). To this end we note the following asymptotic expansions (see App. F)

$$\operatorname{Ai}(-b^2) \sim \frac{1}{\sqrt{\pi b}} \cos(\zeta - \pi/4), \quad \operatorname{Ai}'(-b^2) \sim \frac{\sqrt{b}}{\sqrt{\pi}} \sin(\zeta - \pi/4), \tag{H.11}$$

where $\zeta = 2b^3/3$. Accordingly, we obtain

$$G_1\, e^{+i\pi/4} = \left[\frac{r}{2\sqrt{\pi b}} + \frac{s\sqrt{b}}{2i\sqrt{\pi}}\right], \quad G_2\, e^{-i\pi/4} = \left[\frac{r}{2\sqrt{\pi b}} - \frac{s\sqrt{b}}{2i\sqrt{\pi}}\right], \tag{H.12}$$

where

$$G_i = g(x_i)\left[\frac{2\pi i}{\lambda f''(x_i)}\right]^{1/2}. \tag{H.13}$$

Therefore, the coefficients in Eq. (H.10) are given by

$$r = \sqrt{\pi b}\left[G_1\, e^{+i\pi/4} + G_2\, e^{-i\pi/4}\right], \quad s = i\sqrt{\frac{\pi}{b}}\left[G_1\, e^{+i\pi/4} - G_2\, e^{-i\pi/4}\right]. \tag{H.14}$$

H.2. Two nearly coalescing complex stationary points

Normally, the location of the two stationary points x_1 and x_2 under consideration is determined by a parameter α. In the following we assume that they are distinct for $\alpha < \alpha_0$, coalesce for $\alpha = \alpha_0$ and become complex for $\alpha > \alpha_0$ [OT94]. The Airy uniform approximation as presented above can be used until the two real stationary points coalesce, i.e. for for $\alpha < \alpha_0$. However, the contribution to the integral from the region under consideration should (in general) depend smoothly on α. Thus, significant contributions to the integral are also expected for $\alpha > \alpha_0$, as long as $f'(x) \neq 0$ is "small". We therefore consider the point x_0 defined by $f''(x_0) = 0$, where the oscillations along the real integration line are as slow as possible. Around this point we can approximate the phase by a cubic polynomial as before

$$f(x) \approx f(x_0) + f'(x_0)(x - x_0) + \frac{f'''(x_0)}{6}(x - x_0)^3. \tag{H.15}$$

Here, we assume that all higher derivatives are of the same order as $f'''(x_0)$ and that $f'''(x_0) \gg f'(x_0)$. The last condition ensures that far away from x_0 the

oscillations are fast, i.e. that the integral is formed around $x = x_0$. Within this approximation we obtain

$$f'(x) \approx f'(x_0) + \frac{f'''(x_0)}{2}(x - x_0)^2, \tag{H.16}$$

meaning that the stationary points x_s of the phase are now complex and approximately given by

$$x_s \approx x_0 \pm i \sqrt{2 \frac{f'(x_0)}{f'''(x_0)}}. \tag{H.17}$$

Thus, the assumption $f'''(x_0) \gg f'(x_0)$ ensures that the imaginary part of the true stationary points is small, i.e. that they are located close to the real line (in the following we can assume that the first and the third derivative have the same sign, as otherwise the stationary points are real).

As long as the imaginary part in Eq. (H.17) is small, the two complex stationary points still influence the integral along the real line and significant contributions arise from the region around x_0. By using the expansion in Eq. (H.15), the contribution to the integral coming from the region of the real line close to the complex stationary points is approximately given by [see Eq. (H.1)]

$$I \approx \frac{2\pi g(x_0)}{\sqrt[3]{\lambda f'''(x_0)/2}} e^{i\lambda f(x_0)} \operatorname{Ai}\left[\frac{\lambda^{2/3} f'(x_0)}{\sqrt[3]{f'''(x_0)/2}} \right]. \tag{H.18}$$

This result is valid as long as the imaginary part of the stationary points is small, i.e. for $f'(x_0) \ll f'''(x_0)$ [see Eq. (H.17)] [if $g(x_0) = 0$ the linear term of the preexponent must be used in the approximation].

Summarizing, we can apply Eq. (H.2) for isolated stationary points, Eq. (H.10) for two (nearly) coalescing real stationary points and Eq. (H.18) for two (nearly) coalescing complex stationary points, as long as they are close to the real integration line (complex stationary points far away from the real line can be neglected).

I. Numerical calculation of Fourier integrals

In this appendix we consider Fourier integrals with finite boundaries

$$\int\limits_a^b dx\, e^{i\omega x} g(x). \tag{I.1}$$

As long as the required precision is not too high and the integral must be computed for many different oscillation frequencies ω, the method of choice is the fast Fourier transform (FFT). If, however, the integral should be computed for a single frequency with a very high precision, the second approach based on Chebyshev expansions is more suitable.

I.1. Fast Fourier transform (FFT)

Fourier-integrals (with finite limits) can be calculated very efficiently using the fast Fourier transform (FFT) algorithm [CT65]. To this end we apply the approximation

$$\int\limits_a^b dx\, e^{ipx} f(x) = \sum_{j=0}^{n-1} \int\limits_{x_j}^{x_{j+1}} dx\, e^{ipx} f(x) \approx \delta \sum_{j=0}^{n-1} e^{ipx_j} f(x_j), \tag{I.2}$$

where $x_j = a + j\delta$ with $\delta = (b-a)/n$. To be sufficiently general, we introduce $p_k = p_0 + [2\pi/(b-a)]\,k$ and obtain

$$\int\limits_a^b dx\, e^{ip_k x} f(x) \approx e^{i[2\pi a/(b-a)]\,k} \delta \sum_{j=0}^{n-1} e^{2\pi i\,(jk/n)} \left[e^{ip_0 x_j} f(x_j)\right]. \tag{I.3}$$

After fixing a value for n and setting $X_j = e^{ip_0 x_j} f(x_j)$, we can, e.g., use the FFTW_BACKWARD algorithm [FJ05], which computes

$$Y_k = \sum_{j=0}^{n-1} X_j e^{2\pi i\,(jk/n)} \tag{I.4}$$

to obtain an approximation for the Fourier integral with finite boundaries using Eq. (I.3). Note that the case $a = 0$ is particularly convenient.

I.2. Chebyshev integration

Fourier integrals with finite limits can be calculated very precisely using Chebyshev series expansions [PB75; PB84; Pie+83]. To this end we write

$$\int\limits_a^b dx\, e^{i\omega x} g(x) = \delta e^{i\omega c} \int\limits_{-1}^{+1} dt\, e^{i\Omega t} f(t), \tag{I.5}$$

where we used the change of variables $x(t) = c + \delta t$ with $c = (a+b)/2$, $\delta = (b-a)/2$, $f(t) = g[x(t)]$ and $\Omega = \delta\omega$. If the function $f(t)$ is slowly varying, its ex-

pansion into a Chebyshev series is rapidly converging [Boy01; Olv+10]

$$f(t) = \sum_{n=0}^{\infty}{}' c_n T_n(t), \quad T_n(t) = \cos(n\theta), \quad t = \cos\theta, \tag{I.6}$$

where

$$c_n = \frac{2}{\pi}\int\limits_{-1}^{+1} dt\, \frac{T_n(t)f(t)}{\sqrt{1-t^2}} = \frac{2}{\pi}\int\limits_{0}^{\pi} d\theta\, \cos(n\theta)f(\cos\theta) \tag{I.7}$$

(the prime at the sum symbol indicates that the first coefficient in the sum is halved). The Chebyshev series coefficients can be calculated very efficiently using FFT and an estimate for the absolute error induced by the truncation of the Chebyshev series is obtained from the last series coefficients [Boy01].

Having computed the series coefficients, the Chebyshev moments

$$C_n(z) = \int\limits_{-1}^{+1} dt\, T_{2n}(t)e^{izt}, \quad S_n(z) = i\int\limits_{-1}^{+1} dt\, T_{2n+1}(t)e^{izt} \tag{I.8}$$

must be determined in order to evaluate the integral in Eq. (I.5). To this end we note the following three-term recurrence relations [Pie+83]

$$z^2(n-1)(2n-1)C_{n+1}(z) - (n+1)(n-1)\left[4z^2 - 8(2n+1)(2n-1)\right]C_n(z)$$
$$+ z^2(n+1)(2n+1)C_{n-1}(z) = -16(n-1)(n+1)\cos(z) + 12z\sin(z), \tag{I.9a}$$

$$z^2(2n-1)nS_{n+1}(z) - (2n+3)(2n-1)\left[z^2 - 8n(n+1)\right]S_n(z)$$
$$+ z^2(2n+3)(n+1)S_{n-1}(z) = 4(2n-1)(2n+3)\sin(z) + 12z\cos(z). \tag{I.9b}$$

For certain parameters (e.g., for very large frequencies), the Chebyshev moments can be calculated by applying the above relations in the forward direction (e.g., S_n can be calculated by starting from S_0 and S_1). However, this procedure is in general numerically unstable and Olver's algorithm must be used [Olv67; Wim84]. By calculating C_n and S_n independently, we can estimate the numerical error of the calculated Chebyshev moments by evaluating the relation [Pie+83]

$$S_n(z) = \frac{\sin z}{2(n+1)n} - \frac{z}{4n}C_n(z) + \frac{z}{4(n+1)}C_{n+1}(z). \tag{I.10}$$

Bibliography

[AB69]   S. L. Adler and W. A. Bardeen. *Absence of Higher-Order Corrections in the Anomalous Axial-Vector Divergence Equation*. Phys. Rev. **182**, 1517 (1969).

[Adl69]   S. L. Adler. *Axial-Vector Vertex in Spinor Electrodynamics*. Phys. Rev. **177**, 2426 (1969).

[AEE08]   F. T. Avignone III, S. R. Elliott, and J. Engel. *Double beta decay, Majorana neutrinos, and neutrino mass*. Rev. Mod. Phys. **80**, 481 (2008).

[AF03]   M. J. Ablowitz and A. S. Fokas. *Complex Variables: Introduction and Applications*. Cambridge University Press, 2003.

[Aff88]   I. Affleck. *Photon propagation in a plane-wave field*. J. Phys. A **21**, 693 (1988).

[Ahm+09]   I. Ahmad, S. A. Trushin, Z. Major, C. Wandt, S. Klingebiel, T. Wang, et al. *Frontend light source for short-pulse pumped OPCPA system*. Appl. Phys. B **97**, 529 (2009).

[AM13]   R. A. Anikin and N. V. Mikheev. *Radiative neutrino decay in a strong magnetic field*. Phys. Atom. Nucl. **76**, 1541 (2013).

[Aok+82]   K. Aoki, Z. Hioki, R. Kawabe, M. Konuma, and T. Muta. *Electroweak Theory*. Prog. Theor. Phys. Suppl. **73**, 1 (1982).

[ATLAS12]   ATLAS Collaboration. *Combined search for the Standard Model Higgs boson using up to $4.9\,\mathrm{fb}^{-1}$ of pp collision data at $\sqrt{s} = 7\,\mathrm{TeV}$ with the ATLAS detector at the LHC*. Phys. Lett. B **710**, 49 (2012).

[Bai+76]   V. N. Baier, V. M. Katkov, A. I. Milstein, and V. M. Strakhovenko. *The theory of quantum processes in the field of a strong electromagnetic wave*. Sov. Phys. JETP **42**, 400 (1976).

[Ban+09]   A. Bandyopadhyay, S. Choubey, R. Gandhi, S. Goswami, B. L. Roberts, J. Bouchez, et al. *Physics at a future Neutrino Factory and super-beam facility*. Rep. Prog. Phys. **72**, 106201 (2009).

[Bar69]   W. A. Bardeen. *Anomalous Ward Identities in Spinor Field Theories*. Phys. Rev. **184**, 1848 (1969).

[BB67]   R. Baier and P. Breitenlohner. *Photon propagation in external fields*. Acta. Phys. Austr. **25**, 212 (1967).

[BB70]   Z. Bialynicka-Birula and I. Bialynicki-Birula.
             *Nonlinear Effects in Quantum Electrodynamics. Photon
             Propagation and Photon Splitting in an External Field*.
             Phys. Rev. D **2**, 2341 (1970).

[BDF12a]   M. Boca, V. Dinu, and V. Florescu.
             Electron distributions in nonlinear Compton scattering.
             Phys. Rev. A **86**, 013414 (2012).

[BDF12b]   M. Boca, V. Dinu, and V. Florescu. *Spin effects in nonlinear
             Compton scattering in a plane-wave laser pulse*.
             Nucl. Instr. Meth. Phys. Res. B **279**, 12 (2012).

[Bec+02]   W. Becker, F. Grasbon, R. Kopold, D. B. Milošević, G. G. Paulus,
             and H. Walther. *Above-Threshold Ionization: From Classical
             Features to Quantum Effects*.
             Adv. At. Mol. Opt. Phys. **48**, 35 (2002).

[Ber+06]   J. S. Berg, S. A. Bogacz, S. Caspi, J. Cobb, R. C. Fernow,
             J. C. Gallardo, et al. *Cost-effective design for a neutrino factory*.
             Phys. Rev. ST Accel. Beams **9**, 011001 (2006).

[Ber69]   I. Berson. *Electron in the quantized field of a monochromatic
             electromagnetic wave*. Sov. Phys. JETP **29**, 871 (1969).

[Bet47]   H. A. Bethe. *The Electromagnetic Shift of Energy Levels*.
             Phys. Rev. **72**, 339 (1947).

[BF11]   M. Boca and V. Florescu.
             Thomson and Compton scattering with an intense laser pulse.
             Eur. Phys. J. D **61**, 449 (2011).

[BG03]   K. Bhattacharya and A. K. Ganguly. *Axial-vector–vector amplitude
             and neutrino effective charge in a magnetized medium*.
             Phys. Rev. D **68**, 053011 (2003).

[BGS12]   C. Broggini, C. Giunti, and A. Studenikin.
             Electromagnetic Properties of Neutrinos.
             Adv. High Energy Phys. **2012**, 459526 (2012).

[BH34]   H. Bethe and W. Heitler. *On the Stopping of Fast Particles and on
             the Creation of Positive Electrons*. Proc. R. Soc. A **146**, 83 (1934).

[BI70]   E. Brezin and C. Itzykson.
             Pair Production in Vacuum by an Alternating Field.
             Phys. Rev. D **2**, 1191 (1970).

[Bil10]   S. Bilenky.
             Introduction to the Physics of Massive and Mixed Neutrinos.
             Springer, 2010.

[BJ69]   J. S. Bell and R. Jackiw. *A PCAC puzzle: $\pi^0 \to \gamma\gamma$ in the σ-model*.
             Nuovo Cimento A **60**, 47 (1969).

[BK08]   A. R. Bell and J. G. Kirk.
             Possibility of Prolific Pair Production with High-Power Lasers.
             Phys. Rev. Lett. **101**, 200403 (2008).

[BKM99]   M. Y. Borovkov, A. V. Kuznetsov, and N. V. Mikheev. *One-Loop Amplitude of the Transition $j \to f\bar{f} \to j'$ in an External Electromagnetic Field*. Phys. Atom. Nucl. **62**, 1601 (1999).

[BKS75]   V. N. Baier, V. M. Katkov, and V. M. Strakhovenko. *Operator approach to quantum electrodynamics in an external field: The mass operator*. Sov. Phys. JETP **40**, 225 (1975).

[BKS98]   V. N. Baier, V. M. Katkov, and V. M. Strakhovenko. *Electromagnetic Processes at High Energies in Oriented Single Crystals*. World Scientific, 1998.

[Ble50]   K. Bleuler. *Eine neue Methode zur Behandlung der longitudinalen und skalaren Photonen*. Helv. Phys. Acta **23**, 567 (1950).

[BLM90]   W. Becker, S. Long, and J. K. McIver. *Higher-harmonic production in a model atom with short-range potential*. Phys. Rev. A **41**, 4112 (1990).

[BM75]   W. Becker and H. Mitter. *Vacuum polarization in laser fields*. J. Phys. A **8**, 1638 (1975).

[BM76]   V. N. Baier and A. I. Milstein. *Radiation effects in the field of an electromagnetic wave*. Sov. Phys. Dokl. **21**, 734 (1976).

[BMS76]   V. N. Baier, A. I. Milstein, and V. M. Strakhovenko. *Interaction between a photon and an intense electromagnetic wave*. Sov. Phys. JETP **42**, 961 (1976).

[BMT59]   V. Bargmann, L. Michel, and V. L. Telegdi. *Precession of the Polarization of Particles Moving in a Homogeneous Electromagnetic Field*. Phys. Rev. Lett. **2**, 435 (1959).

[Bog+14]   M. Bogomilov et al. *Neutrino factory*. Phys. Rev. ST Accel. Beams **17**, 121002 (2014).

[Boy01]   J. P. Boyd. *Chebyshev and Fourier spectral methods*. Dover, 2001.

[BP87]   S. M. Bilenky and S. T. Petcov. *Massive neutrinos and neutrino oscillations*. Rev. Mod. Phys. **59**, 671 (1987).

[BP99]   D. Bardin and G. Passarino. *The Standard Model in the Making: Precision Study of the Electroweak Interactions*. Oxford University Press, 1999.

[BPP77]   S. M. Bilenky, S. T. Petcov, and B. Pontecorvo. *Lepton mixing, $\mu \to e + \gamma$ decay and neutrino oscillations*. Phys. Lett. B **67**, 309 (1977).

[BPP98]   S. J. Brodsky, H. Pauli, and S. S. Pinsky. *Quantum chromodynamics and other field theories on the light cone*. Phys. Rep. **301**, 299 (1998).

[BR13]   R. Battesti and C. Rizzo. *Magnetic and electric properties of a quantum vacuum*. Rep. Prog. Phys. **76**, 016401 (2013).

[Bro02]   C. Brouder. *Renormalization of QED in an external field*.
            EPJ direct **4**, 1 (2002).

[BS68]   I. A. Batalin and A. E. Shabad. FIAN Preprint **166**, (1968).

[BS71]   I. A. Batalin and A. E. Shabad. *Green's Function of a Photon in a
            Constant Homogeneous Electromagnetic Field of General Form*.
            Sov. Phys. JETP **33**, 483 (1971).

[BSH86]   M. Böhm, H. Spiesberger, and W. Hollik.
            *On the 1-Loop Renormalization of the Electroweak Standard Model
            and its Application to Leptonic Processes*.
            Fortschr. Physik **34**, 687 (1986).

[BTZ93]   A. V. Borisov, A. I. Ternov, and V. C. Zhukovsky. *Electron-positron
            pair production by a neutrino in an external electromagnetic field*.
            Phys. Lett. B **318**, 489 (1993).

[Bul+10a]   S. S. Bulanov, T. Z. Esirkepov, A. G. R. Thomas, J. K. Koga, and
            S. V. Bulanov.
            Schwinger Limit Attainability with Extreme Power Lasers.
            Phys. Rev. Lett. **105**, 220407 (2010).

[Bul+10b]   S. S. Bulanov, V. D. Mur, N. B. Narozhny, J. Nees, and
            V. S. Popov. *Multiple Colliding Electromagnetic Pulses: A Way to
            Lower the Threshold of e^+e^- Pair Production from Vacuum*.
            Phys. Rev. Lett. **104**, 220404 (2010).

[Bul+13]   S. S. Bulanov, C. B. Schroeder, E. Esarey, and W. P. Leemans.
            *Electromagnetic cascade in high-energy electron, positron, and
            photon interactions with intense laser pulses*.
            Phys. Rev. A **87**, 062110 (2013).

[Bul+96]   C. Bula, K. T. McDonald, E. J. Prebys, C. Bamber, S. Boege,
            T. Kotseroglou, et al.
            Observation of Nonlinear Effects in Compton Scattering.
            Phys. Rev. Lett. **76**, 3116 (1996).

[Bur+97]   D. L. Burke, R. C. Field, G. Horton-Smith, J. E. Spencer, D. Walz,
            S. C. Berridge, et al.
            Positron Production in Multiphoton Light-by-Light Scattering.
            Phys. Rev. Lett. **79**, 1626 (1997).

[BV81]   J. Bergou and S. Varro. *Nonlinear scattering processes in the
            presence of a quantised radiation field. II. Relativistic treatment*.
            J. Phys. A **14**, 2281 (1981).

[BW34]   G. Breit and J. A. Wheeler. *Collision of Two Light Quanta*.
            Phys. Rev. **46**, 1087 (1934).

[CFU57]   C. Chester, B. Friedman, and F. Ursell.
            An extension of the method of steepest descents.
            Math. Proc. Cambridge Philos. Soc. **53**, 599 (1957).

[Ché+12]   G. Chériaux, F. Giambruno, A. Fréneaux, F. Leconte,
            L. P. Ramirez, P. Georges, et al.
            Apollon-10P: Status and implementation.
            AIP Conf. Proc. **1462**, 78 (2012).

[Chu+13]   Y. Chu, X. Liang, L. Yu, Y. Xu, L. Xu, L. Ma, et al.
            High-contrast 2.0 Petawatt Ti:sapphire laser system.
            Opt. Express **21**, 29231 (2013).

[CI69]   E. A. Choban and A. N. Ivanov.
            *The Production of Lepton Pairs by High-Energy Neutrinos in the
            Field of a Strong Electromagnetic Wave*.
            Sov. Phys. JETP **29**, 109 (1969).

[CL82]   T. Cheng and L. Li. *Gauge theory of elementary particle physics*.
            Oxford University Press, 1982.

[CLF]   *Central Laser Facility* (CLF).

[CM02]   M. V. Chistyakov and N. V. Mikheev.
            Photon-Neutrino Interactions in Strong Magnetic Field.
            Mod. Phys. Lett. A **17**, 2553 (2002).

[CM69]   S. Chang and S. Ma. *Feynman Rules and Quantum
            Electrodynamics at Infinite Momentum*.
            Phys. Rev. **180**, 1506 (1969).

[CMS12]   CMS Collaboration. *Combined results of searches for the standard
            model Higgs boson in pp collisions at $\sqrt{s} = 7\,\mathrm{TeV}$*.
            Phys. Lett. B **710**, 26 (2012).

[Col84]   J. C. Collins. *Renormalization*. Cambridge University Press, 1984.

[Cor+13]   H. M. C. Cortés, C. Müller, C. H. Keitel, and A. Pálffy.
            Nuclear recollisions in laser-assisted α decay.
            Phys. Lett. B **723**, 401 (2013).

[Cor93]   P. B. Corkum.
            Plasma perspective on strong field multiphoton ionization.
            Phys. Rev. Lett. **71**, 1994 (1993).

[CT65]   J. W. Cooley and J. W. Tukey.
            An algorithm for the machine calculation of complex Fourier series.
            Math. Comp. **19**, 297 (1965).

[Cut60]   R. E. Cutkosky.
            Singularities and Discontinuities of Feynman Amplitudes.
            J. Math. Phys. **1**, 429 (1960).

[DD11]   C. K. Dumlu and G. V. Dunne. *Interference effects in Schwinger
            vacuum pair production for time-dependent laser pulses*.
            Phys. Rev. D **83**, 065028 (2011).

[Den93]   A. Denner.
            *Techniques for the Calculation of Electroweak Radiative Corrections
            at the One-Loop Level and Results for W-physics at LEP 200*.
            Fortschr. Phys. **41**, 307 (1993).

[DG00]   W. Dittrich and H. Gies. *Probing the Quantum Vacuum.*
           Springer, 2000.

[DGH94]   J. F. Donoghue, E. Golowich, and B. R. Holstein.
           Dynamics of the Standard Model.
           Cambridge University Press, 1994.

[DGS09]   G. V. Dunne, H. Gies, and R. Schützhold.
           Catalysis of Schwinger vacuum pair production.
           Phys. Rev. D **80**, 111301 (2009).

[DHK09]   A. Di Piazza, K. Z. Hatsagortsyan, and C. H. Keitel.
           *Strong Signatures of Radiation Reaction below the
           Radiation-Dominated Regime*. Phys. Rev. Lett. **102**, 254802 (2009).

[Di+09]   A. Di Piazza, E. Lötstedt, A. I. Milstein, and C. H. Keitel.
           Barrier Control in Tunneling e^+–e^- Photoproduction.
           Phys. Rev. Lett. **103**, 170403 (2009).

[Di+12]   A. Di Piazza, C. Müller, K. Z. Hatsagortsyan, and C. H. Keitel.
           *Extremely high-intensity laser interactions with fundamental
           quantum systems*. Rev. Mod. Phys. **84**, 1177 (2012).

[Di+13]   A. Di Piazza. *On refractive processes in strong laser field quantum
           electrodynamics*. Ann. Phys. **338**, 302 (2013).

[Dic+09]   D. A. Dicus, A. Farzinnia, W. W. Repko, and T. M. Tinsley.
           Muon decay in a laser field. Phys. Rev. D **79**, 013004 (2009).

[Din+14a] V. Dinu, T. Heinzl, A. Ilderton, M. Marklund, and G. Torgrimsson.
           Photon polarization in light-by-light scattering: Finite size effects.
           Phys. Rev. D **90**, 045025 (2014).

[Din+14b] V. Dinu, T. Heinzl, A. Ilderton, M. Marklund, and G. Torgrimsson.
           Vacuum refractive indices and helicity flip in strong-field QED.
           Phys. Rev. D **89**, 125003 (2014).

[Din13]   V. Dinu. *Exact final-state integrals for strong-field QED*.
           Phys. Rev. A **87**, 052101 (2013).

[Dir27]   P. A. M. Dirac.
           The Quantum Theory of the Emission and Absorption of Radiation.
           Proc. R. Soc. A **114**, 243 (1927).

[Dir28]   P. A. M. Dirac. *The Quantum Theory of the Electron*.
           Proc. R. Soc. A **117**, 610 (1928).

[Dir30]   P. A. M. Dirac. *A Theory of Electrons and Protons*.
           Proc. R. Soc. A **126**, 360 (1930).

[Dir49]   P. A. M. Dirac. *Forms of Relativistic Dynamics*.
           Rev. Mod. Phys. **21**, 392 (1949).

[DMD76]   L. L. DeRaad, K. A. Milton, and N. D. H. Dass.
           Photon decay into neutrinos in a strong magnetic field.
           Phys. Rev. D **14**, 3326 (1976).

[DMK07]   A. Di Piazza, A. I. Milstein, and C. H. Keitel.
           Photon splitting in a laser field. Phys. Rev. A **76**, 032103 (2007).

[DMN13]   A. A. Dobrynina, N. V. Mikheev, and E. N. Narynskaya.
           Neutrino self-energy operator and neutrino magnetic moment.
           Phys. Atom. Nucl. **76**, 1352 (2013).

[DRT07]   D. A. Dicus, W. W. Repko, and T. M. Tinsley. *Pair production
           with neutrinos in an intense background magnetic field*.
           Phys. Rev. D **76**, 025005 (2007).

[DS01]   M. S. Dvornikov and A. I. Studenikin. *Neutrino oscillations in the
           field of a linearly polarized electromagnetic wave*.
           Phys. Atom. Nucl. **64**, 1624 (2001).

[DS04a]   M. S. Dvornikov and A. I. Studenikin.
           Electromagnetic form factors of a massive neutrino.
           J. Exp. Theor. Phys. **99**, 254 (2004).

[DS04b]   M. S. Dvornikov and A. I. Studenikin. *Parametric resonance in
           neutrino oscillations in periodically varying electromagnetic fields*.
           Phys. Atom. Nucl. **67**, 719 (2004).

[DS04c]   M. Dvornikov and A. Studenikin.
           Electric charge and magnetic moment of a massive neutrino.
           Phys. Rev. D **69**, 073001 (2004).

[Dys49a]   F. J. Dyson.
           The Radiation Theories of Tomonaga, Schwinger, and Feynman.
           Phys. Rev. **75**, 486 (1949).

[Dys49b]   F. J. Dyson. *The S Matrix in Quantum Electrodynamics*.
           Phys. Rev. **75**, 1736 (1949).

[EKK09]   F. Ehlotzky, K. Krajewska, and J. Z. Kamiński.
           *Fundamental processes of quantum electrodynamics in laser fields of
           relativistic power*. Rep. Prog. Phys. **72**, 046401 (2009).

[ELI]   *Extreme Light Infrastructure* (ELI).

[Elk+11]   N. V. Elkina, A. M. Fedotov, I. Y. Kostyukov, M. V. Legkov,
           N. B. Narozhny, E. N. Nerush, et al.
           QED cascades induced by circularly polarized laser fields.
           Phys. Rev. ST Accel. Beams **14**, 054401 (2011).

[ELS00]   A. M. Egorov, A. E. Lobanov, and A. I. Studenikin.
           Neutrino oscillations in electromagnetic fields.
           Phys. Lett. B **491**, 137 (2000).

[ER66]   J. H. Eberly and H. R. Reiss.
           Electron Self-Energy in Intense Plane-Wave Field.
           Phys. Rev. **145**, 1035 (1966).

[Erd09]   A. Erdas. *Neutrino self-energy in an external magnetic field*.
           Phys. Rev. D **80**, 113004 (2009).

[Esc+05]   S. Escoffier, P. Y. Bertin, M. Brossard, E. Burtin, C. Cavata,
           N. Colombel, et al. *Accurate measurement of the electron beam
           polarization in JLab Hall A using Compton polarimetry*.
           Nucl. Instrum. Meth. A **551**, 563 (2005).

[ESL09]   E. Esarey, C. B. Schroeder, and W. P. Leemans.
            Physics of laser-driven plasma-based electron accelerators.
            Rev. Mod. Phys. **81**, 1229 (2009).

[Eva94]   G. A. Evans. *An alternative method for irregular oscillatory
            integrals over a finite range*. Int. J. Comput. Math. **52**, 185 (1994).

[Far+09]   A. Farzinnia, D. A. Dicus, W. W. Repko, and T. M. Tinsley.
            Muon decay in a linearly polarized laser field.
            Phys. Rev. D **80**, 073004 (2009).

[FE64]   Z. Fried and J. H. Eberly. *Scattering of a High-Intensity,
            Low-Frequency Electromagnetic Wave by an Unbound Electron*.
            Phys. Rev. **136**, B871 (1964).

[Fed+10]   A. M. Fedotov, N. B. Narozhny, G. Mourou, and G. Korn.
            Limitations on the Attainable Intensity of High Power Lasers.
            Phys. Rev. Lett. **105**, 080402 (2010).

[Fer34a]   E. Fermi. *Tentativo di una Teoria Dei Raggi β*.
            Il Nuovo Cimento **11**, 1 (1934).

[Fer34b]   E. Fermi. *Versuch einer Theorie der β-Strahlen. I*.
            Z. Phys. **88**, 161 (1934).

[Fey48a]   R. P. Feynman. *Relativistic Cut-Off for Quantum Electrodynamics*.
            Phys. Rev. **74**, 1430 (1948).

[Fey48b]   R. P. Feynman.
            Space-Time Approach to Non-Relativistic Quantum Mechanics.
            Rev. Mod. Phys. **20**, 367 (1948).

[Fey49a]   R. P. Feynman. *Space-Time Approach to Quantum Electrodynamics*.
            Phys. Rev. **76**, 769 (1949).

[Fey49b]   R. P. Feynman. *The Theory of Positrons*.
            Phys. Rev. **76**, 749 (1949).

[Fey50]   R. P. Feynman. *Mathematical Formulation of the Quantum Theory
            of Electromagnetic Interaction*. Phys. Rev. **80**, 440 (1950).

[Fey51]   R. P. Feynman. *An Operator Calculus Having Applications in
            Quantum Electrodynamics*. Phys. Rev. **84**, 108 (1951).

[FGS91]   E. S. Fradkin, D. M. Gitman, and S. M. Shvartsman.
            Quantum Electrodynamics with Unstable Vacuum. Springer, 1991.

[Fil85]   P. Filipowicz. *Relativistic electron in a quantised plane wave*.
            J. Phys. A **18**, 1675 (1985).

[FJ05]   M. Frigo and S. G. Johnson.
            The Design and Implementation of FFTW3.
            Proc. IEEE **93**, 216 (2005).

[FM13]   A. M. Fedotov and A. A. Mironov. *Pair creation by collision of an
            intense laser pulse with a high-frequency photon beam*.
            Phys. Rev. A **88**, 062110 (2013).

[Fuj79]   K. Fujikawa.
            Path-Integral Measure for Gauge-Invariant Fermion Theories.
            Phys. Rev. Lett. **42**, 1195 (1979).

[Fur51]   W. H. Furry. *On Bound States and Scattering in Positron Theory*.
            Phys. Rev. **81**, 115 (1951).

[Gau+10]   E. W. Gaul, M. Martinez, J. Blakeney, A. Jochmann, M. Ringuette,
            D. Hammond, et al.
            *Demonstration of a 1.1 petawatt laser based on a hybrid optical
            parametric chirped pulse amplification/mixed Nd:glass amplifier*.
            Appl. Opt. **49**, 1676 (2010).

[Gee12]   S. Geer. *Muon colliders and neutrino factories. Muon colliders and
            neutrino factories*, (2012).

[Gee98]   S. Geer. *Neutrino beams from muon storage rings: Characteristics
            and physics potential*. Phys. Rev. D **57**, 6989 (1998).

[GH14]   D. G. Green and C. N. Harvey.
            Transverse Spreading of Electrons in High-Intensity Laser Fields.
            Phys. Rev. Lett. **112**, 164801 (2014).

[GIM70]   S. L. Glashow, J. Iliopoulos, and L. Maiani.
            Weak Interactions with Lepton-Hadron Symmetry.
            Phys. Rev. D **2**, 1285 (1970).

[GJ72]   D. J. Gross and R. Jackiw.
            Effect of Anomalies on Quasi-Renormalizable Theories.
            Phys. Rev. D **6**, 477 (1972).

[GK07]   C. Giunti and C. W. Kim.
            Fundamentals of Neutrino Physics and Astrophysics.
            Oxford University Press, 2007.

[GKS14]   H. Gies, F. Karbstein, and R. Shaisultanov.
            Laser photon merging in an electromagnetic field inhomogeneity.
            Phys. Rev. D **90**, 033007 (2014).

[Gla63]   R. J. Glauber.
            Coherent and Incoherent States of the Radiation Field.
            Phys. Rev. **131**, 2766 (1963).

[GMV92]   A. A. Gvozdev, N. V. Mikheev, and L. A. Vassilevskaya.
            *The magnetic catalysis of the radiative decay of a massive neutrino
            in the standard model with lepton mixing*.
            Phys. Lett. B **289**, 103 (1992).

[GMV93]   A. A. Gvozdev, N. V. Mikheev, and L. A. Vassilevskaya.
            *The radiative decay $\nu_i \to \nu_j \gamma$ $(i \neq j)$ of a massive neutrino in the
            field of an intensive electromagnetic wave*.
            Phys. Lett. B **313**, 161 (1993).

[GMV94a]   A. A. Gvozdev, N. V. Mikheev, and L. A. Vassilevskaya.
            *Electromagnetic catalysis of the radiative transitions of $\nu_i \to \nu_j \gamma$
            type in the field of an intense monochromatic wave*.
            Phys. Lett. B **321**, 108 (1994).

[GMV94b]   A. A. Gvozdev, N. V. Mikheev, and L. A. Vassilevskaya. *The radiative decay of a high energy neutrino in the Coulomb field of a nucleus*. Phys. Lett. B **323**, 179 (1994).

[GMV96]   A. A. Gvozdev, N. V. Mikheev, and L. A. Vassilevskaya. *Radiative decay of the massive neutrino in external electromagnetic fields*. Phys. Rev. D **54**, 5674 (1996).

[GMV97]   A. A. Gvozdev, N. V. Mikheev, and L. A. Vassilevskaya. *Resonance neutrino bremsstrahlung $\nu \to \nu\gamma$ in a strong magnetic field*. Phys. Lett. B **410**, 211 (1997).

[GN72]   D. V. Galtsov and N. S. Nikitina. *Photoneutrino Processes in a Strong Field*. Sov. Phys. JETP **35**, 1047 (1972).

[GR07]   I. S. Gradshteyn and I. M. Ryzhik. *Table of Integrals, Series, and Products*. Academic Press, 2007.

[GR11]   H. Gies and L. Roessler. *Vacuum polarization tensor in inhomogeneous magnetic fields*. Phys. Rev. D **84**, 065035 (2011).

[GR96]   W. Greiner and J. Reinhardt. *Field Quantization*. Springer, 1996.

[GS00a]   H. Gies and R. Shaisultanov. *Axial vector current in an electromagnetic field and low-energy neutrino-photon interactions*. Phys. Rev. D **62**, 073003 (2000).

[GS00b]   H. Gies and R. Shaisultanov. *Neutrino interactions with a weak slowly varying electromagnetic field*. Phys. Lett. B **480**, 129 (2000).

[GS01]   H. Gies and C. Schubert. *Vacuum polarisation tensors in constant electromagnetic fields: Part III*. Nucl. Phys. B **609**, 313 (2001).

[GS09]   C. Giunti and A. Studenikin. *Neutrino electromagnetic properties*. Phys. Atom. Nucl. **72**, 2089 (2009).

[GSL]   *GNU Scientific Library* (GSL).

[Gup50]   S. N. Gupta. *Theory of Longitudinal Photons in Quantum Electrodynamics*. Proc. Roy. Soc. **63A**, 681 (1950).

[Hag+07]   K. Hagiwara, A. D. Martin, D. Nomura, and T. Teubner. *Improved predictions for $g - 2$ of the muon and $\alpha_{\mathrm{QED}}(M_Z^2)$*. Phys. Lett. B **649**, 173 (2007).

[HE36]   W. Heisenberg and H. Euler. *Folgerungen aus der Diracschen Theorie des Positrons*. Z. Phys. **98**, 714 (1936).

[Hei01]   T. Heinzl. *Light-Cone Quantization: Foundations and Applications*. Springer, 2001, 55.

[HHI09]   C. Harvey, T. Heinzl, and A. Ilderton. *Signatures of high-intensity Compton scattering*. Phys. Rev. A **79**, 063407 (2009).

[HHK04]   B. Henrich, K. Z. Hatsagortsyan, and C. H. Keitel.
            Positronium in Intense Laser Fields.
            Phys. Rev. Lett. **93**, 013601 (2004).

[HI09]   T. Heinzl and A. Ilderton.
            A Lorentz and gauge invariant measure of laser intensity.
            Opt. Commun. **282**, 1879 (2009).

[HIK15]   C. N. Harvey, A. Ilderton, and B. King.
            Testing numerical implementations of strong-field electrodynamics.
            Phys. Rev. A **91**, 013822 (2015).

[HIM10]   T. Heinzl, A. Ilderton, and M. Marklund.
            Finite size effects in stimulated laser pair production.
            Phys. Lett. B **692**, 250 (2010).

[HIM11]   F. Hebenstreit, A. Ilderton, and M. Marklund.
            Pair production: The view from the lightfront.
            Phys. Rev. D **84**, 125022 (2011).

[HMK06]   K. Z. Hatsagortsyan, C. Müller, and C. H. Keitel.
            Microscopic laser-driven high-energy colliders.
            Europhys. Lett. **76**, 29 (2006).

[Hol90]   W. F. L. Hollik. *Radiative Corrections in the Standard Model and
            Their Rôle for Precision Tests of the Electroweak Theory*.
            Fortschr. Phys. **38**, 165 (1990).

[HSK10]   T. Heinzl, D. Seipt, and B. Kämpfer.
            Beam-shape effects in nonlinear Compton and Thomson scattering.
            Phys. Rev. A **81**, 022125 (2010).

[IDS]   *The International Design Study for the Neutrino Factory* (IDS).

[Ipp+11]   A. Ipp, J. Evers, C. H. Keitel, and K. Z. Hatsagortsyan.
            Streaking at high energies with electrons and positrons.
            Phys. Lett. B **702**, 383 (2011).

[IR97]   A. N. Ioannisian and G. G. Raffelt.
            Cherenkov radiation by massless neutrinos in a magnetic field.
            Phys. Rev. D **55**, 7038 (1997).

[ISS]   *International scoping study of a future Neutrino Factory and
            super-beam facility* (ISS).

[IT13]   A. Ilderton and G. Torgrimsson. *Scattering in plane-wave
            backgrounds: Infrared effects and pole structure*.
            Phys. Rev. D **87**, 085040 (2013).

[IZ05]   C. Itzykson and J. B. Zuber. *Quantum field theory*. Dover, 2005.

[Jac98]   J. D. Jackson. *Classical Electrodynamics*. John Wiley & Sons, 1998.

[JJ69]   R. Jackiw and K. Johnson. *Anomalies of the Axial-Vector Current*.
            Phys. Rev. **182**, 1459 (1969).

[JKP12]   C. J. Joachain, N. J. Kylstra, and R. M. Potvliege.
            Atoms in Intense Laser Fields. Cambridge University Press, 2012.

[JM13]   M. J. A. Jansen and C. Müller. *Strongly enhanced pair production in combined high- and low-frequency laser fields*.
Phys. Rev. A **88**, 052125 (2013).

[Kap14]   D. M. Kaplan. *Muon Colliders and Neutrino Factories*. *Muon Colliders and Neutrino Factories*, (2014).

[Kar+08]   S. Karsch, Z. Major, J. Fülöp, I. Ahmad, T. Wang, A. Henig, et al.
The Petawatt Field Synthesizer: A New Approach to Ultrahigh Field Generation. Advanced Solid-State Photonics, WF1 (2008).

[Kar+12]   F. Karbstein, L. Roessler, B. Döbrich, and H. Gies.
Optical Probes of the Quantum Vacuum: The Photon Polarization Tensor in External Fields.
Int. J. Mod. Phys. Conf. Ser. **14**, 403 (2012).

[Kar13]   F. Karbstein. *Photon polarization tensor in a homogeneous magnetic or electric field*. Phys. Rev. D **88**, 085033 (2013).

[Kay03]   B. Kayser. *Neutrino Mass, Mixing, and Flavor Change*.
Springer, 2003.

[Kay81]   B. Kayser. *On the quantum mechanics of neutrino oscillation*.
Phys. Rev. D **24**, 110 (1981).

[KER13]   B. King, N. Elkina, and H. Ruhl.
Photon polarization in electron-seeded pair-creation cascades.
Phys. Rev. A **87**, 042117 (2013).

[KI09]   F. Krausz and M. Ivanov. *Attosecond physics*.
Rev. Mod. Phys. **81**, 163 (2009).

[Kim+13]   H. T. Kim, K. H. Pae, H. J. Cha, I. J. Kim, T. J. Yu, J. H. Sung, et al. *Enhancement of Electron Energy to the Multi-GeV Regime by a Dual-Stage Laser-Wakefield Accelerator Pumped by Petawatt Laser Pulses*. Phys. Rev. Lett. **111**, 165002 (2013).

[Kin15]   B. King. *Double Compton scattering in a constant crossed field*.
Phys. Rev. A **91**, 033415 (2015).

[Kir+12]   H. Kiriyama, T. Shimomura, H. Sasao, Y. Nakai, M. Tanoue, S. Kondo, et al.
Temporal contrast enhancement of petawatt-class laser pulses.
Opt. Lett. **37**, 3363 (2012).

[KK12a]   K. Krajewska and J. Z. Kamiński.
Breit-Wheeler process in intense short laser pulses.
Phys. Rev. A **86**, 052104 (2012).

[KK12b]   K. Krajewska and J. Z. Kamiński.
Compton process in intense short laser pulses.
Phys. Rev. A **85**, 062102 (2012).

[KK13]   K. Krajewska and J. Z. Kamiński. *Spin effects in nonlinear Compton scattering in ultrashort linearly-polarized laser pulses*.
Laser Part. Beams **31**, 503 (2013).

[KK14]   K. Krajewska and J. Z. Kamiński.
            Breit-Wheeler pair creation by finite laser pulses.
            J. Phys.: Conf. Ser. **497**, 012016 (2014).

[Kle29]   O. Klein. *Die Reflexion von Elektronen an einem Potentialsprung
            nach der relativistischen Dynamik von Dirac*.
            Z. Phys. **53**, 157 (1929).

[KM03]   A. Kuznetsov and N. Mikheev.
            Electroweak Processes in External Electromagnetic Fields.
            Springer, 2003.

[KM13]   A. Kuznetsov and N. Mikheev.
            Electroweak Processes in External Active Media. Springer, 2013.

[KM97]   A. V. Kuznetsov and N. V. Mikheev.
            *Neutrino energy and momentum loss through the process
            $\nu \to \nu e^- e^+$ in a strong magnetic field*.
            Phys. Lett. B **394**, 123 (1997).

[KMR00]   A. V. Kuznetsov, N. V. Mikheev, and D. A. Rumyantsev.
            *Lepton pair production by high-energy neutrino in an external
            electromagnetic field*. Mod. Phys. Lett. A **15**, 573 (2000).

[KMR02]   A. V. Kuznetzov, N. V. Mikheev, and D. A. Rumyantsev.
            *Lepton-pair production by a neutrino in an external electromagnetic
            field*. Phys. Atom. Nucl. **65**, 277 (2002).

[KMR03]   A. V. Kuznetsov, N. V. Mikheev, and D. A. Rumyantsev.
            Process $\gamma\gamma \to \nu\bar{\nu}$ in a strong magnetic field.
            Phys. Atom. Nucl. **66**, 294 (2003).

[KMV98]   A. V. Kuznetsov, N. V. Mikheev, and L. A. Vassilevskaya.
            Photon splitting $\gamma \to \nu\bar{\nu}$ in an external magnetic field.
            Phys. Lett. B **427**, 105 (1998).

[Koh+12]   M. C. Kohler, T. Pfeifer, K. Z. Hatsagortsyan, and C. H. Keitel.
            Frontiers of Atomic High-Harmonic Generation.
            Adv. At. Mol. Opt. Phys. **61**, 159 (2012).

[Kor+11]   A. V. Korzhimanov, A. A. Gonoskov, E. A. Khazanov, and
            A. M. Sergeev. *Horizons of petawatt laser technology*.
            Phys. Usp. **54**, 9 (2011).

[KR13]   B. King and H. Ruhl.
            Trident pair production in a constant crossed field.
            Phys. Rev. D **88**, 013005 (2013).

[Kuc07]   M. Y. Kuchiev. *Production of High-Energy Particles in Laser and
            Coulomb Fields and the $e^+ e^-$ Antenna*.
            Phys. Rev. Lett. **99**, 130404 (2007).

[Kuc87]   M. Y. Kuchiev. *Atomic antenna*. JETP Lett. **45**, 404 (1987).

[Kuz+06]   A. V. Kuznetsov, N. V. Mikheev, G. G. Raffelt, and
            L. A. Vassilevskaya. *Neutrino dispersion in external magnetic fields*.
            Phys. Rev. D **73**, 023001 (2006).

[KW97]   M. Kachelrieß and G. Wunner.
           Radiative neutrino decays in very strong magnetic fields.
           Phys. Lett. B **390**, 263 (1997).

[Lan59]   L. D. Landau.
           On analytic properties of vertex parts in quantum field theory.
           Nucl. Phys. **13**, 181 (1959).

[Law79]   J. D. Lawson. *Lasers and Accelerators*.
           IEEE Trans. Nucl. Sci. **26**, 4217 (1979).

[Lea01]   E. Leader. *Spin in Particle Physics*.
           Cambridge University Press, 2001.

[Lee+06]   W. P. Leemans, B. Nagler, A. J. Gonsalves, C. Tóth, K. Nakamura,
           C. G. R. Geddes, et al.
           GeV electron beams from a centimetre-scale accelerator.
           Nature Phys. **2**, 696 (2006).

[Lee+14]   W. P. Leemans, A. J. Gonsalves, H. Mao, K. Nakamura,
           C. Benedetti, C. B. Schroeder, et al.
           *Multi-GeV Electron Beams from Capillary-Discharge-Guided
           Subpetawatt Laser Pulses in the Self-Trapping Regime*.
           Phys. Rev. Lett. **113**, 245002 (2014).

[LL81]   L. D. Landau and L. M. Lifshitz. *Quantum Mechanics*.
           Butterworth-Heinemann, 1981.

[LL82]   L. D. Landau and E. M. Lifshitz. *Quantum Electrodynamics*.
           Butterworth-Heinemann, 1982.

[LL87]   L. D. Landau and E. M. Lifshitz. *The Classical Theory of Fields*.
           Butterworth-Heinemann, 1987.

[LM14]   E. Lötstedt and K. Midorikawa.
           *Nuclear Reaction Induced by Carrier-Envelope-Phase Controlled
           Proton Recollision in a Laser-Driven Molecule*.
           Phys. Rev. Lett. **112**, 093001 (2014).

[Lon56]   I. M. Longman. *Note on a method for computing infinite integrals
           of oscillatory functions*.
           Math. Proc. Cambridge Philos. Soc. **52**, 764 (1956).

[LR47]   W. E. Lamb and R. C. Retherford.
           Fine Structure of the Hydrogen Atom by a Microwave Method.
           Phys. Rev. **72**, 241 (1947).

[LS01]   A. E. Lobanov and A. I. Studenikin.
           *Neutrino oscillations in moving and polarized matter under the
           influence of electromagnetic fields*. Phys. Lett. B **515**, 94 (2001).

[LS03]   A. Lobanov and A. Studenikin.
           Spin light of neutrino in matter and electromagnetic fields.
           Phys. Lett. B **564**, 27 (2003).

[LS77]   B. W. Lee and R. E. Shrock.
             Natural suppression of symmetry violation in gauge theories: Muon-
             and electron-lepton-number nonconservation.
             Phys. Rev. D **16**, 1444 (1977).

[Lya+11]   A. Lyachev, O. Chekhlov, J. Collier, R. Clarke, M. Galimberti,
             C. Hernandez-Gomez, et al.
             The 10PW OPCPA Vulcan Laser Upgrade.
             High Intensity Lasers and High Field Phenomena, HThE2 (2011).

[Mag05]   M. Maggiore. *A Modern Introduction to Quantum Field Theory.*
             Oxford University Press, 2005.

[Mai60]   T. H. Maiman. *Stimulated Optical Radiation in Ruby.*
             Nature **187**, 493 (1960).

[MAP]   *Muon Accelerator Program* (MAP).

[MD11]   F. Mackenroth and A. Di Piazza.
             Nonlinear Compton scattering in ultrashort laser pulses.
             Phys. Rev. A **83**, 032106 (2011).

[MD13]   F. Mackenroth and A. Di Piazza. *Nonlinear Double Compton*
             Scattering in the Ultrarelativistic Quantum Regime.
             Phys. Rev. Lett. **110**, 070402 (2013).

[MDK10]   F. Mackenroth, A. Di Piazza, and C. H. Keitel. *Determining the*
             Carrier-Envelope Phase of Intense Few-Cycle Laser Pulses.
             Phys. Rev. Lett. **105**, 063903 (2010).

[Mer98]   E. Merzbacher. *Quantum Mechanics.* John Wiley & Sons, 1998.

[Meu10]   S. Meuren.
             Radiative corrections to electron states in intense laser fields.
             Ruprecht-Karls-Universität Heidelberg (Diploma thesis), (2010).

[Mey71]   J. W. Meyer.
             Covariant Classical Motion of Electron in a Laser Beam.
             Phys. Rev. D **3**, 621 (1971).

[MHK08]   C. Müller, K. Z. Hatsagortsyan, and C. H. Keitel. *Muon pair*
             creation from positronium in a linearly polarized laser field.
             Phys. Rev. A **78**, 033408 (2008).

[Mil+06]   A. I. Milstein, C. Müller, K. Z. Hatsagortsyan, U. D. Jentschura,
             and C. H. Keitel.
             Polarization-operator approach to electron-positron pair production
             in combined laser and Coulomb fields.
             Phys. Rev. A **73**, 062106 (2006).

[Mit75]   H. Mitter. *Quantum Electrodynamics in Laser Fields.*
             Acta Phys. Austriaca, Suppl. **XIV**, 397 (1975).

[MNS62]   Z. Maki, M. Nakagawa, and S. Sakata.
             Remarks on the Unified Model of Elementary Particles.
             Progr. Theor. Phys. **28**, 870 (1962).

[MP04]   R. N. Mohapatra and P. B. Pal.
            Massive Neutrinos in Physics and Astrophysics.
            World Scientific, 2004.

[MS06]   M. Marklund and P. K. Shukla. *Nonlinear collective effects in photon-photon and photon-plasma interactions*.
            Rev. Mod. Phys. **78**, 591 (2006).

[MS77]   W. J. Marciano and A. I. Sanda.
            Exotic decays of the muon and heavy leptons in gauge theories.
            Phys. Lett. B **67**, 303 (1977).

[MTB06]   G. A. Mourou, T. Tajima, and S. V. Bulanov.
            Optics in the relativistic regime. Rev. Mod. Phys. **78**, 309 (2006).

[MTN12]   P. J. Mohr, B. N. Taylor, and D. B. Newell. *CODATA recommended values of the fundamental physical constants: 2010*.
            Rev. Mod. Phys. **84**, 1527 (2012).

[Mur+14]   N. Muramatsu, Y. Kon, S. Daté, Y. Ohashi, H. Akimune,
            J. Y. Chen, et al. *Development of high intensity laser-electron photon beams up to 2.9 GeV at the SPring-8 LEPS beamline*.
            Nucl. Instrum. Meth. A **737**, 184 (2014).

[MW55]   L. Michel and A. S. Wightman. *Covariant formalism describing the polarization of spin one-half particles*. Phys. Rev. **98**, 1190 (1955).

[Nar69]   N. B. Narozhnyi.
            Propagation of Plane Electromagnetic Waves in a Constant Field.
            Sov. Phys. JETP **28**, 371 (1969).

[Ner+11]   E. N. Nerush, I. Y. Kostyukov, A. M. Fedotov, N. B. Narozhny,
            N. V. Elkina, and H. Ruhl. *Laser Field Absorption in Self-Generated Electron-Positron Pair Plasma*.
            Phys. Rev. Lett. **106**, 035001 (2011).

[Nie03]   J. F. Nieves. *Electromagnetic vertex of neutrinos in an electron background and a magnetic field*. Phys. Rev. D **68**, 113003 (2003).

[Nie82]   J. F. Nieves. *Electromagnetic properties of Majorana neutrinos*.
            Phys. Rev. D **26**, 3152 (1982).

[Nis51]   K. Nishijima. *Generalized Furry's Theorem for Closed Loops*.
            Progr. Theor. Phys. **6**, 614 (1951).

[NNR65]   N. B. Narozhny, A. I. Nikishov, and V. I. Ritus. *Quantum processes in the field of a circularly polarized electromagnetic wave*.
            Sov. Phys. JETP **20**, 622 (1965).

[Nou+12]   T. Nousch, D. Seipt, B. Kämpfer, and A. I. Titov.
            Pair production in short laser pulses near threshold.
            Phys. Lett. B **715**, 246 (2012).

[NR64a]   A. I. Nikishov and V. I. Ritus. *Quantum processes in the field of a plane electromagnetic wave and in a constant field*.
            Sov. Phys. JETP **19**, 1191 (1964).

[NR64b]   A. I. Nikishov and V. I. Ritus. *Quantum processes in the field of a plane electromagnetic wave and in a constant field. I*. Sov. Phys. JETP **19**, 529 (1964).

[NR67]   A. I. Nikishov and V. I. Ritus. *Pair production by a photon and photon emission by an electron in the field of an intense electromagnetic wave and in a constant field*. Sov. Phys. JETP **25**, 1135 (1967).

[NR71]   R. A. Neville and F. Rohrlich. *Quantum Electrodynamics on Null Planes and Applications to Lasers*. Phys. Rev. D **3**, 1692 (1971).

[OHA11]   M. Orthaber, F. Hebenstreit, and R. Alkofer. *Momentum spectra for dynamically assisted Schwinger pair production*. Phys. Lett. B **698**, 80 (2011).

[Olv+10]   F. W. J. Olver, D. W. Lozier, R. F. Boisvert, and C. W. Clark, eds. *NIST Handbook of Mathematical Functions*. Cambridge University Press, 2010.

[Olv67]   F. W. J. Olver. *Numerical solution of second-order linear difference equations*. J. Res. Nat. Bur. Stand. **71B**, 101 (1967).

[OP33]   J. R. Oppenheimer and M. S. Plesset. *On the Production of the Positive Electron*. Phys. Rev. **44**, 53 (1933).

[OT94]   A. B. Olde Daalhuis and N. M. Temme. *Uniform Airy-Type Expansions of Integrals*. SIAM J. Math. Anal. **25**, 304 (1994).

[PB75]   R. Piessens and M. Branders. *Computation of oscillating integrals*. J. Comput. Appl. Math. **1**, 153 (1975).

[PB84]   R. Piessens and M. Branders. *Computation of Fourier transform integrals using Chebyshev series expansions*. Computing **32**, 177 (1984).

[Pet77]   S. T. Petcov. *The processes $\mu \to e + \gamma$, $\mu \to e + e + \bar{e}$, $\nu' \to \nu + \gamma$ in the Weinberg-Salam model with neutrino mixing*. Sov. J. Nucl. Phys. **25**, 340 (1977).

[Phu+12]   K. T. Phuoc, S. Corde, C. Thaury, V. Malka, A. Tafzi, J. P. Goddet, et al. *All-optical Compton gamma-ray source*. Nature Photon. **6**, 308 (2012).

[Pie+83]   R. Piessens, E. de Doncker-Kapenga, C. W. Überhuber, and D. K. Kahaner. *Quadpack - A Subroutine Package for Automatic Integration*. Springer, 1983.

[Poh+13]   R. Pohl, R. Gilman, G. A. Miller, and K. Pachucki. *Muonic Hydrogen and the Proton Radius Puzzle*. Annu. Rev. Nucl. Part. Sci. **63**, 175 (2013).

[Pok00]   S. Pokorski. *Gauge Field Theories*. Cambridge University Press, 2000.

[Pon57]   B. Pontecorvo. *Mesonium and antimesonium.*
            Sov. Phys. JETP **6**, 429 (1957).

[Pon58]   B. Pontecorvo.
            Inverse beta processes and nonconservation of lepton charge.
            Sov. Phys. JETP **7**, 172 (1958).

[Pow+14]   N. D. Powers, I. Ghebregziabher, G. Golovin, C. Liu, S. Chen,
            S. Banerjee, et al. *Quasi-monoenergetic and tunable X-rays from a
            laser-driven Compton light source.* Nature Photon. **8**, 28 (2014).

[PS95]   M. E. Peskin and D. V. Schroeder.
            An Introduction to Quantum Field Theory. Addison-Wesley, 1995.

[PW82]   P. B. Pal and L. Wolfenstein.
            Radiative decays of massive neutrinos.
            Phys. Rev. D **25**, 766 (1982).

[Rei62]   H. R. Reiss. *Absorption of Light by Light.*
            J. Math. Phys. **3**, 59 (1962).

[Rit70a]   V. I. Ritus. *Mass Operator and Exact Green's Function of an
            Electron in an Intense Field.* JETP Lett. **12**, 289 (1970).

[Rit70b]   V. I. Ritus. *Radiative Effects and Their Enhancement in an Intense
            Electromagnetic Field.* Sov. Phys. JETP **30**, 1181 (1970).

[Rit72a]   V. I. Ritus. *Radiative corrections in quantum electrodynamics with
            intense field and their analytical properties.*
            Ann. Phys. **69**, 555 (1972).

[Rit72b]   V. I. Ritus.
            *Vacuum polarization correction to elastic electron and muon
            scattering in an intense field and pair electro- and muoproduction.*
            Nucl. Phys. B **44**, 236 (1972).

[Rit85]   V. I. Ritus. *Quantum effects of the interaction of elementary
            particles with an intense electromagnetic field.*
            J. Sov. Laser Res. **6**, 497 (1985).

[RPP14]   Particle Data Group. *Review of Particle Physics.*
            Chin. Phys. C **38**, 090001 (2014).

[RVX10]   R. Ruffini, G. Vereshchagin, and S. Xue. *Electron–positron pairs in
            physics and astrophysics: From heavy nuclei to black holes.*
            Phys. Rep. **487**, 1 (2010).

[Ryd96]   L. H. Ryder. *Quantum Field Theory.*
            Cambridge University Press, 1996.

[Sal+99]   P. Salières, A. L'Huillier, P. Antoine, and M. Lewenstein. *Study of
            the Spatial and Temporal Coherence of High-Order Harmonics.*
            Adv. At. Mol. Opt. Phys. **41**, 83 (1999).

[Sau31]   F. Sauter. *Über das Verhalten eines Elektrons im homogenen
            elektrischen Feld nach der relativistischen Theorie Diracs.*
            Z. Phys. **69**, 742 (1931).

[Sch+93]   K. J. Schafer, B. Yang, L. F. DiMauro, and K. C. Kulander.
             Above threshold ionization beyond the high harmonic cutoff.
             Phys. Rev. Lett. **70**, 1599 (1993).

[Sch00a]   C. Schubert. *Vacuum polarisation tensors in constant
             electromagnetic fields: Part I*. Nucl. Phys. B **585**, 407 (2000).

[Sch00b]   C. Schubert. *Vacuum polarisation tensors in constant
             electromagnetic fields: Part II*. Nucl. Phys. B **585**, 429 (2000).

[Sch48a]   J. Schwinger. *On Quantum-Electrodynamics and the Magnetic
             Moment of the Electron*. Phys. Rev. **73**, 416 (1948).

[Sch48b]   J. Schwinger.
             Quantum Electrodynamics. I. A Covariant Formulation.
             Phys. Rev. **74**, 1439 (1948).

[Sch49a]   J. Schwinger. *On Radiative Corrections to Electron Scattering*.
             Phys. Rev. **75**, 898 (1949).

[Sch49b]   J. Schwinger. *Quantum Electrodynamics. II. Vacuum Polarization
             and Self-Energy*. Phys. Rev. **75**, 651 (1949).

[Sch49c]   J. Schwinger. *Quantum Electrodynamics. III. The Electromagnetic
             Properties of the Electron – Radiative Corrections to Scattering*.
             Phys. Rev. **76**, 790 (1949).

[Sch51]   J. Schwinger. *On Gauge Invariance and Vacuum Polarization*.
             Phys. Rev. **82**, 664 (1951).

[SFK13]   O. D. Skoromnik, I. D. Feranchuk, and C. H. Keitel.
             Collapse-and-revival dynamics of strongly laser-driven electrons.
             Phys. Rev. A **87**, 052107 (2013).

[SGD08]   R. Schützhold, H. Gies, and G. Dunne.
             Dynamically Assisted Schwinger Mechanism.
             Phys. Rev. Lett. **101**, 130404 (2008).

[Sha00]   R. Shaisultanov.
             νν γ amplitude in an external homogeneous electromagnetic field.
             Phys. Rev. D **62**, 113005 (2000).

[Sha98]   R. Shaisultanov. *Photon-Neutrino Interactions in Magnetic Fields*.
             Phys. Rev. Lett. **80**, 1586 (1998).

[Shr82]   R. E. Shrock. *Electromagnetic properties and decays of Dirac and
             Majorana neutrinos in a general class of gauge theories*.
             Nucl. Phys. B **206**, 359 (1982).

[SK11]   D. Seipt and B. Kämpfer.
             Nonlinear Compton scattering of ultrashort intense laser pulses.
             Phys. Rev. A **83**, 022101 (2011).

[SK12]   D. Seipt and B. Kämpfer.
             Two-photon Compton process in pulsed intense laser fields.
             Phys. Rev. D **85**, 101701 (2012).

[SK13]   D. Seipt and B. Kämpfer.
             Asymmetries of azimuthal photon distributions in nonlinear
             Compton scattering in ultrashort intense laser pulses.
             Phys. Rev. A **88**, 012127 (2013).

[SK14]   D. Seipt and B. Kämpfer.
             Laser-assisted Compton scattering of x-ray photons.
             Phys. Rev. A **89**, 023433 (2014).

[Sko76]   V. V. Skobelev.
             The $\gamma \to \nu\bar{\nu}$ and $\nu \to \gamma\nu$ reactions in strong magnetic fields.
             Sov. Phys. JETP **44**, 660 (1976).

[Sko91]   V. V. Skobelev.
             Interaction between a massive neutrino and a plane-wave field.
             Sov. Phys. JETP **73**, 40 (1991).

[SLAC376]   The FFTB Collaboration.
             Final Focus Test Beam (Project Design Report). SLAC-376, (1991).

[SLAC9961]   V. A. Alexandrof et al. *Results of Final Focus Test Beam*.
             SLAC-PUB-9961, (1995).

[SM85]   D. Strickland and G. Mourou.
             Compression of amplified chirped optical pulses.
             Opt. Commun. **55**, 447 (1985).

[SPring8]   *Super Photon Ring – 8 GeV* (SPring8).

[Sre07]   M. Srednicki. *Quantum Field Theory*.
             Cambridge University Press, 2007.

[SS70]   E. S. Sarachik and G. T. Schappert. *Classical Theory of the*
             Scattering of Intense Laser Radiation by Free Electrons.
             Phys. Rev. D **1**, 2738 (1970).

[ST05]   A. Studenikin and A. Ternov.
             Neutrino quantum states and spin light in matter.
             Phys. Lett. B **608**, 107 (2005).

[ST07]   B. E. A. Saleh and M. C. Teich. *Fundamentals of Photonics*.
             John Wiley & Sons, 2007.

[Sun+10]   J. H. Sung, S. K. Lee, T. J. Yu, T. M. Jeong, and J. Lee.
             0.1 Hz 1.0 PW Ti:sapphire laser. Opt. Lett. **35**, 3021 (2010).

[Tak57]   Y. Takahashi. *On the generalized ward identity*.
             Il Nuovo Cimento **6**, 371 (1957).

[Tay72]   J. R. Taylor. *Scattering Theory: The Quantum Theory of*
             Nonrelativistic Collisions. John Wiley & Sons, 1972.

[TE14]   A. I. Ternov and P. A. Eminov.
             Neutrino radiative decay in external field and medium.
             Phys. Part. Nuclei **45**, 397 (2014).

[The+09]   The ISS Accelerator Working Group et al.
             Accelerator design concept for future neutrino facilities.
             J. Instrum. **4**, P07001 (2009).

[Tin05]   T. M. Tinsley.
            Pair production with neutrinos and high-intensity laser fields.
            Phys. Rev. D **71**, 073010 (2005).

[Tit+11]   A. I. Titov, B. Kämpfer, H. Takabe, and A. Hosaka. *Neutrino pair
            emission off electrons in a strong electromagnetic wave field*.
            Phys. Rev. D **83**, 053008 (2011).

[Tit+12]   A. I. Titov, H. Takabe, B. Kämpfer, and A. Hosaka.
            Enhanced Subthreshold e^+e^- Production in Short Laser Pulses.
            Phys. Rev. Lett. **108**, 240406 (2012).

[Tit+13]   A. I. Titov, B. Kämpfer, H. Takabe, and A. Hosaka.
            Breit-Wheeler process in very short electromagnetic pulses.
            Phys. Rev. A **87**, 042106 (2013).

[TO48]   S. Tomonaga and J. R. Oppenheimer.
            On Infinite Field Reactions in Quantum Field Theory.
            Phys. Rev. **74**, 224 (1948).

[Tol56]   H. A. Tolhoek. *Electron Polarization, Theory and Experiment*.
            Rev. Mod. Phys. **28**, 277 (1956).

[Tom46]   S. Tomonaga. *On a Relativistically Invariant Formulation of the
            Quantum Theory of Wave Fields*. Progr. Theor. Phys. **1**, 27 (1946).

[Tuc10]   K. Tuchin. *Non-linear pair production in scattering of photons on
            ultra-short laser pulses at high energy*.
            Phys. Lett. B **686**, 29 (2010).

[Vol35]   D. M. Volkov.
            Über eine Klasse von Lösungen der Diracschen Gleichung.
            Z. Phys. **94**, 250 (1935).

[VS04]   O. Vallée and M. Soares.
            Airy Functions and Applications to Physics. World Scientific, 2004.

[Wan+11]   Z. Wang, C. Liu, Z. Shen, Q. Zhang, H. Teng, and Z. Wei.
            *High-contrast 1.16 PW Ti:sapphire laser system combined with a
            doubled chirped-pulse amplification scheme and a femtosecond
            optical-parametric amplifier*. Opt. Lett. **36**, 3194 (2011).

[Wan+13]   X. Wang, R. Zgadzaj, N. Fazel, Z. Li, S. A. Yi, X. Zhang, et al.
            *Quasi-monoenergetic laser-plasma acceleration of electrons to 2
            GeV*. Nat. Commun. **4**, 1988 (2013).

[War50]   J. C. Ward. *An Identity in Quantum Electrodynamics*.
            Phys. Rev. **78**, 182 (1950).

[Wei95]   S. Weinberg. *The Quantum Theory of Fields I*.
            Cambridge University Press, 1995.

[Wei96]   S. Weinberg. *The Quantum Theory of Fields II*.
            Cambridge University Press, 1996.

[Wim84]   J. Wimp. *Computation with Recurrence Relations*.
            Pitman Publishing, 1984.

[WL48]   P. M. Woodward and J. D. Lawson.
             The theoretical precision with which an arbitrary radiation-pattern
             may be obtained from a source of finite size.
             J. Inst. Electr. Eng. 3 **95**, 363 (1948).

[Wöl+15]   A. Wöllert, M. Klaiber, H. Bauke, and C. H. Keitel.
             Relativistic tunneling picture of electron-positron pair creation.
             Phys. Rev. D **91**, 065022 (2015).

[Won01]   R. Wong. *Asymptotic Approximation of Integrals.* SIAM, 2001.

[XCELS]   *Exawatt Center for Extreme Light Studies* (XCELS).

[Yan+08]   V. Yanovsky, V. Chvykov, G. Kalinchenko, P. Rousseau,
             T. Planchon, T. Matsuoka, et al.
             Ultra-high intensity 300 TW laser at 0.1 Hz repetition rate.
             Opt. Express **16**, 2109 (2008).

[Yu+12]   T. J. Yu, S. K. Lee, J. H. Sung, J. W. Yoon, T. M. Jeong, and
             J. Lee. *Generation of high-contrast, 30 fs, 1.5 PW laser pulses from*
             chirped-pulse amplification Ti:sapphire laser.
             Opt. Express **20**, 10807 (2012).

[ZEG96]   C. V. Zhukovsky, P. A. Eminov, and A. E. Grigoruk.
             Radiative Decay of a Massive Neutrino in the Weinberg–Salam
             Model with Mixing in a Constant Uniform Magnetic Field.
             Mod. Phys. Lett. A **11**, 3119 (1996).

Acknowledgments